QUANTUM DYNAMICS IN LOW-TEMPERATURE CHEMISTRY

V.A. BENDERSKII, V.I. GOLDANSKII and D.E. MAKAROV

Institute of Chemical Physics of the Russian Academy of Sciences, 142 432 Chernogolovka, Moscow Region, Russia

NORTH-HOLLAND

PHYSICS REPORTS (Review Section of Physics Letters) 233, Nos. 4 & 5 (1993) 195–339
North-Holland

PHYSICS REPORTS

Quantum dynamics in low-temperature chemistry

V.A. Benderskii, V.I. Goldanskii and D.E. Makarov[1,2]

Institute of Chemical Physics of the Russian Academy of Sciences, 142 432 Chernogolovka, Moscow Region, Russia

Received October 1992; editor: J. Eichler

Contents:

Abstract:

A contemporary review of quantum models of chemical reactions is presented. At low temperatures tunneling prevails over thermally activated transitions and results in non-Arrhenius behavior of the rate constant, which cannot be described in terms of classical transition state theory and requires explicit incorporation of environment dynamics. The correlation between the quantum rate constant and spectral properties of the heat bath and dynamics of intramolecular vibrations is considered. The spectroscopic evidence of tunneling in molecules is also discussed. The theoretical consideration is illustrated by a number of experimental examples.

[1] Present address: School of Chemical Sciences, University of Illinois, 505 S. Mathews Avenue, Urbana, IL 61 801, USA.
[2] To whom correspondence should be addressed.

1. Introduction

1.1. Historical background

Any elementary chemical reaction is a conversion of reactant molecules, which are stable on the time scale of their vibration frequencies, to the product molecules. This process is associated with surmounting an energy barrier dividing the quasistationary states. Stability of reactants implies in particular that the transition proceeds so slowly that the populations of energy levels in the initial state are close to the equilibrium ones. In order for this stability to take place, the barrier height should be greater than both the thermal energy and the energy level spacing in the initial state,

$$V_0 \gg \hbar\omega_0 , \qquad \beta V_0 \gg 1 , \quad \beta = (k_B T)^{-1} . \tag{1.1}$$

Under the conditions (1.1) the rate constant is determined by the statistically averaged reactive flux from the initial to the final state.

The quintessence of the classical chemical kinetics is the Arrhenius law

$$k(T) = k_0 \exp(-\beta V_0) , \tag{1.2}$$

which means that those initial states mostly contribute to the rate constant, which lie in the vicinity of the barrier top. The prefactor k_0 depends on the statistical weight of these states. The classical transition state theory (CLTST) [Eyring 1935; Glasstone et al. 1941; Eyring et al. 1983] developed, in the first place, by Eyring, takes into account solely the over-barrier transitions with energy $E > V_0$. The history of CLTST has been written up by Leidler [1969]. The Arrhenius law particularly requires that, even for the lowest barrier still satisfying the first of the conditions (1.1), the rate constant should vanish at sufficiently low temperature. For instance, even for a very fast reaction with $k_0 = 10^{13}\,s^{-1}$, $V_0 = 5\,kJ/mol$, $k = 10^{12}\,s^{-1}$ at 300 K, the rate constant decreases to below $10^{-9}\,s^{-1}$ at $T = 10\,K$. Such a low value of k means the full absence of any conversion on a time scale available in a measurement.

Quantum mechanics has brought new essential features into the chemical reaction theory. First, the nature of the chemical bond itself has been established, and the concept of potential energy surface (PES) on which the chemical reaction occurs has emerged. Second, the quantum partition functions (for discrete energy spectra) are calculated in CLTST for both the initial and transition states; the transition state is chosen from the condition that a classical trajectory of free motion along the reaction coordinate, having once crossed the transition state, does not return [Wigner 1938; Miller 1976]. Third, quantum mechanics allows for tunneling, i.e., penetration of particles through the classically forbidden areas. This possibility has been considered within CLTST only as giving rise to small corrections to the rate constant. Wigner was the first to calculate this correction for a parabolic barrier [Wigner 1932, 1938]. He discovered that the apparent activation energy,

$$E_a = k_B T^2 \partial \ln k / \partial T , \tag{1.3}$$

becomes less than the barrier height and decreases with decreasing temperature,

$$E_a = V_0 - \tfrac{1}{24}\beta(\hbar\omega^{\#})^2 , \tag{1.4}$$

where $\omega^{\#}$ is the upside-down parabolic barrier frequency,

$$V(Q) = V_0 - \tfrac{1}{2} m\omega^{\#2}Q^2 , \tag{1.5}$$

and the reaction coordinate Q is considered separately from the remaining degrees of freedom.

Earlier investigations [Hund 1927; Roginsky and Rozenkevitsch 1930] had pointed out that the tunneling corrections should be observable in the case of high and narrow barriers, and that they should be taken into account for reactions involving transfer of light particles, and in particular, for hydrogen atoms. Although Bell's solution [Bell 1933, 1935, 1937] to the Wigner problem for low temperatures ($\beta\hbar\omega^{\#}/2\pi > 1$) has demonstrated that at $T \to 0$ the rate constant is no longer subject to the Arrhenius law, this result has passed unnoticed for two reasons primarily: partly because of exoticity of that situation which could not be implemented given the experimental perspective at the moment, and partly because the parabolic barrier model (1.5) was apparently incorrect at $E \ll V_0$, when the initial and final states should be explicitly considered.

The next three decades were a period of overwhelming domination of CLTST, which has become the basis of a universal description of various gas- and liquid-phase chemical reactions. Tunneling was drawing just a little attention in the context of chemical kinetics during those years. Only Bell's prolonged investigations, summarized in his renowned books [Bell 1973, 1980], have ascertained the two main consequences of proton tunneling in liquid phase reactions, i.e., the lowering of the apparent activation energy and the growth of the isotope H/D effect (ratio of the rate constants of H and D atom transfer) with decreasing temperature. The same results had been found by the early 60s in the gas-phase reactions of the H atom [Johnston 1960]. In both cases tunneling was considered to occur from thermally activated reactant states and to give rise to only small corrections to the Arrhenius law.

In 1959 Goldanskii showed [Goldanskii 1959, 1979] that at low enough temperatures, when the population of thermally activated energy levels vanishes, only tunneling from the ground state contributes to the transition, and the rate constant approaches its low-temperature quantum limit k_c, becoming temperature-independent. According to [Goldanskii 1959], the Arrhenius dependence $k(T)$ evens out at the low-temperature plateau in a relatively narrow temperature domain determined by the characteristic temperature T_c, which was later called the "cross-over temperature". It depends not only on V_0, but also on the barrier width and tunneling mass m,

$$\beta_c^{-1} = k_B T_c = a(\hbar^2 V_0/2md^2)^{1/2} , \tag{1.6}$$

where d is the barrier width corresponding to the zero-point energy in the initial state, and a is a factor of order unity, depending on the specific barrier shape. It equals $\frac{1}{2}$, $2/\pi$, $\frac{3}{4}$ and 1 for rectangular, parabolic and triangular barriers, and for the barrier constructed from two shifted paraboloids, respectively. For the parabolic barrier (1.5), eq. (1.6) assumes the equivalent form

$$k_B T_c = \hbar\omega^{\#}/2\pi . \tag{1.7}$$

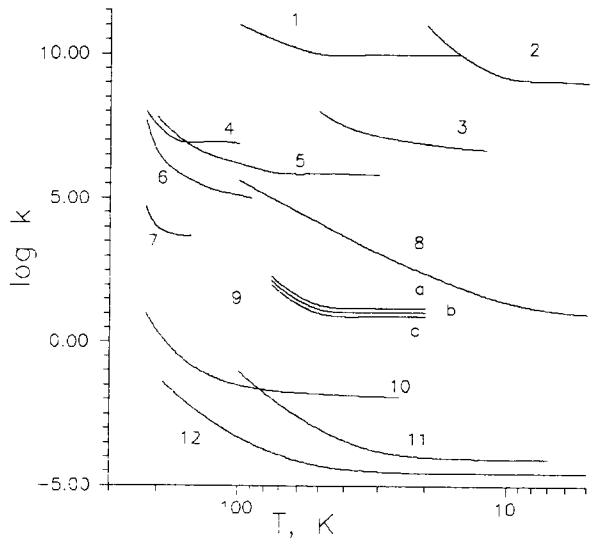

Fig. 1. Examples of temperature dependence of the rate constant for the reactions in which the low-temperature rate-constant limit has been observed: 1. hydrogen transfer in the excited singlet state of the molecule represented by (6.16); 2. molecular reorientation in methane crystal; 3. internal rotation of CH_3 group in radical (6.25); 4. inversion of radical (6.40); 5. hydrogen transfer in "halved" molecule (6.16); 6. isomerization of molecule (6.17) in excited triplet state; 7. tautomerization in the ground state of 7-azoindole dimer (6.1); 8. polymerization of formaldehyde in reaction (6.44); 9. limiting stage (6.45) of (a) chain hydrobromination, (b) chlorination and (c) bromination of ethylene; 10. isomerization of radical (6.18); 11. abstraction of H atom by methyl radical from methanol matrix [reaction (6.19)]; 12. radical pair isomerization in dimethylglyoxime crystals [Toriyama et al. 1977].

The quantum limit k_c relates to V_0 and T_c through the approximate formula

$$k_c = Ak_0 \exp(-\beta_c V_0), \quad A \sim (\beta_c V_0)^{-1}, \tag{1.8}$$

where the factor A accounts for the decrease in $k(T)$ in the intermediate region between the Arrhenius dependence and low-temperature plateau. As follows from (1.6)–(1.8), the rate constant of the tunneling reaction, unlike the classical case, depends not only on the barrier height, but also on the additional parameter $\hbar^2/2md^2$ (or $\omega^{\#}$), which does not show up in CLTST. As a function of this parameter, the rate constant changes in a range which is not narrower than when it is considered a function of V_0. Typical values of d and m ($d = 0.5$–2.5 Å, $m/m_H = 1$–20) at a fixed barrier height correspond with a variation of k_c over more than 10–12 orders of magnitude, thus covering the entire experimentally permissible range of the rate constant.

The experimental studies of a large number of low-temperature solid-phase reactions undertaken by many groups in 70s and 80s have confirmed the two basic consequences of the Goldanskii model, the existence of the low-temperature limit and the cross-over temperature. The aforementioned difference between quantum-chemical and classical reactions has also been established, namely, the values of k_c turned out to vary over many orders of magnitude even for reactions with similar values of V_0 and hence with similar Arrhenius dependence. For illustration, fig. 1 presents a number of typical experimental examples of $k(T)$ dependence.

At $T < T_c$ tunneling occurs not only in irreversible chemical reactions, but also in spectroscopic splittings. Tunneling eliminates degeneracy and gives rise to tunneling multiplets, which can be detected with various spectroscopic techniques, from inelastic neutron scattering to optical and microwave spectroscopy. The most illustrative examples of this sort are the inversion of the

ammonium molecule and the rotations of the methyl group. In this case it is impossible to prepare the initial nonstationary state, i.e., one cannot talk about reactants and products. The tunneling splittings Δ involved in spectroscopy range from 10^5 to $10^{12}\,s^{-1}$. Surprisingly, they can be measured at temperatures for which the thermal energy is several orders greater than $\hbar\Delta$. At $T > T_c$ tunneling splittings are not detected, because the over-barrier transitions from the energy levels belonging to the continuous spectrum compete with tunneling.

The data presented in the following sections of this review demonstrate, however, that k_c and T_c taken from the experimental curves $k(T)$ are usually at dramatic variance with crystallographic and spectroscopic data concerning the geometric configuration of the initial state, from which the tunneling distance is usually inferred. In contradiction with (1.6), T_c was found to depend weakly on the mass of the tunneling particle. The explanation for this lies in realizing that the PES of any, even the simplest, chemical reaction is multidimensional (of dimension $N \geq 2$), and the potential barrier $V(Q)$ corresponds to the saddle point, which is the energy minimum on the $(N-1)$-dimensional surface dividing the reactant and product valleys. All of the N degrees of freedom participate in the classical motion of the system, and in the vicinity of the initial minimum on the PES this motion is composed of the normal vibrations, including the ones with sufficiently low frequencies. In particular, when an atom or fragment is transferred between the crystal lattice nodes, intermolecular vibrations may have low frequencies, compared to the other characteristic frequencies of the problem. When the frequencies of these vibrations ω are less than $\omega^{\#}$, then the Arrhenius dependence, although with smaller activation energy, will persist at $T < T_c$, until these vibrations freeze out at $k_B T < \frac{1}{2}\hbar\omega$ or cease to participate in the transition.

In the first case the cross-over temperature is given by

$$k_B T_c' = \tfrac{1}{2}\hbar\omega < k_B T_c \,, \tag{1.9}$$

and is not related with $\omega^{\#}$. In the case of "switching-off" of the low-frequency modes, the tunneling trajectories should differ from the classical ones, so that they do not pass through the saddle point. Consequently, the height of the barrier through which the particle tunnels is greater than that for the classical transition. Both effects take place in tunneling reactions and this explains why k_c and T_c differ from the values calculated within one-dimensional static-barrier models. This leads one to recognize the need for multidimensional tunneling models in which the multidimensional reactant motion creates a dynamical barrier whose parameters differ considerably from those of the static barrier.

A simple dynamical model of a low-temperature reaction, referred to as the "fluctuational barrier preparation" model (or "vibration-assisted tunneling"), was put forth in the beginning of the 80s [Ovchinnikova 1979; Benderskii et al. 1980; Trakhtenberg et al. 1982]. Only later was the proximity of this model to the contemporary quantum transition state theory (QTST) realized. QTST has been under intensive development since the 70s as the problem of multidimensional tunneling trajectories [Truhlar and Kuppermann 1971; Miller 1974, 1983; Babamov and Marcus 1981] stimulating both theoretical and experimental studies of quantum-chemical reactions. Since these reactions, unlike the classical ones, correspond to low transition probabilities and they are observed in the absence of thermal activation, the results, which were earlier obtained in low-temperature chemistry and to which not much attention was paid for a long time, have at last been incorporated into the mainstream of development of fundamental concepts in chemical kinetics. The advance of the last decade in quantum-chemical dynamics has enabled one to describe from a unique perspective such, at first glance, distant phenomena as spectroscopic tunneling splitting (with transition probabilities 10^{10}–$10^{11}\,s^{-1}$) and slow low-temperature chemical conversions (with rate constants up to $10^{-5}\,s^{-1}$).

Computations have shown that in the quantum region it is possible to have various most probable transition paths (ranging from the classical minimum energy path (MEP) to the straight-line one-dimensional tunneling of early models), depending on the PES geometry.

The quantum effects in low-temperature chemistry are discussed in a book [Goldanskii et al. 1989] and in reviews [Jortner and Pullman 1986; Benderskii et al. 1989; Benderskii and Goldanskii 1992]. In the last two reviews the current state of affairs in low-temperature chemistry is considered in connection with advances in quantum-chemical dynamics in general. However, all these reviews except [Benderskii and Goldanskii 1992] relied only on radiationless transition theory [Kubo and Toyasava 1955], developed for studying impurity centers in crystals, and did not reflect the rampant progress in the general quantum theory of chemical reactions.

Judging from our present knowledge, such a description is far from the whole story. The article of Benderskii and Goldanskii [1992] addressed mostly the vast amount of experimental data accumulated thus far. On the other hand, the major applications of QTST involved gas-phase chemical reactions, where quantum effects were not dominant. All this implies that there is a gap between the possibilities offered by modern quantum theory and the problems of low-temperature chemistry, which apparently are the natural arena for testing this theory. This prompted us to propose a new look at this field, and to consistently describe the theoretical approaches which are adequate even at $T = 0$.

1.2. Routes of simplifying the problem

The main problem of elementary chemical reaction dynamics is to find the rate constant of the transition in the reaction complex interacting with its environment. This problem, in principle, is close to the general problem of statistical mechanics of irreversible processes (see, e.g., Blum [1981], Kubo et al. [1985]) about the relaxation of initially nonequilibrium state of a particle in the presence of a reservoir (heat bath). If the particle is coupled to the reservoir weakly enough, then the properties of the latter are fully determined by the spectral characteristics of its susceptibility coefficients.

Moreover, in this linear-response (weak-coupling) limit any reservoir may be thought of as an infinite number of oscillators $\{q_j\}$ with an appropriately chosen spectral density, each coupled linearly in q_j to the particle coordinates. The coordinates q_j may not have a direct physical sense; they may be just unobservable variables whose role is to provide the correct response properties of the reservoir. In a chemical reaction the role of a particle is played by the reaction complex, which itself includes many degrees of freedom. Therefore the separation of reservoir and particle does not suffice to make the problem manageable, and a subsequent reduction of the internal degrees of freedom in the reaction complex is required. The possible ways to arrive at such a reduction are summarized in table 1.

By convention, we divide the total system characterized by nuclear coordinates and composed of a reaction complex and the environment into the PES coordinates and the heat bath, by using the weak-coupling criterion. Thus the set of PES coordinates will not in general be identical to the reaction complex because it contains only those degrees of freedom which cannot be split off and put into the harmonic heat bath because of their strong coupling. On the other hand, the PES coordinates may include the intermolecular vibrations strongly coupled to the motion of the transferred atom or fragment.

Since the calculation of multidimensional PES is a very difficult task, in most cases the choice of the internal PES coordinates is based on models, which take into account the information about the structure, barrier height and characteristic frequencies of the reaction complex and

Table 1
Reduction of the general quantum dynamics problem

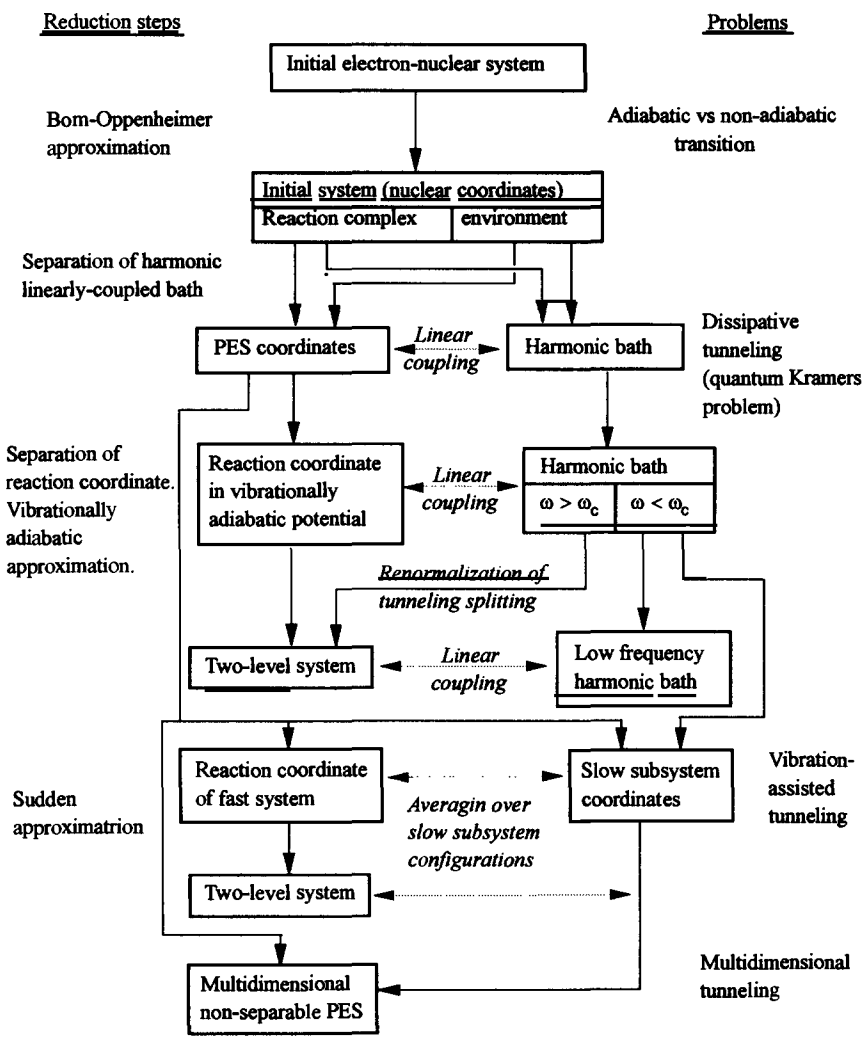

environment. In fact, at this stage simplifications come about, which allow one to choose a PES with a restricted number of degrees of freedom.

Often the consideration of low-temperature chemical reactions is restricted to a single-sheet PES. In general, a chemical reaction is the passage between two (or several) electronic states, each characterized by its own PES (reactant and product "diabatic terms"). The interaction between these states ("diabatic coupling") eliminates their intersection and creates two new adiabatic PES one of which (the lower one) connects the reactant and product states in a continuous way. The upper and lower adiabatic terms are separated by the adiabatic splitting. In the usual case for low-temperature chemistry, this splitting is large enough, and the influence of the upper term is immaterial, so that tunneling occurs on a single adiabatic PES; the effect of nonadiabaticity is to modify the preexponential factor.

The obtained PES forms the basis for the subsequent dynamical calculation, which starts with determining the MEP. The next step is to use the vibrationally adiabatic approximation for those PES degrees of freedom whose typical frequencies ω_j are greater than ω_0 and $\omega^\#$. Namely, for the high-frequency modes the vibrationally adiabatic potential [Miller 1983] is introduced,

$$V_{\mathrm{vad}}(Q) = V(Q) + \sum_j \tfrac{1}{2}\hbar\omega_j(Q) \,. \tag{1.10}$$

If all the PES coordinates are split off in this way, the original multidimensional problem reduces to that of one-dimensional tunneling in the effective barrier (1.10) of a particle which is coupled to the heat bath. This problem is known as the dissipative tunneling problem, which has been intensively studied for the past 15 years, primarily in connection with tunneling phenomena in solid state physics [Caldeira and Leggett 1983]. Interaction with the heat bath leads to the friction force that acts on the particle moving in the one-dimensional potential (1.10), and, as a consequence, $\omega^\#$ is replaced by the Kramers frequency $\lambda^\#$ [Kramers 1940] defined by

$$\lambda^\# = \omega^\#\{[1 + (\eta/2\omega^\#)^2]^{1/2} - \eta/2\omega^\#\} \,, \tag{1.11}$$

where η is the friction coefficient. The cross-over temperature decreases to [Hanggi 1986; Hanggi et al. 1990]

$$k_{\mathrm{B}}T_{\mathrm{c}} = \hbar\lambda^\#/2\pi \,. \tag{1.12}$$

In order that CLTST be valid, in addition to conditions (1.1) it is necessary that friction, while leaving the transition rate unaffected, should maintain thermal equilibrium in the initial state. This leads to the additional requirement

$$(\beta V_0)^{-1} < \eta/2\omega^\# < 1 \,. \tag{1.13}$$

At low temperatures ($\beta\hbar\omega_0 \gg 1$) only the lowest initial eigenstate actually participates in the transition, and the problem permits further reduction to the two-level system Hamiltonian [Leggett et al. 1987; Suarez and Silbey 1991a]. In doing so, one separates the high-frequency part of the bath spectrum (vibrations with frequencies $\omega > \omega_{\mathrm{c}}$ where ω_{c} is a characteristic cutoff frequency). The tunneling is considered instantaneous on the time scale of the low-frequency bath vibrations ($\omega < \omega_{\mathrm{c}}$) and thus it is described by a tunneling matrix element $\frac{1}{2}\hbar\Delta$, which is renormalized by the high-frequency vibrations [Leggett et al. 1987]. In essence, the rate theory version based on the model of a two-level system (TLS) coupled to a low-frequency heat bath is a golden-rule approach, exploiting the basic formula

$$k = (2\pi/\hbar)(\hbar\Delta/2)^2\,\rho_{\mathrm{f}}\mathrm{FC} \,, \tag{1.14}$$

where $\hbar\Delta$ is the tunneling splitting in the isolated TLS, ρ_{f} the density of energy levels in the final state and FC is the Franck–Condon factor (square of the overlap integral of oscillator wave functions in the initial and final states).

This model permits one to immediately relate the bath frequency spectrum to the rate-constant temperature dependence. For the classical bath ($\beta\hbar\omega_c < 1$) the Franck–Condon factor is proportional to $\exp(-\frac{1}{4}\beta E_r)$ with the reorganization energy equal to

$$E_r = \tfrac{1}{2}\sum m_j\omega_j^2\Delta q_j^2 \tag{1.15}$$

where Δq_j is the shift of the jth oscillator due to the transition. The heat bath reorganization creates the barrier $V_0 = \frac{1}{4}E_r$. At $\beta\hbar\omega_c \gg 1$ the contributions from one-phonon, two-phonon processes, etc., can be systematically extracted from the general expression for the rate constant, and the type of the dominant process is determined by the bath spectrum. The results of Leggett et al. [1987] show that the quantum dynamics of a TLS crucially depends upon the spectrum of the bath and, in particular, the bath may dramatically slow tunneling down and even localize the particle in one of the wells at sufficiently strong coupling. The strong dependence on the bath spectrum is inherent to the quantum dynamics and it does not show up in classical transitions.

Aside from the reorganization of the bath, there is one more phenomenon which has to be accounted for in description of a chemical reaction. Namely, there are vibrational modes which are not reorganized in the transition, but which efficiently modulate the barrier thereby dramatically increasing the tunneling rate. The dissipative tunneling model, formulated by Leggett et al. [1987], does not properly account for such "promoting" vibrational modes which are strongly coupled to the particle, and which, in fact, do not belong to the heat bath in the above weak-coupling sense.

As an example of such a situation consider the tunneling of the hydrogen atom in an OH ··· O fragment (fig. 2). The height and width of the barrier for the H atom depend on the O–O distance. On the other hand, the O–O distance is the same in the initial and final states, i.e., the reorganization energy corresponding with the O–O vibration equals zero. If the promoting vibration has a high frequency, it can be incorporated by using the vibrationally adiabatic potential along MEP (1.10). In the opposite case tunneling occurs instantaneously on the timescale of the promoting vibrations of the heavy fragments, and its rate results from averaging over the slow subsystem configurations [Ovchinnikova 1979; Benderskii et al. 1980; Trakhtenberg et al. 1982]. The most probable tunneling path in this case differs from the MEP.

This idea, christened later as the sudden approximation, has recently been developed in detail by Levine et al. [1989], in connection with dissipative tunneling in the framework of quantum

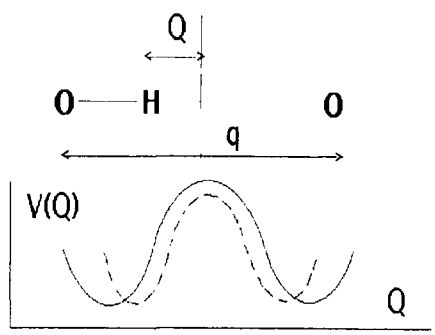

Fig. 2. Transfer of a hydrogen atom in an OH ··· O fragment promoted by stretching O–O vibration. Solid line corresponds to equilibrium O–O distance, $q = q_0$, dotted line $q < q_0$.

transition state theory. For the TLS model the promoting vibrations (q_p) are incorporated by introducing the tunneling matrix element dependence on q_p [Suarez and Silbey 1991a; Bogris et al. 1989; Siebrand et al. 1984]

$$\Delta = \Delta_0 \exp(-\gamma q_p) , \tag{1.16}$$

where γ^{-1} is small compared to the tunneling distance. For OH ··· O fragments the value of γ is in the range 25–35 $Å^{-1}$ [Bogris et al. 1989].

In realistic systems, the separation of the modes according to their frequencies and subsequent reduction to one dimension is often impossible with the above-described methods. In this case an accurate multidimensional analysis is needed. Another case in which a multidimensional study is required and which obviously cannot be accounted for within the dissipative tunneling model is that of complex PES with several saddle points and therefore with several MEPs and tunneling paths.

While the goal of the previous models is to carry out analytical calculations and gain insight into the physical picture, the multidimensional calculations are expected to give a quantitative description of concrete chemical systems. However at present we are just at the beginning of this process, and only a few examples of numerical multidimensional computations, mostly on rather idealized PES, have been performed so far. Nonetheless these pioneering studies have established a number of novel features of tunneling reactions, which do not show up in the effectively one-dimensional models.

The most general problem should be that of a particle in a nonseparable potential, linearly coupled to an oscillator heat bath, when the dynamics of the particle in the classically accessible region is subject to friction forces due to the bath. However, this multidimensional quantum Kramers problem has not been explored as yet.

To conclude this section, it is worth pointing out one more basic peculiarity of quantum dynamics, as opposed to classical dynamics. Since in classical mechanics trajectories with energies $E < V_0$ are banned, the treatment of tunneling necessitates considering a phase space in which the coordinates are real and the conjugate momenta imaginary. This is being done by introducing imaginary time for motion in classically inaccessible regions. An appropriate language for these trajectory studies is the Feynman path-integral formulation of quantum mechanics [Feynman and Hibbs 1965; Feynman 1972], where the probability amplitude of the transition equals the path integral over all the ways connecting the initial and final states.

This review largely follows the above reduction scheme. In section 2 we discuss the main peculiarities of tunneling reactions, as compared to thermally activated ones. The most salient theoretical conclusions are given without derivation. The next three sections pursue the pedagogical task and systematically deal with the theoretical imaginary-time path-integral approach. In section 6 some illuminating experimental results are selected in order to illustrate the previous discussion. The reader who is not interested in the details of the theory may skip sections 3–5, because the conclusions that are necessary for understanding the last section are presented in section 2.

2. From thermal activation to tunneling

2.1. Cross-over temperature

Although the inadequacy of the one-dimensional model [Goldanskii 1959, 1979] is well by now understood, we start with discussing the simplest one-dimensional version of the theory, since it

will permit us to elucidate some important features of tunneling reactions inherent in more realistic approaches. The one-dimensional model relies on the following assumptions:

(i) the reaction coordinate is selected from the total set of PES coordinates;

(ii) the energy spectra of reactants and products are continuous;

(iii) the thermal equilibrium is maintained in the course of the transition;

(iv) tunneling and over-barrier transitions proceed along the same coordinate.

Assumptions (i)–(iii) form, according to Wigner, the basis of CLTST; in a sense, the one-dimensional model straightforwardly extends the CLTST to the subbarrier energy region. These assumptions necessitate in particular the validity of condition (1.13).

The rate constant is the statistical average of the reactive flux from the initial to the final state

$$k = Z_0^{-1} \int_0^\infty \mathrm{d}E\, \rho(E) w(E) \exp(-\beta E)\,, \tag{2.1}$$

where $\rho(E)$ is the density of the energy levels in the initial state, $w(E)$ is the barrier transparency at the energy E, and Z_0 is the partition function in the initial state included in (2.1) in order to normalize the flux. In this formula the reader will readily recognize the traditional CLTST expression (see, e.g., Eyring et al. [1983]), in which the transformation from the (P, Q) phase space to the (E, t) variables (where t is the time of motion along the classical trajectory with the energy E) has been carried out,

$$k_{\mathrm{cl}} = Z_0^{-1} \int \mathrm{d}P\, \mathrm{d}Q\, \frac{P}{m} \exp[-\beta E(P, Q)]\, \theta(E - V_0) \delta(Q)\, \theta(P)\,. \tag{2.2}$$

Equation (2.2) defines the statistically averaged flux of particles with energy $E = P^2/2m + V(Q)$ and $P > 0$ across the dividing surface with $Q^{\#} = 0$. The step function $\theta(E - V_0)$ is introduced because the classical passage is possible only at $E > V_0$. In classically forbidden regions, $E < V_0$, the barrier transparency is exponentially small and given by the well known WKB expression (see, e.g., Landau and Lifshitz [1981])

$$\rho(E)\, w(E) = (2\pi\hbar)^{-1} \exp[-2S(E)/\hbar]\,, \tag{2.3}$$

where $S(E)$ is the quasiclassical action in the barrier,

$$S(E) = \int_{Q_1(E)}^{Q_2(E)} \mathrm{d}Q\, [2m(V(Q) - E)]^{1/2}, \tag{2.4}$$

and $Q_1(E)$ and $Q_2(E)$ are the turning points defined by $V(Q_1) = V(Q_2) = E$ (see fig. 3).

After substituting (2.3) and (2.4) for (2.1), the integral can be evaluated with the method of steepest descents. The stationary point $E = E_a$ is given by the equation derived by Miller and George [1972]

$$\hbar\beta = -2\frac{\partial S(E)}{\partial E} = 2 \int_{Q_1(E_a)}^{Q_2(E_a)} \mathrm{d}Q \left(\frac{m}{2[V(Q) - E_a]}\right)^{1/2} = \tau(E_a)\,, \tag{2.5}$$

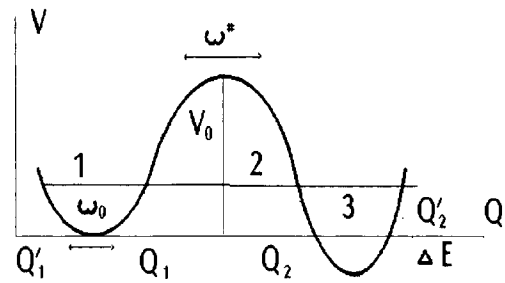

Fig. 3. One-dimensional barrier along the coordinate of an exoergic reaction. $Q_1(E)$, $Q_1'(E)$, $Q_2(E)$, $Q_2'(E)$ are the turning points, ω_0 and ω^* initial well and upside-down barrier frequencies, V_0 the barrier height, $-\Delta E$ the reaction heat. Classically accessible regions are 1, 3, tunneling region 2.

where $\tau(E_a)$ is the period of vibrations of a classical particle at energy E_a in the inverse barrier. Finally, (2.1) reduces to

$$k = k_0 \exp[-2S(E_a)/\hbar] \exp(-\beta E_a) , \tag{2.6}$$

where the prefactor is given by

$$k_0 = Z_0^{-1}(2\pi\hbar)^{-1}\left(\frac{\pi}{|\partial^2 S/\partial E^2|_{E=E_a}}\right)^{1/2} , \qquad \frac{2\partial^2 S}{\partial E^2} = \frac{\partial \tau}{\partial E} = \left(\frac{\partial^2[2S(E) + \beta\hbar E]}{\partial(\hbar\beta)^2}\right)^{-1} . \tag{2.7}$$

According to (2.6), when the temperature is decreased, both the apparent activation energy E_a and the apparent prefactor $k_a = k_0 \exp[-2S(E_a)/\hbar]$ decrease. The rate constant k given by (2.6) goes to a finite value k_c at $T \to 0$ when $E_a = 0$, while $\tau(E_a)$ goes to infinity. When the temperature grows, the period τ decreases. It is evident, though, that it cannot be smaller than $2\pi/\omega^{\#}$, where

$$\omega^{\#} = [m^{-1} \mathrm{d}^2 V(Q)/\mathrm{d}Q^2]^{1/2} . \tag{2.8}$$

This means that there is a cross-over temperature defined by (1.7) at which tunneling "switches off", because the quasiclassical trajectories that give the extremum to the integrand in (2.1) cease to exist. This change in the character of the semiclassical motion is universal for barriers of arbitrary shape.

The relative contribution of over-barrier ($E > V_0$) transitions and tunneling ($E < V_0$) to the integral (2.1) is governed by the dimensionless parameter

$$\xi = \delta_T/\delta_0 = (2k_B T/\hbar\omega^{\#})^{1/2} , \qquad \delta_T^2 = k_B T/m\omega^{\#2} , \quad \delta_0^2 = \hbar/2m\omega^{\#} \tag{2.9}$$

where δ_T is the amplitude of thermal vibrations and δ_0 is the zero-point amplitude for the upside-down barrier. When $\xi \gg 1$, the thermal vibration amplitude prevails over δ_0, and thermal fluctuations result in Arrhenius behavior with the activation energy equal to the barrier height. When $\xi \ll 1$, the thermal fluctuations are small, and $k(T)$ approaches the low-temperature limit k_c with $E_a = 0$. At intermediate values of $\xi \sim 1$ the major contribution to the integral (2.1) comes from an energy in the range $0 < E < V_0$ and tunneling occurs from thermally activated energy levels.

Of special interest is the case of parabolic barrier (1.5) for which the cross-over between the classical and quantum regimes can be studied in detail. Note that the above derivation does not hold in this case because the integrand in (2.1) has no stationary points. Using the exact formula for the parabolic barrier transparency [Landau and Lifshitz 1981],

$$w(E) = \{1 + \exp[(2\pi/\hbar\omega^{\#})(V_0 - E)]\}^{-1} , \tag{2.10}$$

which holds above the barrier as well as below it, and taking the integral (2.1) with infinite limits, one finds

$$k = Z_0^{-1}(2\pi\hbar\beta)^{-1}\,[\tfrac{1}{2}\hbar\beta\omega^{\#}/\sin(\tfrac{1}{2}\hbar\beta\omega^{\#})]\exp(-\beta V_0) . \tag{2.11}$$

When $\frac{1}{2}\hbar\beta\omega^{\#} \ll 1$, we recover the basic CLTST relation,

$$k(T) = Z_0^{-1}(k_B T/2\pi\hbar)\exp(-\beta V_0) . \tag{2.12}$$

In the harmonic approximation for the initial state,

$$Z_0^{-1} = 2\sinh(\tfrac{1}{2}\hbar\beta\omega_0) , \tag{2.13}$$

and at $\frac{1}{2}\hbar\beta\omega_0 \ll 1$ we arrive at the classical limit of the rate constant,

$$k_{cl}(T) = (\omega_0/2\pi)\exp(-\beta V_0) . \tag{2.14}$$

Expression (2.11) has been derived by Wigner [1932], who pointed out that the factor

$$f = \tfrac{1}{2}\hbar\beta\omega^{\#}/\sin(\tfrac{1}{2}\hbar\beta\omega^{\#}) \tag{2.15}$$

modifying CLST, corresponds to quantum corrections. Equation (1.4) follows from (2.11) when expanding the sine to third order in $\frac{1}{2}\hbar\beta\omega^{\#}$. The prefactor in (2.11) diverges at the cross-over temperature (1.7). This artefact occurs because the parabolic approximation is acceptable only near the top of the barrier, and at $T \ll T_c$, when the particle explores the bottom of the well, this approximation does not suffice. For this reason the Eckart barrier has been used by Goldanskii [1959] instead of a parabolic one, and the role of the zero-point vibrations at $T \ll T_c$ has been noted. Since the harmonic oscillator period is independent of energy, $\partial\tau/\partial E = 0$ for a parabolic barrier, and eq. (2.5) has no solution. Thus at $T < T_c$ the apparent activation energy falls abruptly until it reaches the region where the potential is no longer parabolic.

Figure 4 demonstrates that in order to variationally describe a realistic barrier shape (Eckart potential) by an effective parabolic one, the frequency of the latter, ω_{eff}, should drop with decreasing temperature. At high temperatures, $T > T_c$, transitions near the barrier top dominate, and the parabolic approximation with $\omega_{eff} = \omega^{\#}$ is accurate.

Let us now turn to the case $T \to 0$. First of all, somewhat suspicious is the combination of the continuous integral (2.1) with the discrete partition function Z_0 (2.13), usual for CLTST. This serious deficiency cannot be circumvented in the framework of this CLTST-based formalism, and a more rigorous reasoning is needed to describe the quantum situation. Introduction of adequate methods will be the objective of the next sections devoted to the path-integral formalism, so here we

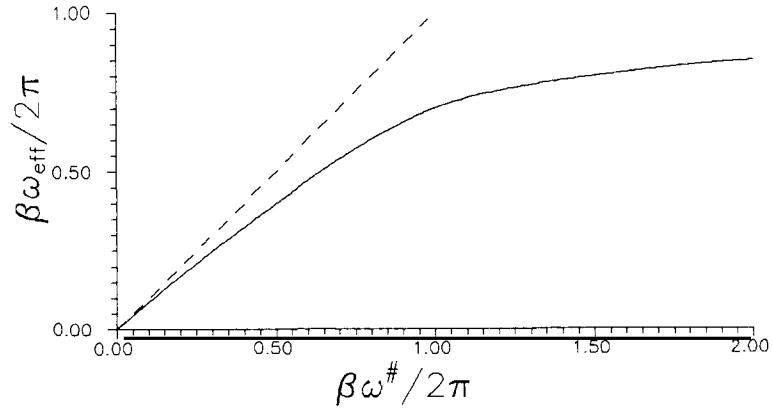

Fig. 4. Variationally determined effective parabolic barrier frequency $\omega^{\#}_{eff}$ for the Eckart barrier in units of $2\pi/\hbar\beta$ [Voth et al. 1989b]. The dotted line is the high-temperature limit $\omega^{\#}_{eff} = \omega^{\#}$.

just note that, fortunately, eqs. (2.6) and (2.7), combined with (2.13) still turn out to be correct in the quasiclassical sense [Waxman and Leggett 1985; Hanggi and Hontscha 1988, 1991].

In order for the prefactor in (2.6) to be finite, the exponential increase in Z_0^{-1} should be compensated by a decrease in $|\partial\tau/\partial E|^{-1/2}$. As shown in appendix A, for β satisfying (2.5) at $\beta \to \infty$ the following equation holds:

$$-\hbar\,\partial\beta/\partial E = -\partial\tau/\partial E = 1/\omega_0 E\,. \tag{2.16}$$

The formal solution of this equation is

$$E = E_0 \exp(-\beta\omega_0)\,, \tag{2.17}$$

where E_0 is the characteristic energy which depends on the barrier shape and is of the order of V_0. When substituting (2.16) and (2.17) in (2.6), the exponents $\exp(\pm\frac{1}{2}\beta\omega_0)$ cancel out in the prefactor and k_c takes the form

$$k_c = (\omega_0/2\pi)(2\pi E_0/\hbar\omega_0)^{1/2}\exp(-2S_0/\hbar)\,, \tag{2.18}$$

where S_0 is the action $S(E)$ (2.4) at $E = 0$. The square root in (2.18) is responsible for the zero-point vibrations in the initial well and is of the order of $(S_0/\hbar)^{1/2}$.

Exploration of the region $0 < T < T_c$ requires numerical calculations using eqs. (2.5)–(2.7). Since the change in k_0 is small compared to that in the leading exponential term [cf. (2.14) and (2.18)], the Arrhenius plot $k(\beta)$ is often drawn simply by setting $k_0 = \omega_0/2\pi$ (fig. 5). Typical behavior of the prefactor k_a and activation energy E_a versus temperature is presented in fig. 6. The narrow intermediate region between the Arrhenius behavior and the low-temperature limit has width

$$\Delta T/T_c \simeq k_B T_c/V_0\,. \tag{2.19}$$

The above discussion concerning eq. (2.1) implied that tunneling transitions were incoherent and characterized by a rate constant. This is predetermined by assumption (ii) mentioned at the

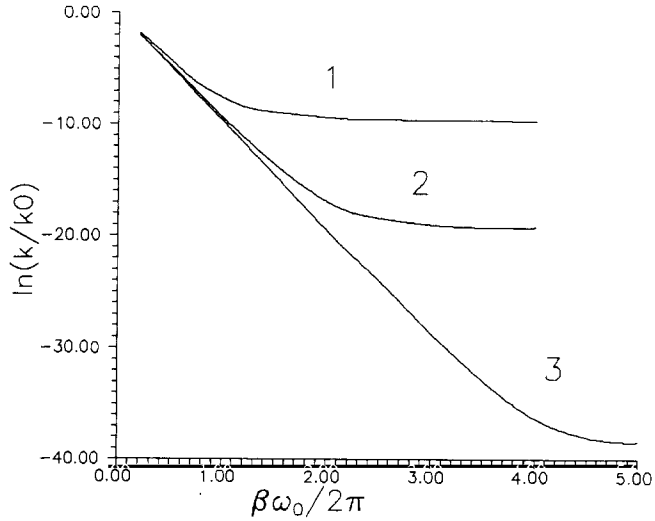

Fig. 5. Arrhenius plot of $k(T)$ for one-dimensional barrier with $\omega^*/\omega_0 = 1, 0.5, 0.25$ for the curves 1–3, respectively; $2\pi V_0/\hbar\omega_0 = 10$, prefactor is taken constant.

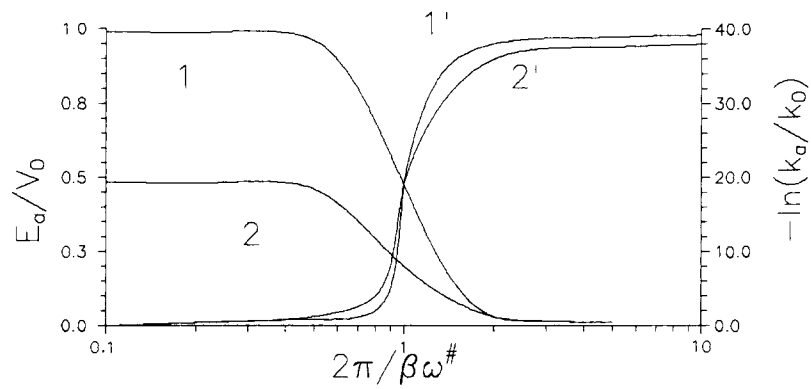

Fig. 6. Apparent activation energy (1, 2) and logarithm of apparent prefactor $\ln k_a$ (1′, 2′) versus temperature. The value $2\pi V_0/\hbar\omega^*$ is taken 40 and 20 for the curves 1, 1′ and 2, 2′, respectively.

beginning of this section. Studying the spectral manifestations of tunneling requires giving up this assumption. In a symmetric double well tunneling results in the splitting of each energy level of a bound state, semiclassically given by

$$\hbar\Delta = [\hbar\omega(E)/\pi] \exp[-S(E)/\hbar] , \tag{2.20}$$

where E is the eigenenergy in the isolated well. This splitting shows up as a doublet of spectral lines, for example, in neutron scattering spectroscopy or optical spectroscopy of high resolution. With increasing temperature these lines are broadened and tend to collapse onto one central line. This central line is observed only at high temperatures, and its width is determined by incoherent thermally activated hopping between the wells. So there should be a characteristic temperature at

the boundary between the two different regimes: incoherent hopping and coherent probability oscillations between the wells. The former is characterized by the rate constant k with Arrhenius behaviour (2.14), while the latter by the oscillation frequency Δ.

Although, strictly speaking, these two quantities are incomparable, one may suggest the following spectral criterion. The doublet disappears when the thermal hopping fully "smears out" the two spectral lines, i.e., $\Delta = k$. The temperature T^* at which this happens comes directly from $\exp(-S/\hbar) = \exp(-V_0/k_B T^*)$. If we compare T^* with T_c given by (1.6), we see that T^* is twice T_c. This reflects the difference between the incoherent tunneling transition, whose rate is proportional to $\exp(-2S/\hbar)$, and oscillations with frequency proportional to $\exp(-S/\hbar)$. In the one-dimensional model at hand, the mechanism of destruction of coherence is connected with the interference of amplitudes in the continuous energy spectrum above the barrier. Interaction with the reservoir provides a more efficient mechanism for this destruction, and it will be considered in section 2.3.

The previous treatment applies to exoergic chemical reactions (with positive energy difference between the minima of the initial and final states $\Delta E = E_1^0 - E_2^0 > 0$). For endoergic reactions ($\Delta E < 0$) the lower bound on the integral (2.1) should be replaced by $-\Delta E$, since tunneling is possible only at $E \geq -\Delta E$. When $T < T_c$, the apparent activation energy of endoergic reactions approaches its low-temperature limit equal to $-\Delta E < V_0$. The Arrhenius plot consists of two nearly straight lines corresponding with the activation energies V_0 and $-\Delta E$ at $T > T_c$ and $T < T_c$, respectively.

2.2. Tunneling and dissipation

The classical motion of a particle interacting with its environment can be phenomenologically described by the Langevin equation

$$m\,\mathrm{d}^2Q/\mathrm{d}t^2 + \eta\dot{Q}(t) + \partial V(Q)/\partial Q = f(t)\,, \tag{2.21}$$

where $f(t)$ is a Gaussian random force. The most remarkable advance in analysing chemical transitions governed by (2.21) lies in the idea that the effect of friction is equivalent to that of linear coupling to a bath of harmonic oscillators (see, e.g., Hanggi et al. [1990], Dekker [1991]). The bath is characterized by its spectral density

$$J(\omega) = \tfrac{1}{2}\pi \sum m_j^{-1}\omega_j^{-1} C_j^2 \delta(\omega - \omega_j)\,, \tag{2.22}$$

where C_j is the parameter of coupling to the oscillator with frequency ω_j. No information is actually available about the coupling constants in molecular crystals, and introduction of the integral characteristic $J(\omega)$ is a phenomenological way to account for environment effects. In order to obtain (2.21) one has to choose

$$J(\omega) = \eta\omega\,. \tag{2.23}$$

Other spectral densities correspond to memory effects in the generalized Langevin equation, which will be considered in section 5. It is the equivalence between the friction force and the influence of the oscillator bath that allows one to extend (2.21) to the quantum region; there the friction coefficient η and $f(t)$ are related by the fluctuation–dissipation theorem (FDT),

$$\int_{-\infty}^{\infty} \mathrm{d}t \langle f(t) f(0) \rangle \exp(\mathrm{i}\omega t) = \eta\hbar\omega \coth(\tfrac{1}{2}\beta\hbar\omega)\,, \tag{2.24}$$

where $\langle f(t)f(0)\rangle$ is the symmetrized correlation function [Chandler 1987]. In the classical limit $f(t)$ is δ-correlated,

$$\langle f(t)f(t')\rangle = 2\beta^{-1}\eta\delta(t-t') . \tag{2.25}$$

As first shown by Caldeira and Leggett [1981], in the tunneling regime friction reduces the transition probability by the factor

$$\exp[-A\eta(\Delta Q)^2/\hbar] , \tag{2.26}$$

where ΔQ is the tunneling distance and A is a factor of order unity depending on the shape of barrier. How friction affects $k(T)$ can be illustrated by a simple example of a cusp-shaped parabolic term depicted in fig. 7. This potential models a strongly exothermic chemical reaction with a sharp descent to the valley of products. The rate constant is proportional to the probability to reach the barrier top $Q = Q^{\#}$, which, in turn, is described by a Gaussian

$$k \propto \exp(-Q^{\#2}/2\delta^2) , \tag{2.27}$$

where the damped harmonic oscillator spread may be found from the FDT,

$$\delta^2(\eta,\beta) = \pi^{-1}m^{-1}\hbar\int_0^\infty d\omega \frac{\eta\omega}{(\omega_0^2-\omega^2)^2+(\eta/m)^2\omega^2}\coth(\tfrac{1}{2}\beta\hbar\omega) . \tag{2.28}$$

This relation may be interpreted as the mean-square amplitude of a quantum harmonic oscillator $\delta^2(\omega) = (2m\omega)^{-1}\hbar\coth(\frac{1}{2}\beta\hbar\omega)$ averaged over the Lorentzian distribution of the system's normal modes. In the absence of friction (2.27) describes thermally activated as well as tunneling processes when $\frac{1}{2}\beta\hbar\omega_0 < 1$, or $\frac{1}{2}\beta\hbar\omega_0 > 1$, respectively. At first glance it may seem surprising that the same formula holds true for the damped oscillator. This statement, borne out in the work of Grabert et al. [1984a], can be explained by the aforementioned averaging. The

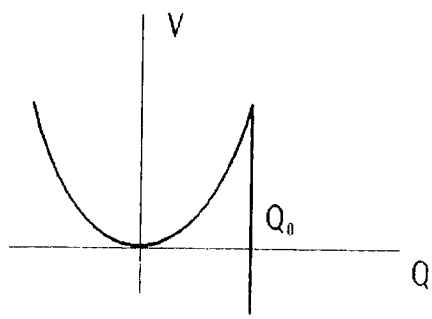

Fig. 7. Cusp-shaped potential, made up of parabola and a vertical wall.

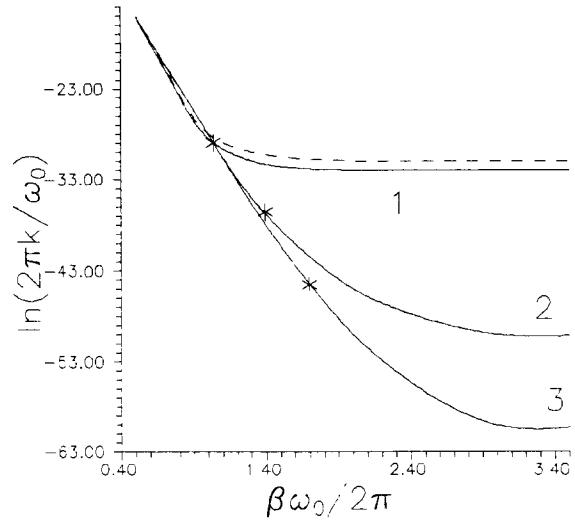

Fig. 8. Arrhenius plot of dissipative tunneling rate in a cubic potential with $V_0 = 5\hbar\omega_0$ and $\eta/2\omega^{\#} = 0$, 0.25 and 0.5 for curves 1–3, respectively. The cross-over temperatures are indicated by asterisks. The dashed line shows $k(T)$ for the parabolic barrier with the same $\omega^{\#}$ and V_0.

asymptotic expressions for δ^2 are

$$\delta^2 = \begin{cases} k_B T/m\omega_0^2 , & k_B T \gg \hbar\omega_0 \\ \hbar(2m\omega_0)^{-1}(1 - \eta/\pi m\omega_0) , & T = 0, \quad \eta/m \ll \omega_0 \\ 2\hbar(\pi\eta)^{-1} \ln(\eta/m\omega_0) , & T = 0, \quad \eta/m \gg \omega_0 \end{cases} \tag{2.29}$$

According to (2.29), dissipation reduces the spread of the harmonic oscillator making it smaller than the quantum uncertainty of the position of the undamped oscillator (de Broglie wavelength). Within exponential accuracy (2.27) agrees with the Caldeira–Leggett formula (2.26), and similar expressions may be obtained for more realistic potentials.

A few comments on (2.27), (2.29), (1.11) and (1.12) are in order. The activation energy in the Arrhenius region is independent of η, since friction changes only the velocity at which a classical particle crosses the barrier and thus affects the prefactor. Friction reduces k_c along with T_c thereby widening the Arrhenius region. Dissipation visibly affects the $k(T)$ dependence when η is strong enough, namely when η/m is comparable to, or greater than $\omega^{\#}$. The function $k(T)$ at various friction coefficients calculated from the data [Grabert et al. 1987] is shown in fig. 8.

Friction also changes the way $k(\beta)$ approaches its low-temperature limit and widens the intermediate region between the two asymptotes of $k(\beta)$. At temperatures far below the cross-over point $k(T)$ behaves as

$$k(T) = k(0)\exp[A(T)] , \quad A(T) \propto T^n , \tag{2.30}$$

where n depends on the spectrum of the bath. In particular, for the frequency-independent friction (2.23) $n = 2$, for the deformation potential model (defects in a 3D crystal lattice with Debye phonon spectrum) $J(\omega) \propto \omega^3$, $n = 4$, while in the absence of friction $A(T) \propto \exp(-\hbar\omega_0/k_B T)$.

Thus far we have discussed the direct mechanism of dissipation, when the reaction coordinate is coupled directly to the continuous spectrum of the bath degrees of freedom. For chemical reactions this situation is rather rare, since low-frequency acoustic phonon modes have much larger wavelengths than the size of the reaction complex, and so they cannot cause a considerable relative displacement of the reactants. The direct mechanism may play an essential role in long-distance electron transfer in dielectric media, when the reorganization energy is created by displacement of equilibrium positions of low-frequency polarization phonons. Another cause of friction may be anharmonicity of solids which leads to multiphonon processes. In particular, the Raman processes may provide small energy losses.

More pertinent to the present topic is the indirect dissipation mechanism, when the reaction coordinate is coupled to one or several active modes which characterize the reaction complex and, in turn, are damped because of coupling to a continuous bath. The total effect of the active oscillators and bath may be represented by the effective spectral density $J_{\text{eff}}(\omega)$. For instance, in the case of one harmonic active oscillator with frequency ω_1, mass m_1 and friction coefficient η, $J_{\text{eff}}(\omega)$ is proportional to the imaginary part of its susceptibility and equals [Garg et al. 1985]

$$J_{\text{eff}}(\omega) = m_1\omega_1^4\chi''(\omega) = \eta\omega\omega_1^4[(\omega_1^2 - \omega^2)^2 + (\eta/m)^2\omega^2]^{-1} . \tag{2.31}$$

Since the susceptibilities can be extracted from the optical spectra of these active modes, a quantitative description based on dissipative tunneling techniques can be developed. Such a program should include the analysis of the motion of the reaction complex PES, with the dissipation of active modes taken into account. The advantage of this procedure is that it would allow one to confine the number of PES degrees of freedom to the relevant modes, and incorporate the environment phenomenologically.

2.3. Coherent versus incoherent tunneling

Aside from merely calculational difficulties, the existence of a low-temperature rate-constant limit poses a conceptual problem. In fact, one may question the actual meaning of the rate constant at $T = 0$, when the TST conditions listed above are not fulfilled. If the potential has a double-well shape, then quantum mechanics predicts coherent oscillations of probability between the wells, rather than the exponential decay towards equilibrium. These oscillations are associated with tunneling splitting measured spectroscopically, not with a chemical conversion. Therefore, a simple one-dimensional system has no rate constant at $T = 0$, unless it is a metastable potential without a bound final state. In practice, however, there are exchange chemical reactions, characterized by symmetric, or nearly symmetric double-well potentials, in which the rate constant is measured. To account for this, one has to admit the existence of some external mechanism whose role is to destroy the phase coherence. It is here that the need to introduce a heat bath arises.

In this section we shall consider in some detail the mechanism of coherence breakdown due to the bath, in order to clarify the physical assumptions which underlie the concept of rate constant at low temperatures. The particular tunneling model we choose is the two-level system (TLS) with the Hamiltonian

$$\hat{H}_0 = \tfrac{1}{2}\hbar\Delta_0\sigma_x + \tfrac{1}{2}\hbar\varepsilon\sigma_z , \tag{2.32}$$

where σ_x and σ_z are the Pauli matrices, $\frac{1}{2}\hbar\Delta_0$ is the "tunneling matrix element", and $\hbar\varepsilon$ is the energy "bias" between the two wells. The Hamiltonian (2.32) includes only the lowest energy doublet of the

actual double well. Given a double well, one is able to approximate it by a TLS (2.32) when $\varepsilon \ll \omega_0$, $\Delta_0 \ll \omega_0$, and, moreover, the temperature is so low that the higher energy levels are not populated, i.e., $k_B T \ll \hbar\omega_0$.

The most complicated case is of no asymmetry, i.e., $\varepsilon = 0$, and it is specially this problem that we shall investigate. At $\varepsilon = 0$ the system, described by H_0, has two energy levels $E_\pm = \mp \frac{1}{2}\hbar\Delta_0$. If the particle is initially put into the left well, the amplitudes of the particle being in the left and right wells oscillate, respectively, as

$$c_L(t) = \cos(\tfrac{1}{2}\Delta_0 t) , \qquad c_R = \sin(\tfrac{1}{2}\Delta_0 t) , \tag{2.33}$$

and the probability of the particle being in the left well equals

$$P_L(t) = |c_L|^2 = [1 + \cos(\Delta_0 t)]/2 . \tag{2.34}$$

The simplest scheme that accounts for the destruction of phase coherence is the so-called "stochastic interruption" model [Nikitin and Korst 1965; Simonius 1978; Silbey and Harris 1989]. Suppose the process of free tunneling is interrupted by a sequence of "collisions" separated by time periods $\nu_0^{-1} = t_0 \ll \Delta_0^{-1}$. After each collision the system "forgets" its initial phase, i.e., the off-diagonal matrix elements of the density matrix ρ go to zero, resulting in the density matrix ρ':

$$\rho = \begin{pmatrix} |c_L|^2 & c_L c_R^* \\ c_R c_L^* & |c_R|^2 \end{pmatrix} , \qquad \rho' = \begin{pmatrix} |c_L|^2 & 0 \\ 0 & |c_R|^2 \end{pmatrix} . \tag{2.35a, b}$$

The density matrix ρ describes the pure state, as seen from the equality $\rho^2 = \rho$, while ρ' does not. The transition from (2.35a) to (2.35b) describes a "strong collision", which fully localizes the particle, but in general the off-diagonal elements may not completely vanish. This however does not affect the qualitative picture.

After each strong collision the system, having been localised in the left or right well, resumes free tunneling from the diagonal state. Thus, after N collisions the probability to survive in the left well is

$$P_L(t) = [\cos^2(\tfrac{1}{2}\Delta_0 t_0)]^N \simeq [1 - \tfrac{1}{8}(\Delta_0 t_0)^2]^{2N} \simeq \exp(-\tfrac{1}{4}\Delta_0^2 t_0 t) , \tag{2.36}$$

where $t = Nt_0$. Therefore, the rate constant is

$$k = \Delta_0^2/4\nu_0 . \tag{2.37}$$

This simple gas-phase model confirms that the rate constant is proportional to the square of the tunneling matrix element divided by some characteristic bath frequency. Now, in order to put more concretness into this model and make it more realistic, we specify the total (TLS and bath) Hamiltonian

$$\hat{H} = \hat{H}_0 + \hat{H}_b + \hat{H}_{int} , \quad \hat{H}_{int} = \hat{f}\sigma_z \tag{2.38}$$

where $\hat{H}_b$ is the free bath Hamiltonian and $\hat{f}$ acts on the bath variables only. The environment, as it were, "observes" whether the particle is on the right or on the left, through the interaction $\hat{f}\sigma_z$, thus destroying the interference between the two eigenstates of the matrix σ_z.

Of particular interest is the model of a bath as a set of harmonic oscillators q_j with frequencies ω_j, which are linearly coupled to the tunneling coordinate

$$\hat{H}_b = \sum p_j^2/2m_j + \tfrac{1}{2} m_j \omega_j^2 q_j^2 \ , \quad \hat{f} = \sum C_j Q_0 q_j \ , \tag{2.39}$$

where $2Q_0$ is the interwell distance. The quantity $Q = Q_0\sigma_z$ is nothing but the particle's coordinate, which, in the present approximation, takes two values, $\pm Q_0$. The bath is characterized by its spectral function $J(\omega)$ (2.22), which is proportional to the mean square of force acting on a particle from oscillators with frequency ω, and it is related with the phonon density $\rho(\omega)$ by

$$J(\omega) = \tfrac{1}{2}\pi C^2(\omega)\rho(\omega)/m\omega \ . \tag{2.40}$$

This model, called the spin-boson Hamiltonian, is probably the only fully manageable problem of this kind (with the possible exception of some very artificial problems) with a transparent solution.

The equation of motion for the expectation $\langle\sigma_z\rangle$ in the weak-coupling limit has a Langevin-like form

$$\mathrm{d}^2\langle\sigma_z\rangle/\mathrm{d}t^2 + \eta_{\mathrm{TLS}}\,\mathrm{d}\langle\sigma_z\rangle/\mathrm{d}t + \Delta_0^2\langle\sigma_z\rangle = 0 \ , \tag{2.41}$$

where the damping coefficient is determined by the spectral density at $\omega = \Delta_0$ [Silbey and Harris 1983],

$$\eta_{\mathrm{TLS}} = \hbar^{-1}\pi Q_0^2 \coth(\tfrac{1}{2}\beta\hbar\Delta_0)\sum C_j^2\,\delta(\omega_j - \Delta_0)/m_j\omega_j = 2\hbar^{-1}Q_0^2 J(\Delta_0)\coth(\tfrac{1}{2}\beta\hbar\Delta_0) \tag{2.42}$$

This damping coefficient η_{TLS} is nothing but the rate constant of transitions between the energy levels of the doublet, and it may be represented as

$$\eta_{\mathrm{TLS}} = k_\uparrow + k_\downarrow \ , \tag{2.43}$$

where $k_\uparrow$ is the probability (per unit time) to escape from the lower energy level to the upper one, and $k_\downarrow$ is the probability of the reverse transition. The explicit form for $k_\uparrow$ and $k_\downarrow$ is the golden rule,

$$\begin{aligned} k_\uparrow &= 2\pi\hbar^{-1}\sum_j\sum_{n=1}^{\infty} |\langle n-1|C_jQ_0q_j|n\rangle|^2\,\delta(\hbar\Delta_0 - \hbar\omega_j)Z_j^{-1}\exp[-\beta\hbar\omega_j(n+\tfrac{1}{2})] \\ &= 2\hbar^{-1}Q_0^2 J(\Delta_0)[\exp(\beta\hbar\Delta_0) - 1]^{-1} \end{aligned} \tag{2.44}$$

where Z_j is the partition function of jth oscillator. From the detailed balance condition we have

$$k_\downarrow = \exp(\beta\hbar\Delta_0)\,k_\uparrow \ . \tag{2.45}$$

As required by the energy-conservation law reflected by the δ-function in (2.44), each intradoublet transition is accompanied by emission or absorption of a phonon with energy $\hbar\Delta_0$.

Equation (2.41) describes either damped oscillations (at $\eta_{\mathrm{TLS}} < 2\Delta_0$) or exponential relaxation ($\eta_{\mathrm{TLS}} > 2\Delta_0$). Since η_{TLS} grows with increasing temperature, there may be a cross-over between these two regimes at β^* such that $2\hbar^{-1}Q_0^2 J(\Delta_0)\coth(\tfrac{1}{2}\beta^*\hbar\Delta_0) = 2\Delta_0$. If the friction coefficient

exceeds by far $2\Delta_0$,*) the long-time behavior of the solution to (2.41) is determined by the exponent $\exp(-\Delta_0^2 t/\eta_{\mathrm{TLS}})$. That is, the rate constant equals

$$k = \Delta_0^2/\eta_{\mathrm{TLS}} \,. \tag{2.46}$$

Expression (2.46) has the same form as (2.37) if we define the collision frequency as $\nu_0 = \frac{1}{4}\eta_{\mathrm{TLS}}$. Both these formulae can be expressed in the golden-rule form [cf. eq. (1.14)],

$$k = 2\pi\hbar(\Delta_0/2)^2\rho_{\mathrm{f}} \,, \quad \rho_{\mathrm{f}} = 2/\pi\hbar\eta_{\mathrm{TLS}} = 1/2\pi\hbar\nu_0 \,, \tag{2.47a, b}$$

where ρ_{f}, the density of final states, was set equal to the expression (2.47b).

The identities in (2.47b) are very illuminating. The first of them indicates that the coupling to the bath broadens the energy levels of the TLS leading to a density of states inversely proportional to the damping coefficient. The second shows that the mean level spacing of the system is formally equal to $2\pi\hbar\nu_0$, where ν_0 is the characteristic bath frequency. Finally, the same result (2.46), (2.47a, b) obtains if one formally supposes that the energy level in the right well (in the original basis, before the Hamiltonian was diagonalized), has an imaginary part $\mathrm{i}\frac{1}{2}\Gamma = \mathrm{i}\frac{1}{2}\eta_{\mathrm{TLS}}$ [Rom et al. 1991]. Such an imaginary part may be interpreted as caused by a process removing the products from the final state. If the width of the energy level associated with this process exceeds the tunneling splitting Δ, the tunneling becomes irreversible.

The solution of the spin-boson problem with arbitrary coupling has been discussed in detail by Leggett et al. [1987]. The displacement of the equilibrium positions of the bath oscillators in the transition results in the effective renormalization of the tunneling matrix element by the bath overlap integral

$$\Delta_{\mathrm{eff}} = \Delta_0 \exp(-\tfrac{1}{2}\Phi_0) \,, \quad \Phi_0 = 2\sum Q_0^2 C_j^2 \hbar^{-1} m_j^{-1} \omega_j^{-3} = 4Q_0^2(\pi\hbar)^{-1} \int_0^\infty \mathrm{d}\omega\, \omega^{-2} J(\omega) \,, \tag{2.48}$$

whereas the quantity $\exp(-\Phi_0)$ is nothing but the bath Franck–Condon factor. This relation expresses the fact that oscillators cause a dynamical asymmetry of the initial and final states, and tunneling occurs only when a bath fluctuation symmetrizes the potential.

We just quote the main results of [Leggett et al. 1987], which cover most of the possible situations. The spectral density is taken in the form

$$J(\omega) \propto \omega^n \xi(\omega/\omega_{\mathrm{c}}) \,, \tag{2.49}$$

where ξ is the cutoff function which equals unity at $\omega \ll \omega_{\mathrm{c}}$ and vanishes at $\omega \gg \omega_{\mathrm{c}}$ [e.g., $\xi = \exp(-\omega/\omega_{\mathrm{c}})$]. The cutoff frequency is supposed to be greater than both the bare tunneling splitting and thermal energy, $\Delta_0 \ll \omega_{\mathrm{c}}$, $k_{\mathrm{B}}T \ll \hbar\omega_{\mathrm{c}}$. The case $n = 1$ [cf. eq. (2.23)] is referred to as ohmic, $n < 1$ subohmic and $n > 1$ superohmic dissipation. The distinction between these cases is due to different lobes of low-frequency vibrations in $J(\omega)$, which is evident from the divergence of Φ_0 at $n \leq 1$.

* Our conclusions about the case of large η_{TLS} have a rather speculative character, and pursue merely an illustrative goal, since (2.41) and (2.42) are obtained in the weak-coupling limit.

Coupling to these low-frequency modes (at $n < 1$) results in localization of the particle in one of the wells (symmetry breaking) at $T = 0$. This case, requiring special care, is of little importance for chemical systems. In the superohmic case at $T = 0$ the system reveals weakly damped coherent oscillations characterised by the damping coefficient η_{TLS} from (2.42) but with Δ_0 replaced by Δ_{eff}. If $1 < n < 2$, then there is a cross-over from oscillations to exponential decay, in accordance with our weak-coupling predictions. In the subohmic case the system is completely localized in one of the wells at $T = 0$ and it exhibits exponential relaxation with the rate $\ln k \propto -(\hbar\omega_c/k_B T)^{1-n}$.

The ohmic case is the most complex. A particular result is that the system is localised in one of the wells at $T = 0$, for sufficiently strong friction, viz. $\eta > \pi\hbar/2Q_0^2$. At higher temperatures there is an exponential relaxation with the rate $\ln k \propto (4\eta Q_0^2/\pi\hbar - 1)\ln T$. Of special interest is the special case $\eta = \pi\hbar/4Q_0^2$. It turns out that the system exhibits exponential decay with a rate constant which does not depend at all on temperature, and equals $k = \pi\Delta_0^2/2\omega_c$. Comparing this with (2.37), one sees that the "collision frequency" turns out to be precisely equal to the cutoff vibration frequency $\nu_0 = \omega_c/2\pi$.

In the biased case coherent oscillations are completely suppressed by the bath when the bias ε is large enough compared to the renormalized tunneling splitting, $\varepsilon > \Delta_{\mathrm{eff}}$. It therefore may be concluded that the increase in both temperature and asymmetry results in a shift from coherent to incoherent behavior. The low-temperature limit of the rate constant, k_c, has meaning mostly for biased systems. The needed asymmetry, though, is actually very small, smaller than the level spacing $\hbar\omega_0$, and it is this circumstance that permits one to study exchange reactions, like strongly exoergic reactions, with the golden rule approach.

Note in passing that the common model in the theory of diffusion of impurities in 3D Debye crystals is the so-called deformational potential approximation with $C(\omega) \propto \omega, \rho(\omega) \propto \omega^2$ and $J(\omega) \propto \omega^3$, which, for a strictly symmetric potential, displays weakly damped oscillations and does not have a well defined rate constant. If the system permits definition of the rate constant at $T = 0$, the latter is proportional to the square of the tunneling matrix element times the Franck–Condon factor, whereas accurate determination of the prefactor requires specifying the particular spectrum of the bath.

The coherent tunneling case is experimentally dealt with in spectroscopic studies. For example, the neutron-scattering structure factor determining the spectral line shape is

$$S(\boldsymbol{k}, \omega) = \cos^2(\boldsymbol{k}\cdot\boldsymbol{Q}_0)\,\delta(\omega) + \pi^{-1}\sin^2(\boldsymbol{k}\cdot\boldsymbol{Q}_0)\,[1 + \exp(\beta\hbar\omega)]^{-1}$$

$$\times \int_{-\infty}^{\infty} \mathrm{d}t \exp(\mathrm{i}\omega t)\, C(t)\,, \tag{2.50}$$

where $\boldsymbol{k}$ is the wavevector, $\hbar\omega$ the absorbed energy; the displacement of the scatterer is represented as $\boldsymbol{Q} = \boldsymbol{Q}_0\sigma_z$. The function $C(t)$ is the symmetrized correlator,

$$C(t) = \tfrac{1}{2}\langle\sigma_z(0)\sigma_z(t) + \sigma_z(t)\sigma_z(0)\rangle\,. \tag{2.51}$$

The δ-part in (2.50) is responsible for elastic scattering, while the second term, proportional to the Fourier transform of $C(t)$, leads to the gain and loss spectral lines. When the system exercises undamped oscillations with frequency Δ_0, this leads to two delta peaks in the structure factor,

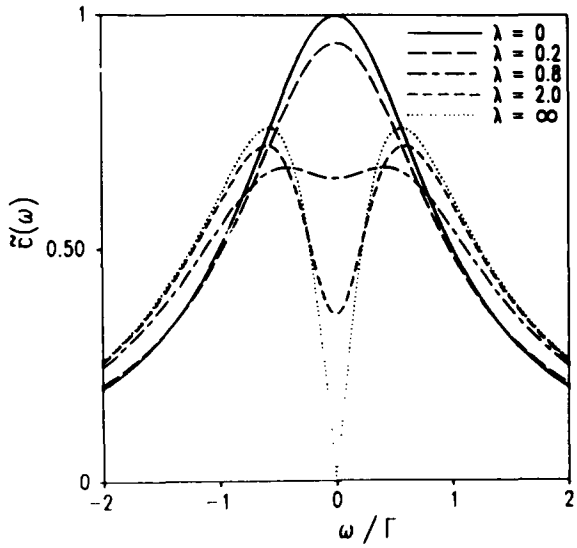

Fig. 9. Spectral line shape for tunneling doublet at different dimensionless temperatures, $\lambda \equiv T/T^*$, as indicated.

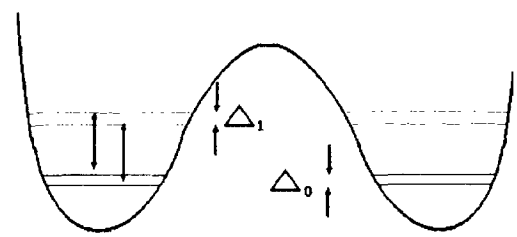

Fig. 10. Energy levels in symmetric double well. Arrows indicate interdoublet transitions induced by vibrations.

placed at $\omega = \pm \Delta_0$. Damping results in broadening of the spectral line. For spectral theory clearly a different object from $\langle \sigma_z(t) \rangle$ is needed, the correlation function [Dattaggupta et al. 1989].

Nevertheless, Leggett et al. [1987] have argued, with some provisos,*) that $\langle \sigma_z(t) \rangle$ [with the initial condition $\sigma_z(0) = 1$] and $C(t)$ may be practically taken the same. If $C(t)$ then obeys the damped oscillator equation (2.41), then the inelastic part of the structure factor has the Lorentzian form with the peaks at $\omega = (\Delta_0^2 - \frac{1}{4}\eta_{\mathrm{TLS}}^2)^{1/2}$ and linewidth $\Gamma = \frac{1}{2}\eta_{\mathrm{TLS}}$. With increasing temperature the peaks come closer to each other, and the lines become broadened. An example of the dependence of the structure factor on ω is given in fig. 9 for the special exactly soluble case of ohmic friction with $\eta = \pi\hbar/4Q_0^2$ [Sasetti and Weiss 1990]. In accord with our predictions, the peaks become indistinguishable, and thus the system fully loses coherence above a certain temperature $T^* = \hbar\Delta_0^2/4k_{\mathrm{B}}\omega_{\mathrm{c}}$.

At temperatures such that $k_{\mathrm{B}}T \simeq \hbar\omega_0$ the two-state approximation breaks down, and the interdoublet dynamics starts to play an essential role in broadening the tunneling splitting spectral line [Parris and Silbey 1985; Dekker 1991]. The energy level scheme for a symmetric double well is presented in fig. 10. In each well we have a vibrational ladder with spacing between the levels $\Delta E \simeq \hbar\omega_0$, and each level is split into a doublet with tunneling splitting $\Delta_n \ll \Delta E$. The contribution of interdoublet transitions into the linewidth may be found with the golden-rule approximation in analogy with (2.44). Namely, in the case of linear coupling the transitions from the ground state $|0\rangle$ to the lth excited doublet $|l\rangle$ with absorption of one phonon are characterized by the overall rate constant

$$\bar{k}_{\uparrow} = \sum_{l \geq 1} k_{\uparrow}(0, l) = 2\hbar^{-1} \sum_{l \geq 1} |\langle 0|Q|l\rangle|^2 J(E_l - E_0)\bar{n}(E_l - E_0)\,, \tag{2.52}$$

*) The long-time behaviour of $\langle \sigma_z(t) \rangle$ may essentially differ from that of $C(t)$, but this affects mostly the form of the spectral line at $\omega \simeq 0$, and seemingly this is immaterial for determining the tunneling splitting [Sasetti and Weiss 1990].

with the mean number of phonons of energy $E_l - E_0$,

$$\bar{n}(E) = [\exp(\beta E) - 1]^{-1} . \tag{2.53}$$

The corresponding level broadening equals half $\bar{k}_\uparrow$. In fact $\bar{k}_\uparrow$ is the diagonal kinetic coefficient characterizing the rate of phonon-assisted escape from the ground state [Ambegaokar 1987]. In harmonic approximation for the well the only nonzero matrix element is that with $l = 1, |\langle 0|Q|l\rangle|^2 = \delta_0^2$, where δ_0 is the zero-point spread of the harmonic oscillator. For an anharmonic potential, other matrix elements contribute to (2.52).

From a comparison between (2.44) and (2.52) one sees that at $T = 0$ only the intradoublet broadening mechanism works. At higher temperatures, $\omega_0^{-1} < \hbar\beta < \Delta_0^{-1}$, the interdoublet contribution provides exponential growth of the linewidths $\propto \exp(-\beta\hbar\omega_0)$. When $\hbar\beta \ll \omega_0^{-1}$, the relative contributions from both mechanisms depend on the spectral density,

$$\bar{k}_\uparrow / k_\uparrow = (\hbar\Delta_0 / 2m\omega_0^2 Q_0^2) J(\omega_0)/J(\Delta_0) . \tag{2.54}$$

The interdoublet transitions may prevail over the intradoublet ones if the spectral density $J(\omega)$ grows with ω faster than ω^2.

The situation drastically changes, when the coupling to the oscillators is symmetric, $C_j f(Q) q_j$, where $f(Q)$ is an even function, or, in the two-state model, when the coupling is proportional to σ_x. In this case the intradoublet matrix elements are identically zero due to symmetry, and, therefore, the intradoublet broadening may appear only in higher orders of perturbation theory, i.e., for multiphonon transitions. Note that the vibrations coupled in this way have the property that they do not contribute to the Franck–Condon factor, because their equilibrium positions are the same in the initial and final states. As we shall see later in subsection 2.5, it is these vibrations that modulate the barrier thereby enhancing tunneling. When the intradoublet transitions are forbidden, the tunneling splitting may be observed even at temperatures close to $k_B T_c \simeq \hbar\omega_0$. This situation is realized, in particular, for tunneling rotations, when the symmetry of the potential is not violated by phonons.

2.4. Vibronic relaxation and electron transfer

Let us return to the nonadiabatic chemical processes. When a PES has been built, a part of the total Hamiltonian may remain unaccounted for, and this part, acting as a perturbation, induces transitions from the initial to the final state. There are several types of such a perturbation, namely: (i) an unaccounted part of the electronic interaction; (ii) non-adiabaticity; (iii) spin–orbit coupling.

The first type of interaction, associated with the overlap of wavefunctions localized at different centers in the initial and final states, determines the electron-transfer rate constant. The other two are crucial for vibronic relaxation of excited electronic states. The rate constant in the first order of the perturbation theory in the unaccounted interaction is described by the statistically averaged Fermi golden-rule formula

$$k = \frac{2\pi}{\hbar} \sum_{i,f} |V_{if}|^2 \exp(-\beta E_i)\, \delta(E_i - E_f) , \tag{2.55}$$

where the matrix element V_{if} equals

$$V_{if} = \langle \psi_i(\boldsymbol{Q}) \psi_i^e(r, \boldsymbol{Q}) | V | \psi_f^e(r, \boldsymbol{Q}) \psi_f(\boldsymbol{Q}) \rangle \tag{2.56}$$

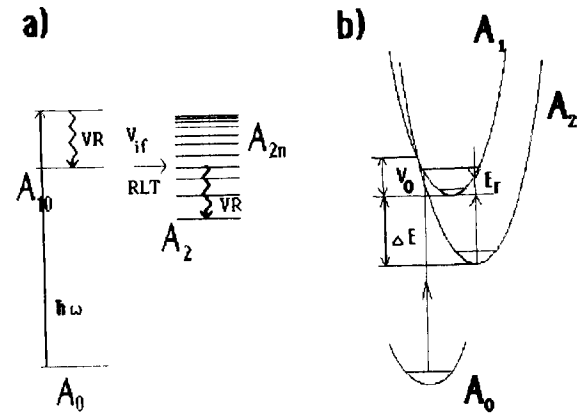

Fig. 11. (a) Diagram of energy levels for a polyatomic molecule. Optical transition occurs from the ground state A_0 to the excited electronic state A_1. A_{2n} are the vibrational sublevels of the optically forbidden electronic state A_2. Arrows indicate vibrational relaxation (VR) in the states A_1 and A_2, and radiationless transition (RLT). (b) Crossing of the terms A_1 and A_2. Reorganization energy E_r is indicated.

and the wave functions are taken in the Born–Oppenheimer approximation as products of electronic (ψ^e) and nuclear functions.

The reactions of electron transfer and vibronic relaxation are ubiquitous in chemistry and many review papers have dealt with them in detail (see, e.g., Ovchinnikov and Ovchinnikova [1982], Ulstrup [1979]), so we discuss them to the extent that the nuclear tunneling is involved.

The fundamental problem that is to be solved is formulated as follows. There are initial and final electronic terms which cross at some surface, which lies in the classically forbidden region. According to the Born–Oppenheimer principle, the transition occurs at fixed nuclear configuration which brings the system to the crossing region. It is tunneling that creates such a configuration. This situation, as shown by Robinson and Frosh [1963], is typical of vibronic relaxation in polyatomic molecules. A diagram of energy levels is shown in fig. 11a. The vertical optical transition to the excited electronic state A_1 is accompanied by rapid vibrational relaxation [Hill and Dlott 1988], which results in populating the lowest vibrational sublevels only. These sublevels lie below the point at which the term A_1 crosses the term of the final state A_2. The minimum of A_2, E_2^0, is situated much lower than that of A_1, E_1^0,

$$\Delta E = E_1^0 - E_2^0 \gg \hbar\omega \,, \tag{2.57}$$

and the transition $A_2 \leftarrow A_1$ entails creation of many vibrational quanta.

Because of the dense spectrum of the highest vibrational sublevels and their rapid vibrational relaxation in the A_2 state, this radiationless transition (RLT) is irreversible and thus it may be characterized by a rate constant k. The irreversibility condition formulated by Bixon and Jortner [1968] reads

$$\tau_R = 2\pi\hbar\rho_f \gg k^{-1} \,, \tag{2.58}$$

where τ_R is recurrence time, i.e., the time it takes the system with a density of the energy levels ρ_f to return to the initial state. This inequality, called statistical limit of the RLT rate constant, is a quantitative embodyment of the second key assumption of TST (see section 2.1).

When the characteristic time of vibrational relaxation τ_v is much shorter than τ_R, the rate constant is independent of τ_v. For molecules consisting of not too many atoms, the inequality (2.58) is not fulfilled. Moreover, τ_v may even become larger than τ_R. This situation is beyond our present consideration. The total set of resonant sublevels partaking in RLT consists of a small number of active "acceptor" modes with nonzero matrix elements (2.56) and many inactive modes with $V_{if} = 0$. The latter play the role of reservoir and insure the resonance $E_i = E_f$.

For aromatic hydrocarbon molecules, in particular, the main acceptor modes are strongly anharmonic C–H vibrations which pick up the main part of the electronic energy in ST conversion. Inactive modes are stretching and bending vibrations of the carbon skeleton. The value of ρ_f provided by these intramolecular vibrations is so large that they act practically as a continuous bath even without intermolecular vibrations. This is confirmed by the similarity of RLT rates for isolated molecules and the same molecules imbedded in crystals.

Owing to the separation of the active and inactive modes, in the Condon approximation the matrix element (2.56) breaks up into the product of overlap integrals for inactive modes and a constant factor V responsible for interaction of the potential energy terms due to the active modes. In this approximation the survival probability of A_1 develops in time as

$$P_i(t) = \exp(-kt)\cos^2(2\pi t/\tau_R)\,, \tag{2.59}$$

$$k = (2\pi/\hbar)V^2\rho_f \mathrm{FC}\,, \qquad \mathrm{FC} = \sum_{n_k}\left(\prod_k |\langle\psi_i(\boldsymbol{Q})|\psi_{f,n_k}(\boldsymbol{Q})\rangle|^2\right), \tag{2.60a, b}$$

where k is the RLT rate constant, and FC is the statistically weighted Franck–Condon factor. The sum in (2.60b) is over all sets of vibrations n_k such that $\sum n_k\hbar\omega_k = E_1^0 - E_2^0$.

The reorganization of the nuclear configuration in exoergic electron-transfer reactions is usually considered in the same framework. A typical diagram of the terms is depicted in fig. 12.

Comparison of (1.14), (2.47a) and (2.60a) reveals the universality of the golden rule in the description of both the nonadiabatic and adiabatic chemical reactions. However, the matrix elements entering into the golden-rule formula have quite a different nature. In the case of an adiabatic reaction it comes from tunneling along the reaction coordinate, while for a nonadiabatic

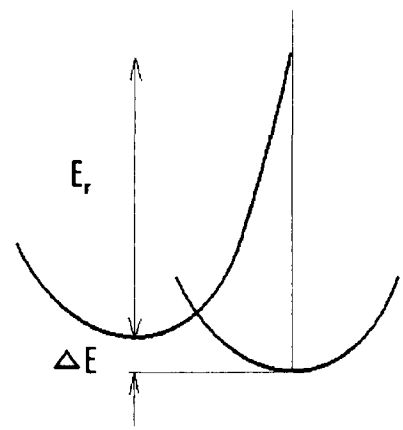

Fig. 12. Marcus model of two harmonic terms in the limit of strong coupling. Reorganization energy E_r is shown.

reaction it originates from the electronic interaction discussed above. The constant matrix-element approximation usually used in RLT theory virtually reduces the problem of transition in a strongly asymmetric potential, as shown in figs. 11 and 12, to that of a two-level system. For the nonadiabatic problem the reduction to a TLS stems from the perturbation theory in electronic interaction, while the adiabatic tunneling theory has no good small parameter; therefore this reduction requires invoking rather delicate reasoning [Leggett et al. 1987].

While being very similar in the general description, the RLT and electron-transfer processes differ in the vibration types they involve. In the first case, those are the high-frequency intramolecular modes, while in the second case the major role is played by the continuous spectrum of polarization phonons in condensed 3D media [Dogonadze and Kuznetsov 1975]. The localization effects mentioned in the previous section, connected with the low-frequency part of the phonon spectrum, still do not show up in electron-transfer reactions because of the asymmetry of the potential.

Another conventional simplification is replacing the whole vibration spectrum by a single harmonic vibration with an effective frequency $\bar{\omega}$. In doing so one has to leave the reversibility problem out of consideration. It is again the model of an active oscillator mentioned in section 2.2 and, in fact, it is friction in the active mode that renders the transition irreversible. Such an approach leads to the well known Kubo–Toyozawa problem [Kubo and Toyozava 1955], in which the Franck–Condon factor FC depends on two parameters, the order of multiphonon process N and the coupling parameter $\bar{S}$

$$N = \Delta E/\hbar\bar{\omega} , \qquad \bar{S} = E_r/\hbar\bar{\omega} = m\bar{\omega}(\Delta R_{if})^2/2\hbar , \tag{2.61}$$

where the reorganization energy E_r indicated in figs. 11b and 12 is determined by the displacement of the vibration equilibrium position.

In this model there is a quantitative difference between RLT and electron transfer stemming from the aforementioned difference in phonon spectra. RLT is the weak-coupling case $\bar{S} \leq 1$, while for electron transfer in polar media the strong-coupling limit is reached, when $\bar{S} \gg 1$. In particular, in the above example of ST conversion in aromatic hydrocarbon molecules $\bar{S} = 0.5–1.0$.

In the strong-coupling limit at high temperatures the electron transfer rate constant is given by the Marcus formula [Marcus 1964]

$$k = (1/\hbar)\, V^2 (\pi\beta/E_r)^{1/2} \exp[-\beta(E_r - \Delta E)^2/4E_r] . \tag{2.62}$$

The transition described by (2.62) is classical and it is characterized by an activation energy equal to the potential at the crossing point. The prefactor is the attempt frequency $\bar{\omega}/2\pi$ times the Landau–Zener transmission coefficient B for nonadiabatic transition [Landau and Lifshitz 1981]

$$B = 2\pi\delta(\bar{v}) , \qquad \delta = V^2/\hbar\bar{v}|\Delta F| , \tag{2.63}$$

where δ is the Massey parameter depending on the mean thermal velocity, and ΔF is the difference in slopes of the initial and final terms at the crossing point. Of course, (2.62) is of typical TST form. It straightforwardly generalizes to an arbitrarily large electronic interaction by replacing B by the Zener transmission factor

$$B = 1 - \exp[-2\pi\delta(\bar{v})] . \tag{2.64}$$

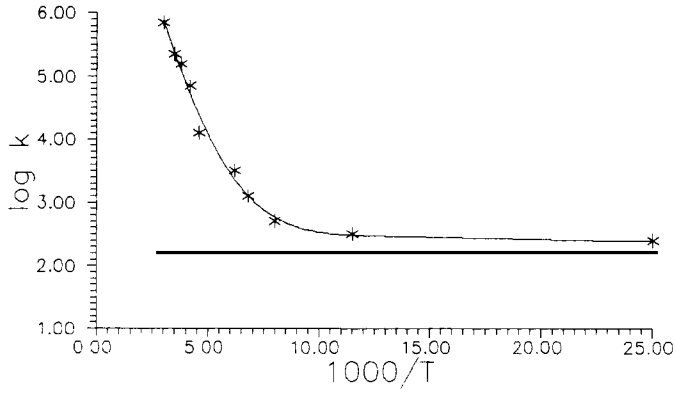

Fig. 13. Arrhenius plot of $k(T)$ for electron transfer from cytochrome c to the special pair of bacteriochlorophylls in the reaction center of c-vinosum.

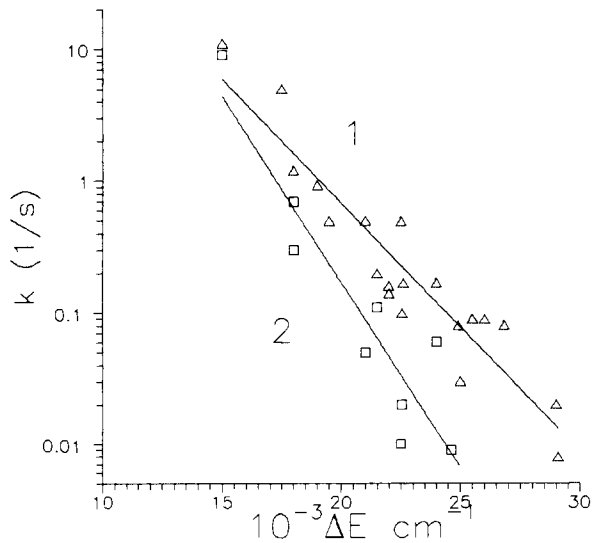

Fig. 14. Energy-gap dependence of the rate constant of intersystem ST: conversion for 1. aromatic hydrocarbons; and 2. their totally deuterated substitutes.

Adiabatic reactions, occurring on a single-sheet PES correspond to $B = 1$, and the adiabatic barrier height occurs instead of E_a. The low-temperature limit of a nonadiabatic-reaction rate constant equals

$$k_c = (2\pi/\hbar^2\bar{\omega})V^2 \exp\{(\Delta E/\hbar\bar{\omega})[1 - \ln(\Delta E/E_r)] - E_r/\hbar\bar{\omega}\} . \tag{2.65}$$

This formula, aside from the prefactor, is simply a one-dimensional Gamov factor for tunneling in the barrier shown in fig. 12. The temperature dependence of k, being Arrhenius at high temperatures, levels off to k_c near the cross-over temperature which, for $\Delta E = 0$, is equal to $k_B T_c \simeq \frac{1}{4}\hbar\bar{\omega}$.

As an illustration of these considerations, the Arrhenius plot of the electron-transfer rate constant, observed by DeVault and Chance [1966] (see also DeVault [1984]), is shown in fig. 13.

Note that only E_r, which is actually the sum of the reorganization energies for all degrees of freedom, enters into the high-temperature rate constant formula (2.62). At low temperature, however, in order to preserve E_r, one has to fit an additional parameter $\bar{\omega}$, which has no direct physical sense for a real multiphonon problem.

By contrast with the Marcus formula, in the RLT case the barrier height increases with increasing ΔE. As seen from fig. 11b, the classically available regions for both terms lie on the same side of the crossing point, and the tunneling behavior at $\hbar\bar{\omega}\beta \gg 1$ is due to the large disparity of the imaginary momenta in the initial and final states. The low-temperature limit for RLT is given by

$$k_c = (2\pi/\hbar)V^2(2\pi/\Delta E\,\hbar\bar{\omega})^{1/2}\exp[-(\Delta E/\hbar\bar{\omega})\ln(\Delta E/\hbar\bar{\omega}) - E_r/\hbar\bar{\omega}] . \tag{2.66}$$

The exponent in this formula is readily obtained by calculating the difference of quasiclassical actions between the turning and crossing points for each term. The most remarkable difference between (2.65) and (2.66) is that the electron-transfer rate constant grows with increasing ΔE, while the RLT rate constant decreases. This exponential dependence $k_c(\Delta E)$ [Siebrand 1967] known as the energy gap law, is exemplified in fig. 14 for ST conversion.

Within CLTST the activation energy E_a depends on ΔE according to the empirical Broensted–Polanyi–Seminov (BPS) rule (see, e.g., Eyring et al. [1983]),

$$E_a(\Delta E) = E_a(0) - \alpha_{cl}\Delta E , \quad 0 < \alpha_{cl} < 1 . \tag{2.67}$$

The symmetry coefficient $\alpha_{cl} = -\beta^{-1}\partial\ln k/\partial\Delta E$ is usually close to $\frac{1}{2}$, in agreement with the Marcus formula. Turning to the quantum limit, one observes that the barrier transparency increases with increasing ΔE as a result of barrier lowering, as well as of a decrease of its width. Therefore, k_c grows faster than the Arrhenius rate constant. At $T = 0$

$$\ln k_c(\Delta E) \simeq \ln k_c(0)[1 + (\Delta E/E_r)(\ln|\Delta E/E_r| - 1)] . \tag{2.68}$$

This relationship is the analogue of the BPS rule for tunneling reactions. The quantum symmetry coefficient $\alpha_q = -\beta_c^{-1}\partial\ln k_c/\partial\Delta E$ is greater than α_{cl} and it may exceed 1.

The origin of the isotope effect is the dependence of ω_0 and $\omega^{\#}$ on the reacting particle mass. Classically, this dependence comes about only via the prefactor ω_0 [see (2.14)], and the ratio of the rate constants of transfer of isotopes with masses m_1 and m_2 ($m_2 > m_1$) is temperature-independent and equal to

$$k_L(m_1)/k_L(m_2) = \omega_0(m_1)/\omega_0(m_2) = (m_2/m_1)^{1/2} . \tag{2.69}$$

In CLTST there appears a kinetic isotope effect owing to the difference in partition functions in the initial state [see eq. (2.12)], and at $\frac{1}{2}\beta\hbar\omega_0 > 1$,

$$k(m_1)/k(m_2) = \exp\{\tfrac{1}{2}\beta\hbar\omega_0[(m_2/m_1)^{1/2} - 1]\} . \tag{2.70}$$

That is, the exponential increase of the isotope effect with β is determined by the difference of the zero-point energies. The cross-over temperature (1.7) depends on the mass by

$$T_c(m_1)/T_c(m_2) = \omega^{\#}(m_1)/\omega^{\#}(m_2) = (m_2/m_1)^{1/2} . \tag{2.71}$$

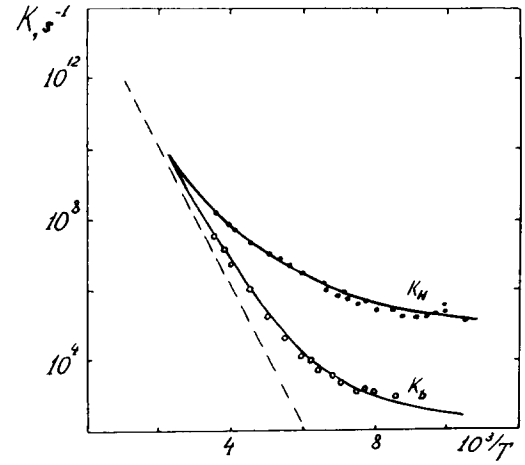

Fig. 15. Arrhenius plot of the rate constant for the transfer of H and D atoms in the CH–O fragment for the reaction (6.17).

In the H/D isotope effect case, $m_2/m_1 = 2$, the interval of temperatures between $T_c(H)$ and $T_c(D)$ is wider than ΔT as predicted by (2.19), and in this interval the H atom tunnels while the D atom classically overcomes the barrier. For this reason the isotope effect becomes several orders larger than that described by (2.70). At $T < T_c(m_2)$ the tunneling isotope effect becomes independent of the temperature,

$$k_c(m_1)/k_c(m_2) = \exp[\beta_c V_0((m_2/m_1)^{1/2} - 1)] . \tag{2.72}$$

The Arrhenius plot of $k(T)$ for H and D transfer is presented in fig. 15. Qualitatively, the conclusions about the isotope effect drawn here on the basis of the one-dimensional model remain correct for more dimensions, but k_c turns out to depend more weakly on m than $\ln k_c \propto m^{1/2}$. This enables observation of transfer of much heavier masses ($m \leq 20m_H$).

2.5. *Vibration-assisted tunneling*

In early papers devoted to the analysis of low-temperature experimental data, the barrier height V_0 was supposed to be the same as in gas-phase reactions, and the barrier widths d were being found by fitting the experimental curves and the theoretical form (2.1). The values of d calculated in this way disagreed with the well known spectroscopic data on the bond lengths in crystals. On the other hand, the experimentally known inter-reactant distances would suggest barriers so large that any reactions would be impossible. Therefore V_0 and d could hardly be reconciled within the one-dimensional model of section 2.1, because the van der Waals distances between reactants in a lattice are usually much longer than in the gas-phase reaction complexes.

To circumvent this difficulty, one has to take into account that the reactants themselves take part in intermolecular vibrations, which may bring them to distances sufficiently short so as to facilitate tunneling, as well as classical transition. Of course, such a rapprochement costs energy, but, because the intermolecular modes are much softer than the intramolecular ones, this energy is smaller than that required for the transition at a fixed intermolecular distance.

As an illustration, let us consider the collinear reaction AB + C → A + BC. It is known that the collinear motion of the linear system ABC relative to its center-of-mass reduces to the motion of the

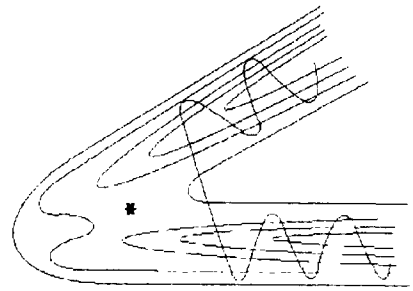

Fig. 16. PES of the collinear exchange reaction AB + A → A + BA in the case $m_B \ll m_A$. The asterisk indicates the saddle point. One of possible realizations of a cutting-corner trajectory is shown. The unbound initial state corresponds to gas-phase reactions.

effective mass

$$m = [m_A m_B m_C/(m_A + m_B + m_C)]^{1/2} , \tag{2.73}$$

on the two-dimensional PES $V(r, R)$ obtained from $V(R_{AB}, R_{BC})$ by scaling the distances R_{AB} and R_{AC}, and reducing the angle between the axes from $\frac{1}{2}\pi$ to β (fig. 16) [Baer 1982],

$$\beta = \tan^{-1}(m_B/m) . \tag{2.74}$$

When $m_B \ll m_A, m_C$, the angle β between the product and reactant valleys becomes small. The longitudinal motion along the reactant valley implies the corresponding displacement of heavy atoms A and C, while the transverse motions are the intramolecular vibrations of B near A. In view of the smallness of m_B, tunneling along the intramolecular coordinate is a fast process on the time scale of slow A–C motion, and, therefore, it may be supposed to occur at fixed A–C distances. This is presented in fig. 16 by a line that cuts straight across the angle between the reactant and product valleys. The overall rate constant then comes from averaging of the tunneling transmission factor over the probability distribution of R_{AC}.

This reasoning was set forth by Johnston and Rapp [1961] and developed by Ovchinnikova [1979], Miller [1975b], Truhlar and Kupperman [1971], Babamov and Marcus [1981], and Babamov et al. [1983] for reactions of hydrogen transfer in the gas phase. A similar model was put forth in order to explain the transfer of light impurities in metals [Flynn and Stoneham 1970; Kagan and Klinger 1974]. Simple analytical expressions were found for an illustrative model [Benderskii et al. 1980] in which the A–B and B–C bonds were assumed to be represented by parabolic terms.

In the case of a strongly exothermic reaction the final term turns into an absorbing wall, and the transition is completed whenever the distance AB reaches a certain value and the A–B bond is broken. The intra- and intermolecular coordinates Q and q are harmonic and have frequencies ω_0 and ω_1, and reduced masses m_0 and m_1. At fixed intermolecular displacement the tunneling probability equals

$$w(Q_0, q) = w_0 \exp[-(Q_0 - q)^2/2\delta_0^2] , \tag{2.75}$$

where Q_0 is the total distance the particle B should overcome, δ_0 the rms amplitude for the intramolecular vibration.

As we have argued above, this probability is to be averaged over the equilibrium distribution for the q-oscillator

$$p(q) = \delta_1^{-1}(2\pi)^{-1/2}\exp(-q^2/\delta_1^2)\,. \tag{2.76}$$

The result is

$$k = w_0[\delta_0/(\delta_0^2+\delta_1^2)^{1/2}]\exp[-Q_0^2/2(\delta_0^2+\delta_1^2)]\,,\quad \delta_i^2 = (\hbar/2m_i\omega_i)\coth\tfrac{1}{2}\beta\hbar\omega_i\,. \tag{2.77a, b}$$

A typical situation is when $\delta_1 > \delta_0$, so that the tunneling distance Q_0 is overcome mostly at the expense of intermolecular vibration q. The probability $p(q)$ is exponentially small, but it is to be compared with the exponentially small barrier transparency, and reduction of the tunneling distance $Q_0 - q$ by promoting vibrations may be very large.

For example, in the case of H tunneling in an asymmetric O_1–H$\cdots O_2$ fragment the O_1–O_2 vibrations reduce the tunneling distance from 0.8–1.2 Å to 0.4–0.7 Å, and the tunneling probability increases by several orders. The expression (2.77a) is equally valid for the displacement of a harmonic oscillator and for an arbitrary Gaussian random value q. In a solid the intermolecular displacement may be contributed by various lattice motions, and the above two-mode model may not work, but once q is Gaussian, eq. (2.77a) will still hold, however complex the intermolecular motion be.

The two-mode model has two characteristic cross-over temperatures corresponding with the "freezing" of each vibration. Above $T_{c1} = \hbar\omega_0/2k_B$ the dependence $k(T)$ is Arrhenius, with activation energy equal to

$$V^{\#} = \tfrac{1}{2}m_0\omega_0^2Q_0^2\,m_1\omega_1^2/(m_0\omega_0^2 + m_1\omega_1^2)\,. \tag{2.78}$$

The transition is fully classical and it proceeds over the barrier which is lower than the static one, $V_0 = \frac{1}{2}m_0\omega_0^2Q_0^2$. Below T_{c1} but above the second cross-over temperature $T_{c2} = \hbar\omega_1/2k_B$, the tunneling transition along Q is modulated by the classical low-frequency q vibration. The apparent activation energy is smaller than V_a. The rate constant levels off to its low-temperature limit k_c only at $T < T_{c2}$, when tunneling starts out from the ground state of the initial parabolic term. The effective barrier in this case is neither $V^{\#}$ nor V_0,

$$V_{\text{eff}} \simeq V^{\#}[1 + (\omega_0/\omega_1)\,\delta_1^2/(\delta_0^2+\delta_1^2)]\,. \tag{2.79}$$

It is noteworthy that it is the lower cross-over temperature T_{c2} that is usually measured. The above simple analysis shows that this temperature is determined by the intermolecular vibration frequencies rather than by the properties of the gas-phase reaction complex or by the static barrier. It is not surprising then, that in most solid state reactions the observed value of T_{c2} is of order of the Debye temperature of the crystal. Although the result (2.77a) has been obtained in the approximation $\omega_1 \ll \omega_0$, the leading exponential term turns out to be exact for arbitrary ω [Benderskii et al. 1990, 1991a]. It is instructive to compare (2.77a) with (2.27) and see that friction slows tunneling down, while the q mode promotes it.

Let us now turn to the influence of vibrations on exchange chemical reactions, like transfer of hydrogen between two O atoms in fig. 2. The potential is symmetric and, depending on the coupling symmetry, there are two possible types of contour plot, schematically drawn in fig. 17a, b. The O atoms participate in different intra- and intermolecular vibrations. Those normal skeleton

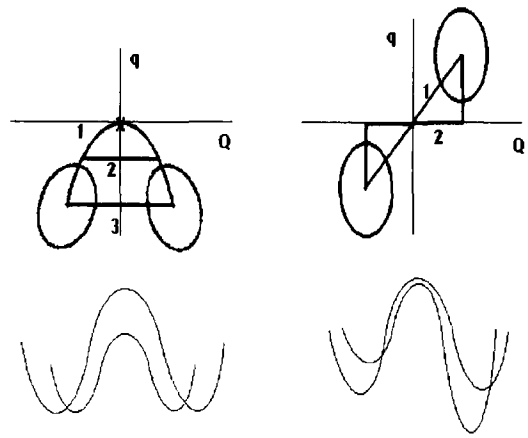

Fig. 17. Contour plots for a q vibration coupled symmetrically (left) and antisymmetrically (right) to the reaction coordinate Q. The cross indicates the saddle point. Lines 1, 2 and 3 correspond to MEP, sudden trajectory, and to the path in the static barrier. Below a sketch of the potential along the tunneling coordinate Q is represented at different q.

vibrations that change the O–O distance keeping the position of the O–O center constant are symmetrically coupled to the proton coordinate, while the other modes that displace the O–O fragment as a whole have antisymmetric coupling. The second case is associated with the Franck–Condon factor introduced in subsections 2.3 and 2.4, while the vibrations of the first type do not contribute to the reorganization energy because their equilibrium positions stay unchanged.

For this reason these vibrations influence tunneling in an entirely different way. For a model in which the reactant and product valleys are represented by paraboloids with frequencies ω_0 and ω_1, the transition probability has been found to be [Benderskii et al. 1991a, b]

$$k_s \propto \exp[-Q_0^2/(\delta_0^2 \cos^2\varphi + \delta_1^2 \sin^2\varphi)] , \qquad k_a \propto \exp(-Q_0^2/\delta_0^2 - q_0^2/\delta_1^2) , \tag{2.80a, b}$$

for symmetric and antisymmetric cases, respectively. Here 2φ is the angle between the reactant and product valleys, $2q_0$ is the displacement of the vibration equilibrium position, and the thermally averaged amplitudes δ_i are those from (2.77b), but taken at $\frac{1}{2}\beta$.

Let us discuss in some detail the reaction path in both cases. At $T > T_c$, since only the barrier height enters into the Arrhenius factor, the transition always passes through the saddle point where the barrier is lowest. In the tunneling regime, the barrier transparency depends on both the height and width of the barrier, and the optimum reaction path is a compromise of these competing factors. Consider first the symmetric case. From what we have said above it is clear that the reaction path (at $T = 0$) should lie between the two extreme lines, the MEP, minimizing the barrier height, and the static barrier, minimizing the path length. For the transfer of light particles, when the angle between the valleys is small and the MEP is strongly curved, the length factor prevails over that of the height, and the reaction path cuts straight across the angle between the valleys. The probability to reach the saddle point is roughly $\ln w_s \propto -\omega_1 q_1^2$, where q_1 is the distance from the minimum to the saddle point, while the probability to "cut the corner", $\ln w_c \propto -\omega_0 Q_0^2$. Therefore, this cutting corner path is realized when $w_c \gg w_s$, that is,

$$1 > \omega_1/\omega_0 \gg \sin^2\varphi , \quad \sin\varphi = Q_0/q_1 . \tag{2.81}$$

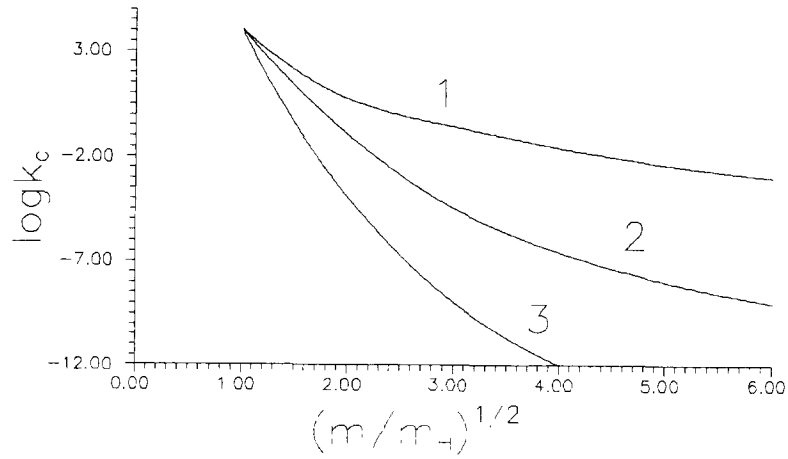

Fig. 18. Rate constant k_c calculated with the use of (2.80a) plotted against $(m/m_H)^{1/2}$. The hydrogen transfer rate is assumed to be $10^4 s^{-1}$, the effective symmetric vibration mass $125m_H$. The ratio of force constants corresponding to the intra (K_0) and intermolecular (K_1) vibrations is $(K_1/K_0)^{1/2} = 2.5\times10^{-2}$, 5×10^{-2} and 1.0×10^{-1} for curves 1–3, respectively.

Physically the cutting-corner trajectory implies that the particle crosses the barrier suddenly on the time scale of the slow q-vibration period. In the literature this approximation is usually called "sudden", "frozen bath" and "fast flip" approximation, or large curvature case. In the opposite case of small curvature (also called adiabatic and "slow flip" approximation), $\omega_1/\omega_0 \ll \sin^2\varphi$, which is relevant for transfer of fairly heavy masses, the MEP may be taken to a good accuracy to be the reaction path.

In the antisymmetric case the possible reaction path ranges from the MEP (when ω_1 and ω_0 are comparable) to the sudden path ($\omega_1 \ll \omega_0$), when the system "waits" until the q vibration "symmetrizes" the potential (the segment of path with $Q = Q_0$) and then instantaneously tunnels in the symmetric potential along the line $q = 0$. All of these types of paths are depicted in fig. 17.*)

When the mass of the tunneling particle is extremely small, it tunnels in the one-dimensional static barrier. With increasing mass, the contribution from the intermolecular vibrations also increases, and this leads to a weaker mass dependence of k_c, than that predicted by the one-dimensional theory. That is why the strong isotope H/D effect is observed along with a weak $k_c(m)$ dependence for heavy transferred particles, as illustrated in fig. 18. It is this circumstance that makes the transfer of heavy reactants (with masses $m \leq 20$–30) possible.

A beautiful experimental piece of evidence of the different roles of antisymmetric and symmetric modes is the vibrational selectivity of tunneling splitting [Fuke and Kaya 1989; Sekiya et al. 1990]. The tunneling splitting Δ in progressions of vibrational levels behaves in different way as a function of the vibrational quantum number n for modes symmetrically and antisymmetrically coupled to the tunneling coordinate. In the former case the splitting increases several times with increasing n from $n = 0$ to $n = 1$–2, while in the latter a decrease of Δ is observed.

This effect can be explained by referring to fig. 17. If the coupling is strong enough so that the q vibration undergoes a displacement q^* greater than its zero-point amplitude, then when moving along the two-dimensional tunneling trajectory, exciting the vibrations of both types changes Δ in

*) It is to be remembered that when the frequencies ω_0, ω_1 and the angle φ are given, only one type of trajectory is actually realized.

a similar way, namely

$$\ln \Delta(n) = \ln \Delta(0) + (2n + 1)\ln(q^*/\delta_{1n}) - \ln(q^*/\delta_{10}) , \quad \delta_{1n}^2 = (n + \tfrac{1}{2})\hbar/m_1\omega_1 . \tag{2.82a, b}$$

This increase in Δ with increasing n is simply due to shortening of the tunneling distance with increasing vibration amplitude δ_{1n}, and it is equivalent to the effect of increasing the temperature for the incoherent tunneling rate [Benderskii et al. 1992b]. For the symmetric case, the qualitative picture does not change in the weak-coupling limit, because all the vibration can do is to modulate the barrier thus facilitating tunneling.

The situation is more subtle for the antisymmetrically coupled mode. As shown in fig. 17, this vibration, in contrast to the symmetric mode, asymmetrizes the potential and violates the resonance. This should lead to a decrease in the splitting. Consider this problem perturbatively. If the vibration and the potential $V(Q)$ were uncoupled, each tunneling doublet E_0, E_1 (we consider only the lowest one) of the uncoupled potential $V(Q)$ would give rise to a progression of vibrational levels with energies

$$E_{0,1}(n) = \hbar\omega_1(n + \tfrac{1}{2}) + E_{0,1} \tag{2.83}$$

Antisymmetric coupling $V_{\text{int}} = CQq$ has the nonzero matrix elements

$$\langle n, 0|CqQ|n + 1, 1\rangle = C\delta_{10}(n + 1)^{1/2}Q_0 , \qquad \langle n, 0|CqQ|n - 1, 1\rangle = C\delta_{10}n^{1/2}Q_0 . \tag{2.84}$$

In the second order of the perturbation theory the shift of the lower level equals

$$\Delta E_0(n) = C^2\delta_{10}^2Q_0^2[n/(\hbar\omega_1 - \hbar\Delta_0) - (n + 1)/(\hbar\omega_1 + \hbar\Delta_0)] , \quad \hbar\Delta_0 = E_1 - E_0 . \tag{2.85}$$

The shift of the upper level, $\Delta E_1(n)$ obtains from (2.85) on changing $\Delta_0 \to -\Delta_0$. Since $\Delta_0 \ll \omega_1$, we finally obtain the renormalized splitting as a function of n,

$$\Delta(n) = \Delta_0[1 - 2C^2(n + \tfrac{1}{2})Q_0^2/\hbar m_1\omega_1^3] . \tag{2.86}$$

Therefore, the tunneling splitting decreases with increasing n, in accord with experiment. The weak-coupling formula holds for $C^2Q_0^2/\hbar m_1\omega_1^3 \ll 1$.

Both the weak- and strong-coupling results (2.82a) and (2.86) could be formally obtained from multiplying Δ_0 by the overlap integral (square root from the Franck–Condon factor) for the harmonic q oscillator,

$$\text{FC}^{1/2} = \int dq\,\psi_n(q + q^*)\psi_n(q - q^*) = \exp(-q^{*2}/2\delta_{10}^2)\,L_n(q^{*2}/\delta_{10}^2) \tag{2.87}$$

where $q^* = CQ_0/m_1\omega_1^2$, and L_n is the Laguerre polynomial. When $n \neq 0$, the harmonic-oscillator wavefunctions have nodes, and for $q^* \leq \delta_{10}$, the overlap of the functions with opposite signs reduces the integral [Huller 1980].

2.6. Is there an alternative to tunneling?

Of course, there is no other explanation to spectroscopic manifestations of tunneling. Such an alternative can be suggested only in the case of an irreversible chemical reaction. We shall discuss

the possibilities to explain large deviations from the Arrhenius law and the existence of a low-temperature limit within CLTST. At $T < T_c$ the apparent prefactor decreases along with the activation energy. In CLTST small prefactors are due to large negative activation entropy $\Delta S^{\#}$ (see, e.g., Eyring et al. [1983]). In this language (2.6) formally gives

$$\Delta S^{\#} = -2\hbar^{-1} k_B S(E_a) , \tag{2.88}$$

although the reason for the appearance of small prefactors in the case of tunneling has nothing to do with the ratio of the partition functions in transition and initial states, which determines $\Delta S^{\#}$ in CLTST. The typical value of $k_c = 10^{-1}$–$10^{-5}\,s^{-1}$ corresponds to a drop in $\Delta S^{\#}$ of 65–85 cal/mol K.

Since only the vibrational degrees of freedom take part in a solid-state reaction, the sole reason for this change may be the increase in their frequencies in the transition state

$$\Delta S^{\#} = k_B \sum_{n=1}^{N} \ln(\omega_n/\omega_n^{\#}) , \tag{2.89}$$

where N is the total number of transverse vibrational modes with frequencies ω_n and $\omega_n^{\#}$ in the initial and transition states. In order to obtain the indicated values of $\Delta S^{\#}$, one has to suppose $N > 10^2$, $\omega_n^{\#} > \omega_n$. Even this somewhat artificial assumption cannot explain the temperature dependence of $\Delta S^{\#}$ shown in fig. 6, because CLTST at $\omega_n^{\#} > \omega_n$ predicts a rise instead of a decrease in $\Delta S^{\#}$ when the vibrations become quantum $\frac{1}{2}\beta\hbar\omega_n \simeq 1$. Therefore, an additional assumption is needed to account for the sharp increase of the number of vibrations involved in the reaction when the temperature approaches T_c.

This model of classical cooperative transitions has been speculated about as an alternative to tunneling. No confirmation for such a scheme exists now. The possibility of representing the experimental form of $k(T)$ as

$$k(T) = k_0 \exp(-\beta E_a) + k_1 \tag{2.90}$$

has also been considered, where the rate $k_1 \ll k_0$ is associated with passing through an activationless channel with a very small transition probability. The origin of such a channel can hardly be substantiated within the framework of CLTST, in view of the above entropy arguments. Although these hypotheses do not clash with any basic principles and they cannot be discarded a priori, they hardly pretend to be a universal explanation to the abundant experimental evidence of the low-temperature limit.

3. One-dimensional models

In this section we shall expand upon the problem of one-dimensional motion in a potential $V(x)$. Although it is a textbook example, we use here the less traditional Feynman path-integral formalism, the advantage of which is a possibility of straightforward extension to many dimensions. In the following portion of the theory we shall use dimensionless units, in which $\hbar = 1$, $k_B = 1$ and the particle has unit mass.

3.1. The main path-integral relations

The path-integral quantum mechanics relies on the basic relation for the evolution operator of the particle with the time-independent Hamiltonian $\hat{H}(x, p) = \frac{1}{2}p^2 + V(x)$ [Feynman and Hibbs 1965],

$$\langle x_f|\exp(-i\hat{H}t_0)|x_i\rangle \equiv K(x_f, x_i|t_0) = \int D[x(t)]\exp(iS[x(t)]) , \tag{3.1}$$

with the normalization

$$K(x, x'|0) = \delta(x - x') , \tag{3.2}$$

where the path integral sums up all the paths connecting the points $x(0) = x_i$ and $x(t_0) = x_f$, each path having the weight $\exp(iS)$. If we discretize time by introducing the points $0 = t_1 < t_2 < \cdots < t_{l-1} < t_l = t_0, l \to \infty$, the symbol $D[x(t)]$, indicating summation over all realizations of path $x(t)$, may be thought of as $D[x(t)] = N\,dx(t_2)\cdots dx(t_{l-1})$, where N is the normalization factor providing the validity of (3.2). The action S is defined via the classical Lagrangian,

$$S = \int_0^{t_0} dt\, L(x, \dot{x}) , \quad L(x, \dot{x}) = \tfrac{1}{2}\dot{x}^2 - V(x) . \tag{3.3}$$

The Fourier transform of the propagator (3.1) gives the energy Green function,

$$G(x, x'|E) = i\int_0^{\infty} dt\, K(x, x'|t)\exp(iEt) , \tag{3.4}$$

which provides a solution to the time-independent Shrödinger equation

$$(\hat{H} - E)G = \delta(x - x') . \tag{3.5}$$

The poles of the spectral function

$$g(E) = \mathrm{Tr}(\hat{H} - E)^{-1} = \int dx\, G(x, x|E) \tag{3.6}$$

correspond to the energy eigenvalues, E_n^0. This function can also be represented as

$$g(E) = i\int_0^{\infty} dt \exp(iEt)\int dx_i \int_{x_i = x_f} D[x(t)]\exp(iS[x(t)]) . \tag{3.7}$$

As seen from (3.7), the closed paths with $x(t_0) = x(0)$ fully determine the energy spectrum of the system. Propagator K has, in terms of the energy eigenfunctions $|n\rangle$, the form

$$K(x_f, x_i|t_0) = \sum \exp(-iE_n^0 t_0)\langle x_f|n\rangle\langle n|x_i\rangle \,. \tag{3.8}$$

The statistical operator (density matrix),

$$\exp(-\beta\hat{H}) = \sum \exp(-\beta E_n^0)|n\rangle\langle n| \,, \tag{3.9}$$

formally obtains from the quantum mechanical evolution operator on replacing it_0 by β. This change of variables $t = -i\tau$, called Wick rotation [Callan and Coleman 1977], "turns upside-down" the potential and therefore replaces the Lagrangian in (3.3) by the classical Hamiltonian

$$t \to -i\tau \,, \qquad x \to x \,, \qquad \dot{x} \to i\dot{x} \,, \qquad V(x) \to -V(x) \,,$$

$$L \to H \equiv \tfrac{1}{2}\dot{x}^2 + V(x) \,, \qquad E \to -E \,. \tag{3.10}$$

The resulting Eucledian action equals

$$-iS = S_E[x(\tau)] = \int_0^\beta d\tau\, H(x, \dot{x}) = \int_{x_i}^{x_f} p\, dx + E\beta \,. \tag{3.11}$$

The density matrix is [Feynman 1972]

$$\rho(x_f, x_i|\beta) \equiv \langle x_f|\exp(-\beta\hat{H})|x_i\rangle = \int_{x(0)=x_i}^{x(\beta)=x_f} D[x(\tau)]\exp(-S_E[x(\tau)]) \,, \tag{3.12}$$

and, consequently, the partition function is

$$Z \equiv \exp(-\beta F) \equiv \mathrm{Tr}\exp(-\beta\hat{H}) = \int dx(0) \int_{x(0)=x(\beta)} D[x(\tau)]\exp(-S_E[x(\tau)]) \,, \tag{3.13}$$

where F is the free energy. As in (3.7), only the closed paths enter into the expression (3.13). The density matrix $\rho(x_f, x_i|\beta)$ obeys the differential equation

$$\partial\rho/\partial\beta = -\hat{H}\rho \,, \tag{3.14}$$

with the initial condition $\rho(x, x'|0) = \delta(x - x')$ [cf. eq. (3.2)].

In conclusion of this section, we write out the expressions for the density matrix of a free particle and a harmonic oscillator. In the former case $\rho(x, x'|\beta)$ is a Gaussian with the half-width equal to the thermal de Broglie wavelength

$$\rho(x, x'|\beta) = (2\pi\beta)^{-1/2}\exp[-(x - x')^2/2\beta] \,. \tag{3.15}$$

For the harmonic oscillator with frequency ω,

$$\rho(x, x'|\beta) = [\omega/(2\pi \sinh \beta\omega)]^{1/2}$$

$$\times \exp\{-[\omega/(2\sinh\beta\omega)][(x^2 + x'^2)\cosh\beta\omega - 2xx']\} \tag{3.16}$$

$$Z = \exp(-\beta F) = [2\sinh(\tfrac{1}{2}\beta\omega)]^{-1} . \tag{3.17}$$

3.2. Decay of metastable state

Consider a potential $V(x)$ having a single minimum separated from the continuous spectrum by a sufficiently large barrier satisfying (1.1), e.g., a cubic parabola (fig. 19)

$$V(x) = \tfrac{1}{2}\omega_0^2 x^2(1 - x/x_0) . \tag{3.18}$$

Since the Hamiltonian is unbounded, the energy of each state is complex [Landau and Lifshitz 1981]

$$E_n = E_n^0 - i\tfrac{1}{2}\Gamma_n , \tag{3.19}$$

whence the wave function falls off exponentially with time,

$$|\psi|^2 \propto \exp(-\Gamma_n t) . \tag{3.20}$$

Metastability implies that $\Gamma_n \ll E_n^0$, so that the wave function inside the well is close to that of a stationary state with energy E_n^0. Strictly speaking, the energy spectrum in this case is quasi-discrete with the density of states

$$\rho(E) = (2\pi)^{-1} \sum_n \Gamma_n/[(E - E_n^0)^2 + \tfrac{1}{4}\Gamma_n^2] . \tag{3.21}$$

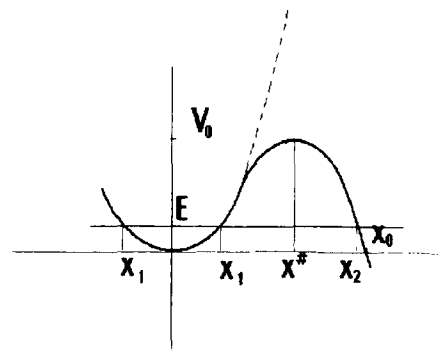

Fig. 19. Cubic parabola potential. Turning points are shown. The dashed line indicates the stable potential with the same well frequency.

We seek the poles of the spectral function $g(E)$ given by (3.7). In the WKB approximation the path integral in (3.7) is dominated by the classical trajectories which give an extremum to the action functional

$$0 = \delta S[x(t)]/\delta x = \mathrm{d}^2x/\mathrm{d}t^2 + \mathrm{d}V(x)/\mathrm{d}x \,. \tag{3.22}$$

In fact, (3.22) is the usual stationary phase approximation, performed however for an infinite-dimensional path integral, which picks up the trajectories with classical action S_{cl}. Further, at fixed time t we take the integral over x_{i} again in the stationary phase approximation, which gives

$$0 = \partial S_{\mathrm{cl}}/\partial x_{\mathrm{i}} = \partial S_{\mathrm{cl}}/\partial x(0) + \partial S_{\mathrm{cl}}/\partial x(t) = \dot{x}(t) - \dot{x}(0) \,. \tag{3.23}$$

This equation shows that only the closed classical trajectories [$x(t) = x(0)$ and $\dot{x}(t) = \dot{x}(0)$] should be taken into account, and the energy spectrum is determined by these periodic orbits [Gutzwiller 1967; Balian and Bloch 1974; Miller 1975a; Rajaraman 1975].

Finally, the stationary phase integration over time yields the identity

$$E = -\partial S_{\mathrm{cl}}/\partial t = E_{\mathrm{cl}}(t) \,, \tag{3.24}$$

which means that the classical periodic orbits should have energy E. Therefore, with exponential accuracy the spectral function is represented by the sum over all periodic orbits,

$$g(E) \propto \sum_{\substack{\text{periodic}\\ \text{orbits}}} \exp[\mathrm{i}(W(E) - \tfrac{1}{2}l\pi)] \,, \quad W(E) = S_{\mathrm{cl}} + Et = \oint p\,\mathrm{d}x \,, \tag{3.25a, b}$$

where $W(E)$ is the short action and the additional phases $\frac{1}{2}l\pi$, l being the number of turning points encountered along the trajectory, emerge because of the breakdown of the WKB approximation near the turning points [Gutzwiller 1967; McLaughlin 1972; Levit et al. 1980a, b]. The vibrations with energy E in the well and the short action of (3.25b) have periods given, respectively, by

$$\tau_1 = 2\int_{x_1'}^{x_1} \mathrm{d}x\,[2(E - V(x))]^{-1/2} \,, \quad W_1(E) = 2\int_{x_1'}^{x_1} \mathrm{d}x\,[2(E - V(x))]^{1/2} \,, \tag{3.26a, b}$$

where x_1' and x_1 are the turning points (see fig. 19). If the state in the well were stable (the potential in fig. 19 shown by a dashed line), these classical vibrations would be the only possible periodic orbits entering into (3.25a).

Summing up the series (3.25a) over the number of passages back and forth, n, we get

$$g(E) \propto \sum_{n=1}^{\infty} \exp[\mathrm{i}n(W_1(E) - \pi)] = \{\exp[-\mathrm{i}(W_1(E) - \pi)] - 1\}^{-1} \,. \tag{3.27}$$

Thus $g(E)$ has an infinite number of poles at

$$W_1(E) = 2\pi(n + \tfrac{1}{2}) \,. \tag{3.28}$$

This expression is nothing but the Bohr–Sommerfeld quantization rule (see, e.g., Landau and Lifshitz [1981]). In the metastable potential of fig. 19 there are also imaginary-time periodic orbits satisfying (3.22) and contained between the turning points inside the classically forbidden region. It is these trajectories that are responsible for tunneling [McLaughlin 1972; Levit et al. 1980a, b]. They have imaginary period and action,

$$i\tau_2 = 2\int_{x_1}^{x_2} dx\,[2(E - V(x))]^{-1/2}\,, \qquad iW_2(E) = 2\int_{x_1}^{x_2} dx\,[2(E - V(x))]^{1/2}\,. \tag{3.29}$$

The classically accessible region to the right of the turning point x_2 does not contain any closed trajectories. An arbitrary periodic orbit which includes n "swings" inside the well and m barrier passages has complex period $\tau_{nm}(E) = n\tau_1(E) + im\tau_2(E)$ and action $nW_1(E) + imW_2(E)$. Each orbit with given n and m ($m + n \geq 1$) enters into the sum (3.25a) with the combinatorial coefficient C^n_{n+m}, and direct summation gives

$$g(E) \propto \frac{\exp[i(W_1 - \pi)] + \exp(-W_2)}{1 - \exp[i(W_1 - \pi)] - \exp(-W_2)}\,, \tag{3.30}$$

whence the quantization condition is

$$\exp[i(W_1(E) - \pi)] + \exp[-W_2(E)] = 1\,. \tag{3.31}$$

Since $\exp(-W_2) \ll 1$, this equation can be solved iteratively by using (3.28) as a zeroth approximation, whence

$$\Gamma_n = (\partial W_1/\partial E)^{-1}_{E=E^0_n} \exp[-W_2(E^0_n)] = [1/\tau_1(E^0_n)]\exp[-W_2(E^0_n)]\,. \tag{3.32}$$

Equation (3.32) demonstrates that the decay rate for a metastable state is equal to the inverse period of classical vibrations in the well ("attempt frequency") times the barrier transparency.

3.3. *The Im F method*

Now we take up the calculation of the rate constant for the decay of a metastable state. In principle it can be done by statistically averaging Γ_n from (3.32), but there is a more elegant and general way which relates the rate constant with the imaginary part of free energy. Recalling (3.19) we write the rate constant as

$$k = Z_0^{-1}\sum \Gamma_n \exp(-\beta E^0_n) = 2\beta^{-1}\,\mathrm{Im}\,Z/Z_0 = 2\,\mathrm{Im}\,F\,, \tag{3.33}$$

where Z_0 is the real part of the free energy in the well which is calculated by neglecting the decay. This expression enables one to use the path-integral expression (3.13).

Again, as in the previous section, we look for the stationary points of the path integral, i.e., the trajectories that extremize the Eucledian action (3.11) and thus satisfy the classical equation of motion in the upside-down barrier,

$$0 = \delta S[x(t)]/\delta x = -\,d^2x/d\tau^2 + dV(x)/dx\,, \tag{3.34}$$

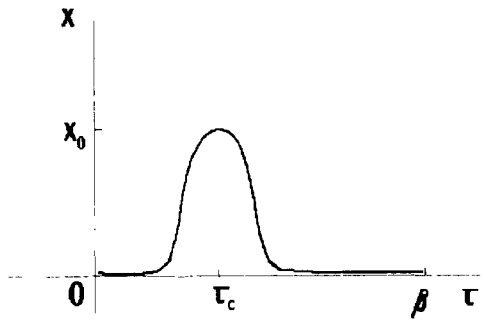

Fig. 20. The bounce trajectory in the cubic potential at $\beta\omega_0 \to \infty$.

with the periodic boundary condition $x(\tau + \beta) = x(\tau)$. These trajectories have the integral of motion

$$E = \tfrac{1}{2}(\mathrm{d}x/\mathrm{d}\tau)^2 - V(x)\,, \tag{3.35}$$

in accordance with the prescription (3.10). There are two trivial solutions to (3.34), $x \equiv 0$, and $x \equiv x^{\#}$. The first of these corresponds to Z_0; the second, to the transition-state partition function.

In addition to the trivial solutions, there is a β-periodic upside-down barrier trajectory called instanton, or "bounce"*) [Langer 1969; Callan and Coleman 1977; Polyakov 1977]. At $\beta \to \infty$ the instanton dwells mostly in the vicinity of the point $x = 0$, attending the barrier region (near $x^{\#}$) only during some finite time $\tau_{\mathrm{ins}} \sim \omega^{\#-1}$ (fig. 20). When β is raised, the instanton amplitude decreases until the trajectory collapses to the point $x(\tau) = x^{\#}$. As follows from the arguments of subsection 2.1, this happens at $\beta_c = 2\pi/\omega^{\#}$. In other words, the cross-over phenomenon is associated with the disappearance of the instanton.

Unlike the trivial solution $x \equiv 0$, the instanton, as well as the solution $x(\tau) \equiv x^{\#}$, is not the minimum of the action $S[x(\tau)]$, but a saddle point, because there is at least one direction in the space of functions $x(\tau)$, i.e. towards the absolute minimum $x(\tau) \equiv 0$, in which the action decreases. Hence if we were to try to use the approximation of steepest descents in the path integral (3.13), we would get divergences from these two saddle points. This is not surprising, because the partition function corresponding to the unbounded Hamiltonian does diverge.

Langer [1969] proposed to extend the integration to the complex space and then use the approximation of steepest descents. This procedure makes the partition function converge, and the latter acquires the sought imaginary part $\mathrm{Im}\,Z$ coming from the above two saddle-point solutions. Accordingly, working with exponential accuracy, one has two contributions to $\mathrm{Im}\,Z$, proportional to $\exp[-S_{\mathrm{ins}}(\beta)]$, where S_{ins} is the instanton action, and to $\exp(-\beta V_0)$. These contributions correspond with tunneling and thermally activated over-barrier transitions. While being crucial at high temperatures $\beta < \beta_c$, at $\beta > \beta_c$ the second contribution becomes negligible, compared to the contribution of the instanton.

The uncertainty principle necessitates that any extremal trajectory should be "spread", and the next step in our calculation is to find the prefactor by incorporating the small fluctuations around

*) Langer, who was the first to introduce the $\mathrm{Im}\,F$ method in his original paper [Langer 1969] on nucleation theory called it "bubble".

the extremal trajectory, in the spirit of the usual method of steepest descents. Following Callan and Coleman [1977] let us expand the action functional around the extremal trajectory up to quadratic terms,

$$S[x(\tau)] = S_{\text{ins}} + \tfrac{1}{2}\int_0^\beta \mathrm{d}\tau\, \delta x(\tau)[-\partial_\tau^2 + \mathrm{d}^2 V(x(\tau))/\mathrm{d}x^2]\,\delta x(\tau)\,, \tag{3.36}$$

where ∂_τ^2 is the second-derivative operator. The linear terms are absent from (3.36) due to the extremality condition (3.34). Suppose that we have found the basis of eigenfunctions of the differential operator $-\partial_\tau^2 + \mathrm{d}^2 V(x(\tau))/\mathrm{d}x^2$,

$$[-\partial_\tau^2 + \mathrm{d}^2 V(x(\tau))/\mathrm{d}x^2]\,x_n(\tau) = \varepsilon_n x_n(\tau)\,. \tag{3.37}$$

Expanding an arbitrary path $x(\tau)$ in this basis,

$$\delta x(\tau) = \sum c_n x_n(\tau)\,, \tag{3.38}$$

we rewrite (3.36) as

$$S = S_{\text{ins}} + \sum \tfrac{1}{2}\varepsilon_n c_n^2\,. \tag{3.39}$$

The path integration reduces to integration over all coefficients c_n with the measure

$$D[x(\tau)] = N\prod_n \mathrm{d}c_n/(2\pi)^{1/2} \tag{3.40}$$

We shall not have to worry about the normalizing factor N because it will eventually cancel out in the ratio $(\mathrm{Im}\,Z)/Z_0$. The integral (3.13) with the action (3.39) is Gaussian and equal to

$$\int N\prod_n \frac{\mathrm{d}c_n}{(2\pi)^{1/2}}\exp(-S_{\text{ins}})\exp\left(-\sum \tfrac{1}{2}\varepsilon_n c_n^2\right) = \tfrac{1}{2}\mathrm{i}N\left(\prod|\varepsilon_n|\right)^{-1/2}\exp(-S_{\text{ins}})$$

$$\equiv \tfrac{1}{2}\mathrm{i}N|\det(-\partial_\tau^2 + \mathrm{d}^2 V/\mathrm{d}x^2)|^{-1/2}\exp(-S_{\text{ins}})\,, \tag{3.41}$$

where we have defined the determinant of a differential operator as the product of its eigenvalues. Since the instanton is a saddle point, one of the eigenvalues, say ε_1, must be negative, and, according to Langer, the integration contour for c_1 should be distorted in the c_1 plane, as shown in fig. 21. This makes the integral (3.41) imaginary and provides an additional factor $\frac{1}{2}$.

A more vexing issue is that one of the ε_n in (3.37) equals zero. To see this, note that the function $x_{\text{ins}}(\tau)$ [where x_{ins} is the instanton solution to (3.34)] can be readily shown to satisfy (3.37) with $\varepsilon_0 = 0$. Since the instanton trajectory is closed, it can be considered to start arbitrarily from one of its points. It is this "zero mode" which is responsible for the time-shift invariance of the instanton solution. Therefore, the non-Gaussian integration over c_0 is expected to be the integration over

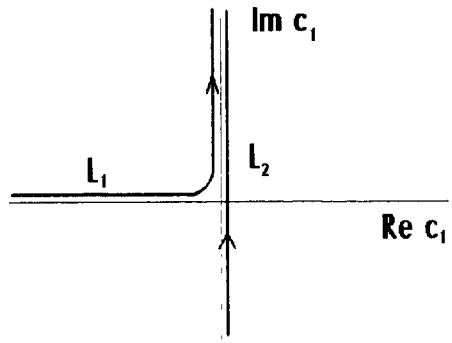

Fig. 21. Integration contours in the complex plane for the unstable mode. Contours L_1 and L_2 are used to calculate Im Z and the barrier partition function, respectively.

positions of the instanton center τ_c (see fig. 20). The eigenfunction x_0 is the properly normalized $\dot{x}_{ins}(\tau)$,

$$x_0(\tau) = N_0 \dot{x}_{ins}(\tau) . \tag{3.42}$$

The normalization condition $\int_0^\beta x_0^2(\tau)\,d\tau = 1$ yields

$$N_0 = S_0^{-1/2} , \quad S_0 = \int_0^\beta \dot{x}_{ins}^2\,d\tau , \tag{3.43}$$

and the integration over c_0 is replaced by

$$(2\pi)^{-1/2}\,dc_0 = (S_0/2\pi)^{1/2}\,d\tau_c , \tag{3.44}$$

where integration over τ_c simply gives the factor β. Eliminating the zero-mode from (3.41) by use of (3.44), and recalling that Z_0 may be represented in the same way as (3.41),

$$Z_0 = N[\det(-\partial_\tau^2 + \omega_0^2)]^{-1/2} = [2\sinh(\tfrac{1}{2}\beta\omega_0)]^{-1} , \tag{3.45}$$

one obtains finally

$$k = 2\,\mathrm{Im}\,F = \left(\frac{S_0}{2\pi}\right)^{1/2} \left|\frac{\det'(-\partial_\tau^2 + d^2V/dx^2)_{ins}}{\det(-\partial_\tau^2 + \omega_0^2)}\right|^{-1/2} \exp(-S_{ins}) , \tag{3.46}$$

where the prime means that the zero-mode is omitted from the determinant.

Callan and Coleman [1977] have obtained this formula in the limit $\beta \to \infty$ by summing up all multi-instanton contributions to Im F, i.e., taking into account the trajectories that pass through the barrier more than twice. These trajectories enter into Im F with factors $\exp(-nS_{ins})/n!$ (where n is the number of passes) and, therefore, they can be neglected when $S_{ins} \gg 1$.

Equation (3.46) has been applied to the cubic parabola (3.18) at $T = 0$ by Caldeira and Leggett [1983]. The result is

$$k_c = 60^{1/2}\omega_0\left(\frac{S_{ins}}{2\pi}\right)^{1/2}\exp(-S_{ins}), \quad S_{ins} = \int_0^{x_0}[2V(x)]^{1/2}\,dx = \frac{36V_0}{5\omega_0}, \tag{3.47}$$

and the cross-over temperature equals $T_c = \omega_0/2\pi$. The same result has been obtained with a more traditional quantum-mechanical treatment by Schmid [1986], by directly solving the Shrödinger equation in the WKB approximation. The calculation of $\Gamma_0 = k_c$ with the aid of (3.31) and (3.32) for the same potential [Wartak and Krzeminski 1989] leads to a result larger than (3.47) by a factor 3.34. This discrepancy is due to the use of the semiclassical quantization condition (3.31) for the lowest energy level, while the instanton method, as well as Schmid's calculation, exploits in fact the exact harmonic oscillator wavefunction in the well.

Meanwhile, eqs. (3.31) and (3.32) may work better than the instanton approach (3.29) when anharmonicity is substantial, even for the ground state [Hontscha et al. 1990]. As shown by Rajaraman [1975], and Waxman and Leggett [1985], the basic instanton relationship (3.29) is equivalent to eqs. (2.6) and (2.7) obtained by the extension of CLTST to the quantum region. Comparing (2.6) and (2.7) with (3.29) gives the semiclassical estimate for Im Z,

$$2\,\mathrm{Im}\,Z = \beta(2\pi)^{-1/2}|d\beta/dE|^{-1/2}\exp(-S_{ins}) = \beta(2\pi)^{-1/2}|d^2S_{ins}/d\beta^2|^{1/2}\exp(-S_{ins}). \tag{3.48}$$

The identity of eqs. (2.6) (at $T = 0$) and (3.47) for the cubic parabola is also demonstrated in appendix A. Although at first glance the infinite determinants in (3.46) might look less attractive than the simple formulas (2.6) and (2.7), or the direct WKB solution by Schmid, it is the instanton approach that permits direct generalization to dissipative tunneling and to the multidimensional problem.

Gillan [1987], in studying tunneling of a particle interacting with a classical oscillator bath, has proposed a physically transparent CLTST-based approach to the quantum rate using the centroid approximation. This idea has been developed and tested by Voth et al. [1989b]. Following Voth et al. [1989b], we wish to modify the CLTST formula (2.12) rewritten as

$$k_{CLTST} = \tfrac{1}{2}u_{cl}Z_0^{-1}Z^{\#}(x^{\#}), \quad Z^{\#}(x^{\#}) = (2\pi\beta)^{-1/2}\int dx\exp[-\beta V(x)]\,\delta(x - x^{\#}), \tag{3.49a, b}$$

where $Z^{\#}(x^{\#})$ is the constrained transition-state partition function, so as to incorporate tunneling effects. The velocity factor $u_{cl} = \langle|\dot{x}|\rangle = (2/\pi\beta)^{1/2}$ in (3.49a) represents the reactive flux for those trajectories that have reached the transition state.

The original idea of approximating the quantum mechanical partition function by a classical one belongs to Feynman [Feynman and Vernon 1963; Feynman and Kleinert 1986]. Expanding an arbitrary β-periodic orbit, entering into the partition-function path integral, in a Fourier series in Matsubara frequencies ν_n,

$$x(\tau) = \beta^{-1}\sum_{n=-\infty}^{\infty} x_n\exp(i\nu_n\tau), \quad \nu_n = 2\pi n/\beta, \tag{3.50}$$

it is easy to see that the kinetic-energy term in the action $S[x(\tau)]$ takes the form

$$\int_0^\beta \tfrac{1}{2}\dot{x}^2\,\mathrm{d}\tau = \tfrac{1}{2}\beta^{-1}\sum_{n=-\infty}^{\infty} \nu_n^2 x_n x_{-n}\,. \tag{3.51}$$

For small β the contribution of paths with large x_n ($n \neq 0$) to the partition function Z is suppressed because they are associated with large kinetic-energy terms proportional to ν_n^2. That is why the partition function actually becomes the integral over the zeroth Fourier component x_0. It is therefore plausible to conjecture that the quantum corrections to the classical TST formula (3.49a) may be incorporated by replacing $Z^\#$ by

$$Z_c^\#(x^\#) = \int D[x(\tau)]\exp(-S[x(\tau)])\,\delta(x_c - x^\#)\,, \tag{3.52}$$

where the "centroid" coordinate equals

$$x_c = x_0/\beta = \beta^{-1}\int_0^\beta x(\tau)\,\mathrm{d}\tau\,. \tag{3.53}$$

To show that this guess is actually consistent with the Im F approach and to see what happens to the velocity factor u_{cl} at low temperatures let us study the statistics of centroids. We introduce the centroid density

$$\begin{aligned} Z_c(R) &= \langle\delta(R - x_c)\rangle = \int D[x(\tau)]\exp(-S[x(\tau)])\,\delta(x_c - R) \\ &= \int_{-\infty}^{\infty}\frac{\mathrm{d}\lambda}{2\pi}\int D[x(\tau)]\exp\{-S[x(\tau)] - \mathrm{i}\lambda(x_c - R)\}\,, \end{aligned} \tag{3.54}$$

where we have used the integral representation of the δ function. Apart from integration over λ and a constant factor, (3.54) is the partition function Z_λ in the complex potential $V_\lambda(x) = V(x) + \mathrm{i}\lambda x$,

$$Z_\lambda = \int D[x(\tau)]\exp(-S_\lambda[x(\tau)])\,,\quad S_\lambda[x(\tau)] = \int_0^\beta \mathrm{d}\tau\,[\tfrac{1}{2}\dot{x}^2 + V_\lambda(x)]\,, \tag{3.55}$$

so that $Z_c(R)$ is the Fourier transform of Z_λ,

$$Z_c(R) = \int_{-\infty}^{\infty}\frac{\mathrm{d}\lambda}{2\pi}\exp(\mathrm{i}\lambda R)\,Z_\lambda\,. \tag{3.56}$$

In fact, Z_λ is twice Im Z defined above,*) taken for V_λ [Stuchebrukhov 1991], and, therefore

$$Z_\lambda = \beta(2\pi)^{-1/2}|\mathrm{d}^2 S_\lambda/\mathrm{d}\beta^2|^{1/2}\exp(-S_{\lambda,\mathrm{ins}})\,. \tag{3.57}$$

Expanding the action $S_{\lambda,\mathrm{ins}}$ around $\lambda = 0$ one obtains

$$S_{\lambda,\mathrm{ins}} = S_{\mathrm{ins}} + (\lambda/\beta)S_1 + (\lambda/\beta)^2 S_2 + \cdots\,, \quad S_1 = \mathrm{i}\beta\langle x\rangle_{\mathrm{ins}}\,, \tag{3.58}$$

$$S_2 = (2\,\mathrm{d}^2 S_{\mathrm{ins}}/\mathrm{d}\beta^2)^{-1}[(\mathrm{d}/\mathrm{d}\beta)\beta\langle x^2\rangle_{\mathrm{ins}} + (\mathrm{d}S_1/\mathrm{d}\beta)^2]\,, \tag{3.59}$$

where $\langle x\rangle_{\mathrm{ins}}$ and $\langle x^2\rangle_{\mathrm{ins}}$ are imaginary-time averages over the instanton trajectory. Neglecting higher-order terms in (3.58), one finds from (3.56) that the centroid density is gaussian

$$Z_{\mathrm{c}}(R) = 2\,\mathrm{Im}\,Z\,\pi^{-1/2}\,\Delta x^{-1}\exp[(R - \langle x\rangle_{\mathrm{ins}})^2/\Delta x^2]\,, \quad \Delta x = -4S_2/\beta^2\,, \tag{3.60a, b}$$

where Δx is the characteristic length. It is obvious from (3.60a) that the modified "transition state" position in the quantum region is given by

$$\tilde{x}^{\#} = \langle x\rangle_{\mathrm{ins}}\,, \tag{3.61}$$

and comparison of (3.33) with (3.60a) gives

$$k = \pi^{1/2}\Delta x\,\beta^{-1} Z_{\mathrm{c}}(\tilde{x}^{\#})/Z_0\,. \tag{3.62}$$

This formula looks like the CLTST one (3.49a), if we introduce the quantum velocity factor

$$u = 2\pi^{1/2}\Delta x\,\beta^{-1}\,. \tag{3.63}$$

At high temperatures ($\beta \to 0$) the centroid (3.53) collapses to a point so that the centroid partition function (3.52) becomes a classical one (3.49b), and the velocity (3.63) should approach the classical value u_{cl}. In particular, it can be directly shown [Voth et al. 1989b] that the centroid approximation provides the correct Wigner formula (2.11) for a parabolic barrier at $T > T_{\mathrm{c}}$, if one uses the classical velocity factor u_{cl}. A direct calculation of Δx for a parabolic barrier at $T > T_{\mathrm{c}}$ gives

$$\Delta x^2_{\mathrm{pb}} = 2/\beta\omega^{\#2}\,. \tag{3.64}$$

That is, the centroids are distributed according to the classical function $Z_{\mathrm{c}}(R) \propto \exp[\frac{1}{2}\beta\omega^{\#2} \times (R - x^{\#})^2]$.

Substituting (3.64) in (3.63), however, does not give the correct value of u_{cl}. To fit smoothly the high- and low-temperature regions, Voth et al. [1989b] have written $u = 2\pi^{1/2}\Delta x\,\beta^{-1}\phi$, where $\phi = 1$ at low temperatures, and $\phi = T_{\mathrm{c}}/T = \beta\omega^{\#}/2\pi$ at $T > T_{\mathrm{c}}$ [Affleck 1981]. This correction factor recovers the correct behavior of u at high temperatures, when the eqs. (3.59) and (3.60a, b) do not work. For the Eckart barrier (eq. 3.65a), a simple empirical formula for the velocity factor

*) In the semiclassical evaluation of the barrier partition function Z_λ the integration goes along the whole imaginary axis in the c_1 plane (see fig. 21).

(eq. 3.65b) has been shown by Voth et al. [1989b] to work within the accuracy of 1% at $\frac{1}{2}T_c \leq T \leq T_c$, where

$$V(x) = V_0 \operatorname{sech}^2(x/x_0) , \qquad u = u_{cl}[1 + \ln(\beta\omega^{\#}/2\pi)] . \tag{3.65a, b}$$

While being very attractive in view of their similarity to CLTST, on closer inspection (3.61)–(3.63) reveal their deficiency at low temperatures. When $\beta \to \infty$, the characteristic length Δx from (3.60b) becomes large, and the expansion (3.58) as well as the gaussian approximation for the centroid density breaks down. In the test of ref. [Voth et al. 1989b], which has displayed the success of the centroid approximation for the Eckart barrier at $T \geq \frac{1}{2}T_c$, the low-temperature limit has not been reached, so there is no ground to trust eq. (3.62) as an estimate for k_c.*)

Furthermore, the situation becomes even worse for an asymmetric potential like that in (3.18), because at low temperature nearly the entire period β is spent on dwelling in the potential well (see appendix A), so that $\lim_{\beta\to\infty} \langle x \rangle_{ins} = 0$. In other words, unless the potential is strictly symmetric,**) the "transition state position" $\tilde{x}^{\#}$ tends to the minimum of the initial state! It is natural to expect that the centroid approximation will work well when $\tilde{x}^{\#}$ does not deviate too far from $x^{\#}$. To summarize, the centroid method is an instructive way to describe in a unique TST-like manner both the high ($T > T_c$) and fairly low ($T < T_c$) temperature regions, but it does not give a reliable estimate for k_c.

3.4. Tunneling splitting in a double well

Coleman's method can be applied to finding the ground state tunneling splitting in a symmetric double well [Vainshtein et al. 1982], for some

$$V(x) = \lambda(x^2 - x_0^2)^2 . \tag{3.66}$$

It is expedient again, as in the previous subsection, to study the partition function Z in the limit $\beta \to \infty$, which is now real. The extremal trajectories satisfying (3.34) are composed of "single passes" or "kinks" and "antikinks". During a single kink the particle spends an infinite time on sliding from the upside-down potential top $x = -x_0$, crosses the barrier region $x \sim 0$ during some finite time and then approaches the point $x = x_0$ during an infinite time. The same event reiterated in the reverse order is antikink. For the potential (3.66) the kink (antikink) is described by

$$x_k(\tau) = \pm x_0 \tanh \tfrac{1}{2}\omega_0(\tau - \tau_c) , \qquad \omega_0 = (8\lambda x_0^2)^{1/2} , \quad 0 < \tau_c < \beta , \tag{3.67}$$

where ω_0 is the frequency of classical vibrations in the well near $x = \pm x_0$, and τ_c is an arbitrary position of the kink center. The single kink action S_k is independent of τ_c:

$$S_k = \int_{-x_0}^{x_0} dx\, [2V(x)]^{1/2} = \omega_0^3/12\lambda . \tag{3.68}$$

*) Strictly speaking, the concept of k_c itself makes no sense for a potential like the Eckart one, unless one artificially introduces Z_0 as the partition function of a bound initial state, which is not described by this potential. That is to say, it is reasonable to consider the combination kZ_0, not k alone.

**) It is the symmetric situation that has been studied by Gillan [1987] and by Voth et al. [1989b].

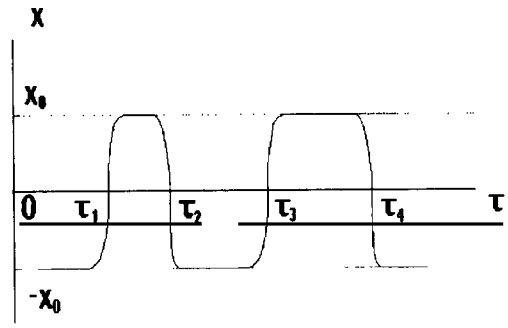

Fig. 22. "Instanton gas".

Each extremal trajectory includes n kink–antikink pairs, where n is an arbitrary integer, and the kink centers are placed at the moments $0 < \tau_1 < \cdots < \tau_{2n} < \beta$ forming the "instanton gas" (fig. 22). Its contribution to the overall path integral may be calculated in exactly the same manner as was done in the previous subsection, with the assumption that the instanton gas is dilute, i.e., the kinks are independent of each other,

$$Z_n = \int_0^\beta d\tau_1 \int_{\tau_{2n-1}}^\beta d\tau_{2n} (\tfrac{1}{2}\Delta)^{2n} = \frac{\beta^{2n}}{(2n)!} (\tfrac{1}{2}\Delta)^{2n} , \tag{3.69}$$

$$\tfrac{1}{2}\Delta = \left(\frac{S_k}{2\pi}\right)^{1/2} \left| \frac{\det'(-\partial_\tau^2 + d^2V/dx^2)_{kink}}{\det(-\partial_\tau^2 + \omega_0^2)} \right|^{-1/2} \exp(-S_k) . \tag{3.70}$$

With Z_0 given by (3.45), summation of all the terms in (3.69) gives

$$Z = Z_0 \left(1 + \sum_{n=1}^{\infty} Z_n\right) = Z_0 \cosh(\tfrac{1}{2}\beta\Delta) . \tag{3.71}$$

What we obtained in (3.71) is the partition function of a two-level system, the levels having energies $\frac{1}{2}\omega_0 \pm \frac{1}{2}\Delta$. Hence (3.70) gives us the desired ground state tunneling splitting Δ. The analytical continuation of relation (3.71) to real time (imaginary β) leads to the two-level system propagator oscillating as $\cos(\frac{1}{2}\Delta t)$. This picture corresponds to coherent oscillations of the probability to find a particle in one of the wells with frequency Δ.

Consider in more detail the calculation of the determinant in (3.70) for the potential (3.66). The eigenvalue equation

$$(-\partial_\tau^2 + d^2V/dx^2)x_n(\tau) = -\partial^2 x_n/\partial\tau^2 + \omega_0^2[1 - \tfrac{3}{2}\operatorname{sech}^2(\tfrac{1}{2}\omega_0\tau)]x_n = \varepsilon_n x_n(\tau) \tag{3.72}$$

is formally equivalent to the stationary Schrödinger equation for the inverted Eckart potential, the exact solution of which is well known [Landau and Lifshitz 1981]. The spectrum of bound states satisfies the relation $(\omega_0^2 - \varepsilon_n)^{1/2} = \omega_0(1 - \frac{1}{2}n)$, $n = 0, 1, \ldots$, and, therefore, there are only two bound states $n = 0, 1$ with eigenvalues $\varepsilon_0 = 0$ and $\varepsilon_1 = \frac{3}{4}\omega_0^2$. The normalized zero mode with $\varepsilon_0 = 0$

is given by

$$x_0(\tau) = (\tfrac{3}{8}\omega_0)^{1/2}\,\mathrm{sech}^2[\tfrac{1}{2}\omega_0(\tau - \tau_c)]\,. \tag{3.73}$$

Equation (3.73) may also be obtained from (3.42). The contribution of x_1 to the ratio of determinants in (3.70) is equal to $\frac{3}{4}$. Apart from the bound states, there is a continuous spectrum of eigenvalues ε_n whose contribution to (3.70) may be shown [Vainshtein et al. 1982] to equal $\frac{1}{12}$. Finally (3.70) gives

$$\Delta = (\omega_0/\pi)(2\pi\,\omega_0^3/\lambda)^{1/2}\exp(-\omega_0^3/12\lambda)\,. \tag{3.74}$$

A disadvantage of this method is that it applies to the lowest energy doublet only. It is natural to calculate the tunneling splittings of the highest energy levels with the same method as in section 3.2. Following Miller [1979], we consider a more general situation of a double well, which is not necessarily symmetric. The spectral function $g(E)$ in (3.25a) comes from summation over closed classical trajectories with energy E. Each such trajectory is composed of the vibrations in the classically accessible regions (1) and (3) and the imaginary-time orbits in the barrier region (2) (see fig. 3, replacing Q by x).

Introducing the phases

$$W_1(E) = 2\int_{x_1'}^{x_1} \mathrm{d}x\,[2(E - V(x))]^{1/2} - \pi\,, \qquad \mathrm{i}W_2 = 2\int_{x_1}^{x_2} \mathrm{d}x\,[2(E - V(x))]^{1/2}\,,$$

$$W_3(E) = 2\int_{x_2}^{x_2'} \mathrm{d}x\,[2(E - V(x))]^{1/2} - \pi\,, \tag{3.75}$$

and, in view of exponential smallness of $\exp(-W_2)$ neglecting the multiple crossings of the barrier, one obtains for $g(E)$

$$g(E) \propto \frac{\exp(\mathrm{i}W_1)}{1 - \exp(\mathrm{i}W_1)} - \exp(-W_2)\,\frac{\exp[\mathrm{i}(W_1 + W_3)]}{[1 - \exp(\mathrm{i}W_1)]^2[1 - \exp(\mathrm{i}W_3)]}\,. \tag{3.76}$$

For a symmetric potential $W_1 = W_3 = W(E)$. Approximating $W(E)$ near the nth energy level E_n of an isolated well by

$$W(E) = 2\pi n + [\mathrm{d}W/\mathrm{d}E]_{E=E_n}(E - E_n)\,, \tag{3.77}$$

so that the Bohr–Sommerfeld condition holds at $E = E_n$, one gets $g(E)$ as

$$g(E) \propto \frac{1}{E - E_n} + \left[\frac{\mathrm{d}W}{\mathrm{d}E}\right]_{E=E_n}^{-2}\frac{\exp(-W_2)}{(E - E_n)^3} \simeq \frac{1}{2}\left(\frac{1}{E - E_n - \frac{1}{2}\Delta_n} + \frac{1}{E - E_n + \frac{1}{2}\Delta_n}\right), \tag{3.78}$$

and the tunneling splitting of the nth energy level equals

$$\Delta_n = [2/W'(E_n)]\exp(-\tfrac{1}{2}W_2) = (2/\tau_n)\exp(-\tfrac{1}{2}W_2)\,, \tag{3.79}$$

where τ_n is the period of classical vibrations in the well with energy E_n.

This formula resembles (3.32) and, as we shall show in due course, this similarity is not accidental. Note that at $n = 0$ the short action $\frac{1}{2}W_2(E_0)$ taken at the ground state energy E_0 is not equal to the kink action S_k (3.68). Since in the harmonic approximation for the well $\tau_0 = 2\pi/\omega_0$, this difference should be compensated by the prefactor in (3.74), but, generally speaking, expressions (3.74) and (3.79) are not identical because eq. (3.79) uses the semiclassical approximation for the ground state, while (3.74) does not.

Let now the potential be asymmetric. If E_1 and E_2 are the individual energy levels in each well so that $W_1(E_1) = 2\pi n_1$ and $W_2(E_2) = 2\pi n_2$, then (3.76) becomes

$$g(E) \propto \frac{1}{E - E_1} + \frac{\exp(-W_2)}{(E - E_1)^2(E_1 - E_2)}[W_1'(E_1)W_2'(E_2)]^{-1}\,. \tag{3.80}$$

Comparing this with $g(E) \propto (E - E_1 - \Delta E)^{-1}$ at $\Delta E \ll |E_1 - E_2|$ one obtains for the shift of the energy level

$$\Delta E = [(E_1 - E_2)W_1'(E_1)W_2'(E_2)]^{-1}\exp(-W_2) = [(E_1 - E_2)\tau_1\tau_2]^{-1}\exp(-W_2)$$

$$= (\omega_1/2\pi)(\omega_2/2\pi)(E_1 - E_2)^{-1}\exp(-W_2)\,, \tag{3.81}$$

where ω_1 and ω_2 are the frequencies of vibrations in the wells. The same procedure performed near $E = E_2$ gives $\Delta E_1 = -\Delta E_2$.

To gain physical insight into the asymmetric situation let us compare Miller's result (3.81) with that obtained by considering a formal two-state problem with the matrix Hamiltonian,

$$\begin{pmatrix} E_1 & V_{12} \\ V_{21} & E_2 \end{pmatrix}. \tag{3.82}$$

If $|V_{12}| \ll |E_1 - E_2|$, then the shift of an energy level appears in the second order in V_{12}, and it equals

$$\Delta E = |V_{12}|^2/(E_1 - E_2)\,. \tag{3.83}$$

Comparing this expression with (3.81), one obtains the formal definition of the quasiclassical tunneling matrix element

$$|V_{12}|^2 = (\omega_1/2\pi)(\omega_2/2\pi)\exp(-W_2)\,. \tag{3.84}$$

This definition is also valid in the symmetric case ($E_1 = E_2$) when $V_{12} = \frac{1}{2}\Delta = (2\pi)^{-1} \times \omega_1 \exp(-\frac{1}{2}W_2)$.

In the time-dependent perturbation theory [Landau and Lifshitz 1981] the transition probability from the state 1 to 2 is related with the perturbation by the golden rule,

$$\Gamma = 2\pi|V_{12}|^2\rho_2 \,. \tag{3.85}$$

Inserting V_{12} from (3.84) into (3.85) and taking into account that the density of the energy levels in the final state ρ_2 is equal to ω_2^{-1} one obtains eq. (3.32) for the decay of the metastable state. Strictly speaking, the solution for the time-dependent Shrödinger equation for a double well would provide coherent oscillations of probability to find the particle in the chosen well, rather than exponential decay. Expression (3.85) comes about either for a metastable state or when there is an additional mechanism destroying the phase coherence, resulting from interaction with other degrees of freedom (the bath). We shall further discuss this problem in section 5.

3.5. Nonadiabatic tunneling

The previous treatment relied on the assumption that the transition occurs on a single potential energy surface $V(x)$ characterized by a barrier separating two wells. This potential is actually created from the terms of the initial and final electronic states. The separation of electron and nuclear coordinates in each of these states gives rise to the diabatic basis with nondiagonal Hamiltonian matrix

$$H = \tfrac{1}{2}p^2\mathbf{1} + \begin{pmatrix} V_i(x) & V_d(x) \\ \tilde{V}_d(x) & V_f(x) \end{pmatrix}, \tag{3.86}$$

where $\mathbf{1}$ is the 2×2 unit matrix. The off-diagonal matrix elements are significant in the vicinity of the crossing point x_c such that $V_i(x_c) = V_f(x_c)$. Diagonalization of (3.86) gives the adiabatic terms

$$V_\pm(x) = \tfrac{1}{2}[V_i(x) + V_f(x)] \pm \tfrac{1}{2}\{[V_i(x) - V_f(x)]^2 + 4V_d^2(x)\}^{1/2} \,, \tag{3.87}$$

which are separated at the crossing point by the adiabatic splitting $2|V_d|$ (fig. 23).

The usual tunneling problem we considered earlier is associated with the situation when this splitting is so large that the influence of the upper term V_+ can be neglected, and tunneling occurs in

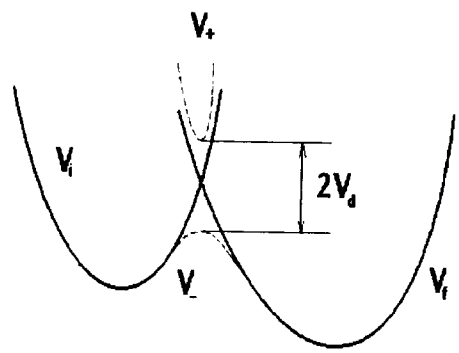

Fig. 23. Diabatic terms of initial and final states (solid lines) and adiabatic terms (dashed lines). Adiabatic splitting is $2V_d$.

the potential V_-. It is obvious, however, that when $V_d = 0$, any transition between non-interacting terms cannot occur at all. Therefore, the relationship between adiabatic splitting and the tunneling probability requires a special study. For a classical transition this is the well known Landau–Zener–Stueckelberg problem [Landau 1932; Zener 1932; Stueckelberg 1932], which has been investigated in detail in molecular collision theory (see, e.g., Child [1974], Nakamura [1991]).

With the assumption that near x_c the diabatic terms are linear, and V_d is independent of x, the probability of transition between the diabatic terms at $E > V_+(x_c)$ depends on the parameter

$$\delta = |V_d|^2/v|F_1 - F_2| , \tag{3.88}$$

where F_1 and F_2 stand for the slopes of the terms, and v is the velocity of classical motion at $x = x_c$, given by

$$B_0(\delta) = 1 - \exp(-2\pi\delta) . \tag{3.89}$$

At $\delta > 1$, $B_0 \sim 1$ and the transition occurs along the lower adiabatic term V_-. At $\delta \ll 1$, $B_0 = 2\pi\delta$, and there is a large probability that the particle passes the crossing point remaining on the initial diabatic term. This is the case when the perturbation theory in V_d is valid yielding the golden rule formula. With increasing energy, the parameter δ decreases thus enhancing non-adiabatic effects.

The problem of nonadiabatic tunneling in the Landau–Zener approximation has been solved by Ovchinnikova [1965]. For further refinements of the theory beyond this approximation see Laing et al. [1977], Holstein [1978], Coveney et al. [1985], Nakamura [1987]. The nonadiabatic transition probability for a more general case of dissipative tunneling is derived in appendix B. We quote here only the result for the dissipationless case obtained in the Landau–Zener limit. When $E < V_-(x_c)$, the total transition probability is the product of the adiabatic tunneling rate, calculated in the previous sections, and the Landau–Zener–Stueckelberg-like factor

$$B = 2\pi\delta^{-1}e^{-2\delta}\delta^{2\delta}/\Gamma^2(\delta) , \tag{3.90}$$

where δ is defined by (3.88) but the classical velocity is replaced by the absolute value of imaginary-time instanton velocity,

$$v = \{2[V_-(x_c) - E]\}^{1/2} . \tag{3.91}$$

According to (3.91), non-adiabaticity increases with decreasing energy, as opposed to the classical case. This is a straightforward consequence of the Wick rotation (3.10).

According to the general ideas formulated in sections 2.3 and 3.4 [see especially eqs. (3.84) and (3.85) and appendix B], the incoherent tunneling rate is proportional to the square of the tunneling splitting. Therefore, when the diabatic terms are symmetric with respect to the crossing point, the tunneling splitting is the product of the factor $B^{1/2}$ and the splitting in the lower adiabatic potential, V_-, Δ_{ad},

$$\Delta = \Delta_{ad}(2\pi)^{1/2}\delta^{-1/2}e^{-\delta}\delta^{\delta}/\Gamma(\delta) . \tag{3.92}$$

In the nonadiabatic regime Δ is proportional to the adiabatic splitting $2|V_d|$. The instanton trajectory crosses the barrier twice, each time bringing the factor Δ/Δ_{ad} associated with the probability to cross the nonadiabaticity region remaining on the same adiabatic term (and thus

jumping from one diabatic term to the other). These two crossings result in the prefactor (3.90) when tunneling is incoherent.

3.6. *Quantum transition state theory*

So far we have considered two limiting cases of transition, the decay of a metastable state and quantum probability oscillations in a double well, of which only the first case permits the use of the concept of the rate constant. The latter, in general, describes the relaxation of a chemical system initially deviated from its equilibrium between reactants and products. According to the Onsager regression hypothesis (see, e.g., Chandler [1987]), this relaxation may be expressed in terms of fluctuations in the equilibrium system. The regression hypothesis together with the fluctuation–dissipation theorem (FDT) leads to the Kubo linear-response theory [Kubo 1957; Kubo and Nakajima 1957], which was first applied to chemistry by Yamamoto [1960]. The decay of the reactant concentration $a(t)$ is characterized by the time-correlation function

$$[a(t) - a(0)]/a(0) = \langle \delta a(t)\, \delta a(0)\rangle / \langle [\delta a(0)]^2 \rangle = \exp(-kt) \,. \tag{3.93}$$

Since the decay is associated with passing through the barrier, the quantity $a(t)$ is nothing but the step function $a = \theta(x^{\#} - x)$. Differentiating (3.93) and finally setting $t = 0$ one obtains [Chandler 1987] the expression for the rate constant,

$$k = -\langle a \rangle^{-1} \langle \dot{x}(0) \delta(x - x^{\#}) \theta(x^{\#} - x) \rangle \,. \tag{3.94}$$

CLTST follows from (3.94) after totally neglecting correlations between the flux $\dot{x}(0)$ and the concentration,

$$k_{\mathrm{CLTST}} = \tfrac{1}{2} \langle a \rangle^{-1} \langle \dot{x}(0) \rangle \langle \delta(x - x^{\#}) \rangle \,, \quad \langle \dot{x}(0) \theta(x^{\#} - x) \rangle \equiv -\tfrac{1}{2} \langle \dot{x}(0) \rangle \,, \tag{3.95}$$

where the identity of the second equation in (3.95) shows that the θ function selects the direction of the flux. The relation (2.2) that we gave earlier is nothing but (3.95) written for a canonical ensemble.

A consistent quantal TST (QTST) has been worked out by Miller and coworkers [Miller 1974; Miller et al. 1983; Tromp and Miller 1986; Voth et al. 1989a]. In quantum mechanics the classical flux $\dot{x}$ is replaced by the symmetrized flux operator

$$\hat{F} = \tfrac{1}{2} [\hat{p} \delta(x - x^{\#}) + \delta(x - x^{\#}) \hat{p}] \,, \quad \hat{p} = -\mathrm{i} \partial / \partial x \,. \tag{3.96}$$

It is readily checked that the matrix elements of the flux operator between two states are

$$|\langle n | \hat{F} | n' \rangle|^2 = \tfrac{1}{4} |\psi_n(x^{\#}) \psi'_{n'}(x^{\#}) - \psi'_n(x^{\#}) \psi_{n'}(x^{\#})|^2 \,.$$

Further, the step function $\theta(x(t) - x^{\#})$ is replaced by the projection operator $\hat{p}$ selecting the states which evolve finally to the product valley at $t \to \infty$,

$$\hat{P} = \lim_{t \to \infty} \exp(\mathrm{i}\hat{H}t)\, \theta(x - x^{\#}) \exp(-\mathrm{i}\hat{H}t) \,. \tag{3.97}$$

Its equivalent representation is [Miller et al. 1983]

$$\hat{P} = \lim_{t\to\infty} \exp(\mathrm{i}\hat{H}t)\,\theta(p)\exp(-\mathrm{i}\hat{H}t)\,. \tag{3.98}$$

The identity of (3.97) and (3.98) means that the particle hits the product valley only having crossed the dividing surface $x = x^{\#}$ from left to right. If we were to use simply the step function $\theta(x - x^{\#})$, we would be neglecting the recrossings of the dividing surface.

At last, the formally exact quantal expression for the rate constant is

$$k = Z_0^{-1} \lim_{t\to\infty} \mathrm{Tr}[\exp(-\beta\hat{H})\,\hat{F}\hat{P}]\,. \tag{3.99}$$

Using the fact that the symmetrized flux operator commutes with the density matrix, and representing the latter as $\exp(-\beta\hat{H}) \equiv \exp(-\lambda\hat{H})\exp[-(\beta-\lambda)\hat{H}]$, one may rewrite (3.99) as

$$k = Z_0^{-1} \lim_{t\to\infty} \mathrm{Tr}\{\hat{F}\exp[\mathrm{i}\hat{H}(t+\mathrm{i}\lambda)]\,\theta(x-x^{\#})\exp[-\mathrm{i}\hat{H}(t-\mathrm{i}(\beta-\lambda))]\}\,. \tag{3.100}$$

It is usual to take $\lambda = \beta/2$, and, after some manipulations, the following expressions for k can be obtained:

$$k = Z_0^{-1} \int_0^{\infty} \mathrm{d}t\, C_{\mathrm{f}}(t) = \lim_{t\to\infty} C_{\mathrm{fx}}(t) = \lim_{t\to\infty} \frac{\mathrm{d}}{\mathrm{d}t} C_{\mathrm{x}}(t) \tag{3.101}$$

where the flux–flux correlation function C_{f} is defined by

$$C_{\mathrm{f}}(t) = \mathrm{Tr}[\hat{F}\exp(\mathrm{i}\hat{H}t_{\mathrm{c}}^{*})\,\hat{F}\exp(-\mathrm{i}\hat{H}t_{\mathrm{c}})]\,, \quad t_{\mathrm{c}} = t - \mathrm{i}\tfrac{1}{2}\beta\,. \tag{3.102}$$

The cross correlation function of position and flux C_{fx},

$$C_{\mathrm{fx}}(t) = \mathrm{Tr}[\hat{F}\exp(\mathrm{i}\hat{H}t_{\mathrm{c}}^{*})\,\theta(x-x^{\#})\exp(-\mathrm{i}\hat{H}t_{\mathrm{c}})]\,, \tag{3.103}$$

and the left–right spatial correlation function C_{x},

$$C_{\mathrm{x}}(t) = \mathrm{Tr}[\theta(x^{\#}-x)\exp(\mathrm{i}\hat{H}t_{\mathrm{c}}^{*})\,\theta(x-x^{\#})\exp(-\mathrm{i}\hat{H}t_{\mathrm{c}})]\,, \tag{3.104}$$

are related with C_{f} by

$$C_{\mathrm{f}}(t) = \mathrm{d}C_{\mathrm{fx}}/\mathrm{d}t = \mathrm{d}^2C_{\mathrm{x}}/\mathrm{d}t^2\,. \tag{3.105}$$

According to (3.95), CLTST approximates $C_{\mathrm{f}}(t)$ by the δ-function, being, in a sense, a zero-time limit of the first of the equations (3.101). In the representation of eigenfunctions $|n\rangle$, $|n'\rangle$ the flux–flux correlation function equals

$$C_{\mathrm{f}}(t) = \sum_{n,n'} \exp[-\tfrac{1}{2}\beta(E_n + E_{n'})]\cos[(E_n - E_{n'})t]\,|\langle n|\hat{F}|n'\rangle|^2\,, \tag{3.106}$$

so that the rate constant is

$$k = \pi Z_0^{-1} \sum_{n,n'} \exp(-\beta E_n) |\langle n|\hat{F}|n'\rangle|^2 \delta(E_n - E_{n'}) . \tag{3.107}$$

The correlation functions (3.102)–(3.104) may be written out explicitly in terms of the propagator $K(x_f, x_i|t_c)$ [Miller et al. 1983] and, in particular, for a parabolic barrier one has

$$C_f = \frac{1}{2\pi\beta} \frac{\beta\omega^{\#}/2}{\sin(\frac{1}{2}\beta\omega^{\#})} \exp(-\beta V_0) \frac{\omega^{\#} \sin^2(\frac{1}{2}\beta\omega^{\#}) \cosh(\omega^{\#} t)}{[\sin^2(\frac{1}{2}\beta\omega^{\#}) + \sinh^2(\omega^{\#} t)]^{3/2}} , \tag{3.108}$$

which after integration over time gives the Wigner formula (2.11). The function C_f falls off exponentially with a characteristic time close to $1/\omega^{\#}$.

The introduced correlation functions may be expressed with the use of path integrals. Consider, for one, the function C_x. Its explicit form is

$$\begin{aligned} C_x(t) &= -\operatorname{Tr}\{\exp(-\beta\hat{H})\,\theta(x - x^{\#}) \exp[i\hat{H}(t + i\lambda)]\,\theta(x - x^{\#}) \exp[-i\hat{H}(t + i\lambda)]\} \\ &= -\langle h(0)\, h(t + i\lambda)\rangle , \end{aligned} \tag{3.109}$$

where $h(t)$ is the $\theta(x - x^{\#})$ operator in the Heisenberg representation $h(t) = \exp(i\hat{H}t)\,\theta(x - x^{\#}) \times \exp(-i\hat{H}t)$. Since the result does not depend on λ, it can be rewritten by the use of the Kubo transform [Kubo 1957]

$$C_x(t) = -\beta^{-1} \int_0^{\beta} d\lambda \langle h(0)\, h(t + i\lambda)\rangle . \tag{3.110}$$

For purely imaginary time $t = i\tau$ the correlator in (3.110) is expressible via the path integral

$$\langle h(0)\, h(\tau)\rangle = Z_0^{-1} \int D[x(\tau)] \exp(-S[x(\tau)])\,\theta(x(0) - x^{\#})\theta(x(\tau) - x^{\#}) , \tag{3.111}$$

where the integration is performed over all closed β-periodic paths. The complex-time correlation function then may be looked for by analytically continuing (3.111). For example, this correlator is readily calculated for a symmetric double well by use of the instanton method of section 3.4 to give [Gillan 1987]

$$\langle h(0)\, h(\tau)\rangle = \cosh[\tfrac{1}{2}\beta\Delta - i(t + i\lambda)\Delta]/\cosh(\tfrac{1}{2}\beta\Delta) \tag{3.112}$$

This correlation function oscillates in real time thus providing no rate constant, as it should be expected for coherent tunneling. This reveals the deficiency of the one-dimensional model, in which the rate constant, strictly speaking, can be obtained only for an unbound initial or final state, i.e., for a gas-phase reaction. In general, the analytical continuation of the imaginary-time correlator is hardly justifiable, especially for long times ($\beta \to \infty$). The real-time correlation function, represented by a triple path integral, has been given by Voth et al. [1989a, b].

Although the correlation function formalism provides formally exact expressions for the rate constant, only the parabolic barrier has proven to be analytically tractable in this way. It is difficult to consistently follow up the relationship between the flux–flux correlation function expression and the semiclassical Im F formulae at $\beta \to \infty$. So far, the correlation function approach has mostly been used for fairly high temperatures in order to accurately study the quantum corrections to CLST, while the behavior of the functions C_f, C_{fx} and C_x far below T_c has not been studied. A number of papers have appeared (see, e.g., Tromp and Miller [1986], Makri [1991]) implementing the correlation function formalism for two-dimensional PES.

For example, the rate constant of the collinear reaction $H + H_2$ has been calculated in the temperature interval 200–1000 K. The quantum correction factor, i.e., the ratio of the actual rate constant to that given by CLTST, has been found to reach ~ 50 at $T = 200$ K. However, in the reactions that we regard as low-temperature ones, this factor may be as large as ten orders of magnitude (see introduction). That is why the present state of affairs in QTST, which is well suited for finding quantum contributions to gas-phase rate constants, does not presently allow one to use it as a numerical tool to study complex low-temperature conversions, at least without further approximations such as the WKB one.*)

4. Two-dimensional tunneling

The discussion so far has dealt with one-dimensional models which as a rule do not directly apply to real chemical systems for the reasons discussed in the introduction. In this section we discuss how the above methods can be extended to many dimensions. In order not to encumber the text and in order to make physics more transparent, we confine ourselves to two dimensions, although the generalization to more dimensions is straightforward.

From the very simple WKB considerations it is clear that the tunneling rate is proportional to the Gamov factor $\exp\{-2\int[2(V(s(\boldsymbol{Q})) - E)]^{1/2}\,\mathrm{d}s\}$, where $s(\boldsymbol{Q})$ is a path in two dimensions ($\boldsymbol{Q} = \{Q_1, Q_2\}$) connecting the initial and final states. The "most probable tunneling path", or instanton, which renders the Gamov factor maximum, represents a compromise of two competing factors, the barrier height and its width. That is, one has to optimise the instanton path not only in time, as has been done in the previous section, but also in space. This complicates the problem so that numerical calculations are usually needed.

4.1. Decay of metastable state

Again we use the Im F method in which the tunneling rate is determined by the nontrivial instanton paths which extremize the Eucledian action in the barrier. Let for definiteness the potential $V(\boldsymbol{Q})$ have a single minimum at $\boldsymbol{Q} = 0$, $V(0) = 0$, separated from the continuous spectrum

*) Near completion of this review, we learned of very promising QTST results obtained by Topaler and Makri [1993] based on the recently developed quasiadiabatic propagator techniques [Makri 1992; Topaler and Makri 1992]. If the multidimensional Hamiltonian can be formulated as that of a system interacting with a harmonic bath, and if it exhibits an exponential relaxation towards equilibrium, their method permits one to advance much further into the low-temperature domain, and to consider tunneling from the ground state of the system, staying within the flux–flux autocorrelator formalism.

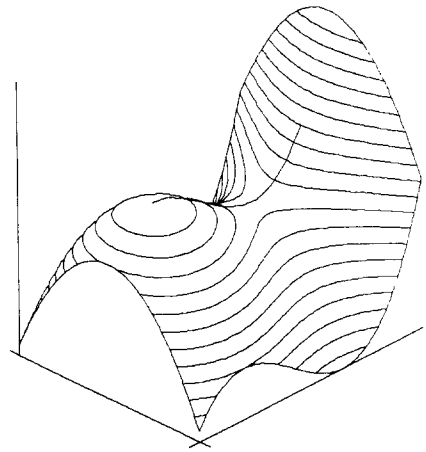

Fig. 24. Instanton trajectory on two-dimensional upside-down PES.

by a high barrier. The extrema of the action,

$$S[\boldsymbol{Q}(\tau)] = \int_0^\beta \mathrm{d}\tau \left[\tfrac{1}{2}\dot{Q}_1^2 + \tfrac{1}{2}\dot{Q}_2^2 + V(Q_1, Q_2)\right], \tag{4.1}$$

are the instanton trajectories subject to the equations

$$\mathrm{d}^2 Q_i/\mathrm{d}\tau^2 = \partial V/\partial Q_i \,. \tag{4.2}$$

These equations form a fourth-order system of differential equations which cannot be solved analytically in almost all interesting nonseparable cases. Further, according to these equations, the particle slides from the "hump" of the upside-down potential $-V(\boldsymbol{Q})$ (see fig. 24), and, unless the initial conditions are specially chosen, it exercises an infinite aperiodic motion. In other words, the instanton trajectory with the required periodic boundary conditions,

$$\boldsymbol{Q}(\tau) = \boldsymbol{Q}(\tau + \beta)\,, \tag{4.3}$$

is unstable with respect to all deviations except the time shift.

Once the instanton trajectory has been numerically found, one proceeds to the calculation of prefactor, which amounts to finding determinants of differential operators. The direct two-dimensional generalization of (3.46) is

$$k = \left(\frac{S_0}{2\pi}\right)^{1/2} \left| \frac{\det'(-\partial_\tau^2 \mathbf{1} + \partial^2 V/\partial Q_i\, \partial Q_j)_{\mathrm{ins}}}{\det(-\partial_\tau^2 \mathbf{1} + K_0)} \right|^{-1/2} \exp(-S_{\mathrm{ins}})\,, \tag{4.4}$$

where $\partial_\tau^2 \mathbf{1}$ is the second-derivative operator multiplied by the unit 2×2 matrix, K_0 the matrix of the form

$$K_0 = \begin{pmatrix} \omega_+^2 & 0 \\ 0 & \omega_-^2 \end{pmatrix}, \tag{4.5}$$

with the squares of the well eigenfrequencies, $\omega_+^2 > \omega_-^2$, on the diagonal. This matrix is simply the diagonal form of the matrix $\partial V/\partial Q_i\,\partial Q_j$, taken at the point $\boldsymbol{Q} = 0$. The same matrix enters into the numerator in (4.4) where it is taken on the instanton trajectory. The action S_0 is

$$S_0 = \int_0^\beta \mathrm{d}\tau(\dot{Q}_1^2 + \dot{Q}_2^2)\,. \tag{4.6}$$

It is interesting to pause now and to highlight some features of the two-dimensional instanton. Let us introduce the local normal coordinates about the potential minimum Q_+ and Q_-, corresponding to the higher and lower vibration frequencies ω_+ and ω_-. The asymptotic behavior of the instanton solution at $\beta \to \infty$, $\tau \to 0$, is described by $Q_\pm = Q_\pm^0 \cosh(\omega_\pm \tau)$ (see appendix A), where Q_+^0 goes to zero faster than Q_-^0 so as to keep $Q_\pm$ finite. Therefore, the asymptotic instanton direction coincides with Q_-. The conclusion we have arrived at is what may be called a "generalized Fukui theorem" (see Tachibana and Fukui [1979]) stating that the reaction path near the minimum goes along the direction of the lowest eigenfrequency. When the temperature is raised, i.e. the period decreases, the instanton amplitude decreases until the trajectory collapses to a point (the saddle point). At the saddle point $\boldsymbol{Q}^\#$ the potential has two normal frequencies, the imaginary longitudinal $\mathrm{i}\omega^\#$, and transverse $\omega_t^\#$. Thus we expect the cross-over temperature to be

$$T_c = \omega^\#/2\pi\,, \tag{4.7}$$

This formula, however, tacitly supposes that the instanton period depends monotonically on its amplitude so that the zero-amplitude vibrations in the upside-down barrier possess the smallest possible period $2\pi/\omega^\#$. This is obvious for sufficiently nonpathological one-dimensional potentials, but in two dimensions this is not necessarily the case. Benderskii et al. [1993] have found that there are certain cases of strongly "bent" two-dimensional PES when the instanton period has a minimum at a finite amplitude. Therefore, the cross-over temperature, formally defined as the lowest temperature at which the instanton still exists, turns out to be higher than that predicted by (4.7). At $T > T_c$ the trivial solution $\boldsymbol{Q} \equiv \boldsymbol{Q}^\#$ ($\boldsymbol{Q}^\#$ is the saddle-point coordinate) emerges instead of instanton, the action equals $S = \beta V^\#$ (where $V^\#$ is the barrier height at the saddle point) and the Arrhenius dependence $k \propto \exp(-\beta V^\#)$ holds.

Although eq. (4.4) gives the formal instanton expression for the rate constant, it is hard to apply directly, because the numerical evaluation of an infinite product of eigenvalues of the differential operator is a rather challenging problem. It is very tempting to reduce the ratio of determinants in (4.4) to something like (3.48). That formula, however, is written solely for one dimension. The way out is to divide (4.4) into transverse and longitudinal parts and to deal with them separately. Namely, we introduce the coordinate s, running along the instanton path, and x, measuring the deviation away from the instanton path. The fluctuations around the instanton trajectory are of two types. The "temporal" or "longitudinal" fluctuations affect only the s-motion keeping x zero. It is this sort of fluctuations that is present in one dimension, leading to (3.46) and (3.48). The transverse fluctuations, lead, as it were, to a finite spatial width of the instanton trajectory, spreading it to a "channel". If this channel is narrow enough, one may use the local harmonic expansion around the points of the instanton trajectory, and it is this expansion that results in the ratio of determinants in (4.4).

In the new coordinates the action, expanded up to quadratic terms, reads

$$S = S_{\mathrm{ins}} + \tfrac{1}{2}\int_0^\beta \delta s(\tau)\,[-\partial_\tau^2 + \partial^2 V/\partial s^2]\,\delta s(\tau)\,\mathrm{d}\tau + \tfrac{1}{2}\int_0^\beta \delta x(\tau)\,[-\partial_\tau^2 + \omega_{\mathrm{t}}^2(s(\tau))]\,\delta x(\tau)\,\mathrm{d}\tau\,, \tag{4.8}$$

where ω_{t} is an s-dependent "transverse vibration frequency", which results from the canonical transformation from the coordinates $\{Q_1, Q_2\}$ to $\{s, x\}$. Its explicit expression in terms of the original potential $V(\boldsymbol{Q})$ can in principle be obtained by the method of Someda and Nakamura [1991], but, as will be seen later, one does not actually need it. There is also an important case when the coordinates s and x are known in advance, without solving the instanton equations of motion, so that the potential is approximately separable, and ω_{t} is the actual transverse frequency with respect to the reaction path s, $\omega_{\mathrm{t}}(s) = \partial^2 V/\partial x^2$.

The most remarkable feature of expression (4.8) is that it does not contain any cross terms $\delta x\,\delta s$. This is a consequence of time-shift invariance of the instanton solution ($\mathrm{d}^2 s/\mathrm{d}\tau^2 = \partial V/\partial s$, $x \equiv 0$). This fact can be expressed as invariance of the action with respect to the infinitesimal transformation $s \to s + c\dot{s}$, $c \to 0$ [cf. eq. (3.42)]. In the new coordinates the determinants break up into longitudinal and transverse parts and (4.4) becomes

$$k = B_{\mathrm{t}} k_{1\mathrm{D}}\,, \tag{4.9}$$

where the "one-dimensional" rate constant equals

$$k_{1\mathrm{D}} = \left(\frac{S_0}{2\pi}\right)^{1/2} \left|\frac{\det'(-\partial_\tau^2 + \partial^2 V/\partial s^2)_{\mathrm{ins}}}{\det(-\partial_\tau^2 + \omega_-^2)}\right|^{-1/2} \exp(-S_{\mathrm{ins}}) \tag{4.10}$$

and the transverse prefactor is

$$B_{\mathrm{t}} = \left(\frac{\det(-\partial_\tau^2 + \omega_{\mathrm{t}}^2)}{\det(-\partial_\tau^2 + \omega_+^2)}\right)^{-1/2}. \tag{4.11}$$

The zero mode, associated with the longitudinal fluctuations, is now put into (4.10), while, when $\omega_{\mathrm{t}} > 0$, the determinants in (4.11) do not suffer from the zero-mode problem. The value $k_{1\mathrm{D}}$ is nothing but the rate of tunneling (3.46) in the dynamical one-dimensional barrier $V(s)$ along the instanton trajectory. As for B_{t}, it incorporates the effect of transverse vibrations around the instanton trajectory. In order to calculate (4.10), one may employ the apparatus of section 3 designed for one-dimensional tunneling. In particular, now it is possible to make use of (3.48) together with (3.45), which gives

$$k_{1\mathrm{D}} = (2/\pi)^{1/2} \sinh(\tfrac{1}{2}\omega_- \beta)\,|\partial E/\partial \beta|^{1/2} \exp(-S_{\mathrm{ins}})\,. \tag{4.12}$$

We proceed now to the calculation of B_{t}, following [Benderskii et al. 1992a]. The denominator in (4.11) (apart from normalization) is equal to the harmonic-oscillator partition function $[2\sinh(\frac{1}{2}\omega_+ \beta)]^{-1}$. The numerator is the product of the ε_n satisfying an equation of the Shrödinger type

$$[-\partial_\tau^2 + \omega_{\mathrm{t}}^2(\tau)]\,x_n(\tau) = \varepsilon_n x_n(\tau)\,, \qquad x_n(\tau + \beta) = x_n(\tau)\,. \tag{4.13}$$

Consider a more general eigenvalue equation without imposing the periodic boundary condition,

$$[-\partial_\tau^2 + \omega_t^2(\tau)]x(\tau) = \varepsilon(z)x(\tau) . \tag{4.14}$$

According to the Floquet theorem [Arnold 1978], this equation has a pair of linearly-independent solutions of the form $x(z,\tau) = u(z, \pm\tau)\exp(\pm 2\pi i z\tau/\beta)$, where the function u is β-periodic. The solution becomes periodic at integer $z = \pm n$, so that the eigenvalues ε_n we need are $\varepsilon_n = \varepsilon(\pm n)$. To find the infinite product of the ε_n we employ the analytical properties of the function $\varepsilon(z)$. It has two simple zeros in the complex plane such that

$$[-\partial_\tau^2 + \omega_t^2(\tau)]x(\tau) = 0 , \qquad x(\tau+\beta) = \exp(\pm\lambda)x(\tau) . \tag{4.15a, b}$$

It is noteworthy that eq. (4.15a) is nothing but the linearized classical upside-down barrier equation of motion ($\delta S/\delta x = 0$) for the new coordinate x. Therefore, while $x \equiv 0$ corresponds to the instanton, the nonzero solution to (4.15a) describes how the trajectory "escapes" from the instanton solution, when it deviates from it. The parameter λ, referred to as the stability angle [Gutzwiller 1967; Rajaraman 1975], generalizes the harmonic-oscillator phase $\omega_t\beta$ which would appear in (4.15), if ω_t were a constant. The fact that λ is real indicates the aforementioned instability of the instanton in two dimensions. Guessing that the determinant $\det(-\partial_\tau^2 + \omega_t^2)$ is a function of λ only, and using the Poisson summation formula, we are able to write

$$\frac{\mathrm{d}[\ln\det(-\partial_\tau^2 + \omega_t^2)]}{\mathrm{d}\lambda} = \sum_{-\infty}^{\infty} \varepsilon_n^{-1}\frac{\mathrm{d}\varepsilon_n}{\mathrm{d}\lambda} = \sum_{-\infty}^{\infty}\int_{-\infty}^{\infty} \mathrm{d}z\,\varepsilon(z)^{-1}\frac{\mathrm{d}\varepsilon(z)}{\mathrm{d}\lambda}\exp(2\pi i n z) , \tag{4.16}$$

which after residuating reduces to

$$\det(-\partial_\tau^2 + \omega_t^2) = (2\sinh\tfrac{1}{2}\lambda)^2 . \tag{4.17}$$

Finally we arrive at

$$B_t = (\sinh\tfrac{1}{2}\omega_+\beta)/(\sinh\tfrac{1}{2}\lambda) . \tag{4.18}$$

Equation (4.9) together with (4.12) and (4.18) is the semiclassical TST result first obtained by Miller [1975a] and developed later by Chapman et al. [1975] and Hanggi and Hontscha [1988, 1991].

As a simple illustration of this technique consider the case of high frequency ω_t, viz. $\omega_t^{-2}\partial\omega_t/\partial\tau \ll 1$ for the instanton trajectory (but $\frac{1}{2}\omega_t$ is still small compared to the total barrier height $V^\#$). Then the quasiclassical approximation can be invoked to solve eq. (4.15a), which yields for λ

$$\lambda = \int_0^\beta \omega_t(s(\tau))\,\mathrm{d}\tau . \tag{4.19}$$

It is readily seen that when β is large enough and the hyperbolic sines in (4.18) can be replaced by exponents, the effect of the prefactor B_t is to replace the potential $V(s)$ by the vibrationally adiabatic

potential

$$V_{\mathrm{vad}}(s) = V(s) + \tfrac{1}{2}\omega_{\mathrm{t}}(s) \,. \tag{4.20}$$

Since usually the transverse vibration frequency at the barrier top is lower than ω_+, the vibrationally adiabatic barrier is lower than the bare one V.

In order to study the deviations from the vibrationally adiabatic approximation Benderskii et al. [1992b] have considered the situation when the transverse frequency ω_{t} switches instantaneously between two values, ω_1 and ω_2 ($\omega_1 > \omega_2$). If τ_1 and $\tau_2 = \beta - \tau_1$ are the times of occurrence of the frequencies ω_1 and ω_2, respectively, then the stability parameter is given by

$$\sinh \tfrac{1}{2}\lambda = \tfrac{1}{2}[4\sinh^2(\tfrac{1}{2}\phi_1 + \tfrac{1}{2}\phi_2) + (\omega_1/\omega_2 + \omega_2/\omega_1 - 2)\sinh\phi_1 \sinh\phi_2]^{1/2} \,,$$

where $\phi_i = \omega_i \tau_i$. When $\omega_1 \gg \omega_2$, this result differs from the adiabatic approximation, $\sinh \frac{1}{2}\lambda_{\mathrm{ad}} = \sinh(\frac{1}{2}\phi_1 + \frac{1}{2}\phi_2)$, by a factor $\frac{1}{2}(\omega_1/\omega_2)^{1/2} > 1$. In other words, nonadiabaticity caused by the stepwise frequency dependence reduces B_{t} by this factor, as compared to the vibrationally adiabatic approximation.

As another illustration, note that above the cross-over point T_{c} the temperature dependence $k(T)$ displays an activation energy equal to

$$E_{\mathrm{a}} \simeq V^{\#} + \tfrac{1}{2}\omega_{\mathrm{t}}^{\#} - \tfrac{1}{2}\omega_+ \,, \tag{4.21}$$

where $V^{\#}$ and $\omega_{\mathrm{t}}^{\#}$ are the barrier height and transverse vibration frequency at the saddle point, and we have neglected the effect of the zero-point energy of the low-frequency vibration ω_-. Unlike eq. (4.20), for (4.21) to hold, no vibrational adiabaticity is needed, and the only requirement is that ω_{t} be quantal, i.e., $\beta\omega_{\mathrm{t}} \gg 1$. In particular, this situation is usually realized in hydrogen transfer reactions, because the intramolecular vibration frequency for hydrogen remains quantal for room temperatures and higher.

The functional (4.8) permits one to study the set of paths which actually contribute to the partition-function path integral thereby leading to the determinant (4.17). Namely, the symmetric Green function for the deviation from the instanton path $x(\tau)$ is given by [Benderskii et al. 1992a]

$$G(\tau,\tau') = \langle (x(\tau)\, x(\tau')\rangle = (2W\sinh\tfrac{1}{2}\lambda)^{-1}[x(\tau)\tilde{x}(\tau')\exp(\tfrac{1}{2}\lambda) + x(\tau')\tilde{x}(\tau)\exp(-\tfrac{1}{2}\lambda)] \,,$$

$$0 < \tau < \tau' < \beta \,, \tag{4.22}$$

where the functions $x(\tau)$ and $\tilde{x}(\tau)$ satisfy (4.15a, b), and W is their Wronskian. The equal-time correlator then gives the "fluctuational width of the tunneling channel", inside which the relevant paths lie,

$$\langle x^2(\tau)\rangle = W^{-1} x(\tau)\tilde{x}(\tau)\coth(\tfrac{1}{2}\lambda) \,. \tag{4.23}$$

In the vibrational–adiabatic limit this formula reduces to the familiar form

$$\langle x^2(\tau)\rangle = [2\omega_{\mathrm{t}}(\tau)]^{-1} \coth\left(\tfrac{1}{2}\int_0^{\beta} \omega_{\mathrm{t}}(s(\tau))\,\mathrm{d}\tau\right) . \tag{4.24}$$

Equation (4.24) indicates that the quantum number $\langle n \rangle$ of the transverse x-vibration is an adiabatic invariant of the trajectory. At $T = 0$ $\langle x^2(\tau) \rangle$ becomes the instantaneous zero-point spread of the transverse vibration $(2\omega_t)^{-1}$, in agreement with the uncertainty principle.

The practical way of calculating λ is different from that used in the derivation of (4.18). Since λ is invariant with respect to canonical transformations, it is preferable to seek it in the initial coordinate system. Writing the linearized equation for deviations from the instanton solution $\delta \boldsymbol{Q}$,

$$(-\partial_\tau^2 \mathbf{1} + [\partial^2 V/\partial Q_i \partial Q_j]_{\text{ins}})\,\delta \boldsymbol{Q} = 0\,, \tag{4.25}$$

we define the monodromy matrix $\boldsymbol{M}$ through which the solution to (4.25) is transformed over the period,

$$\begin{bmatrix} \delta Q_1(\tau+\beta) \\ \delta Q_2(\tau+\beta) \\ \delta \dot{Q}_1(\tau+\beta) \\ \delta \dot{Q}_2(\tau+\beta) \end{bmatrix} = \boldsymbol{M} \begin{bmatrix} \delta Q_1(\tau) \\ \delta Q_2(\tau) \\ \delta \dot{Q}_1(\tau) \\ \delta \dot{Q}_2(\tau) \end{bmatrix}. \tag{4.26}$$

This matrix has two unit eigenvalues corresponding to the zero mode, and the other two eigenvalues are $\exp(\pm\lambda)$ entering into (4.18). The general formulae remain the same when the number of degrees of freedom N is greater than 2. The $2N \times 2N$ monodromy matrix has $2N - 2$ eigenvalues $\exp(\pm\lambda_j)$ and a doubly degenerate unit eigenvalue resulting from the time-shift invariance of the instanton. The transverse prefactor then becomes

$$B_t = \prod (\sinh \tfrac{1}{2}\omega_j \beta)/(\sinh \tfrac{1}{2}\lambda_j)\,, \tag{4.27}$$

where the ω_j are the normal frequencies in the well except for the lowest frequency.

In Benderskii et al. [1993] the numerical instanton analysis of tunneling escape out of the metastable well with the Hamiltonian

$$H(Q,q) = V_0[\tfrac{1}{2}\dot{Q}^2 + \tfrac{1}{2}\dot{q}^2 + \tfrac{1}{2}Q^2(1 + (C^2/\Omega^2) - Q^n) + CQq + \tfrac{1}{2}\Omega^2 q^2] \tag{4.28}$$

has been carried out. The coordinates, "coupling parameter" C and frequency Ω in (4.28) are dimensionless, and time is measured in dimensionless units $\omega_0 \tau$, where ω_0 is the frequency of small vibrations in the well for the "adiabatic" potential $V_a(Q)$, taken along the MEP $q_a(Q)$, defined by

$$\partial V/\partial q = 0\,, \qquad q_a = -CQ/\Omega^2\,, \qquad V_a = \tfrac{1}{2}V_0 Q^2(1 - Q^n)\,. \tag{4.29}$$

For convenience of notation we accept from here on, that each frequency of the problem ω_i has a dimensionless counterpart denoted by a capital Greek letter, so that $\omega_i = \omega_0 \Omega_i$. The model (4.28) may be thought of as a particle in a one-dimensional cubic parabola potential coupled to the q vibration. The saddle-point coordinates, defined by $\partial V/\partial Q = \partial V/\partial q = 0$, are

$$Q^{\#} = [2/(n+2)]^{1/n}\,, \qquad q^{\#} = -(C/\Omega^2)[2/(n+2)]^{1/n}\,, \tag{4.30}$$

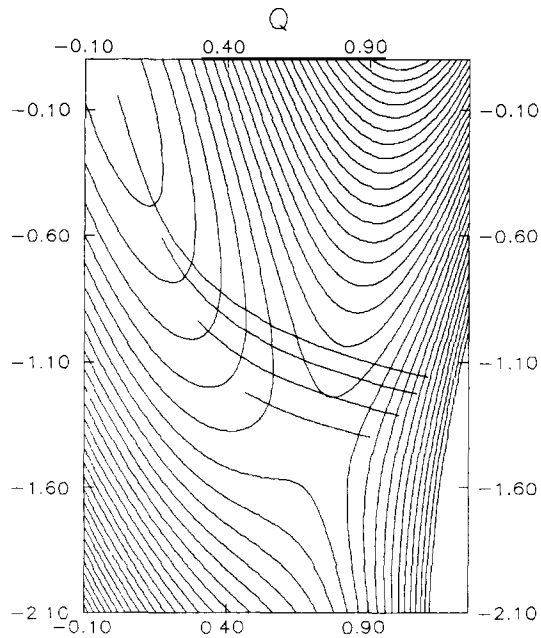

Fig. 25. Contour plot and instanton trajectories at $\beta\omega_0 = 6.4, 7.8, 10.2$ and 25.0 for PES (4.28) with $C = \Omega = 0.5$, $n = 2$. Greater length of trajectory corresponds to greater β.

and the barrier height is

$$V^{\#} = V(Q^{\#}, q^{\#}) = V_0[n/2(n+2)][2/(n+2)]^{2/n} . \tag{4.31}$$

In the limit of large n the potential (4.28) tends to a harmonic well with an absorbing wall placed at $Q = 1$, which has been discussed in section 2.5.

Figure 25 demonstrates the instanton trajectories at different temperatures for $C = 0.5$, $\Omega = 0.5$, $n = 2$. For the temperature close to the cross-over value, the trajectory runs near the saddle point, and it deviates from the saddle point with increasing β. The Hamiltonian (4.28) with $n = 1$ has recently been studied numerically within the complex scaling method [Hontscha et al. 1990]. Using those data we can estimate the accuracy of the instanton method. Note however that the method of Hontscha et al. [1990] was suited for not too high barriers, namely $V^{\#}/\omega_0 \leq 3$, while the instanton method is expected to work best at higher barriers. The ratio $\omega_0/V^{\#}$ may be regarded as the parameter of "quantumness", and the smaller it is, the better the instanton approximation works.

In fig. 26 the Arrhenius plot $\ln[k(T)/\omega_0]$ versus $T_0/T = \beta/2\pi$ is shown for $V^{\#}/\omega_0 = 3$, $\omega = 0.1$, $C = 0.0357$. The disconnected points are the data from Hontscha et al. [1990]. The solid line was obtained with the two-dimensional instanton method. One sees that the agreement between the instanton result and the exact quantal calculations is perfect. The low-temperature limit found with the use of the periodic-orbit theory expression for k_{1D} (dashed line) also excellently agrees with the exact result. Figure 27 presents the dependence $\ln(k_c/\omega_0)$ on the coupling strength defined as C^2/Ω^2. The dashed line corresponds to the exact result from Hontscha et al. [1990], and the disconnected points are obtained with the instanton method. For most practical purposes the instanton results may be considered exact.

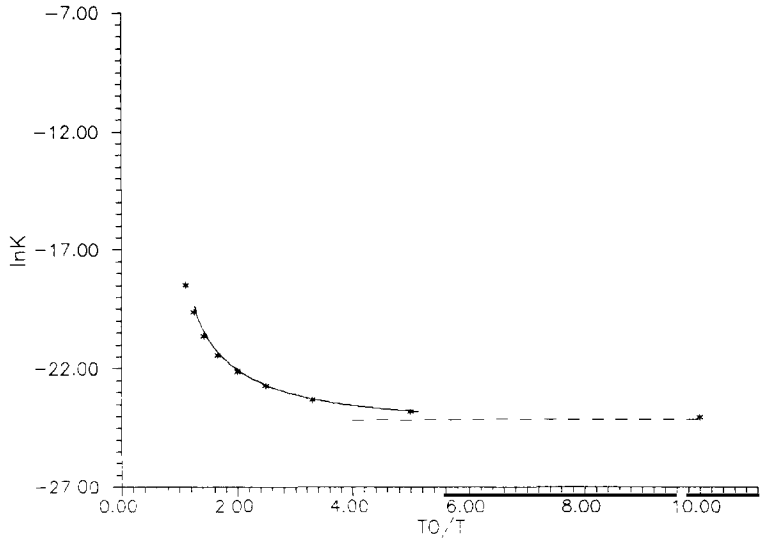

Fig. 26. Arrhenius plot [$\ln(k/\omega_0)$ against $\omega_0\beta/2\pi$] for the PES (4.28) with $\Omega = 0.1$, $C = 0.0357$, $n = 1$, $V^*/\omega_0 = 3$. Solid line shows instanton result; separate points, numerical calculation data from Hontscha et al. [1990]; and dashed line, low-temperature limit using (3.32) for k_{1D}.

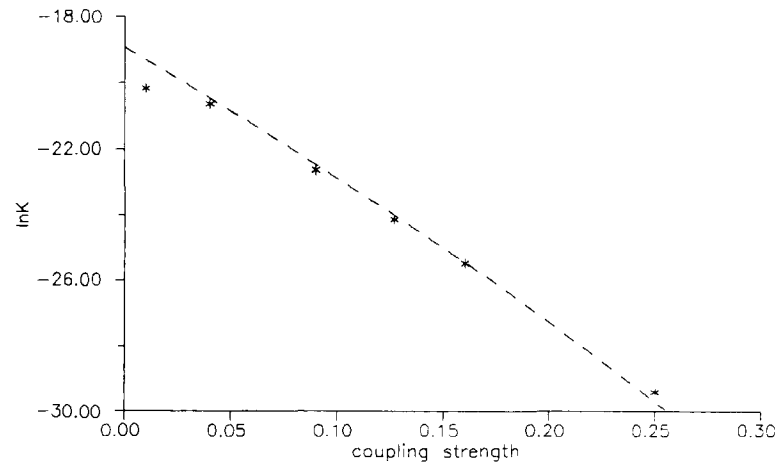

Fig. 27. Logarithm of normalized rate constant $\ln(k/\omega_0)$ versus dimensionless coupling strength C^2/Ω^2 for PES (4.28) with $\Omega = 0.1$, $n = 1$, $V^*/\omega_0 = 3$. Separate points and dashed line correspond to instanton result and numerical data [Hontscha et al. 1990].

Figure 28 shows an instanton trajectory for the parameters chosen in fig. 26. It is very instructive to see that, in contrast to fig. 25, the trajectory consists of two fairly straight segments, the angle between which is nearly 90°. This sharp "bend" of the tunneling path becomes more salient with decreasing Ω. This phenomenon can be understood on the basis of the sudden theory of tunneling, developed in Benderskii et al. [1980], Pollak [1986a, b], Levine et al. [1989]. This theory exploits the fact that when $\Omega \ll 1$, the tunneling event may be considered instantaneous on the time scale of the q-vibration.

More accurately, one rewrites the problem in terms of the coordinates Q_+ and Q_-. The probability to be at a certain point Q_- is given by the diagonal element of the density matrix

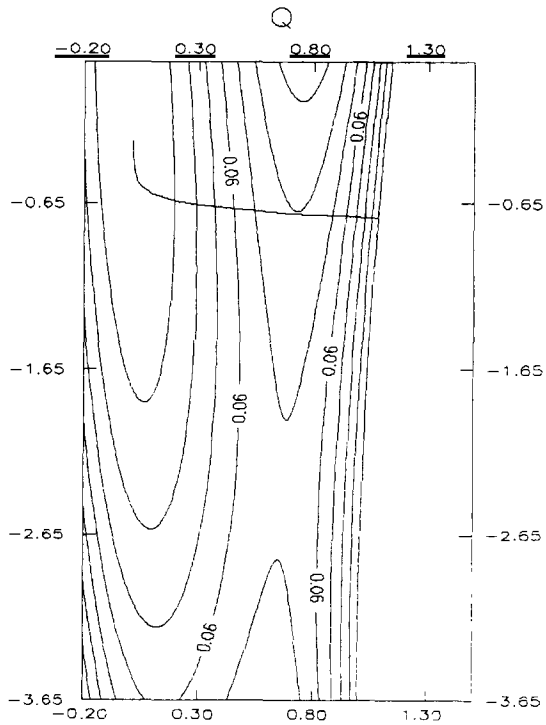

Fig. 28. Contour plot and instanton trajectory for PES (4.28) with the parameters of fig. 25, $\omega_0\beta = 35$.

$P(Q_-) = \rho(Q_-, Q_-, \beta)$, which in the harmonic approximation is described by (3.16), $\rho_h(Q_-, Q_-, \beta) \propto \exp(-\omega_- Q_-^2 \tanh \frac{1}{2}\beta\omega_-)$. Having reached the point Q_-, the particle is assumed to suddenly tunnel along the fast coordinate Q_+ with probability $k_{1D}(Q_-)$, which is described in terms of the usual one-dimensional instanton. The rate constant comes from averaging the one-dimensional tunneling rate over positions of the slow vibration mode,

$$k = \int dQ_- \, \rho(Q_-, Q_-, \beta) k_{1D}(Q_-) \,. \tag{4.32}$$

In the light of the path-integral representation, the density matrix $\rho(Q_-, Q_-, \beta)$ may be semiclassically represented as $\propto \exp[-S_1(Q_-)]$, where $S_1(Q_-)$ is the Eucledian action on the β-periodic trajectory that starts and ends at the point Q_- and visits the potential minimum $Q_- = 0$ for $T = 0$. The one-dimensional tunneling rate, in turn, is proportional to $\exp[-S_2(Q_-)]$, where S_2 is the action in the barrier for the closed straight trajectory which goes along the line with constant Q_-. The integral in (4.32) may be evaluated by the method of steepest descents, which leads to an optimum value of $Q_- = Q_-^*$. This amounts to minimization of the total action $S_1 + S_2$ over the positions of the "bend point" Q_-.

In fact, in the sudden approximation one looks for the minimum of the barrier action taken on a certain class of paths, each consisting of two straight segments. If the actual extremal path is close to one of the paths from this class – and this is indeed the case for low enough Ω – then the sudden approximation provides accurate results. In particular, the sudden approximation has been shown [Hontscha et al. 1990] to provide accuracy within less than 10% for the rate constant at

$V^{\#}/\omega_0 = 3$, $\Omega = 0.1$, $C \leq 0.05$. For the cubic parabola [$n = 1$ in eq. (4.28)] at small values of the coupling parameter, the rate constant in the sudden approximation may be evaluated analytically by using the one-dimensional instanton result (3.47) for k_{1D},

$$k_{c,\,\mathrm{sudden}} = 60^{1/2}\omega_0\,(S_{1D}/2\pi)^{1/2}(1 + 7C^2/4\omega^2)\exp\{-S_{1D}[1 + (5C^2/2\omega^2)(1 - 3\Omega)]\}\,, \quad (4.33)$$

where S_{1D} is the one-dimensional instanton action defined in (3.47).

4.2. Tunneling splitting

The formula for the tunneling splitting in two dimensions is a simple generalization of (3.70),

$$\Delta = 2\left(\frac{S_k}{2\pi}\right)^{1/2}\left(\frac{\det'(-\partial_\tau^2\mathbf{1} + \partial^2 V/\partial Q_i\,\partial Q_j)_{\mathrm{kink}}}{\det(-\partial_\tau^2\mathbf{1} + K_0)}\right)^{-1/2}\exp(-S_k)\,, \quad (4.34)$$

where S_k is the one-kink action at $\beta \to \infty$,

$$S_k = \int_{-\infty}^{\infty} d\tau\,[\tfrac{1}{2}\dot{Q}_1^2 + \tfrac{1}{2}\dot{Q}_2^2 + V(Q_1, Q_2)]\,, \quad (4.35)$$

and K_0 is the eigenfrequency matrix in the well. In order to apply the Floquet procedure of the previous subsection, it is expedient to "double" the kink, i.e., to use the periodic instanton trajectory with the action $S_{ins} = 2S_k$ at $\beta \to \infty$. When the kink and antikink on this trajectory are separated by an infinite time, each eigenvalue of the operator $-\partial_\tau^2 + \partial^2 V/\partial Q_i\,\partial Q_j$ will be doubled in the spectrum of the same operator taken for the whole instanton. Thus we may rewrite (4.35) as

$$\Delta = \left(\frac{S_{ins}}{\pi}\right)^{1/2}\left(\frac{\det''(-\partial_\tau^2\mathbf{1} + \partial^2 V/\partial Q_i\,\partial Q_j)_{ins}}{\det(-\partial_\tau^2\mathbf{1} + K_0)}\right)^{-1/4}\exp(-\tfrac{1}{2}S_{ins})\,, \quad (4.36)$$

where the operators are taken now for the full periodic trajectory, and the double prime indicates that two zero eigenvalues are left out.

Now we are in position to use the results of the previous section to get

$$\Delta = \Delta_{1D}\tilde{B}_t \quad (4.37)$$

where Δ_{1D} is the "one-dimensional" tunneling splitting given by (3.79) or (3.70),

$$\Delta_{1D} = \left(\frac{S_{ins}}{\pi}\right)^{1/2}\left(\frac{\det''(-\partial_\tau^2 + \partial^2 V/\partial s^2)}{\det(-\partial_\tau^2 + \omega_-^2)}\right)^{-1/4}\exp(-\tfrac{1}{2}S_{ins})\,, \quad (4.38)$$

and $\tilde{B}_t$ is the transverse prefactor

$$\tilde{B}_t = \lim_{\beta\to\infty}\exp\{\tfrac{1}{4}[\beta\omega_+ - \lambda(\beta)]\} = \lim_{\beta\to\infty} B_t^{1/2}\,. \quad (4.39)$$

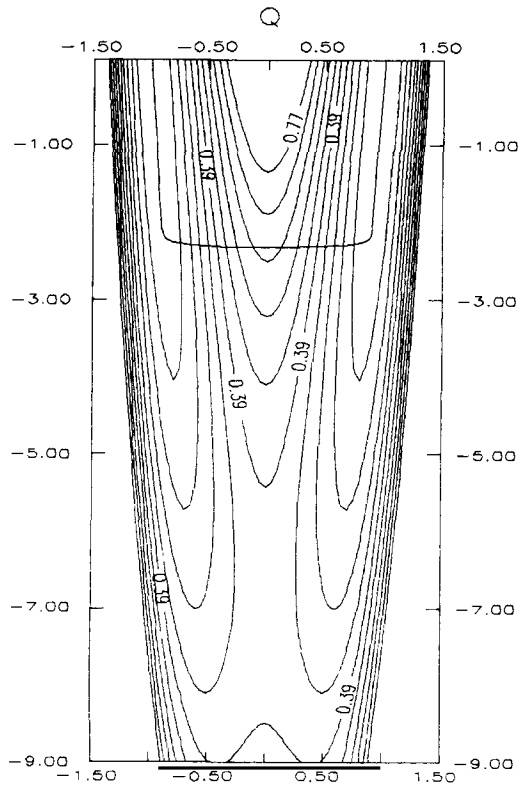

Fig. 29. Contour plot and instanton trajectory for PES (4.40) with $\beta = \infty$, $C = 0.185$, $\Omega = 0.163$.

A similar expression was obtained by Auerbach and Kivelson [1985] based on quite a different methodology, the so-called path-decomposition expansion, which allows one to join semiclassical propagators in the barrier regions with exact (or perturbatively calculated) propagators near the potential minima. Because the joining point lies far outside the classically accessible region, that procedure rids one of the problem of turning points (or, more generally, caustics) inherent to the more traditional semiclassical treatments [Huang et al. 1990; Razavy and Pimpale 1988] and leads, in the limit of $\hbar \to 0$, to the instanton. It should be mentioned that the above papers provide also semiclassically obtained numerical data on some model potentials.

An example of a numerically calculated trajectory in a symmetric double well is presented in fig. 29 for the Hamiltonian

$$H(Q,q) = V_0[\tfrac{1}{2}\dot{Q}^2 + \tfrac{1}{2}\dot{q}^2 + Q^4 - 2Q^2 - CQ^2q + \tfrac{1}{2}\Omega^2(q + C/\Omega^2)^2 + 1 - C^2/2\Omega^2] \qquad (4.40)$$

with $\Omega = 0.163$, $C = 0.185$. All the parameters but V_0 are dimensionless here. The time is gauged in dimensionless units $r = \omega_0 t$, where $8^{1/2}\omega_0$ is the vibration frequency in the well of the one-dimensional potential taken at $q \equiv 0$,

$$V_{1D}(Q) = V_0(Q^2 - 1)^2 \,. \qquad (4.41)$$

Since we are going to rather extensively use the Hamiltonian (4.40) in the sequel, as a simplest two-dimensional model for an exchange chemical reaction, it is beneficial to establish some of

its salient features in advance. The minimum energy path (MEP) is determined by $\partial V/\partial q = 0$, whence

$$q_a = C(Q^2 - 1)/\Omega^2 , \tag{4.42}$$

and the adiabatic barrier along this path is

$$V_a(Q) = V_0(1 - b)(Q^2 - 1)^2 , \quad b = C^2/2\Omega^2 . \tag{4.43}$$

The dimensionless upside-down barrier frequency equals $\Omega^{\#} = 2(1 - b)^{1/2}$, and the transverse frequency $\Omega_t^{\#} = \Omega$. The instanton action at $\beta = \infty$ in the one-dimensional potential (4.41) equals [cf. eq. (3.68)]

$$S_{\text{ins, 1D}} = 2^{7/2} V_0/3\omega_0 . \tag{4.44}$$

The situation presented in fig. 29 corresponds to the sudden limit, as we have already explained in the previous subsection. Having reached a bend point at the expense of the low-frequency vibration, the particle then cuts straight across the angle between the reactant and product valley, tunneling along the Q-direction. The sudden approximation holds when the vibration frequency Ω is less than the characteristic instanton frequency, which is of the order of $\Omega^{\#}$. In particular, the reactions of proton transfer (see fig. 2), characterised by high intramolecular vibration frequency, are being usually studied in this approximation [Ovchinnikova 1979; Babamov and Marcus 1981].

At high transverse frequency $\Omega \gg \Omega^{\#}$ there is another possibility to dispense with actually solving the instanton equations. In this case the factor of the barrier height becomes prevalent over that of its width, because any deviations of the trajectory from the MEP (4.42) entail a great rise of the barrier. Therefore, the q vibration adiabatically follows the motion along the Q coordinate, according to eq. (4.42), and the trajectory of tunneling is the MEP. This is the adiabatic ("small-curvature") approximation [Miller 1983]. Projected onto the Q axis, this motion looks like that of a particle with kinetic energy $\frac{1}{2}\dot{Q}^2(1 + \alpha Q^2)$, $\alpha = 4C^2/\Omega^4$, and thus with variable effective dimensionless mass $M^* = 1 + \alpha Q^2$. The evaluation of the instanton action is straightforward and it gives [Benderskii et al. 1991a–c]

$$S_{\text{ad}} = \tfrac{3}{4} S_{\text{ins, 1D}}(1 - b)^{1/2} [(1 + \alpha)^{1/2}(\tfrac{1}{2} - 1/\alpha) + \alpha^{-1/2}[1 + (4\alpha)^{-1}]\sinh^{-1}(\alpha^{1/2})] . \tag{4.45}$$

It is not hard to show that the inequality $\Omega \ll \Omega^{\#}$, which should be met for the sudden approximation to hold, is equivalent to (2.81), if we introduce the angle 2φ between the reactant and product valleys $\tan\varphi = \Omega^2/C$. The regions of applicability of the sudden and adiabatic approximations in the (C, Ω) plane are symbolically drawn in fig. 30.

Naturally, neither of these approximations is valid near the border between the two regions. Physically sensible are only such parameters, for which $b < 1$. Note that even for a low vibration frequency Ω, the adiabatic limit may hold for large enough coupling parameter C (see the "bill" of the adiabatic approximation domain in fig. 30). This situation is referred to as strong-fluctuation limit by [Benderskii et al. 1991a–c], and it actually takes place for heavy particle transfer, as described in the experimental section of this review. In the section 5 we shall describe how both the sudden and adiabatic limits may be viewed from a unique perspective.

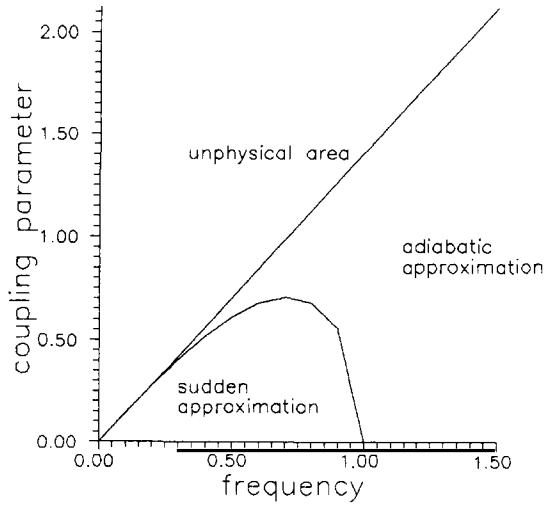

Fig. 30. Domains of validity of sudden and adiabatic approximations in the (C, Ω) plane for PES (4.40).

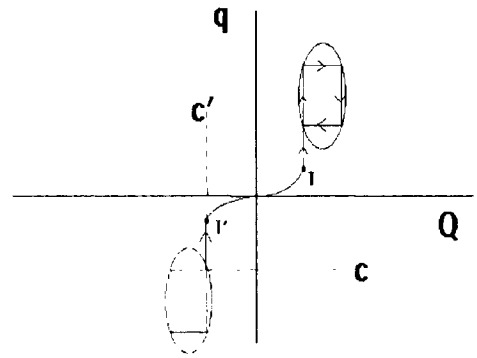

Fig. 31. Two-dimensional periodic orbits for vibration coupled antisymmetrically to the reaction coordinate. Caustics (C) and take-off points (T) are indicated.

4.3. *Periodic orbits in symmetric double well*

Here we shall describe how the periodic-orbit theory of section 3.4, relating the energy levels with the poles of the spectral function $g(E)$, can be extended to two dimensions. For simplicity we shall exemplify this extension by the simplest model in which the total PES is constructed of two paraboloids crossing at some dividing line. Each paraboloid is characterized by two eigenfrequencies, ω_+ and ω_-. As explained in section 2.5 (see fig. 17), the paraboloids are placed either symmetrically with respect to the dividing line (symmetric case), or they are symmetric with respect to a point (antisymmetric case). Our discussion draws on the work of Benderskii et al. [1992b].

In accordance with the one-dimensional periodic orbit theory, any orbit contributing to $g(E)$ is supposedly constructed from closed classical orbits in the well and subbarrier imaginary-time trajectories. These two classes of trajectories are bordering on the turning points. For the present model the classical motion in the well is separable, and the harmonic approximation for classical motion is quite reasonable for more realistic potentials, if only relatively low energy levels are involved.

Consider for definiteness the antisymmetric case. We choose the origin of the coordinate system in one of the wells, and the center of symmetry has the coordinates $(Q_+^{\#}, Q_-^{\#})$ (fig. 31). Inside the well the classical trajectories are Lissajous figures bordering on the rectangle formed by the lines $Q_\pm = Q_\pm^t$, and $Q_\pm = -Q_\pm^t$, where $Q_\pm^t$ are the turning-point coordinates,

$$Q_\pm = Q_\pm^t \cos(\omega_\pm t + \psi_\pm) \,. \tag{4.46}$$

The energy equals

$$E = E_1 + E_2 = \tfrac{1}{2}\omega_+^2 Q_+^{t2} + \tfrac{1}{2}\omega_-^2 Q_-^{t2} \approx E_+^0 + E_-^0 = (n_+ + \tfrac{1}{2})\omega_+ + (n_- + \tfrac{1}{2})\omega_- \,, \tag{4.47}$$

where tunneling is neglected in the zeroth approximation.

Equation (4.46), however, regardless of the phases $\psi_\pm$, does not describe periodic orbits, unless the frequencies $\omega_\pm$ are commensurate. Thus the first question that is to be answered is, how to semiclassically quantize a separate well. Furthermore, because of symmetry, a tunneling orbit should pass through the point $\boldsymbol{Q}^\# = (Q_+^\#, Q_-^\#)$. However, if it sets out from the turning point $\boldsymbol{Q}_t$ at $\tau = 0$, it will not necessarily hit the point $\boldsymbol{Q}^\#$, because it is impossible to satisfy simultaneously two imaginary-time equations of motion

$$Q_\pm = Q_\pm^t \cosh(\omega_\pm \tau) \tag{4.48}$$

when setting $\boldsymbol{Q} = \boldsymbol{Q}^\#$.

The way out is to sacrifice the classical trajectories. The crux of the matter is that we are trying to solve the variational problem for the action S with given energy and fixed end points, while in the instanton theory the ends of the path are allowed to be free. The solution of the problem at hand is not a classical trajectory but a path which consists of segments of classical trajectories and caustics. The caustics are the envelopes of families of classical trajectories [Arnold 1978]. Both the classical trajectories and caustics, and only they, possess a property which distinguishes them from all other paths. Namely, if we find for each point $\boldsymbol{Q}$ the momentum $\boldsymbol{P}(\boldsymbol{Q})$ of a trajectory that passes through this point, then, for a caustic or a classical trajectory, $\boldsymbol{P}$ is directed along its tangent. Moreover, the manifold $\boldsymbol{P}(\boldsymbol{Q})$ is single-valued in the regions bordering on caustics. The absolute value of momentum is obviously equal to $[2(V-E)]^{1/2}$ and, therefore, the Eucledian action equals $S = E\tau + \int ds\,[2(V-E)]^{1/2}$, where s is the coordinate along the path.

In the parabolic model the equations for caustics are simply $Q_+ = Q_+^t$, and $Q_- = Q_-^t$. The periodic orbits inside the well are not described by (4.46), but they run along the borders of the rectangle formed by caustics. It is these trajectories that correspond to topologically irreducible contours on a two-dimensional torus [Arnold 1978] and lead to the quantization condition (4.47).

The semiclassical picture of tunneling then looks as follows (fig. 31). The particle starts out from one of the turning points*) and runs along a subbarrier caustic, say that with $Q_+ = Q_+^t$, until it reaches a "take-off" point $Q_- = Q'_-$, from which it begins to exercise the classical (upside-down barrier) motion. The coordinate and momenta are continuous on the whole path. From each turning point a pair of caustics comes out, and the correct caustic and the position of the "take-off" point are picked up so that the path hits the point $\boldsymbol{Q}^\#$. When moving along the caustic, the "faster" degree of freedom is frozen, so as to eventually "synchronize" the arrival at the point $\boldsymbol{Q}^\#$ for both degrees of freedom. The explicit equation for the take-off point coordinate is [Benderskii et al. 1992b]

$$Q'_- = Q_-^t \cosh[\omega_-(\tau_- - \tau_+)]\,, \qquad \tau_\pm = \omega_\pm^{-1} \cosh^{-1}(Q_\pm^\#/Q_\pm^t)\,, \tag{4.49}$$

where $\tau_\pm$ is the time of motion from the turning point to $Q_\pm^\#$ for each coordinate.

In the symmetric case the requirement to cross the point $\boldsymbol{Q}^\#$ is replaced by the requirement to cross the dividing line at right angles.

For an N-dimensional paraboloid in the space $\boldsymbol{Q} = \{Q_1, \ldots, Q_N\}$ let us order the times to reach the point $\boldsymbol{Q}^\#$, $\tau_i = \omega_i^{-1} \cosh^{-1}(Q_i^\#/Q_i^t)$, as follows: $\tau_1 > \tau_2 > \cdots > \tau_N$. Then the tunneling path

*) There are actually four turning points in each well. It does not matter from which one we start, because the straight-line segments between the turning points are incorporated into that part of $g(E)$ which is responsible for the single well quantization.

consists of segments separated by "take-off" points. At the kth segment classical motion in the k-dimensional space of "slow" coordinates occurs, while the other $N-k$ degrees of freedom are "frozen". The genuine classical motion takes place only at the last segment, when all the times τ_i are "equalized".

In conclusion note that for a sufficiently dense energy spectrum the caustic segments have been shown [Benderskii et al. 1992b] to disappear after statistical averaging, which brings one back to the instanton and, for the present model, leads to eqs. (2.80a, b).

5. Chemical dynamics in the presence of a heat bath

When the system has a very large number of degrees of freedom the multidimensional method treating all of them as having equal rights is no longer of use. There is usually just one (or several) reactive coordinate that is of primary interest, while the other may be considered as a heat bath coupled to this tagged degree of freedom. For example, in the OH ··· O fragment drawn in fig. 2 such a relevant degree of freedom is the proton coordinate, i.e., the position of the H atom relative to the O–O center. The O atoms, in turn, may participate in various intermolecular vibrations in a condensed medium. These vibrations are nonreactive and they may be considered a bath. The choice of the bath is rather conventional, because, for example, one could consider the two-dimensional reaction complex with one more relevant coordinate, say the O–O distance, and relegate the rest of the degrees of freedom to the bath. Once the total Hamiltonian has a system–bath form, the main objective of the theory is to eliminate the bath degrees of freedom in order to write down the problem in terms of the reactive coordinate only. This is done by introducing the so-called influence functionals.

As seen from our discussion concerning the one-dimensional problems, in many relevant cases, in order to find the rate constant, one does not actually need the knowledge of the behavior of the system in real time. As a matter of fact, the rate constant is expressible solely in terms of equilibrium partition-function imaginary-time path integrals. This approximation is closely related with the key assumptions of TST, and it is not always valid, as mentioned in section 2.3. The general real-time description of a particle coupled to a heat bath is the Feynman–Vernon influence functional theory [Feynman and Vernon 1963] which expresses the particle's reduced density matrix as a double path integral over the paths developing in real time*). The only dissipative tunneling problem that has so far been thoroughly studied in real time is that of a two-level system coupled to a harmonic oscillator bath [Leggett et al. 1987], and those results have provided an opportunity to estimate the accuracy of much more feasible imaginary-time methods.

As long as the system can be described by the rate constant – this rules out the localization as well as the coherent tunneling case – it can with a reasonable accuracy be considered in the imaginary-time framework. For this reason we rely on the Im F approach in the main part of this section. In a separate subsection the TLS real-time dynamics is analyzed, however on a simpler but less rigorous basis of the Heisenberg equations of motion. A systematic and exhaustive discussion of this problem may be found in the review [Leggett et al. 1987].

*) The influence functional theory, as it was formulated by Feyman and Vernon, relies on the additional assumption concerning factorization of the total (system and bath) density matrix in the past. Without this assumption the theory requires a triple path integral, with one "thermal" integration over the imaginary time axis [Grabert et al. 1988].

5.1. Quasienergy method

The total space of system coordinates consists of a tagged coordinate Q (conjugate momentum P) and a set of mass-scaled bath coordinates $\boldsymbol{q}$ (conjugate momenta $\boldsymbol{p}$). The Hamiltonian reads

$$H(P,Q,\boldsymbol{p},\boldsymbol{q}) = H_0(P,Q) + H_b(\boldsymbol{p},\boldsymbol{q}) + V_{int}(Q,\boldsymbol{q}) ,$$

$$H_0(P,Q) = \tfrac{1}{2}P^2 + V(Q) , \quad H_b(\boldsymbol{p},\boldsymbol{q}) = \sum \tfrac{1}{2}p_j^2 + V(\boldsymbol{q}) . \tag{5.1}$$

Following the Im F method, one looks for the partition function of the system

$$Z = \int d\boldsymbol{q}_i \, dQ_i \int D[Q(\tau)]\, D[\boldsymbol{q}(\tau)] \exp\left(- \int_0^\beta (H_0 + H_b + V_{int})\, d\tau \right) , \tag{5.2}$$

where the path integral is taken over the closed paths with the periodic boundary conditions

$$Q(\tau) = Q(\tau + \beta) , \qquad \boldsymbol{q}(\tau) = \boldsymbol{q}(\tau + \beta) , \qquad Q(0) = Q_i , \qquad \boldsymbol{q}(0) = \boldsymbol{q}_i . \tag{5.3}$$

If we fix a realization of the path $Q(\tau)$, then, when performing the path integration over $\boldsymbol{q}$, the particle may be treated as acted on by a time-dependent potential $V_{int}(Q(\tau),\boldsymbol{q})$. From traditional quantum mechanics it is clear that this integration is equivalent to the solution of the time-dependent Shrödinger equation in imaginary time,

$$-\partial\phi(\boldsymbol{q},\tau)/\partial\tau = (H_b + V_{int}(Q(\tau),\boldsymbol{q}))\phi(\boldsymbol{q},\tau) , \tag{5.4}$$

which allows one to find the bath propagator,

$$K_b(\boldsymbol{q}_f,\boldsymbol{q}_i|\,-i\beta) \equiv \hat{T}\exp\left(- \int_0^\beta d\tau\,(H_b + V_{int}) \right) = \int D[q(\tau)] \exp\left(- \int_0^\beta d\tau\,(H_b + V_{int}) \right) , \tag{5.5}$$

where the time-ordering operator $\hat{T}$ has appeared in the expression for the propagator because the Hamiltonian is now time-dependent, unlike the problems we have discussed so far. The trace of K_b may be expressed in an elegant form if we exploit the periodicity of the potential V_{int} in (5.4). Namely, there is the so-called Floquet basis of solutions ϕ_n to (5.4) [Casati and Molinari 1989] satisfying condition

$$\phi_n(\tau + \beta) = \exp(-\tilde{\varepsilon}_n\beta)\,\phi_n(\tau) . \tag{5.6}$$

The parameters $\tilde{\varepsilon}_n$ called quasienergies play the same role for periodic motion as the usual energies do for time-independent Hamiltonians. By using the definition (5.6) it is easy to obtain [Benderskii and Makarov 1992]

$$\mathrm{Tr}\, K_b = \int d\boldsymbol{q}_i\, K_b(\boldsymbol{q}_i,\boldsymbol{q}_i|\,-i\beta) \equiv \tilde{Z}[Q(\tau)] = \sum_n \exp(-\beta\tilde{\varepsilon}_n[Q(\tau)]) . \tag{5.7}$$

This equation defines the quasienergy partition-function functional. Its use results in the total partition function written in terms of the coordinate Q alone

$$Z = \int \mathrm{d}Q_i \int D[Q(\tau)] \exp\{-S_{\mathrm{eff}}[Q(\tau)]\} ,$$
$$S_{\mathrm{eff}}[Q(\tau)] = \int_0^\beta H_0 \, \mathrm{d}\tau - \ln \tilde{Z}[Q(\tau)] , \quad Q(\tau) = Q(\tau + \beta) . \tag{5.8}$$

If one expressed the bath Hamiltonian as an $N \times N$ matrix, eqs. (5.4)–(5.7) may be represented as follows. Let F be a fundamental $N \times N$ matrix of the equation

$$-\partial F/\partial\tau = (H_b + V_{int}) F . \tag{5.9}$$

Then define the monodromy matrix M [Shirley 1965],

$$F(\tau + \beta) = MF(\tau) , \qquad M = F(\tau + \beta) F(\tau)^{-1} . \tag{5.10}$$

The matrices F and M can be found from straightforward integration of (5.9) with the initial conditions being N linearly independent vectors. Then the quasienergy partition function equals

$$\tilde{Z}[Q(\tau)] = \mathrm{Tr}\, M . \tag{5.11}$$

Note also that M meets the Wronsky theorem,

$$\det M = \exp\left(- \int_0^\beta \mathrm{Tr}(H_b + V_{int}) \, \mathrm{d}\tau \right) . \tag{5.12}$$

Thus for Hamiltonians of finite dimension the effective action functional can be found by immediately integrating a system of ordinary differential equations. The simplest yet very important case is a bath of two-level systems,

$$H_b + V_{int} = \tfrac{1}{2} \Delta(Q) \sigma_x + \tfrac{1}{2} \varepsilon(Q) \sigma_z . \tag{5.13}$$

The quasienergy partition function equals

$$\tilde{Z} = 2 \cosh(\beta \tilde{\varepsilon}) , \tag{5.14}$$

where $\pm \tilde{\varepsilon}$ correspond to the Floquet solutions to the Shrödinger equation

$$-2\partial c_1/\partial\tau = \varepsilon c_1 + \Delta c_2 , \qquad -2\partial c_2/\partial\tau = -\varepsilon c_2 + \Delta c_1 . \tag{5.15}$$

That is, $c_{1,2}(\tau + \beta) = c_{1,2}(\tau)\exp(\pm\beta\tilde{\varepsilon})$. In fact, when the temperature is less than the separation between the two lowest energy levels of the bath, the latter can be approximated by a set of two-level systems [Caldeira and Leggett 1983; Mermin 1991].*)

Generally speaking, the calculation of quasienergies is itself a very complex problem. There are, however, several limiting cases when it may be done at low cost.

5.1.1. Adiabatic approximation

Suppose that typical frequency of the environment is greater than that of the Q-system. Then eq. (5.4) can readily be solved in the adiabatic approximation and the quasienergies are

$$\tilde{\varepsilon}_n = \beta^{-1}\int_0^\beta \varepsilon_n(Q(\tau))\,\mathrm{d}\tau\,, \tag{5.16}$$

where $Q(\tau)$ is considered a parameter, that is, the ε_n are the energy levels corresponding to (5.4) at constant values of Q. At sufficiently low temperatures when only the ground state [with energy $\varepsilon_0(Q)$] survives in the partition function, the latter renormalizes the effective potential from $V(Q)$ to

$$V_{\mathrm{eff}}(Q) = V(Q) + \varepsilon_0(Q)\,. \tag{5.17}$$

At arbitrary temperatures and in the perturbative limit the energy can be estimated as the matrix element taken over the unperturbed ϕ-functions $\tilde{\varepsilon}_n[Q(\tau)] \simeq \varepsilon_n + \beta^{-1}\int_0^\beta [V_{\mathrm{int}}(Q(\tau))]_{nn}\,\mathrm{d}\tau$. Inserting this equality into the partition function one obtains to first order in V_{int},

$$\ln(\tilde{Z}[Q(\tau)]/Z_0) = -\int_0^\beta \langle V_{\mathrm{int}}(\boldsymbol{q}, Q(\tau))\rangle_{\mathrm{bath}}\,\mathrm{d}\tau\,, \tag{5.18}$$

where the partition function Z_0 and averaging correspond to the unperturbed bath. Thus we arrive at the adiabatically renormalized effective potential

$$V_{\mathrm{eff}}(Q) = V(Q) + \langle V_{\mathrm{int}}(\boldsymbol{q}, Q(\tau))\rangle_{\mathrm{bath}}\,. \tag{5.19}$$

The adiabatic approximation in the form (5.17) or (5.19) allows one to eliminate the high-frequency modes and to concentrate only on the low-frequency motion. The most frequent particular case of adiabatic approximation is the vibrationally adiabatic potential

$$V_{\mathrm{v\,ad}}(Q) = V(Q) + \sum \tfrac{1}{2}\hbar\omega_i(Q)\,, \tag{5.20}$$

where the ω_i are the frequencies of transverse vibrations.

*) Therefore, at extremely low temperatures one may equally choose between TLS and say oscillator bath. The latter is usually supposed to be simpler to handle, but the TLS bath model, apart from its apparent relevance for glass theory, has some very attractive features [Mermin 1991; Suarez and Silbey 1991b; Shimshoni and Cefen 1991].

5.1.2. Classical low-frequency heat bath

In the opposite case of very low-frequency bath degrees of freedom there is a wide range of temperatures in which the bath is classical while the Q-coordinate is quantum. If ω_c is the characteristic frequency of the bath, the latter remains classical so long as $\beta\omega_c \ll 1$. The right-hand side of the Shrödinger equation (5.4) contains now a rapidly oscillating potential V_{int} and the most evident way to treat it is simply to average it over the period. A more accurate approach is based on Kapitsa's method of effective potential for fast oscillations (see, e.g., Bas' et al. [1971]). Expanding V_{int} in a Fourier series in the Matsubara frequencies $\nu_n = 2\pi n/\beta$,

$$V_{int}(Q(\tau), \boldsymbol{q}) = \beta^{-1} \sum_{n=-\infty}^{\infty} V_n([Q(\tau)], \boldsymbol{q}) \exp(i\nu_n \tau) , \tag{5.21}$$

we get the effective interaction potential $V_{eff}(q)$ as

$$V_{eff}(\boldsymbol{q}) = \beta^{-1} \int_0^{\beta} V_{int}(Q(\tau), \boldsymbol{q})\, d\tau - \sum_{n=1}^{\infty} |(\partial V_n/\partial \boldsymbol{q})|^2/(2\pi n)^2 . \tag{5.22}$$

The classical bath "sees" the quantum particle potential as averaged over the characteristic time, which – if we recall that in conventional units it equals $\hbar/k_B T$ – vanishes in the classical limit $\hbar \to 0$. The quasienergy partition function for the classical bath now simply turns into an ordinary integral in configuration space,

$$\tilde{Z}[Q(\tau)] \propto \int d\boldsymbol{q} \exp[-\beta V_{eff}(\boldsymbol{q})] , \tag{5.23}$$

where V_{eff} is a functional of path $Q(\tau)$ and we have omitted the integration over the momenta as a constant factor which is canceled out when the ratio of Im Z and Re z is taken. Inserting the latter expression into (5.8) one obtains

$$Z = \int d\boldsymbol{q} \int dQ_i \oint D[Q(\tau)] \exp\left(- \int_0^{\beta} [H_0 + V_{int}(Q, \boldsymbol{q})]\, d\tau + \beta \sum_{n=1}^{\infty} \frac{|(\partial V_n/\partial \boldsymbol{q})|^2}{(2\pi n)^2} \right) . \tag{5.23a}$$

Except for the nonlocal last term in the exponent, this expression is recognized as the average of the one-dimensional quantum partition function over the static configurations of the bath. This formula without the last term has been used by Dakhnovskii and Nefedova [1991] to handle a bath of classical anharmonic oscillators. The integral over $\boldsymbol{q}$ was evaluated with the method of steepest descents leading to the most favorable bath configuration.

5.2. Bath of harmonic oscillators

There are just a few Hamiltonians for which the path integration can be carried out exactly, and the best known case is the driven harmonic oscillator [Feynman and Hibbs, 1965;

Feynman 1972],

$$H_b(p,q) = \sum_j \tfrac{1}{2}p_j^2 + \tfrac{1}{2}\omega_j^2 q_j^2 , \quad V_{int}(Q,\boldsymbol{q}) = \sum_j q_j f_j(Q) . \tag{5.24}$$

A usual, but not always valid, assumption about f_j is $f_j(Q) = C_j Q$. A great deal of the literature is devoted to the analysis of this Hamiltonian, both classical and quantum mechanical.

Two most appealing features of this model draw so much attention to it. First, although microscopically one has very little information about the parameters entering into (5.24), it is known [Caldeira and Leggett 1983] that when the bath responds linearly to the particle motion, the operators $\boldsymbol{q}$ and $\boldsymbol{p}$ satisfying (5.24) can always be constructed, and the only quantity entering into the various observables obtained from the model (5.24) is the spectral density

$$J(\omega) = \tfrac{1}{2}\pi \sum \omega_j^{-1} C_j^2 \delta(\omega - \omega_j) . \tag{5.25}$$

Second, the classical dynamics of this model is governed by the generalized Langevin equation of motion in the adiabatic barrier [Zwanzig 1973; Hanggi et al. 1990; Schmid 1983],

$$\begin{aligned} &\frac{d^2Q}{dt^2} + \int_{-\infty}^{t} dt' \, \eta(t-t') \frac{dQ}{dt'} + \frac{dV_{ad}}{dQ} = f(t) , \qquad \eta(t) = 2\pi^{-1} \int_0^\infty d\omega \, J(\omega) \frac{\cos(\omega t)}{\omega}, \\ &V_{ad}(Q) = V(Q) - \sum \frac{C_j^2 Q^2}{2\omega_j^2} , \end{aligned} \tag{5.26}$$

where the fluctuating force $f(t)$ satisfies the usual fluctuation–dissipation relation

$$\tfrac{1}{2}\langle f(t)f(0) + f(0)f(t)\rangle = \pi^{-1} \int_0^\infty d\omega \, J(\omega) \coth(\tfrac{1}{2}\beta\omega) \cos(\omega t) . \tag{5.27}$$

From the quantum-mechanical point of view the Langevin equation (5.26) describes the evolution of the Heisenberg operator $Q(t)$. The simplicity of this equation is, however, deceptive. For example, it is usually impossible to write down the equation of motion for the mean position $\langle Q \rangle$ in a closed form, because averaging of (5.26) leads to the term $\langle dV_{ad}/dQ \rangle$, which is not equal to $dV_{ad}(\langle Q \rangle)/d\langle Q \rangle$, unless $V_{ad}(Q)$ is a harmonic-oscillator potential. That is why the quantum Langevin equation, being at first glance similar to the classical Langevin equation, may describe tunneling, i.e., penetration to classically forbidden regions.

The situation simplifies when $V(Q)$ is a parabola, since the mean position of the particle now behaves as a classical coordinate. For the parabolic barrier (1.5) the total system consisting of particle and bath is represented by a multidimensional harmonic potential, and all one should do is diagonalize it. On doing so, one finds a single unstable mode with imaginary frequency $i\lambda^\#$ and a spectrum of normal modes orthogonal to this coordinate. The quantity $\lambda^\#$ is the renormalized parabolic barrier frequency which replaces $\omega^\#$ in a multidimensional theory. In order to calculate

it we rewrite the Langevin equation (5.26) in terms of Fourier components. Namely, if we take $Q = \sum Q_v \exp(\mathrm{i}vt)$, then

$$-(v^2 + \omega^{\#2})Q_v + \mathrm{i}v\eta_v Q_v = f_v \,, \tag{5.28}$$

where the subscript v indicates the corresponding Fourier component.

If we further define the susceptibility χ of the system as

$$\chi(v) \equiv \langle Q_v \rangle / \langle f_v \rangle = [-(v^2 + \omega^{\#2}) + \mathrm{i}v\eta_v]^{-1} \,, \tag{5.29}$$

then the eigenfrequency $\lambda^{\#}$ will correspond to the resonance, i.e., to the pole of χ. Setting $v = \mathrm{i}\lambda^{\#}$ we thus find

$$\lambda^{\#} = \omega^{\#2}/[\lambda^{\#} + \hat{\eta}(\lambda^{\#})] \,, \tag{5.30}$$

where $\hat{\eta}(\lambda^{\#})$ is the Laplace transform of $\eta(t)$ [Pollak 1986a, b; Ford et al. 1988]. Use of conventional TST now will give the following result for the classical rate constant [Grote and Hynes 1980; Pollak 1986a, b]

$$k = (\omega_0/2\pi)(\lambda^{\#}/\omega^{\#})\exp(-\beta V_0) \,. \tag{5.31}$$

For Ohmic friction $\eta(t) = \eta\delta(t)$, $\lambda^{\#} = [\omega^{\#2} + (\frac{1}{2}\eta)^2]^{1/2} - \frac{1}{2}\eta$, and (5.31) goes to the celebrated Kramers' formula for classical escape out of a metastable well in the case of moderate and strong damping [Kramers 1940]. In accord with the multidimensional theory predictions, the crossover temperature should be equal to

$$T_c = \lambda^{\#}/2\pi \,. \tag{5.32}$$

If the potential is parabolic, it seems credible that the inverted barrier frequency $\lambda^{\#}$ should be substituted for the parabolic barrier transparency to give the dissipative tunneling rate as

$$k \propto [1 + \exp(2\pi E/\lambda^{\#})]^{-1} \,. \tag{5.33}$$

Such a treatment, while being accurate above T_c, suffers from the total neglect of the actual form of the potential near the well. It can be the basis for a variational procedure with a parabolic reference [Pollak 1986a].

Proceeding now to the instanton treatment of the Hamiltonian (5.24) we observe that the spectrum of quasienergies differs from that of the unperturbed harmonic oscillator, $f(Q) = 0$, only by a shift independent of n [Bas' et al. 1971],

$$\tilde{\varepsilon}_n^i = (n + \tfrac{1}{2})\omega_i + (2\beta)^{-1}\int_0^{\beta} f_i(Q(\tau))\xi(\tau)\,\mathrm{d}\tau \,, \tag{5.34}$$

where ξ is the periodic solution to the classical equation,

$$-\partial^2\xi/\partial\tau^2 + \omega_i^2\xi = -f_i(Q(\tau)) . \tag{5.35}$$

As shown by Benderskii and Makarov [1992], one could consider an even more general problem with oscillator frequencies ω_i dependent on Q. The result would be

$$\tilde{\varepsilon}_n^i = (n + \tfrac{1}{2})\lambda_i/\beta + (2\beta)^{-1}\int_0^\beta f_i(Q(\tau))\xi(\tau)\,d\tau \tag{5.36}$$

where λ_i is the stability parameter of the ith oscillator defined precisely as in the previous section. In particular, when $f_j \equiv 0$, the bath partition function would be $\tilde{Z} = \prod(2\sinh\frac{1}{2}\lambda_j)^{-1}$. For not very large λ_j/β, the dependence of the quasienergy partition function is relatively weak and the factor $\tilde{Z}$ could be removed from the path integral. This gives another derivation of the prefactor (4.27) in the multidimensional instanton theory.

Substituting (5.34) and (5.35) for (5.8) and dropping in Z the constant partition function of unperturbed harmonic oscillator we get the nonlocal effective action derived by Feynman (see also Caldeira and Leggett [1983]),

$$S_{\text{eff}} = S_0 - \frac{1}{2}\int_0^\beta \sum_j d\tau\, d\tau'\, G_j(\tau - \tau')f_j(Q(\tau))f_j(Q(\tau')) , \tag{5.37}$$

where S_0 is the particle action in the bare potential $V(Q)$, $G_i(\tau - \tau')$ are the phonon Green's functions, whose Fourier components are $(\omega_j^2 + \nu_n^2)^{-1}$ in the expansion in the Matsubara frequencies $\nu_n = 2\pi n/\beta$. For linear functions $f_j(Q) = C_jQ$ eq. (5.37) takes the form

$$S_{\text{eff}} = \int_0^\beta d\tau\left(\tfrac{1}{2}\dot{Q}^2 + V_{\text{ad}}(Q) + \frac{1}{2}\int_0^\beta d\tau'\, K(\tau - \tau')Q(\tau)Q(\tau')\right) , \tag{5.38}$$

$$K(\tau) = \beta^{-1}\sum_j\sum_n \frac{C_j^2\nu_n^2}{\omega_j^2(\omega_j^2 + \nu_n^2)}\exp(i\nu_n\tau) = \beta^{-1}\sum_n \hat{\eta}(|\nu_n|)\,|\nu_n|\exp(i\nu_n\tau) .$$

In the derivation of (5.38) we have extracted the δ-function term from the phonon Green's function which, in turn, renormalized the bare potential V to the adiabatic one V_{ad}. An expression similar to (5.37) can be obtained for an arbitrary bath whenever the coupling is sufficiently weak and the functional $\tilde{Z}[Q(\tau)]$ can be expanded into the series

$$\tilde{Z}[Q(\tau)] = Z_0 + \int\frac{\delta\tilde{Z}}{\delta Q}Q(\tau)\,d\tau + \frac{1}{2}\int\int\frac{\delta^2\tilde{Z}}{\delta Q(\tau)\,\delta Q(\tau')}Q(\tau)Q(\tau')\,d\tau\,d\tau' .$$

The first-order term in this expansion renormalizes the potential $V(Q)$ while the bilinear term is analogous to the last term in (5.38). This is the linear-response theory for the bath. In fact, it shows

that, to the extent that the bath quasienergy partition function is approximated by a quadratic functional, any bath is representable as a set of effective harmonic oscillators.

However, the Green's function of the bath $G_b(\tau, \tau') = \delta^2 \tilde{Z}/\delta Q(\tau)\,\delta Q(\tau')$ may have a form quite different from a single-phonon Green's function and may exhibit a strong temperature dependence. It would be interesting, for example, to see explicitly how this kernel, say, for a liquid, reduces to the phonon Green's function but with temperature-dependent parameters so that the friction coefficient η depends on temperature. To the authors' knowledge this has not been done as yet.

Returning to the tunneling, we assume a metastable state like that in fig. 19 and use the Im F method. The extremal trajectories for S_{eff} satisfy the instanton equation of motion ($\delta S_{\text{eff}}/\delta Q = 0$),

$$-\frac{d^2Q}{d\tau^2} + \frac{dV_{ad}(Q)}{dQ} + \int_0^\beta d\tau' \, K(\tau - \tau')Q(\tau') = 0 \,. \tag{5.39}$$

In the same way as is done in the absence of dissipation, one obtains the instanton formula for the rate constant,

$$k = 2\,\text{Im}\,F = \left(\frac{S_0}{2\pi}\right)^{1/2} \left|\frac{(\det' \hat{L})_{\text{ins}}}{(\det \hat{L})_0}\right|^{-1/2} \exp(-S_{\text{ins}}) \,, \tag{5.40}$$

where $\hat{L}$ is the integro-differential operator defined by

$$\hat{L}Q \equiv \left(-\partial_\tau^2 + \frac{d^2V_{ad}}{dQ^2}\right) Q(\tau) + \int_0^\beta d\tau' \, K(\tau - \tau')Q(\tau') \,, \tag{5.41}$$

and the subscripts "ins" and 0 indicate that the operators are taken on the instanton trajectory and on the static path $Q = 0$, respectively. The action S_{ins} is the action from (5.38) on the instanton trajectory, and $S_0 = \int_0^\beta d\tau \, \dot{Q}^2$.

At temperatures above T_c there is no instanton, and escape out of the initial well is accounted for by the static solution $Q \equiv Q^\#$ with the action $S_{\text{eff}} = \beta V_0$ (where V_0 is the adiabatic barrier height here) which does not depend on friction. This follows from the fact that the zero Fourier component of $K(\tau)$ equals zero and hence the dissipative term in (5.38) vanishes if Q = constant. The dissipative effects come about only through the prefactor which arises from small fluctuations around the static solution. Decomposing the trajectory into Fourier series,

$$Q(\tau) = Q^\# + \beta^{-1} \sum_{n=-\infty}^{\infty} Q_n \exp(i\nu_n \tau) \,, \tag{5.42}$$

and using the harmonic approximation for the potential near $Q = Q^\#$ one gets for the action

$$S_{\text{eff}} = \beta V_0 + \frac{1}{2\beta} \sum_{n=-\infty}^{\infty} [\nu_n^2 - \omega^{\#2} + \hat{\eta}(|\nu_n|)|\nu_n|]\, Q_n^2 \,, \tag{5.43}$$

where we recall that $Q_n = Q_{-n}$ because $Q(\tau)$ is real-valued.

A similar expansion can be written in the vicinity of $Q = 0$. Path integration amounts to the Gaussian integration over the Q_n, whereas the integration over the unstable mode Q_0 is understood as described in section 3.3. In that section we also justified the correction factor $\phi = T_c/T = \beta\lambda^{\#}/2\pi$ which should multiply the Im F result in order to reproduce the correct high-temperature behavior. Direct use of the Im F formula finally yields

$$k = 2\beta^{-1}\phi \frac{\mathrm{Im}\, Z}{\mathrm{Re}\, Z} = \frac{\omega_0}{2\pi}\frac{\lambda^{\#}}{\omega^{\#}} \exp(-\beta V_0) \prod_{n=1}^{\infty} \frac{\nu_n^2 + \nu_n \hat{\eta}(\nu_n) + \omega_0^2}{\nu_n^2 + \nu_n \hat{\eta}(\nu_n) - \omega^{\#2}} \tag{5.44}$$

The last term in (5.44) accounts for quantum corrections to the classical escape rate (5.31) [Wolynes 1981; Melnikov and Meshkov 1983; Grabert and Weiss 1984; Dakhnovskii and Ovchinnikov 1985].

In the case of ohmic dissipation the product in (5.44) can be calculated explicitly and one obtains for the quantum correction factor

$$\frac{k}{k_{\mathrm{Kramers}}} = \frac{\Gamma(1 - \beta\Lambda_+^{\#}/2\pi)\,\Gamma(1 - \beta\Lambda_-^{\#}/2\pi)}{\Gamma(1 - \beta\Lambda_+/2\pi)\,\Gamma(1 - \beta\Lambda_-/2\pi)}, \tag{5.45}$$

where k_{Kramers} is the Kramers' rate constant (5.31) and

$$\Lambda_\pm = -\tfrac{1}{2}\eta \pm ((\tfrac{1}{2}\eta)^2 - \omega_0^2)^{1/2}, \quad \Lambda_\pm^{\#} = -\tfrac{1}{2}\eta \pm ((\tfrac{1}{2}\eta)^2 + \omega^{\#2})^{1/2} \tag{5.46}$$

Interestingly, the correction factor is to a good accuracy approximated by the Wigner formula (2.15) and it is practically independent of friction [Hanggi 1986], by contrast with the relatively strong dependence of T_c on η.

The situation changes when moving on to low temperature. Friction affects not only the prefactor but also the instanton action itself, and the rate constant depends strongly on η. In what follows we restrict ourselves to the action alone, and for the calculation of the prefactor we refer the reader to the original papers cited. For the cusp-shaped harmonic potential

$$V(Q) = \tfrac{1}{2}\omega_0^2 Q^2, \quad Q \le Q^{\#}; \qquad V(Q) \to -\infty, \quad Q > Q^{\#}, \tag{5.47}$$

the instanton equation (5.39) can be solved exactly in the Fourier representation for $Q(\tau)$ to give (Grabert et al. 1984a]

$$k \propto \exp(-Q_0^2/2\delta^2), \tag{5.48}$$

where $\delta(\eta, \beta)$ is the zero-point spread of the damped harmonic oscillator,

$$\delta^2(\eta, \beta) = \beta^{-1} \sum_{n=-\infty}^{\infty} [\nu_n^2 + \omega_0^2 + |\nu_n|\hat{\eta}(|\nu_n|)]^{-1}. \tag{5.49}$$

For ohmic friction this sum reduces to

$$\delta^2(\eta, \beta) = 2(\omega_0^2\beta)^{-1} + (2\pi)^{-1}(\Lambda_- - \Lambda_+)^{-1}[\Psi(1 - \Lambda_+\beta/2\pi) - \Psi(1 - \Lambda_-\beta/2\pi)], \tag{5.50}$$

where Ψ is the digamma function, $\Lambda_\pm$ are defined in (5.46). In the case of the undamped oscillator, $\delta^2 = (2\omega_0)^{-1}\coth(\frac{1}{2}\beta\omega_0)$. Else the following asymptotic formulae hold:

$$\delta^2 = \begin{cases} T/\omega_0^2\,, & T \gg \omega_0, \\ (2\omega_0)^{-1}(1-\eta/\pi\omega_0)\,, & T=0\,, \quad \eta \ll \omega_0\,, \\ 2(\pi\eta)^{-1}\ln(\eta/\omega)_0\,, & T=0, \quad \eta \gg \omega_0\,. \end{cases} \tag{5.51}$$

As seen from (5.48) and (5.51), at high temperatures the leading exponential term in the expression for k is independent of η and it displays the Arrhenius dependence with activation energy $E_a = V_0 = \frac{1}{2}\omega_0^2 Q^{\#2}$. Formally, because of the cusp, the instanton in this model never disappears and the cross-over temperature defined by (5.32) is infinite. Practically, however, it is natural to define T_c as the temperature at which the dependence $\ln k(1/T)$, or $\delta^2(1/T)$ levels off. That is, $T_c = \frac{1}{2}\omega_0$ in the absence of dissipation, and T_c decreases with increasing η. At strong friction and zero temperature $\delta^2 \propto 1/\eta$, apart from the weak logarithmic dependence, and the instanton action increases linearly with increasing η. This behavior is universal for different barrier shapes, as can be shown for more realistic potentials from the scaling properties of the instanton solution [Grabert et al. 1984b].

Specifically, let us rewrite (5.39) at $\beta = \infty$, having integrated the dissipative term by parts,

$$\frac{-\mathrm{d}^2 Q}{\mathrm{d}\tau^2} + \frac{\mathrm{d}V_{ad}(Q)}{\mathrm{d}Q} + \int_0^\infty \mathrm{d}\tau'\, g(\tau-\tau')\dot{Q}(\tau') = 0\,, \tag{5.52}$$

where the Fourier components of the new kernel $g(\tau-\tau')$ are $g_n = -\mathrm{i}\hat{\eta}(|\nu_n|)\operatorname{sign} n$. In the ohmic case the explicit form for g is

$$g(\tau) = \eta(\pi\tau)^{-1}\,. \tag{5.53}$$

If we scale time as $\tau = \tilde{\tau}\eta$, then the frst term in (5.52) decreases as $1/\eta^2$, while the other two are independent of friction. Therefore, at large η the second derivative term in (5.52), as well as the kinetic energy term in the action, can be neglected, and the entire effect of friction is to change the timescale. That is, the solution to (5.52) is $Q(\tau) = \tilde{Q}(\tau/\eta)$ where $\tilde{Q}$ is a function independent of η. The instanton velocity is scaled as $\dot{Q} \propto \eta^{-1}$, and the action (5.38) grows linearly with η, $S_{ins} \propto \eta$.

The exact solution of the instanton equation in the large ohmic friction limit has been found by Larkin and Ovchinnikov [1984] for the cubic parabola (3.18). At $T = 0$

$$Q_{ins}(\tau) = \tfrac{4}{3}Q_0\,[1 + (\omega_0^2\tau/\eta)^2]^{-1}\,, \qquad S_{ins} = \tfrac{2}{9}\pi\eta Q_0^2\,. \tag{5.54}$$

The instanton action behaves in accord with the scaling predictions and is independent of ω_0. Loosely speaking, the frequency ω_0 is replaced by the friction coefficient η. Grabert et al. [1984b] have studied the energy loss ΔE_{diss} in the dissipative tunneling process and found that ΔE_{diss} is saturated at large friction and becomes independent of η. For a cubic parabola, the maximum energy loss has been found to be $\Delta E_{diss} = 4V_0$.

5.3. Dynamics of the dissipative two-level system

When the potential $V(Q)$ is symmetric or its asymmetry is smaller than the level spacing ω_0, then at low temperature ($T \ll \omega_0$) only the lowest energy doublet is occupied, and the total energy spectrum can be truncated to that of a TLS. If $V(Q)$ is coupled to the vibrations whose frequencies are less than ω_0 and $\omega^{\#}$, it can be described by the spin–boson Hamiltonian

$$H_{sb} = \tfrac{1}{2}\Delta_0\sigma_x + \tfrac{1}{2}\varepsilon\sigma_z + \sum \tfrac{1}{2}\omega_j^2 q_j^2 + \tfrac{1}{2}p_j^2 + Q_0\sigma_z C_j q_j \,, \tag{5.55}$$

where $\frac{1}{2}\Delta_0$ is the tunneling matrix element and ε the energy bias. The tunneling matrix element may be found from the instanton analysis, as described in section 3.4. The extended coordinate Q is replaced in the spin–boson model by the matrix $Q_0\sigma_z$ which has two eigenvalues, $\pm Q_0$, corresponding to the minima of the original potential. If there are high-frequency vibrations among the bath oscillators ($\omega_j \gg \omega_0, \omega^{\#}$), their effect is to renormalize Δ_0 [Leggett et al. 1987], so we can assume that (5.55) contains only the low-frequency vibrations. Since we expect the coherence effects to show up in a symmetric potential, it is not obvious in the least that the Im F method can be used for the spin–boson model. Yet the truncation we have done has simplified the model to such an extent that the explicit real-time dynamics can be investigated.

There is a vast field in chemistry where the spin–boson model can serve practical purposes, namely, the exchange reactions of proton transfer in condensed media [Borgis et al. 1989; Suarez and Silbey 1991a; Borgis and Hynes 1991; Morillo et al. 1989; Morillo and Cukier 1990].

The early approaches to this model used perturbative expansion for weak coupling [Silbey and Harris 1983]. Generally speaking, perturbation theory allows one to consider a TLS coupled to an arbitrary bath via the term $\hat{f}\sigma_z$, where $\hat{f}$ is an operator that acts on the bath variables. The equations of motion in the Heisenberg representation for the $\hat{\sigma}$ operators, $\partial\hat{\sigma}/\partial t = \mathrm{i}\hbar^{-1}[\hat{H}, \hat{\sigma}]$, have the form

$$\dot{\sigma}_x = -2\sigma_y\hat{f}\,, \qquad \dot{\sigma}_y = -\Delta_0\sigma_z + 2\sigma_x\hat{f}\,, \qquad \dot{\sigma}_z = \Delta_0\sigma_y\,. \tag{5.56}$$

Note that, since the von Neumann equation for the evolution of the density matrix, $\partial\hat{\rho}/\partial t = -\mathrm{i}\hbar^{-1}[\hat{H}, \hat{\rho}]$, differs from the equation for $\hat{\sigma}$ only by a sign, similar equations can be written out for $\hat{\rho}$ in the basis of the Pauli matrices, $\hat{\rho} = \sigma_x\rho_x + \sigma_y\rho_y + \sigma_z\rho_z + \frac{1}{2}\mathbf{1}$. In the incoherent regime this leads to the master equation [Zwanzig 1964; Blum 1981]. For this reason the following analysis can be easily reformulated in terms of the density matrix.

From (5.56) one can obtain an integro-differential equation for operator σ_z. What we need is the mean particle position, $\langle\sigma_z\rangle$, and in order to find it two approximations are made. First, in taking the bath averages we assume free bath dynamics. Second, we decouple the bath and pseudospin averages, guided by perturbation theory. The result is a Langevin-like equation for the expectation $\langle\sigma_z\rangle$ [Dekker 1987a; Meyer and Ernst 1987; Waxman 1985],

$$\mathrm{d}^2\langle\sigma_z\rangle/\mathrm{d}t^2 + \Delta_0^2\langle\sigma_z\rangle + 4\int_0^t \mathrm{d}t' \,\langle\hat{f}(t)\hat{f}(t')\rangle_s\langle\dot{\sigma}_z(t')\rangle = 0\,, \tag{5.57}$$

where $\langle\hat{f}(t)\hat{f}(t')\rangle_s$ is the symmetrized autocorrelation function for $\hat{f}$, taken for the free bath. A damped oscillator equation of this type was obtained for the first time by Nikitin and Korst

[1965] for the gas-phase model of a stochastically kicked TLS. For the spin–boson Hamiltonian this correlator becomes

$$\langle \hat{f}(t)\hat{f}(t')\rangle_s = Q_0^2\pi^{-1}\int_0^\infty d\omega\, J(\omega)\coth(\tfrac{1}{2}\beta\omega)\cos[\omega(t-t')]\,. \tag{5.58}$$

In the limit of extremely weak coupling, eq. (5.57) becomes Markovian and takes the form (2.41), (2.42). As discussed in section 2.3, for strong enough coupling $\langle\sigma_z\rangle$ exhibits exponential fall off with the rate constant proportional to Δ_0^2, and a prefactor dependent on the bath spectrum. This perturbative treatment however cannot be counted on in the strong friction case, and it applies rather to the spectroscopic problem of broadening of the tunneling splitting spectral line due to dissipation.

The weak-coupling scheme breaks down when the reorganization energy of jth oscillator $E_{rj} = 2Q_0^2C_j^2\omega_j^{-2}$ exceeds its levels spacing ω_j. If $E_{rj} > \omega_j$, when the tunneling particle changes its position, the oscillator equilibrium positions shift through a considerable distance, so that the bath cannot be considered as unperturbed by the particle. It is impossible then to write down the perturbation series by using coupling as a small parameter. This obstacle may be circumvented with the aid of the so-called polaron transformation, which partially diagonalizes the Hamiltonian in the shifted oscillator basis [Silbey and Harris 1984; Leggett et al. 1987]. The new Hamiltonian is

$$\hat{H}' = \hat{U}\hat{H}\hat{U}^{-1} = \tfrac{1}{2}\Delta_0(\sigma_+ e^{-i\hat{\Omega}} + \sigma_- e^{i\hat{\Omega}}) + \tfrac{1}{2}\varepsilon\sigma_z + \sum\tfrac{1}{2}\omega_j^2 q_j^2 + \tfrac{1}{2}p_j^2\,,$$

$$\hat{U} = \exp(-\tfrac{1}{2}i\sigma_z\hat{\Omega})\,, \qquad \hat{\Omega} = 2\sum p_j Q_0 C_j/\omega_j^2\,, \qquad \sigma_\pm = \tfrac{1}{2}(\sigma_x \pm i\sigma_y)\,. \tag{5.59}$$

The operator $\hat{U}$ shifts the q_j oscillator coordinate to its equilibrium through the distance $\pm Q_0C_j/\omega_j^2$, the sign depending on the state of the TLS. All the coupling now is put into the term proportional to the tunneling matrix element and the small parameter of the theory is Δ_0 rather than C_j.

In order to better understand the origin of the first term in (5.59) we separate from the Hamiltonian the part proportional to σ_x and average it over the equilibrium oscillators. This gives rise to an effective tunneling splitting Δ_{eff},

$$\tfrac{1}{2}\Delta_{\text{eff}}\sigma_x = \tfrac{1}{4}\Delta_0\langle e^{-i\hat{\Omega}} + e^{i\hat{\Omega}}\rangle = \tfrac{1}{2}\Delta_0\sigma_x\exp(-\tfrac{1}{2}\langle\hat{\Omega}^2\rangle)$$

$$= \tfrac{1}{2}\Delta_0\sigma_x\exp\Big(-\sum_j\tfrac{1}{2}\Phi_j\Big) = \tfrac{1}{2}\Delta_0\sigma_x\exp(-\tfrac{1}{2}\Phi)\,, \tag{5.60}$$

$$\Phi = \sum_j\Phi_j = 2\sum_j Q_0^2C_j^2\omega_j^{-3}\coth(\tfrac{1}{2}\omega_j\beta) = 4Q_0^2\pi^{-1}\int_0^\infty d\omega\, J(\omega)\omega^{-2}\coth(\tfrac{1}{2}\beta\hbar\omega)\,.$$

The term proportional to σ_y after averaging goes to zero. It is easy to verify that $\exp(-\frac{1}{2}\Phi_j)$ is the statistically averaged overlap integral for the jth oscillator [cf. eq. (2.87)],

$$\exp(-\tfrac{1}{2}\Phi_j) = Z_j^{-1}\sum_n\exp[-\beta\omega_j(n+\tfrac{1}{2})]\int dq_j\,\psi_n(q_j + 2Q_0C_j/\omega_j^2)\psi_n(q_j)\,, \tag{5.61}$$

where Z_j is its partition function. In the strong-coupling case (in which we are interested at present) the absolute value of the overlap integral increases with increasing n (see section 2.5). Nevertheless, as seen from (5.60), the average $\exp(-\frac{1}{2}\Phi_j)$ decreases with increasing temperature because of the alternating sign of the summand in (5.61). Yet the transition probability should increase with increasing temperature, because, according to the golden rule, it is the thermal average of a positive quantity, the *square* of the overlap integral (Franck–Condon factor).

Solving now the Heisenberg equations of motion for the σ operators perturbatively in the same way as in the weak-coupling case, one arrives (at $\varepsilon = 0$) at the celebrated "non-interacting blip approximation" [Dekker 1987b; Aslangul et al. 1985]

$$\mathrm{d}\langle\sigma_z(t)\rangle/\mathrm{d}t + \int_0^t f(t-t')\langle\sigma_z(t')\rangle\,\mathrm{d}t' = 0\,, \tag{5.62}$$

$$f(t) = \Delta_0^2 \cos[4Q_0^2 R_1(t)/\pi] \exp[-4Q_0^2 R_2(t)/\pi]\,,$$

$$R_1(t) = \int_0^\infty \omega^{-2} J(\omega) \sin\omega t\,\mathrm{d}\omega\,, \qquad R_2(t) = \int_0^\infty \omega^{-2} J(\omega)(1-\cos\omega t)\coth\tfrac{1}{2}\beta\hbar\omega\,\mathrm{d}\omega\,. \tag{5.63}$$

This approximation has been originally derived and extensively explored in the path-integral techniques (see the review [Leggett et al. 1987]). Most of the results cited in section 2.3 can be obtained from (5.62) and (5.63). Equation (5.62) makes it obvious that only when the integrand $f(t)$ falls off sufficiently fast, can the rate constant be defined, and it equals

$$k = \int_0^\infty \mathrm{d}t f(t)\,. \tag{5.64}$$

Moreover, eq. (5.64) is nothing but the omnipresent golden rule. To see this just notice that the density of final states is identically equal to

$$\rho_\mathrm{f} = \sum_\mathrm{f} \delta(E_\mathrm{i} - E_\mathrm{f}) = (2\pi)^{-1} \sum_\mathrm{f} \int_{-\infty}^\infty \mathrm{d}t \exp[\mathrm{i}(E_\mathrm{i} - E_\mathrm{f})t]\,. \tag{5.65}$$

Substitution of this for the golden-rule expression (1.14) together with the renormalized tunneling matrix element from (5.60) gives (5.64), after thermally averaging over the initial energies E_i. In the biased case the expression for the forward rate constant is

$$\vec{k} = \int_0^\infty \mathrm{d}t \cos(\varepsilon t) f(t)\,. \tag{5.66}$$

So far we took the tunneling matrix element Δ_0 to be independent of the vibration coordinates. In terms of our original model with extended tunneling coordinate Q this assumption means that

the vibrations asymmetrize the instantaneous potential $V(Q, \{q_j\})$ but do not modulate its height or width. This model does not describe the effect of fluctuational barrier preparation dealt with in section 2.5.

For example, consider the OH ··· O fragment shown in fig. 2. The relative O–O distance is clearly the same in the initial and final states, and hence the O–O vibration cannot be considered linearly coupled to the reaction coordinate. Such a mode (call it q_1) is not associated with any reorganization energy, and this necessitates $C_1 = 0$. However, the O–O vibration, changing the tunneling distance, strongly modulates the barrier transparency and facilitates tunneling. For an asymmetric potential one also has to give up the condition $C_1 = 0$. To describe the effect of such "promoting modes" within the spin–boson Hamiltonian the latter is to be modified by replacing Δ_0 with

$$\Delta = \Delta_0 \exp(\gamma q_1) \tag{5.67}$$

[Borgis et al. 1989; Suarez and Silbey 1991a], where q_1 is a particular "coupling" coordinate from the set $\{q_j\}$ which modulates the barrier (we assume for simplicity that there is only one such coordinate), and the exponential form of Δ is accounted for by the Gamov-factor nature of this term.

A similar approach which does not use explicitly the spin–boson Hamiltonian but exploits the assumption that tunneling is sudden in the time scale of the bath vibration period was developed in quantum diffusion theory [Flynn and Stoneham 1970; Kagan and Klinger 1974] and in chemical reaction theory [Goldanskii et al. 1989; Siebrand et al. 1984] within the method of radiationless transition theory [Kubo and Toyazava 1955]. Carrying out the same polaron transformation one gets the effective tunneling matrix element for the case (5.67),

$$\Delta_{\text{eff}} = \Delta_0 \exp[(\gamma^2/4\omega_1)\coth(\tfrac{1}{2}\beta\omega_1)] \exp(-\tfrac{1}{2}\Phi) \,. \tag{5.68}$$

The promoting effect of the q_1 vibration is represented in this formula by the first exponent, which has the sense of the tunneling matrix element (5.67) averaged over the gaussian distribution of q_1 with a spread equal to $\langle q_1^2 \rangle = (2\omega_1)^{-1}\coth(\frac{1}{2}\beta\omega_1)$. The effect of reorganization of the heat bath in transition, which always hinders tunneling, is described by the second exponent. Integrals like (5.64) and (5.66) are usually calculated with the method of steepest descents by deforming the integration contour to the imaginary axis.

The analytic results for the spin–boson Hamiltonian with fluctuating tunneling matrix element (5.67) are investigated in detail by Suarez and Silbey [1991a]. Here we discuss only the situation when the q_1 vibration is quantum, i.e., $\omega_1\beta \gg 1$. When the bath is classical, $\omega_j\beta \ll 1, j \neq 1$, the rate constant for the transition from left to right is given by

$$k = \tfrac{1}{4}\Delta_0^2 \exp[(\tfrac{1}{2}\gamma^2 - E_r')/\omega_1] (\pi\beta/E_r')^{1/2} \exp[-\beta(E_r' - \varepsilon)^2/4E_r'] \,, \tag{5.69}$$

where E_r' means the reorganization energies for all oscillators but q_1, $E_r' = \sum_{j\neq 1} E_{rj}$. The rate constant (5.69) exhibits Arrhenius behavior associated with the activation of classical degrees of freedom, and the tunneling rate is enhanced by the factor $\exp(\gamma^2/2\omega_1)$. At $\gamma = 0$ the result (5.69) is readily recognized as the well known Holstein formula [Holstein 1959], and it is formally equivalent to the Marcus formula (2.62) for a radiationless transition, except that the matrix element V in (2.62) corresponds with diabatic coupling between the terms rather than with tunneling in an adiabatic potential. This analogy suggests that (5.69) is equally valid for electronically adiabatic and nonadiabatic chemical reactions, once the matrix element is properly defined.

At low temperatures, when the bath is quantum ($\beta\omega_j \gg 1$), the rate expression, expanded in series over the coupling strength, breaks up into the contributions from the various processes involving the bath phonons

$$k = k_{1P} + k_{2P} + k_R + k'_R + \cdots , \tag{5.70}$$

where k_{1P} corresponds to one-phonon emission or absorption, k_{2P} to two-phonon emission and absorption, k_R to two-phonon Raman processes and k'_R to the Raman processes involving one phonon and one quantum of the q_1 vibration. The one-phonon contribution, e.g., for an exothermic reaction ($\varepsilon > 0$) at zero temperature equals

$$k_{1P} = 2\varepsilon\eta Q_0^2 \Delta_{eff}^2/\omega_c^2 \tag{5.71}$$

in the deformational potential approximation $J(\omega) = \eta\omega^3\omega_c^{-1}\exp(-\omega/\omega_c)$. With increasing temperature k_{1P} increases linearly with T at $\beta\varepsilon > 1$, while k_{2P} and k_R manifest, respectively, T^2 and T^3 dependences. The low-temperature limit k_c is proportional to Δ_{eff}^2, while the prefactor depends on the concrete spectral properties of the bath.

A disadvantage of the two-state methods is that modelling of a real potential energy surface (PES) by a TLS cannot always been done*). Moreover, this truncated treatment does not cover the high-temperature regime since the truncation scheme does not hold at $T > \omega_0$. With the assumption that transition is incoherent, similar approximations can be worked out immediately from the nonlocal effective action, as shown in Sethna [1981] and Chakraborty et al. [1988] for $T = 0$, and in Gillan [1987] for the classical heat bath.

Consider the $T = 0$ case. Integrating the nonlocal term in (5.38) by parts, we recast it in the form

$$S_{eff} = \int_{-\infty}^{\infty} d\tau \left[\tfrac{1}{2}\dot{Q}^2 + V_{ad}(Q) + \frac{1}{2}\int_{-\infty}^{\infty} d\tau' \left(\sum_j (C_j^2/2\omega_j^3)\exp(-\omega_j|\tau - \tau'|) \right) \dot{Q}(\tau)\dot{Q}(\tau') \right] \tag{5.72}$$

In the case of a symmetric (or just slightly asymmetric) potential the instanton trajectory consists of kink and antikink, which are separated by infinite time and do not interact with each other.**) In other words, we may change the boundary conditions, namely, suppose that the time spans from $-\infty$ to $+\infty$ for a single kink, and then multiply the action in (5.72) by factor 2.

Sethna [1981] considered two limiting cases. The calculation of action in the fast flip approximation ($\omega_j \ll \omega^{\#}$) proceeds by utilizing the expansion $\exp(-\omega_i|\tau|) \simeq 1 - \omega_i|\tau|$. After substituting the first term, i.e. the unity, in (5.72) we get precisely the quantity $\frac{1}{2}\Phi$, which yields the Franck–Condon factor in the rate constant. The next term cancels the adiabatic renormalization and changes $V_{ad}(Q)$

*) Leggett et al. [1987] have set forth a rigorous scheme that reduces a symmetric (or nearly symmetric) double well, coupled linearly to phonons, to the spin–boson problem, if the temperature is low enough. However, in the case of nonlinear coupling (which is necessary to introduce in order to describe the promoting vibrations), no such scheme is known, and the use of the spin–boson Hamiltonian together with (5.67) relies rather on intuition, and is not always justifiable.

**) This approximation is not valid, say, for the ohmic case, when the bath spectrum contains too many low-frequency oscillators. The nonlocal kernel falls off according to a power law, and kink interacts with antikink even for large time separations. We assume here that the kernel falls off sufficiently fast. This requirement also provides convergence of the Franck–Condon factor, and it is fulfilled in most cases relevant for chemical reactions.

back to the bare potential $V(Q)$. Thus, with exponential accuracy one gets the rate constant proportional to the Franck–Condon factor times the tunneling rate in the potential $V(Q)$, in agreement with (5.60) and (5.71).

In the opposite case of slow flip limit, $\omega_j \gg \omega^{\#}$, the exponential kernel can be approximated by the delta function, $\exp(-\omega_j|\tau|) \simeq 2\delta(\tau)/\omega_j$, thus renormalizing the kinetic energy and, consequently, multiplying the particle's effective mass by the factor $M^* = 1 + \sum C_j^2/\omega_j^4$. The rate constant equals the tunneling probability in the adiabatic barrier $V_{ad}(Q)$ with the renormalized mass M^*,

$$k \propto \exp\left[-S_{\text{ins, 1D}}\left(1 + \sum C_j^2/\omega_j^4\right)^{1/2}\right]. \tag{5.73}$$

As discussed before, the mass renormalization is a reflection of the fact that the particle traces a distance longer than $2Q_0$ in the total multidimensional coordinate space.

The promoting vibrational modes, like q_1 in the above spin–boson treatment, cannot be introduced within the Hamiltonian (5.24) with the linear coupling functions $f_j = C_jQ$, because such couplings suppress tunneling via the Franck–Condon factor, and in order to study vibration-assisted tunneling in symmetric potentials it is necessary to introduce couplings of a more general form. Due to the symmetry, the coupling functions $f_j(Q)$ are either even or odd in Q. The symmetrically coupled vibrations corresponding to the even functions f_j, such as $f_j = C_jQ^2$, are not reorganised in transition (their equilibrium positions do not shift) so that they do not contribute to the Franck–Condon factors [in Sethna's language this means that the first term in the expansion of the exponent $\exp(-\omega_j|\tau|)$ after substitution to the formula for the action gives zero]. On the other hand, they can strongly modulate the potential $V(Q)$ and promote tunneling. The antisymmetrically coupled vibrations (with odd functions f_j) lead to Franck–Condon factors in the usual way described in Sethna [1981] and Chakraborty et al. [1988]. For the situation presented in fig. 2, for instance, the normal lattice modes that shift the O-atoms in opposite directions, are symmetrically coupled to the H-coordinate, while those vibrations that move both O-atoms as a whole are coupled antisymmetrically.

The symmetric coupling case has been examined by using Sethna's approximations for the kernel by Benderskii et al. [1990, 1991a]. For low-frequency bath oscillators the promoting effect appears in the second order of the expansion of the kernel in $\omega_j|\tau|$, and for a single bath oscillator in the model Hamiltonian (4.40) the instanton action has been found to be

$$\begin{aligned} &S_{\text{sud}} = S_{\text{ins, 1D}}(Q_t^3 + 2^{-3/2}\,3aQ_t^2)\,, \quad a = C^2/4\Omega\,, \\ &Q_t = -2^{-1/2}a(1-b)^{-1} + [1 + \tfrac{1}{2}a^2(1-b)^{-2}]^{1/2}, \quad \Omega \ll (1-b)^{1/2}\,. \end{aligned} \tag{5.74}$$

This is the sudden approximation for a symmetric potential. According to (5.74), the tunneling distance decreases from $2Q_0$*) to $2Q_t$. The corresponding tunneling trajectory in (Q,q) space is shown in fig. 17. In the opposite limit of high bath oscillator frequency the action is given by (4.45), and the trajectory is shown in the same figure. The exact instanton action value is compared in fig. 32 with both the sudden and adiabatic approximations. For definiteness, the adiabatic barrier height has been taken to be half the one-dimensional barrier $V^{\#} = \frac{1}{2}V_0$, so that $b = \frac{1}{2}$, $C = \Omega$. One sees that the sudden approximation is realized only for fairly low vibration frequencies, while the adiabatic approximation becomes excellent for $\Omega \geq 2$.

*) $Q_0 = 1$ in dimensionless units of (4.40).

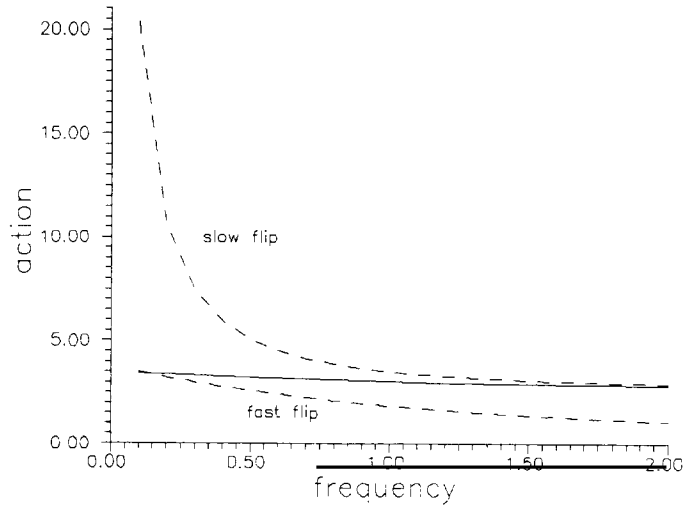

Fig. 32. Dimensionless instanton action $S_{ins}\omega_0/V_0$ plotted against the q-vibration frequency $\Omega = C$ for PES (4.28). Solid line corresponds to exact instanton solution, dashed lines, to sudden and adiabatic approximations.

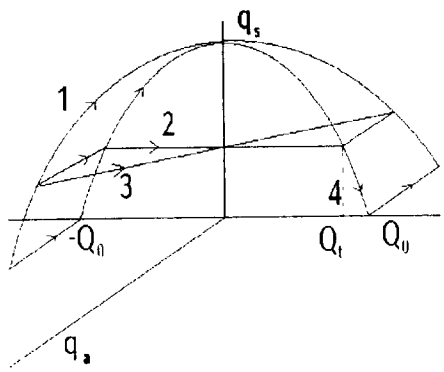

Fig. 33. Three-dimensional instanton trajectories of a particle in a symmetric double well, interacting with symmetrically and antisymmetrically coupled vibrations with coordinates and frequencies q_s, ω_s, and q_a, ω_a, respectively. The curves are: 1, ω_a, $\omega_s \gg \omega_0$ (MEP); 2. ω_a, $\omega_s \ll \omega_0$ (sudden approximation); 3. $\omega_s \ll \omega_0$, $\omega_a \gg \omega_0$; 4. $\omega_s \gg \omega_0$, $\omega_a \ll \omega_0$.

Suppose now that both types of vibrations are involved in the transition. The symmetric modes decrease the effective tunneling distance to $2Q_t$, while the antisymmetric ones create the Franck–Condon factor in which the displacement $2Q_0$ now is to be replaced by the shorter tunneling distance $2Q_t$ [Benderskii et al. 1991a]

$$\Phi = 2\sum Q_t^2 C_j^2 \omega_j^{-3}. \tag{5.75}$$

Thus the promoting vibrations reduce the Franck–Condon factor itself, which is not reflected in the spin–boson model (5.55), (5.67). As an illustration, three-dimensional trajectories for various interrelations between symmetric (ω_s) and antisymmetric (ω_a) vibration frequencies, and ω_0 are shown in fig. 33.

When both vibrations have high frequencies, $\omega_{a,s} \gg \omega_0$, the transition proceeds along the MEP (curve 1). In the opposite case of low frequencies, $\omega_{a,s} \ll \omega_0$, the tunneling occurs in the barrier, lowered and reduced by the symmetrically coupled vibration q_s, so that the position of the antisymmetrically coupled oscillator q_a shifts through a shorter distance, than that in the absence of coupling to q_s (curve 2). The cases $\omega_s \gg \omega_0$, $\omega_a \ll \omega_0$, and $\omega_s \ll \omega_0$, $\omega_a \gg \omega_0$, characterized by combined trajectories (sudden limit for one vibration and adiabatic for the other) are also presented in this picture.

5.4. *Dissipative nonadiabatic tunneling*

The problem of nonadiabatic tunneling has been already formulated in section 3.5, and in this subsection we study how dissipation affects the conclusions drawn there. The two-state Hamiltonian for the system coupled to a bath is conveniently rewritten via the Pauli matrices

$$H = \{\tfrac{1}{2}P^2 + \tfrac{1}{2}[V_i(Q) + V_f(Q)]\}\mathbf{1} + \tfrac{1}{2}[V_f(Q) - V_i(Q)]\sigma_z + V_d(Q)\sigma_x + \sum[\tfrac{1}{2}p_j^2 + \tfrac{1}{2}\omega_j^2(q_j + C_jQ/\omega_j^2)^2]\mathbf{1} \,. \tag{5.76}$$

Here V_i and V_f are the terms of initial and final states, V_d the diabatic coupling. We have explicitly added the counterterm $\sum C_j^2Q^2/2\omega_j^2$ in order to cancel the adiabatic renormalization caused by vibrations. We shall consider the particular case of two harmonic diabatic terms,

$$H = \tfrac{1}{2}P^2 + \tfrac{1}{2}\omega_0^2(Q + F\sigma_z/\omega_0^2)^2 + V_d\sigma_x + \tfrac{1}{2}\varepsilon\sigma_z + \sum[\tfrac{1}{2}p_j^2 + \tfrac{1}{2}\omega_j^2(q_j + C_jQ/\omega_j^2)^2] \,, \tag{5.77}$$

where the diabatic coupling V_d is supposed to be constant, F is half the difference of the slopes of the terms,

$$F = \tfrac{1}{2}[\mathrm{d}V_i/\mathrm{d}Q - \mathrm{d}V_f/\mathrm{d}Q]_{Q=Q_c} \,, \tag{5.78}$$

and the crossing point has the coordinate $Q_c = -\varepsilon/2F$.

The formal structure of (5.77) suggests that the reaction coordinate Q can be combined with the bath coordinates to form a new fictitious "bath", so that the Hamiltonian takes the standard form of dissipative TLS (5.55). Suppose that the original spectrum of the bath is ohmic, with friction coefficient η. Then diagonalization of the total system $(Q, \{q_j\})$ gives the new effective spectral density [Garg et al. 1985]

$$J_{\mathrm{eff}}(\omega) = \omega_0^4\chi''(\omega) = \eta\omega\omega_0^4/[(\omega_0^2 - \omega^2)^2 + \eta^2\omega^2] \,, \tag{5.79}$$

where χ'' is the imaginary part of the susceptibility of the damped harmonic oscillator with frequency ω_0 and friction coefficient η. After formal substitution $Q_0 = F/\omega_0^2$, $\frac{1}{2}\Delta_0 = V_d$ for (5.55), the Hamiltonian (5.77) becomes formally equivalent to (5.55) with the spectral density (5.79).

It is to be emphasized that, despite the formal similarity, the physical problems are different. Moreover, in general, diabatic coupling V_d is not small, unlike the tunneling matrix element, and this circumstance does not allow one to apply the noninteracting blip approximation. So even having been formulated in the standard spin–boson form, the problem still remains rather sophisticated. In particular, it is difficult to explore the intermediate region between nonadiabatic and adiabatic transition.

When V_d is small so that the transition is nonadiabatic, the usual golden-rule analysis based on (5.66) can be performed to give [Garg et al. 1985; Wolynes 1987]

$$k = V_d^2(\pi\beta_{\text{eff}}/E_0)^{1/2}\exp(-Q^{\#2}/2\delta^2)\,, \qquad Q^{\#} = Q_0 - \varepsilon/2F\,,$$

$$E_0 = 2\omega_0^2 Q_0^2 = 2F^2/\omega_0^2\,, \tag{5.80}$$

where $Q^{\#}$ is the distance from the minimum of the initial well to the barrier top. The "effective temperature" is defined as

$$T_{\text{eff}} = \beta_{\text{eff}}^{-1} = \omega_0^2\delta^2(\eta, \beta)\,, \tag{5.81}$$

where δ is defined in (5.50). At high temperatures $T_{\text{eff}} = T$, and (5.80) is nothing but the Marcus formula, irrespective of friction.

As the temperature drops, (5.80) starts to incorporate quantum corrections. When friction increases, T_{eff} decreases and the prefactor in (5.80) increases. This means that the reaction becomes more adiabatic. However, the rise of the prefactor is suppressed by the strong decrease in the leading exponent itself. The result (5.80) may be recast in a TST-like form. If the transition were classical, the rate constant could be calculated as the average flux towards the product valley

$$k = \frac{1}{2}\int \mathrm{d}v\,\mathrm{d}Q\,B(v)v\rho_{\text{cl}}(v, Q)\delta(Q - Q^{\#})\,, \tag{5.82}$$

where v is the velocity, $B(v)$ is the Landau–Zener prefactor (3.88) $B(v) = \pi V_d^2/vF$, $\rho_{\text{cl}}(v, Q)$ is the classical equilibrium distribution function in the initial well.

In the quantum case this function is to be replaced by its quantum counterpart, the Wigner function [Feynman 1972; Garg et al. 1985; Dakhnovskii and Ovchinnikov 1985] expressed via the density matrix as

$$W(v, Q) = (2\pi)^{-1}\int \mathrm{d}Q'\exp(\mathrm{i}Q'v)\,\rho(Q - \tfrac{1}{2}Q', Q + \tfrac{1}{2}Q') \tag{5.83}$$

Substitution of this in (5.82) gives

$$k = \pi V_d^2\rho(Q^{\#}, Q^{\#})/2F\,, \tag{5.84}$$

identical to (5.80). The effect of friction is to slow down the motion, i.e., to decrease v, thereby increasing the Landau–Zener factor.

In the deep tunneling regime, $T \to 0$, the velocity entering into the Landau–Zener factor is formally imaginary. For an asymmetric potential this limit can be studied with the usual Im F techniques. In order to explore the whole range of Landau–Zener parameters it is more expedient to deal with the original Hamiltonian (5.76). Further, the σ operators, as well as the q oscillators, can be integrated out of the problem by use of the quasienergy method, leading to the problem formulated in terms of the reaction coordinate alone. This program is realized in appendix B, and here we just write out the final result,

$$k = Bk_{\text{ad}}\,, \tag{5.85}$$

where k_{ad} is the rate of dissipative tunneling in the lower adiabatic term V_- (fig. 23), found according to the recipe of section 5.2, and B is the prefactor

$$B = 2\pi\delta^{-1}e^{-2\delta}\delta^{2\delta}/\Gamma^2(\delta)\,, \quad \delta = V_d^2/2Fv_{ins}\,, \tag{5.86a, b}$$

where v_{ins} is the imaginary-time instanton velocity.

In the nonadiabatic limit ($\delta \ll 1$) $B = \pi V_d^2/v_{ins}F$, and at $\delta \gg 1$ the adiabatic result $k = k_{ad}$ holds. As shown in section 5.2, the instanton velocity decreases as η increases, and the transition tends to be more adiabatic, as in the classical case. This conclusion is far from obvious, because one might expect that, when the particle loses energy, it should increase its upside-down barrier velocity. Instead, the energy losses are saturated to a finite η-independent value, and friction slows the tunneling motion down.

6. Examples of quantum chemical reactions

Low-temperature chemistry has originated as a branch of solid state chemistry, and major attention has been paid to studying incoherent chemical conversions at cryogenic temperatures. Spectroscopic studies of tunneling splittings in cryogenic matrices of noble gases appeared after suitable laser techniques were developed. In the 80s this field was given impetus by the new supersonic cooling technique, which permitted one to study gas-phase reactions with low translational and internal temperatures of reactants. Use of supersonic beams of heavy noble gases with seeded molecules made the vibrational temperatures below 50 K available. The translational temperature is as low as 5–7 K, so that the reactant molecules form van der Waals complexes even with noble gas molecules [Amirav et al. 1980]. In this regard these reactions differ from the usual gas-phase reactions with continuous energy spectrum, being closer to solid-state reactions with bound initial and final states.

By now, numerous examples of tunneling in chemistry have been studied. The exhaustive list of these pieces of evidence may be found in the review by Benderskii and Goldanskii [1992], and here we confine the discussion to just a number of the most typical examples.

6.1. Hydrogen transfer

We start with the reaction of abstraction of a hydrogen atom by a CH_3 radical from molecules of different matrices (see, e.g., Le Roy et al. [1980], Pacey [1979]). These systems were the first to display the need to go beyond the one-dimensional consideration. The experimental data are presented in table 2 together with the barrier heights and widths calculated so as to fit the theoretical dependence (2.1) with a symmetric gaussian barrier.

The one-dimensional model assumes that tunneling occurs when the C–C distance, R_{CC}^0, is fixed. This distance corresponds to the sum of the van der Waals radii, and the distance the tunneling particle should overcome equals $d = R_{CC}^0 - 2R_{CH}^0$, where R_{CH}^0 is the equilibrium CH bond length. The calculated PES for the methyl radical reactions analogous to those given in table 2 predicts that the length of the CH bond in the transition and initial states is 1.23–1.28 Å and 1.07–1.08 Å, respectively [Sana et al. 1984]. The C–C distance in the reaction complex is 2.7–2.8 Å and the displacement of the hydrogen atom does not exceed 0.54–0.58 Å. It is this displacement that is consistent with the barrier height measured for the gas-phase reactions.

Table 2
Effective parameters of the one-dimensional gaussian barrier for the H atom in the reactions (6.18) (see below)

Matrix	k_c [s^{-1}]	T_c [K]	V_0 [kcal/mol]	Effective tunneling distance [Å]
CH_3OH	2×10^{-4}	45	11.9	1.08
C_2H_5OH	3×10^{-4}	47	12.1	1.04
CH_3CN	1.4×10^{-5}	44	14.3	0.93

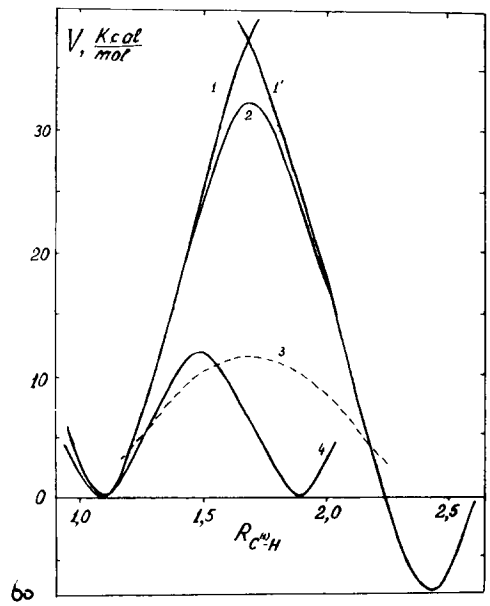

Fig. 34. PES cuts for the reaction (6.19) $C^{(1)}H_3 + C^{(2)}H_3OH \rightarrow C^{(1)}H_4 + C^{(2)}H_2OH$ for the C–C distance corresponding to the hydrogen atom tunneling distance 1.0 Å. 1, 1′ are the diabatic Morse terms, 2 the corresponding adiabatic potential, 3 the one-dimensional parabolic barrier fitted to the experimental data, 4 potential along MEP for the exchange gas-phase reaction $CH_3 + CH_4 \rightarrow CH_4 + CH_3$ [Hipes and Kupperman 1986].

However, for these parameters of the barrier, the cross-over temperature would exceed 500 K, while the observed values are $T_c \simeq 50$ K. If one were to start from the d values calculated from the experimental data, the barrier height would go up to 30–40 kcal/mol, making any reaction impossible. This disparity between V_0 and d is illustrated in fig. 34 which shows the PES cuts for the transition via the saddle-point and for the values of d indicated in table 2.

In view of the correlation between V_0 and d, it is important to remember that the van der Waals distances between the reactants in a lattice are much longer than the inter-reactant distances in gas-phase reaction complexes. For instance, for the reactions in question the C–C distance corresponding to the minimum of the atom–atom potential is 3.7 Å [Pertsin and Kitaigorodskii 1987], so that the tunneling distance for the H-atom in the fragment $C^{(1)}$–H ⋯ $C^{(2)}$ should exceed 1.5 Å (1.3 Å if the zero-point energy is taken into account). Therefore, the problem lies not only in explaining the $k(T)$ dependence from the relationship between V_0 and d, but also in reconciling these values with the inter-reactant distances in the lattice.

Table 3
Tunneling splittings of different vibrational levels in the excited A^1B_2 electronic state of the tropolon molecule

Band assignment	Vibration frequency [cm^{-1}]	Tunneling splitting [cm^{-1}]	
		TrOH	TrOD
0_0^0	–	18.9[4 a)]	2.2
11_0^1	511	13	–
12_0^1	640	17	–
13_0^1	414	32[a)]	3
14_0^1	296	30.4[a)]	11
14_0^2	2 × 296	28	13
19_0^2	2 × 269	9	–
25_0^2	2 × 171	4.2[a)]	–
26_0^2	2 × 39	7.2[a)]	–
26_0^4	4 × 39	4.7	–
26_0^6	6 × 39	3.5	–
26^8	8 × 39	0.8	–

[a)] Data from [Redington et al. 1988], other values are taken from [Sekiya et al. 1990a].

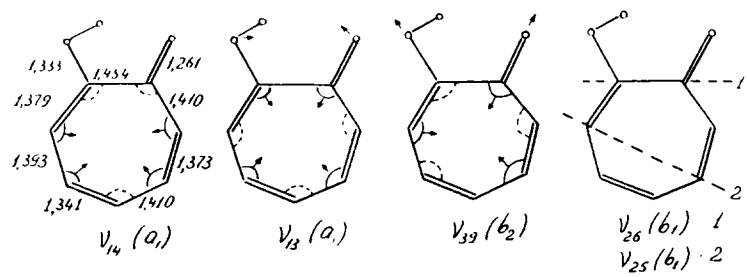

Fig. 35. Normal modes of tropolon molecule participating in tunneling tautomerization. Symmetry of modes is given in brackets. For the off-plane vibrations ν_{25} and ν_{26} the symmetry plane is shown. The equilibrium bond lengths are indicated in the leftmost diagram.

Obviously, these requirements cannot be met in the framework of a one-dimensional model. As explained in section 2.5, these difficulties are naturally circumvented in the vibration-assisted tunneling model. This model has been directly confirmed by the elegant experiments with supercooled jets [Redington et al. 1988; Redington 1990; Sekiya et al. 1990a, b; Fuke and Kaya 1989, Tsuji et al. 1991]. Redington et al. [1988] and Redington [1990] have observed the vibrational selectivity of tautomerization of the tropolon.

The hydrogen-atom tunneling (observed spectroscopically as tunneling splitting Δ) in the OH ··· O fragment connected to the seven-membered carbon atom ring, is enhanced in progressions of the symmetrically coupled vibrations, ν_{13} and ν_{14}, and it is suppressed by the antisymmetrically coupled vibrations ν_{26} and ν_{39} (table 3). The kinematics of these vibrations is featured in fig. 35. The explanation to the vibrational selectivity and relevant formulae (2.82a) and (2.86) are given in section 2.5.

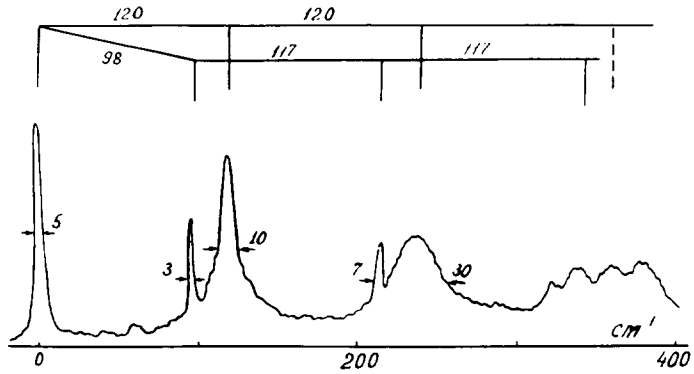

Fig. 36. Laser fluorescence excitation spectrum of 7-azoindole dimer (6.1).

Fuke and Kaya [1989] studied the vibrational selectivity of concerted two-proton transfer in 7-azoindole in the excited electronic state

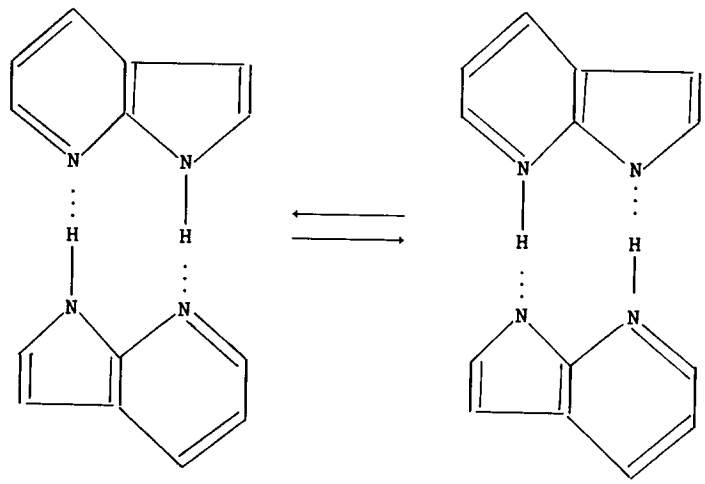

(6.1)

Tunneling in the NH ··· N fragments leads to broadening of certain vibrational bands. This broadening disappears after deuteration. As shown in fig. 36, the tunneling is promoted by the symmetric vibration with frequency $120\,cm^{-1}$. The widths of bands with $n = 0, 1, 2$ are equal to 5, 10 and $30\,cm^{-1}$, respectively. The bending vibration $98\,cm^{-1}$ rather reduces the transition probability. Reaction (6.1) has been studied by Tokumura et al. [1986] (see fig. 1 for the temperature dependence of the rate constant.

It is noteworthy that this example of proton exchange presents a spectroscopic manifestation of incoherent tunneling, which gives rise to spectral line broadening rather than its splitting. This problem is reminiscent of the spin-exchange problem known in magnetic resonance spectroscopy. In the latter problem there are two Zeeman frequencies, ω_1 and ω_2, corresponding to two spin types, and a frequency of double flip-flop exchange between these spins, ω_{ex}. The latter is analogous to the rate constant of the exchange reaction in the problem of proton transfer.

In order to describe the incoherent exchange, in the pulse collision model [Lynden-Bell 1964; Johnson 1967; Stunzes and Benderskii 1971] an effective exchange term, whose real part is

proportional to ω_{ex}, is introduced in the von Neumann equation,

$$\partial\hat{\rho}/\partial t = -i\hbar^{-1}[\hat{H}, \hat{\rho}] + (\partial\hat{\rho}/\partial t)_{ex} \tag{6.2}$$

This results in two Lorentzian spectral lines with positions

$$\tilde{\omega}_{1,2} = \tfrac{1}{2}(\omega_1 + \omega_2) \pm [\tfrac{1}{4}(\omega_1 - \omega_2)^2 - \omega_{ex}^2]^{1/2}\,, \tag{6.3}$$

and widths $\Gamma = \Gamma_0 + \omega_{ex}$, where Γ_0 is the intrinsic width. Therefore, due to incoherent exchange the lines tend to merge and to widen, in contrast with the coherent case, when the lines move apart without broadening [cf. eq. (3.83)].

Sato and Iwata [1988] solved straightforwardly the Shrödinger equation in two dimensions and found the increase in tunneling probability in a three-atom fragment ABA, resulting from an increase in the quantum number of the low-frequency A–A vibration, n. For a barrier height equal to $1300\,cm^{-1}$ (3.72 kcal/mol), a vibration frequency of $450\,cm^{-1}$, and $m_A/m_B = 100$, the tunneling splitting was found to be 111, 133, 151, 166, 193 and $202\,cm^{-1}$ at $n = 0, 1, \ldots 5$, respectively. The two-dimensional picture of the wavefunctions showed that at large n the tunneling particle became delocalized. This result is in agreement with the semiclassical picture set forth in sections 2.5, 4.2 and 4.3.

This simulation performed on the borderline of up-to-date computational capabilities is beyond the framework of the semiclassical approximation, since Δ is comparable with ω_0. As far as real systems are concerned, such simulations are often hardly feasible for higher barriers and more degrees of freedom. On the other hand, as tests show (see section 4.1 and sequel), semiclassical methods cost incomparably less, being at the same time quite accurate, even when the barrier is not too high.

One of the most thoroughly studied examples of intramolecular tunneling is isomerization of malonaldehyde involving the transfer of an H atom in an OH ··· O fragment,

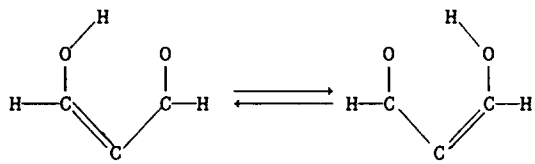

(6.4)

which gives rise to tunneling splitting observable in microwave and IR-spectra. In the ground vibrational state this splitting equals 21.6 and $3\,cm^{-1}$ for the transfer of H and D, respectively [Banghcum et al. 1984; Turner et al. 1984]. The calculation of the one-dimensional tunneling probability [de la Vega 1982] between two equivalent equilibrium states at fixed positions of the O atoms gives the value of Δ, which is nearly two orders smaller than the experimental one.

The cause of this discrepancy, as was pointed out by Bicerano et al. [1983], and Carrington and Miller [1986], is that the transition is accompanied by a considerable displacement of heavy atoms and it cannot be reduced to tunneling in the static barrier. The self-consistent calculation of PES for multidimensional tunneling has been made by Shida et al. [1989]. The transfer of a hydrogen atom is accompanied by a number of large-amplitude motions, including, in addition to OH-bond stretching, the bending vibrations COH and OCC and the stretching vibration CO. All these vibrations supply the dynamical shortening of the tunneling distance.

A major role is played by vibrations with frequencies $318\,cm^{-1}$ and $1378\,cm^{-1}$. The tunneling splitting increases by several times as the quantum numbers of these vibrations increase. The

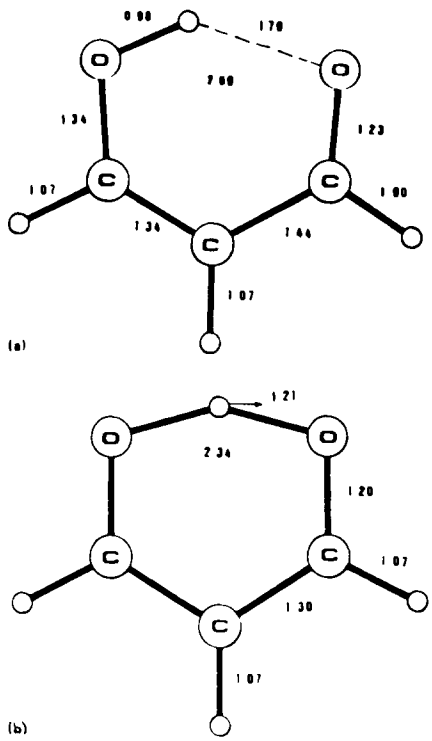

Fig. 37. Geometry of (a) equilibrium and (b) transition state of malonaldehyde (6.4).

deformation of the molecular skeleton in the transition state in comparison with the initial state is shown in fig. 37. As suggested by Shida et al. [1989], Makri and Miller [1987, 1989], Bosch et al. [1990], and Rom et al. [1991], the major multidimensional features of this system can be represented by a two-dimensional PES (4.40). The PES parameters, taking into account the vibrational–adiabatic corrections from high-frequency degrees of freedom, are [Bosch et al. 1990] $V_0 = 18.01$ kcal/mol, $C = 0.86$, $\Omega = 0.71$, $\omega_0 = 1.79 \times 10^{14}\,s^{-1}$, $V^{\#} = V_0(1 - b) = 4.98$ kcal/mol. The contour plot is presented in fig. 38.

A number of empirical tunneling paths have been proposed in order to simplify the two-dimensional problem. Among those are MEP [Kato et al. 1977], sudden straight line [Makri and Miller 1989], and the so-called expectation-value path [Shida et al. 1989]. The results of these papers are hard to compare because slightly different PES were used. As to the expectation-value path, it was constructed as a parametric line $q(Q)$ on which the vibration coordinate q takes its expectation value when Q is fixed. Clearly, for the PES at hand this path coincides with MEP, since q is a harmonic oscillator.

The results for the tunneling splitting calculated with the use of some of the earlier proposed reaction paths for a single PES (4.40) (with the parameters adopted here) are collected by Bosch et al. [1990]. All of them underestimate by at least an order of magnitude the numerically exact value $10.6\,cm^{-1}$, which is also given in that paper. The parameters C and Ω hit the intermediate region between the sudden and adiabatic approximations, described in sections 2.5 and 4.2, and neither of these approximations is quantitatively applicable to the problem.

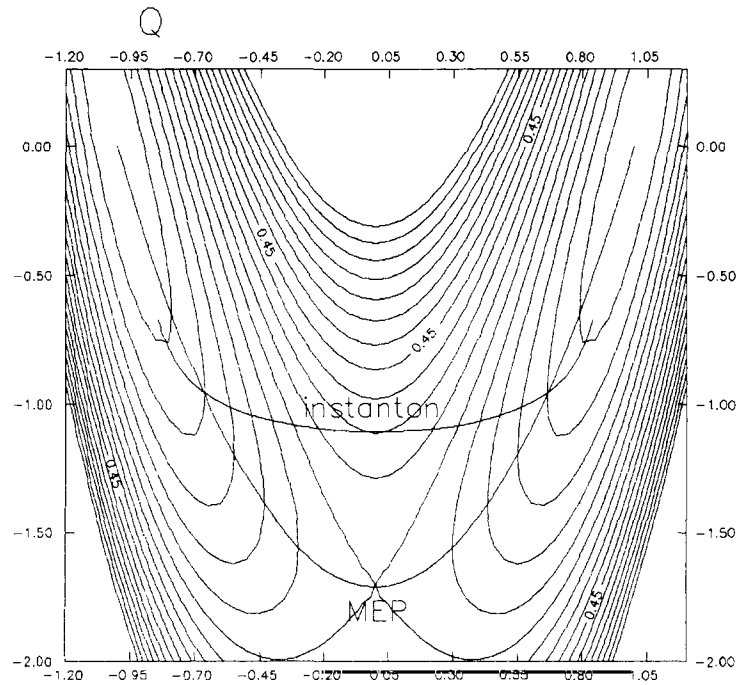

Fig. 38. Contour plot, MEP and instanton trajectory for isomerization of malonaldehyde (6.4). The instanton is drawn for large but finite β; in the limit $\beta = \infty$ it emanates from the potential minimum.

The tunneling trajectory has been numerically calculated by using the instanton techniques of section 4.2 [Benderskii et al. 1993], and it is shown in fig. 38 together with the MEP. The extremal trajectory reveals that tunneling is essentially a two-dimensional process, which involves both degrees of freedom in a manner which is not described by the aforementioned approximate methods. The value of the prefactor obtained is $\tilde{B}_t = 110$, and the tunneling splitting is $13\,\mathrm{cm}^{-1}$, which compares well with both the experimental value and with the quantal calculations of Bosch et al. [1990] ($10.6\,\mathrm{cm}^{-1}$). The large value of the prefactor is due to the fact that the transverse vibration frequency ω_t strongly softens down from the initial to the transition state. It is to be noted that this is a common feature of the proton transfer, and for this reason the primitive semiclassical calculations done with exponential accuracy underestimate the tunneling splitting.

Unlike in the case of the gas-phase measurements, no tunneling has been detected in the IR spectra of the malonaldehyde molecule in the noble matrices at 15–30 K [Firth et al. 1989]. The lack of tunneling is caused by "detuning" of the potential as a result of weak antisymmetric coupling to the environment.

In contrast to malonaldehyde, in the tropolon molecule the tunneling splitting is almost the same in the gas phase and in the neon matrix [Rosetti and Brus 1980]. Note that in both cases there is a similarity not only in Δ but in the equilibrium distances in the O_1HO_2 fragment. The analysis [Redington 1990] of the tropolon IR spectra in the neon matrix, based on the crystallographic data of Shimanouchi and Sasada [1973] for the change of the bond lengths upon transfer of the H-atom (fig. 35), has shown that the displacements of non-tunneling heavy atoms are comparable with the zero-point amplitude, or are even larger. The transfer of hydrogen is strongly coupled with

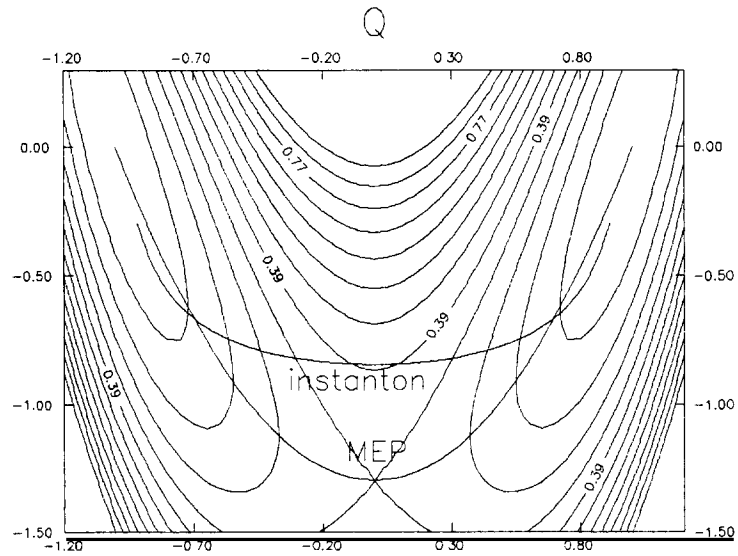

Fig. 39. Contour plot, MEP and instanton trajectory for isomerization of hydrogenoxalate anion (6.5).

the plane vibrations C=O/C–O and C–C=C/C=C–C (coordinates R and S, respectively). The projection of the three-dimensional PES $V(r, R, S)$ onto the R–S plane is characterized by two saddle points.

Such a configurational degeneracy of the reaction path, typical also of two-proton transfer as well as the transfer of the interstitial H-atom between the neighboring sites of a lattice, will be considered below. Since the motion of the H-atom entails strong skeleton deformation, the barrier is higher than for the malonaldehyde (13.7 kcal/mol). The energy bias equals 2–3 cm^{-1}. Unlike the excited state, in the ground state the isotope effect is small, in agreement with the model of vibration-assisted tunneling for the case when the chief contribution comes from the R–S displacements of heavy atoms.

To feature the vibration-assisted tunneling, a convenient object for simulations, is the hydrogenoxalate anion

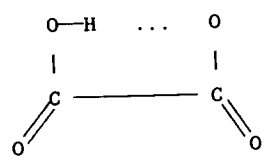

(6.5)

In this case the adjustable parameters of PES (4.40) are $V_0 = 18.52$ kcal/mol, $V^{\#} = 5.62$ kcal/mol, $C = 1.07$, $\Omega = 0.91$, $\omega_0 = 1.50 \times 10^{14}\,s^{-1}$ [Bosch et al. 1990]. Again, as for malonaldehyde, the PES parameters fall between the sudden and adiabatic regimes. The PES contour map and the instanton trajectory for this case are shown in fig. 39. Benderskii et al. [1993] have obtained through the instanton analysis a value for the prefactor, $\tilde{B}_t = 54$, and for the tunneling splitting 1.4 cm^{-1}, in excellent agreement with the quantal calculation value of Bosch et al. [1990], 1.30 cm^{-1}.

The two-proton exchange in pairs of OH ··· O fragments of various carbonic acid dimers

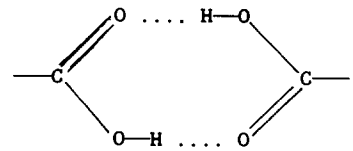

(6.6)

is well studied with NMR relaxation measurements (T_1-NMR) [Meier et al. 1982; Nagaoka et al. 1983; Idziak and Pislewski 1987], incoherent inelastic neutron scattering (IINS) [Horsewill and Aibout 1989a], impurity fluorescence of high spectral resolution [Rambaud et al. 1989, 1990]. In these systems, as well as in other cases of translational tunneling, the energy bias imparted by the asymmetry of crystalline fields precludes proton delocalization. In carbonic acid crystals the bias ε is usually about $60\,\mathrm{cm}^{-1}$, being two orders larger than Δ. For this reason tunneling splitting is hard to observe.

A unique example of observation of tunneling splitting is given by Oppenlander et al. [1989]. Upon replacing the host benzoic acid dimer by a thioindigo molecule of nearly the same size, the resulting bias accidentally turns out to be small, of order of Δ. The 4×4 Hamiltonian of the complex of two dimers and the guest molecule is

$$H = \begin{array}{c} \begin{matrix} \alpha\alpha & \alpha\beta & \beta\alpha & \beta\beta \end{matrix} \\ \begin{pmatrix} -A & \frac{1}{2}\Delta & \frac{1}{2}\Delta & 0 \\ \frac{1}{2}\Delta & B & 0 & \frac{1}{2}\Delta \\ \frac{1}{2}\Delta & 0 & B & \frac{1}{2}\Delta \\ 0 & \frac{1}{2}\Delta & \frac{1}{2}\Delta & A \end{pmatrix} \end{array}, \tag{6.7}$$

where α and β enumerate two possible states of a single dimer, A is twice the bias of a bare dimer, and B is the shift in energy due to the guest molecule. Although $B, A \gg \Delta$, $|B - A| \sim \Delta$. The eigenfunctions of the three lowest energy levels are

$$\begin{aligned} &0.82|\alpha\alpha\rangle - 0.41(|\alpha\beta\rangle + |\beta\alpha\rangle) + 0.05|\beta\beta\rangle\,, \qquad 0.71(|\alpha\beta\rangle - |\beta\alpha\rangle)\,, \\ &0.58|\alpha\alpha\rangle + 0.57(|\alpha\beta\rangle + |\beta\alpha\rangle) - 0.10|\beta\beta\rangle\,, \end{aligned} \tag{6.8}$$

whence delocalization is seen. The "hole burning" spectra measured by Oppenlander et al. [1989] are presented in fig. 40, giving tunneling splitting $\Delta = 8.4 \pm 0.1\,\mathrm{GHz}$, $|A - B| = 4.8 \pm 0.3\,\mathrm{GHz}$.

The other two methods, T_1-NMR and IINS, allow measuring the thermal hopping rates. For different acids in the temperature interval from 40 to 160 K the hopping rate constant, k, ranges from 10^8 to $2\times10^{10}\,\mathrm{s}^{-1}$, and the apparent activation energy is 1–2 kcal/mol. For benzoic acid cyrstals, where both tunneling splitting and thermal hopping were observed, the transition between these two regimes occurs at $\sim 40\,\mathrm{K}$. Formally it is the cross-over temperature introduced in section 2.1 on the basis of the spectral criterion.

As argued in section 2.3, when the asymmetry ε far exceeds Δ, phonons should easily destroy coherence, and relaxation should persist even in the tunneling regime. Such an incoherent tunneling, characterized by a rate constant, requires a change in the quantum numbers of the vibrations coupled to the reaction coordinate. In section 2.3 we derived the expression for the intradoublet relaxation rate with the assumption that only the one-phonon processes are relevant.

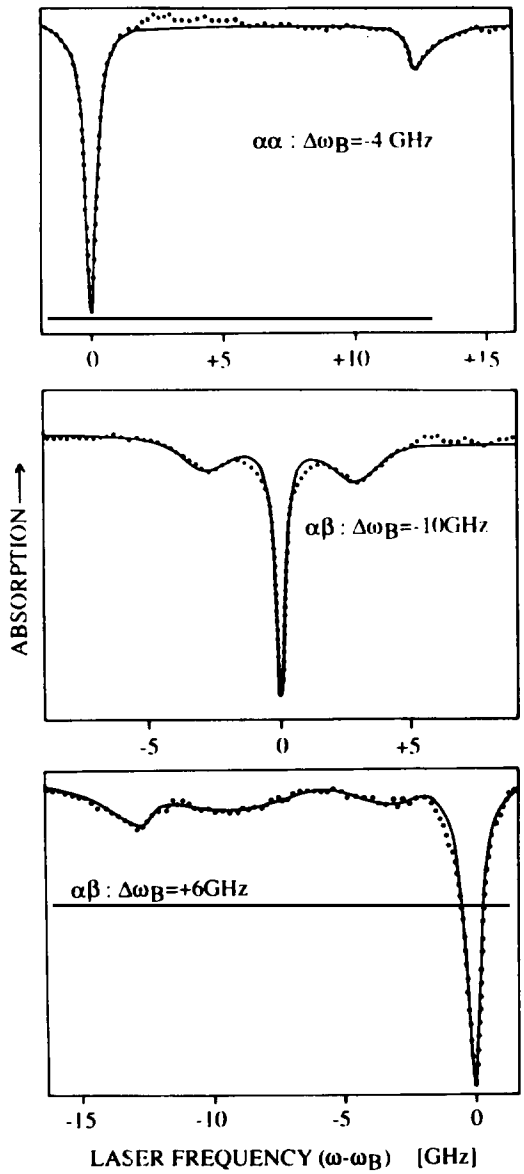

Fig. 40. Hole-burning spectra of thioindigo in benzoic acid crystal at 1.35 K. The scanning laser frequency ω is measured with respect to the burning laser frequency ω_b; $\Delta\omega_b$ is detuning of the burning laser frequency relative to the center of absorption line.

Working in the same weak-coupling approximation, it takes little effort to produce the expression for the rate constant in the asymmetric case, by simply replacing Δ in (2.42)–(2.44) by the energy bias ε.

This expression has been obtained by Skinner and Trommsdorf [1988]. The rate constants for the direct ($\vec{k}$) and reverse ($\overleftarrow{k}$) transition at $\beta\varepsilon > 1$ are proportional to $\bar{n}(\varepsilon)$, and $\bar{n}(\varepsilon) + 1$, respectively, and the relaxation rate equals

$$k = \vec{k} + \overleftarrow{k} = k_0 \coth(\tfrac{1}{2}\beta\varepsilon)\,, \tag{6.9}$$

where $\bar{n}(\varepsilon)$ is the equilibrium number of phonons with energy ε (2.53), and k_0 is determined by the coupling coefficient (see section 2.3). The crossover temperature predicted by (6.9) is associated with the bias ($T_c \simeq \varepsilon/2k_B$). This model is based on the weak-coupling approximation and it takes into account neither reorganization, nor vibration assistance in the sense of section 2.5. Although the term "vibration-assisted tunneling" is also applied to the Skinner–Trommsdorf model, this "assistance" signifies that vibrations supply the energy needed to provide resonance.

The role of two-phonon processes in the relaxation of tunneling systems has been analyzed by Silbey and Trommsdorf [1990]. Unlike the model of TLS coupled linearly to a harmonic bath (2.39), bilinear coupling to phonons of the form $C_{ij}q_iq_j\sigma_z$ was considered. In the deformation potential approximation the coupling constant C_{ij} is proportional to $\omega_i\omega_j$. There are two leading two-phonon processes with different dependence of the relaxation rate on temperature and energy gap, $\tilde{\Delta} = (\Delta^2 + \varepsilon^2)^{1/2}$. Two-phonon emission prevails at low temperatures, and it is temperature-independent and proportional to $\tilde{\Delta}^5$, when $\beta\tilde{\Delta} \gg 1$.

In the opposite case, $\beta\tilde{\Delta} < 1$, the Raman process with the rate constant proportional to $T^7/\tilde{\Delta}^2$ is dominant. At $\beta\tilde{\Delta} \ll 1$ the rate of this process is proportional to $\tilde{\Delta}T^4$. The nonmonotonic dependence of k on $\tilde{\Delta}$ predicted by this model has not been observed experimentally because this effect is pertinent to inaccessibly low temperatures. The T^4 dependence has actually been borne out by Oppenlander et al. [1989].

Quantum-chemical calculations of PES for carbonic acid dimers [Meier et al. 1982] have shown that at fixed heavy-atom coordinates the barrier is higher than 30 kcal/mol, and distance between O atoms is 2.61–2.71 Å. Stretching skeleton vibrations reduce this distance in the transition state to 2.45–2.35 Å, when the barrier height becomes less than 3 kcal/mol. Meier et al. [1982] have stressed that the transfer is possible only due to the skeleton deformation, which shortens the distances for the hydrogen atom tunneling from 0.6–0.7 Å to $\sim$ 0.3 Å. The effective tunneling mass exceeds $2m_H$.

A calculation of tunneling splitting in formic acid dimer has been undertaken by Makri and Miller [1989] for a model two-dimensional polynomial potential with antisymmetric coupling. The semiclassical approximation exploiting a version of the sudden approximation has given $\Delta = 0.9\,\mathrm{cm}^{-1}$, while the numerically exact result is $1.8\,\mathrm{cm}^{-1}$. Since this comparison was the main goal pursued by this model calculation, the asymmetry caused by the crystalline environment has not been taken into account.

Semiempirical two-dimensional PES for O–H $\cdots$ O, O–H $\cdots$ N, N–H $\cdots$ O, and N–H $\cdots$ N can be inferred from the experimental dependence of stretching vibration frequencies and bond lengths on the distance between the heavy atoms. These parameters were extracted from the spectroscopic and crystallographic data for various species containing these fragments [Lippincott and Schröder 1955, 1957]. A further analysis along these lines has been carried out by Sokolov and Savel'ev [1977], Lautie and Novak [1980], and Saitoh et al. [1981]. In fig. 41 taken from the last reference the relationship between V_0, transfer distance ($d = r_{OO} - 2r_{OH}$) and r_{OO} is presented. Using this correlation and the experimental values of r_{OO} and $V^{\#}$, one can immediately estimate the coupling parameter. In particular, for the model PES (4.40)

$$b = C^2/2\Omega^2 = 1 - V^{\#}/V_0\,, \qquad \Omega = 2^{3/2}\,\omega_{OO}/\omega_{OH}\,. \tag{6.10}$$

In addition, the frequency ω_{OO}, as well as the tunneling distance can also be extracted from the same empirical data. Thus all the information needed to construct a PES is available. Of course, this PES is a rather crude approximation, since all the skeleton vibrations are replaced by a single mode with effective frequency ω_{OO} and coupling parameter C. From the experimental data it is known that the strong hydrogen bond ($r_{OO} \leq 2.6$ Å) is usually typical of intramolecular hydrogen transfer.

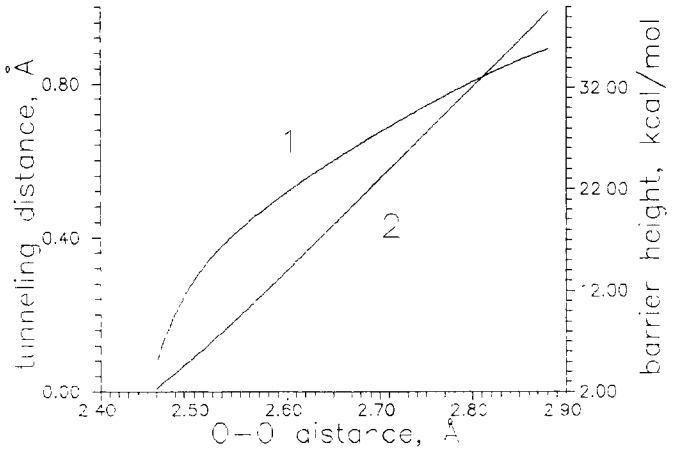

Fig. 41. Empirical correlation between O–O distance, barrier height and hydrogen-atom transfer distance in OH–O fragment.

In this case the parameters C and Ω are of order of unity, and therefore they correspond to the intermediate situation between the sudden and adiabatic tunneling regimes. Examples are malonaldehyde, tropolon and its derivatives, and the hydrogen-oxalate anion discussed above. For intermolecular transfer, corresponding to a weak hydrogen bond, the parameters C, Ω and b are typically much smaller than unity, and the sudden approximation is valid. In particular, carbonic acids fulfill this condition, as was illustrated by Makri and Miller [1989].

Let us now turn to the incoherent case. In the 2-hydroxyphenoxyl radicals

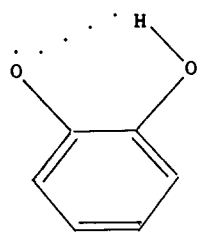

(6.11)

the hydrogen-atom hopping in the fragment O_1HO_2 occurs with the rates 10^5–$10^7\,s^{-1}$, ensuring changes in the hyperfine structure of the electron paramagnetic resonance spectra [Loth et al. 1976]. The distance $O_1H\cdots O_2$ here is much longer than in the above compounds, so that the strong angular deformation is responsible for the transfer. The adiabatic barrier height equals ~ 17 kcal/mol. The bending C–O–H and C–C–O vibrations reduce the tunneling distance from 1.26 Å to 0.36 Å. The transition state corresponds to strong angular deformations (up to 11°).

In the genuine low-temperature chemical conversion, which implies the incoherent tunneling regime, the time dependence of the reactant and product concentrations is detected in one way or another. From these kinetic data the rate constant is inferred. An example of such a case is the important in biology tautomerization of free-base porphyrines (H_2P) and phtalocyanins (H_2Pc), involving transfer of two hydrogen atoms between equivalent positions in the square formed by four N atoms inside a planar 16-member heterocycle (fig. 42).

In the stable trans-form the H atoms lie along the diagonal of the square. The energy of the cis-form, in which the atoms are positioned on one of the edges, is 3–5 kcal/mol higher than that of the trans-form [Smedarchina et al. 1989]. The transition state energies for trans–cis and

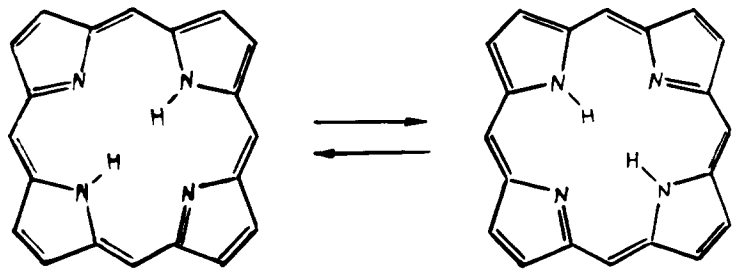

Fig. 42. Two-proton transfer in porphyrine.

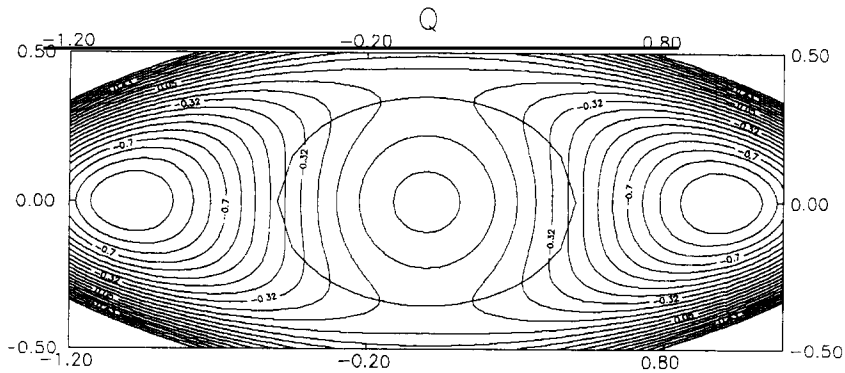

Fig. 43. Contour plot of potential (6.13) with two transition states. $V(Q)=(Q^4-2Q^2)V_0$, $C=20V_0$, $A=90V_0$, $Q_0=0.5$. MEPs are shown.

trans–trans isomerization, calculated in that paper with semiempirical quantum-chemical methods, are equal to $V_0 = 36$–42 kcal/mol and $V'_0 = 60$–66 kcal/mol, respectively.

The temperature dependence of the rate constant for the two-proton exchange in H_2P, HDP and D_2P has been measured with NMR methods in the interval 160–320 K, where k grows from 10 to $10^5\,s^{-1}$ [Hening and Limbach 1979; Schlabach et al. 1986; Crossley et al. 1988; Frydman et al. 1988; Limbach et al. 1982]. In the range 95–110 K the rate constants of H and D transfer, k_H and k_D, measured by Buttenhoff and Moore [1988] with the method of "hole-burning" in the fluorescence spectrum, are 10^{-4}–$10^{-2}\,s^{-1}$. Comparison of the data of both methods shows that the dependence of $k_H(T)$ and $k_D(T)$ on T does not obey the Arrhenius law (E_a^H varies from 10.4 kcal/mol at $T = 200$–320 K to 6.4 kcal/mol at 95–110 K). The activation energy for the D-atom exchange is 3.3 kcal/mol greater than for H-atom. The isotope effect is ~ 25 and ~ 250 at 250 K and 111 K, respectively. Schlabach et al. [1986] have concluded that at $T \geq 200$ K tautomerization corresponds to stepwise transfer of the two H atoms, because the rate constants for HDP and D_2P are similar, i.e., in both species the same stage of D-transfer is rate-limiting.

The PES found by Smedarchina et al. [1989] has two cis-form local minima, separated by four saddle-points from the main trans-form minima. The step-wise transfer (trans–cis, cis–trans) – because of endoergicity of the first stage – displays Arrhenius behavior even at $T < T_c$. The concerted transfer of two hydrogen atoms was supposed to become prevalent at sufficiently low temperatures. However, because of too high a barrier for the concerted trans–trans transition, this

region was experimentally inaccessible. According to Sarai [1982], hydrogen transfer is accompanied by a strong deformation of the heterocycle.

The total reorganization energy equals 7.4 kcal/mol. Owing to the skeleton vibrations, the tunneling distance at the energy E_{ct} of the local minimum of cis-form is decreased to 0.6 Å, while the geometric tunneling distance between the global minima is 1.7 Å. Buttenhoff and Moore [1988] have explained the persistence of the Arrhenius behavior with a small activation energy together with a large isotope effect at low temperatures by supposing that tunneling occurs via a thermally activated state with energy E_{ct}. Accordingly, as in the endoergetic reaction, there are two apparent activation energies E_{ct} and V_0 at $T < T_c$ and $T > T_c$, respectively. To obtain an estimate, they have made use of the simple one-dimensional formula (2.6).

Two-proton transfer has also been observed in naphtazarin crystals in the NMR spectra of C^{13}.

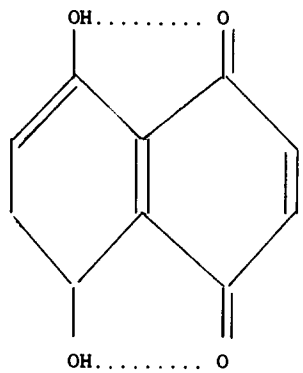

(6.12)

The rate constants k_H and k_D were equal to 3×10^6 and $\sim 10^4\,s^{-1}$, respectively [Shian et al. 1980; Bratan and Strohbusch 1980]. There are two equivalent ways of stepwise transfer, and, therefore, the transition state and MEP are two-fold, if the stepwise transfer is energetically preferable. On the other hand, there is only one way of concerted transfer, which lies between the saddle points. Based on this reasoning, de la Vega et al. [1982] have found that the barrier for stepwise transfer (25 kcal/mol) is 3.1 kcal/mol lower than that for concerted transfer. These authors have proposed a model two-dimensional PES,

$$V(Q,q) = V(Q) + \tfrac{1}{2}Cq^2(Q^2 - Q_0^2) + \tfrac{1}{4}Aq^4 \,. \tag{6.13}$$

One-dimensional motion along Q corresponds to concerted transfer, while the two MEPs, corresponding with stepwise transfer, are

$$q = \pm (C/A)^{1/2}\,(Q_0^2 - Q^2)^{1/2} \,. \tag{6.14}$$

The energy difference between the saddle point and the maximum of the potential (at $Q = q = 0$) equals

$$\Delta V = C^2 Q_0^4/4A \,. \tag{6.15}$$

The contour plot is given in fig. 43. As remarked by Miller [1983], the existence of more than one transition states and, therefore, the bifurcation of the reaction path, is a rather common event. This implies that at least one transverse vibration, q in the case at hand, turns into a double-well potential. The instanton analysis of this PES has been carried out by Benderskii et al. [1991b]. The

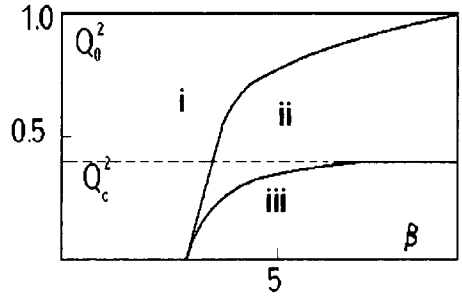

Fig. 44. Bifurcational diagram for the potential (6.13) in the (Q_0^2, β) plane. Domains (i), (ii) and (iii) correspond to Arrhenius dependence (stepwise thermally activated transfer), two-dimensional instanton and one-dimensional instanton (concerted transfer), respectively.

existence of a one-dimensional extremal trajectory with $q = 0$, corresponding to concerted transfer, is evident.

On the other hand, it is clear that in the classical regime, $T > T_{c1}$ (T_{c1} is the crossover temperature for stepwise transfer), the transition should be step-wise and occur through one of the saddle points. Therefore, there should exist another characteristic temperature. T_{c2}, above which there exist two other two-dimensional tunneling paths with smaller action than that of the one-dimensional instanton. It is these trajectories that collapse to the saddle points at $T = T_{c1}$. The existence of the second crossover temperature, T_{c2}, for two-proton transfer has been noted by Dakhnovskii and Semenov [1989].

Earlier, a similar instanton analysis for a PES with two transition states had been performed by Ivlev and Ovchinnikov [1987], in connection with tunneling in Josephson junctions. In the language of stability parameters introduced in section 4.1 the appearance of two-dimensional tunneling paths is signalled by the vanishing of the stability parameter. As follows from (4.23), the one-dimensional tunneling path formally becomes infinitely wide, i.e., it loses its stability, and inclusion of the higher order terms in q results in splitting of the unstable instanton path. Formally, the small stability parameter $\lambda \ll 1$ is equivalent to the existence of a classical transverse degree of freedom, and this mode contributes an Arrhenius dependence with a small activation energy $E_a \leq \Delta V$.

The bifurcational diagram (fig. 44) shows how the (Q_0, β) plane breaks up into domains of different behavior of the instanton. In the Arrhenius region at $T > T_{c1}$ classical transitions take place throughout both saddle points. When $T < T_{c2}$ the extremal trajectory is a one-dimensional instanton, which crosses the maximum barrier point, $Q = q = 0$. Domains (i) and (iii) are separated by domain (ii), where quantum two-dimensional motion occurs. The crossover temperatures, T_{c1} and T_{c2}, depend on ΔV. When $\Delta V \ll V_0$ domain (ii) is narrow ($T_{c1} \simeq T_{c2}$), so that in the classical regime the transfer is stepwise, while the quantum motion is a two-proton concerted transfer. This is the case when the tunneling path differs from the classical one. The concerted transfer changes into the two-dimensional motion at the critical value of parameter $Q_0^* = (2/C)^{-1/4}$. That is, when $\Delta V \geq 2C/A$, two-dimensional behavior, which corresponds to an intermediate case between the stepwise and concerted regimes, persists up to zero temperature.

An Arrhenius plot of the rate constant, consisting of the three domains above, is schematically shown in fig. 45. Although the two-dimensional instanton at $T_{c1} < T < T_{c2}$ for this particular model has not been calculated, having established the behavior of $k(T)$ at $T > T_{c1}$ and $T < T_{c2}$, one is able to suggest a small apparent activation energy (shown by the dashed line) in this intermediate region. This consideration can be extended to more complex PES having a number of equivalent transition states, such as those of porphyrines.

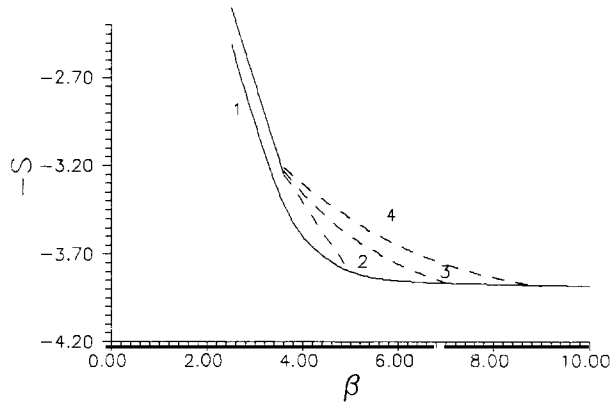

Fig. 45. Action (in units V_0/ω_0) versus β for potential (6.13) at $Q_0 = 0$, 0.33, 0.346, 0.350 for the curves 1–4, respectively; $C = 16V_0$, $A = 90V_0$. Dashed line corresponds to the two-dimensional instanton region.

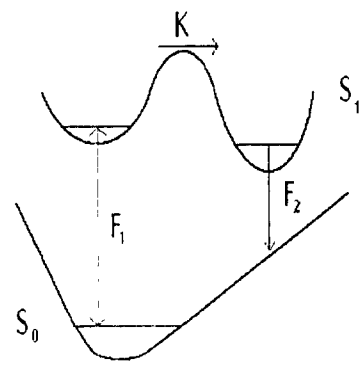

Fig. 46. Scheme of optical transitions, explaining the dual fluorescence resulting from proton transfer in excited electronic state.

Hydrogen transfer in excited electronic states is being intensively studied with time-resolved spectroscopy. A typical scheme of electronic terms is shown in fig. 46. A vertical optical transition, induced by a picosecond laser pulse, populates the initial well of the excited S_1 state. The reverse optical transition, observed as the fluorescence band F_1, is accompanied by proton transfer to the second well with lower energy. This transfer is registered as the appearance of another fluorescence band, F_2, with a large anti-Stokes shift. The rate constant is inferred from the time dependence of the relative intensities of these bands in dual fluorescence. The experimental data obtained by this method have been reviewed by Barbara et al. [1989]. We only quote the example of hydrogen transfer in the excited state of

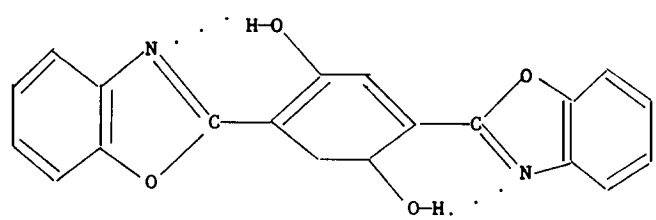

(6.16)

The temperature dependence of the rate constant of rapid hydrogen transfer, measured by Mordzinski and Kuhnle [1986], is given in fig. 1. A similar dependence has been found by Grellmann et al. [1989] for one-proton transfer in "half" of the above molecule (6.16), which does not include the two rightmost rings.

Slower rates ($k = 10^1$–$10^6\,s^{-1}$) are measured with the method of time-resolved triplet–triplet absorption of the product after flash-photolysis (see, e.g., Grellmann et al. [1983]).

The keto-enol tautomerization in the excited triplet state of 2-methylacetophenone involves the transfer of an H atom in the CHO fragment

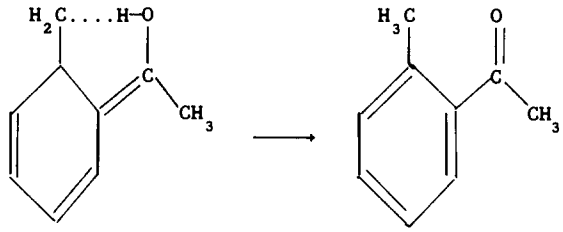

(6.17)

The measured dependence of $k_H(T)$ and $k_D(T)$ consists of an Arrhenius region ($E_a = 9.6$ kcal/mol) going over to the low-temperature plateau below 110 K, where $k_H \simeq 10^5\,s^{-1}$. The isotope effect grows as the temperature drops, $k_H/k_D \simeq 20$ at $T = 100$ K (fig. 15). Tunneling is promoted by the torsional vibrations of the OH and CH groups, as well as the oxy-group bending vibration.

In the trans–enol form the transition does not occur because of the large tunneling distance for the hydrogen atom (2.8 Å). In the cis-form this length decreases to ~ 1 Å, but the transition to this form is unfavorable energetically ($-\Delta E \simeq 3$ kcal/mol). In the transition state the OH bond lies out of plane of the ring. Siebrand et al. [1984] have demonstrated that the experimental curves $k_H(T)$ and $k_D(T)$ can be fitted by the golden-rule formula [see eqs. (5.67) and (5.68)], with the tunneling matrix element modulated by a collinear vibration of frequency 120 cm^{-1} and reduced mass 15 m_H. The evaluated tunneling distance for the H atom is 1.8 Å. In the framework of the golden-rule approach Siebrand et al. [1984] have also considered several other systems.

The transfer of a hydrogen atom resulting in isomerization of the radical

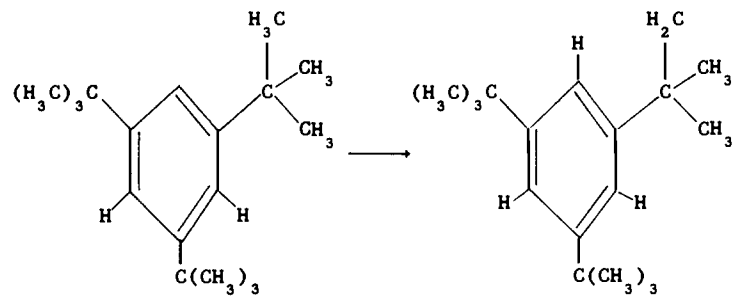

(6.18)

has been studied by Burton et al. [1978]. As in the previous example, the transfer is promoted by internal rotation (see Siebrand et al. [1984]). The temperature dependence of the rate constant for (6.18) is presented in fig. 1.

Abstraction of an H atom from crystalline and glass-like matrices of saturated organic compounds (RH) gives rise to formation of a matrix radical R,

$$CH_3 + RH \rightarrow CH_4 + R\,. \tag{6.19}$$

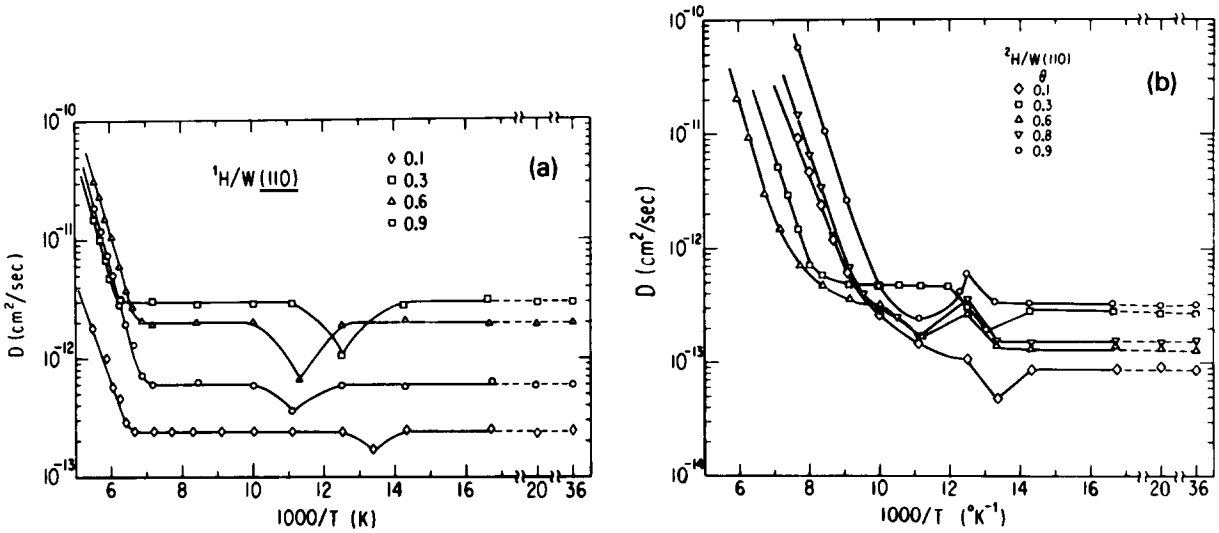

Fig. 47. Arrhenius plot of diffusion coefficient for (a) H and (b) D atoms on the (110) face of a tungsten crystal at coverage degree 0.1–0.9 as indicated. The cusps on the curves correspond to the phase transition.

This is one of the most thoroughly studied examples of intermolecular tunneling. The reaction in the γ-irradiated matrices of aliphatic alcohols is registered with the EPR method by observing the decrease in intensity of the lines of the primary CH_3 radical and the increase in intensity of the lines of the matrix radical (CH_2OH and C_2H_4OH in methanol and ethanol, respectively) [Le Roy et al. 1972, 1980; Sprague and Williams 1971; Campion and Williams 1972; Hudson et al. 1977; Bolshakov et al. 1980; Doba et al. 1984]. The cross-over temperature is 40–50 K, $k_c = 10^{-3}$–$10^{-5}\,s^{-1}$. The apparent activation energy at $T = 50$–100 K is far lower (≤ 2 kcal/mol) than in the gas-phase reaction, where E_a coincides with the barrier height $V_0 = 11.5$–12.5 kcal/mol [Furue and Pacey 1986]. In the γ-irradiated crystalline methanol at 4.2 K the CH_3 radical dies out, forming the new radical CH_2OH, with a characteristic time of $\sim 3 \times 10^3$ s [Toriyama and Iwasaki 1979].

Historically, it was this class of reactions, that fostered the development of the vibration-assisted tunneling model. The tunneling dynamics has been studied by Ovchinnikova [1979] and Trakhtenberg et al. [1982] (see also the review by Goldanskii et al. [1989]). The sudden trajectory bypasses the saddlepoint (see figs. 16 and 29) so that the height of the barrier along it is $\sim$ 15kcal/mol. Owing to the intermolecular vibrations, the "cutting-corner" trajectory corresponds to a C–C distance 3.0–3.1 Å, which is only 0.2–0.3 Å longer than the corresponding distance in the transition state of the same reactions in the gas phase.

Difoggio and Gomer [1982] and Wang and Gomer [1985] have discovered tunneling diffusion of H and D atoms on the (110) face of tungsten. They saw that the Arrhenius dependence of the diffusion coefficient D sharpy levels-off to the low-temperature limit ($D = D_c$) at 130–140 K (fig. 47); the values of D_c depend but slightly on the mass of the tunneling particle: D_c for the D and T atoms is just 10 and 15 times smaller than that for H. The value $D_c \simeq 2 \times 10^{-13}\,cm^2/s$ corresponds to the rate constant of transfer between two adjacent sites, $k_c \sim 10^3\,s^{-1}$ ($k_c = 4D_c/d^2$ where d is the distance between equilibrium positions equal to ~ 2.7 Å).

It follows from the spectrum of the electron energy losses that the hydrogen atom on the (110) face of a tungsten crystal participates in vibrations with frequencies $1310\,cm^{-1}$, $820\,cm^{-1}$ and,

probably, 660 cm^{-1} [Blanchet et al. 1982]. The last two vibrations are the motions along the face and, therefore, they could be candidates to promote tunneling. However, the Debye frequency of the surface vibrations corresponds better to the observed value of T_c. The $D(T)$ dependence undoubtedly testifies to the quantal character of the surface diffusion of hydrogen isotopes. However, the weak dependence of D_c on the mass apparently disagrees with the one-dimensional model.

Jaquet and Miller [1985] have studied the transfer of hydrogen atom between neighbouring equilibrium positions on the (100) face of W by using a model two-dimensional chemosorption PES [McGreery and Wolken 1975]. In that calculation, performed for fairly high temperatures ($T \geq T_c$) the flux–flux formalism along with the vibrationally adiabatic approximation (section 3.6) were used. It has been noted that the increase of the coupling to the lattice vibrations and decrease of the frequency of the latter increase the transition probability.

More realistic PES were used in the calculations of Lauderdale and Truhlar [1985] and Truong and Truhlar [1987]. The Franck–Condon factors entering into the golden-rule formula (1.14) have been analysed by Tringides and Gomer [1986] and Auerbach et al. [1987]. Muttalib and Sethna [1985] have demonstrated that the weak dependence $D(m)$ may be explained with the aid of the adiabatic (slow-flip) model, where the effective mass is the sum of the bare mass and the vibration contributions (see section 5.3). The analysis of the experimental data within this model has shown that the effective H-atom mass spans from $10m_H$ to $6m_H$, depending on the change of the transverse vibration frequency along the trajectory. Since M^* includes the bare mass, m, as only a small component, and $S \sim M^{*1/2}$ [see (eq. 5.73)] the rate constant is a weak function of m.

Muttalib and Sethna [1985] have explained the non-monotonic dependence of D on the coverage degree ϑ discovered by Wang and Gomer [1985], by the change in the adsorption potential. When some of the neighboring nodes are occupied by the adsorbate and, hence, shifted from the equilibrium positions, an additional reorganization energy is involved in the transition. The increase in D with increasing ϑ for $\vartheta < 0.5$ is due to decrease in the vibrationally adiabatic barrier. As ϑ further increases, the diffusion of vacancies in the two-dimensional adsorption layer replaces the H-atom diffusion, reducing D.

The diffusion of H and D atoms in the molecular crystals of hydrogen isotopes was explored with the EPR method. The atoms were generated by γ-irradiation of crystals or by photolysis of a dopant. In the H_2 crystals the initial concentration of the hydrogen atoms 4×10^{-8} mol/cm^2 is halved during $\sim 10^4$ s at 4.2 K as well as at 1.9 K [Miyazaki et al. 1984; Itskovskii et al. 1986]. The bimolecular recombination (with rate constant $k_H = 82\,cm^3\,mol^{-1}\,s^{-1}$) is limited by diffusion, where, because of the low concentration of H atoms, each encounter of the recombinating partners is preceded by 10^5–10^6 hops between adjacent sites.

The diffusion coefficient corresponding to the measured values of k_H ($D = k_H/4\pi R_H$, R_H is the reaction diameter, supposed to be equal to 2 Å) equals $2.7 \times 10^{-16}\,cm^2\,s^{-1}$ at 4.2 K and 1.9 K. The self-diffusion in H_2 crystals at 11–14 K is thermally activated with $E_a = 0.4$ kcal/mol [Weinhaus and Meyer 1972]. At $T \leq 11$ K self-diffusion in the H_2 crystal involves tunneling of a molecule from the lattice node to the vacancy, formation of the latter requiring 0.22 kcal/mol [Silvera 1980], so that the Arrhenius behavior is preserved. Were the mechanism of diffusion of the H atom the same, the diffusion coefficient at 1.9 K would be ten orders smaller than that at 4.2 K, while the measured values coincide. The diffusion coefficient of the D atoms in the D_2 crystal is also the same for 1.9 and 4.2 K. It is ~ 4 orders of magnitude smaller ($3 \times 10^{-20}\,cm^2/s$) than the diffusion coefficient for H in H_2 [Lee et al. 1987].

This clearly indicates quantum diffusion of H and D atoms, rather than molecular diffusion. In mixed crystals of D_2 and HD (with the H_2/D_2 ratio being from 20:1 to 7:1) the concentration of

the D atoms decreases in time, while that of H increases, while the total concentration remains unchanged [Miyazaki and Lee 1986; Miyazaki et al. 1989]. This points to the exchange reaction

$$HD + D = H + D_2 , \tag{6.20}$$

with the exoergicity of 2 kcal/mol caused by the difference in the zero-point energies. The reaction (6.20) does not occur until the D atom encounters an HD molecule as a result of diffusion. The diffusion coefficient for D in D_2 is inferred from the measured rate constant of the exchange reaction in the same way as for H in H_2.

Miyazaki et al. [1984] and Itskovskii et al. [1986] have supposed that the mechanism of diffusion consists in the exchange reactions

$$H + H_2 = H_2 + H , \qquad D + D_2 = D_2 + D , \tag{6.21a, b}$$

causing the atom's transfer to the nearest equilibrium site. The rate constants of reactions (6.21) are related with the diffusion coefficients by the simple formula: $k = 6D/d^2V_0$, where d is the jump distance equal to 4.6 Å for the H_2 crystal, V_0 is the crystal molar volume equal to 20.0, 20.6 and 22.2 cm^3/mol for H_2, HD and D_2, respectively. For the reactions (6.21a), (6.20) and (6.21b) k_c is, respectively, 0.9 s^{-1}, 1.1×10^{-4} s^{-1} and 7.8×10^{-5} s^{-1}.

The spatial localization of H atoms in H_2 and HD crystals found from analysis of the hyperfine structure of the EPR spectrum, is caused by the interaction of the uncoupled electron with the matrix protons [Miyazaki 1991; Miyazaki et al. 1991]. The mean distance between an H atom and protons of the nearest molecules was inferred from the ratio of line intensities for the allowed (without change in the nuclear spin projections, $\Delta m_i = 0$) and forbidden ($\Delta m_i = \pm 1$) transitions. It equals 3.6–4.0 Å and $\sim$ 2.3 Å for the H_2 and HD crystals respectively. It follows from comparison of these distances with the parameters of the hcp lattice of H_2 that the H atoms in the H_2 crystal replace the molecules in the lattice nodes, while in the HD crystal they occupy the octahedral positions.

The intermolecular distance in the H_2 crystal (3.79 Å) is almost five times longer than the H–H bond length, being close to the equilibrium distance in the linear van der Waals complex H_3 (3.5 Å) [Silvera 1980]. The hydrogen atom, as a substituting impurity, moves almost freely in the cavity with radius $\sim$ 0.6 Å. This allows one, when looking for the rate constants of reactions (6.20) and (6.21), to use the gas-phase model, studied quite thoroughly (see, e.g., Garrett and Truhlar [1983, 1991]), as a first approximation.

Such calculations have been performed by Takayanagi et al. [1987] and Hancock et al. [1989]. The minimum energy of the linear H_3 complex is only 0.055 kcal/mol lower than that of the isolated H and H_2. The intermolecular vibration frequency is smaller than 50 cm^{-1}. The height of the vibrational-adiabatic barrier is $\sim$ 9.4 kcal/mol, the H–H distance 0.82 Å. The barrier was approximated by an Eckart potential with width 1.5–1.8 Å. The rate constant has been calculated from eq. (2.1), using the barrier height as an adjustable parameter. This led to a value of V_0 similar to that of the gas-phase reaction $H + H_2$.

The temperature dependences of k, calculated by Hancock et al. [1989], are given in fig. 48. The crossover temperature equals 25–30 K. The weak increase of $k(T)$ with decreasing temperature below T_c is an artefact caused by extending the gas-phase theory prefactor to low temperatures without taking into account the zero-point vibrations of the H atom in the crystal. For the same reason the values of the constants differ by 1–2 orders of magnitude from the experimental ones.

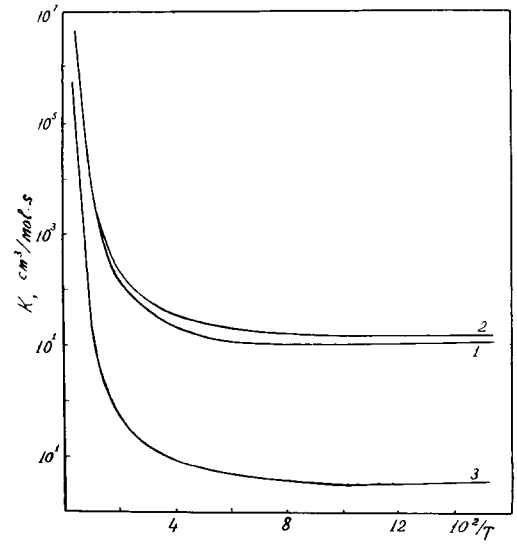

Fig. 48. Calculated temperature dependence of the rate constant of exchange reactions: 1. $H_2 + H$; 2. $H_2 + D$; and 3. $HD + D \rightarrow H + D_2$.

The exchange reactions (6.20) and (6.21) have been among the basic objects of chemical-reaction theory for half a century. Clearly further investigation is needed, incorporating real crystal dynamics. It is worth noting that the adiabatic model, upon which the cited results are based, can prove to be insufficient because of the low frequency of the promoting vibrations.

6.2. Tunneling rotation of methyl group

The fine structure of torsion–vibration spectra of small symmetric molecules and groups such as CH_3, CH_4, NH_3, and NH_4 is one of the most illustrative manifestations of tunneling. This problem has been discussed in detail in several reviews and books (see, e.g., Press [1981], Heidemann et al. [1987]).

The CH_3 group connected to the rest of the molecule by the fourth C-atom bond can rotate around this bond. The potential $V(\varphi)$ the rotating group experiences is three-fold. In the extreme case when the barrier is absent, the group rotates freely, while in the opposite limit of an infinite barrier, it oscillates in one of three minima. How the energy levels change when moving on from free rotation to torsional vibration is shown in fig. 49. Tunneling partially eliminates the triple degeneracy of each vibrational level creating a singlet (A) and doublet (E_a, E_b) in accordance with the irreducible representations of the C_3 symmetry group, which is isomorphous to the permutation group. Figure 49 shows that the A and E levels alternate in the progression of torsional multiplets $n = 0, 1, 2, \ldots$, and the sign of the tunneling splitting is $(-1)^n$.

The potential $V(\varphi)$ may be expanded in a Fourier series, and usually the first harmonic suffices,

$$V(\varphi) = \tfrac{1}{2} V_0 (1 - \cos 3\varphi) , \tag{6.22}$$

where φ is the dihedral angle of rotation of the CH_3 group. The frequency of small torsional vibrations is related with the barrier height by

$$V_0 = \tfrac{2}{9} I \omega_0^2 , \quad I^{-1} = I_1^{-1} + I_2^{-1} , \tag{6.23}$$

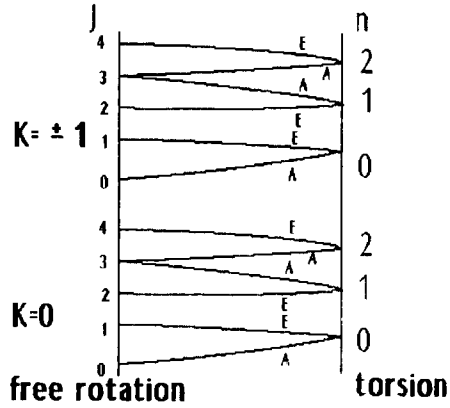

Fig. 49. Correlation between the energy levels of (1) free rotation of the symmetric top, and (2) torsion vibrations in the potential with symmetry C_3. Quantum numbers J and K enumerate rotational levels, n vibrational levels. Relative positions of A and E levels are shown on the right.

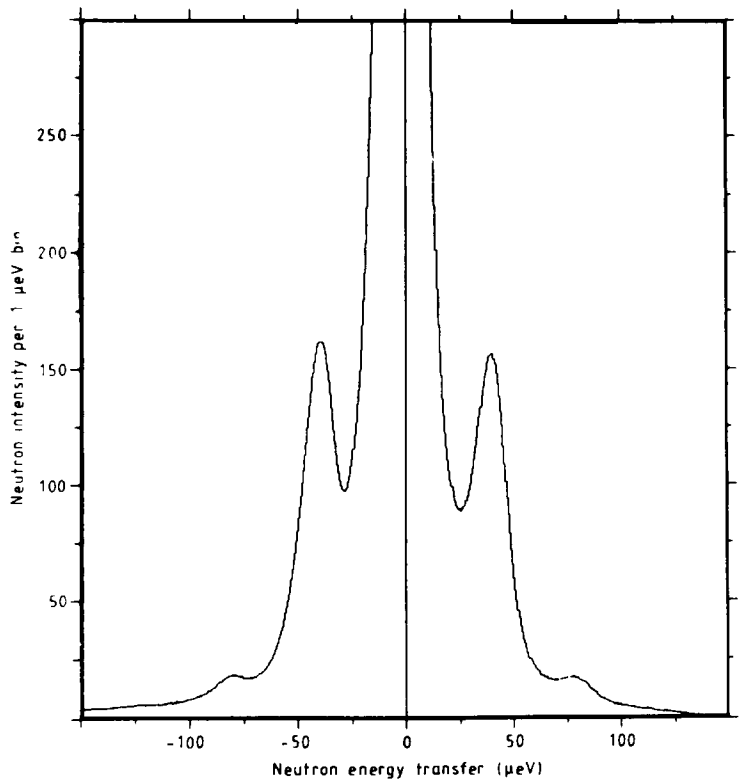

Fig. 50. The INS spectrum of acetylacetone recorded at 4.5 K.

where I is the reduced moment of inertia, and I_1 and I_2 stand for the moments of inertia of the CH_3 group and the remaining molecules.

The magnetic interaction of neutrons with protons or deuterons of the CH_3 (CD_3) group leads to the appearance of peaks of quasielastic and inelastic scattering, corresponding to AE and E_aE_b

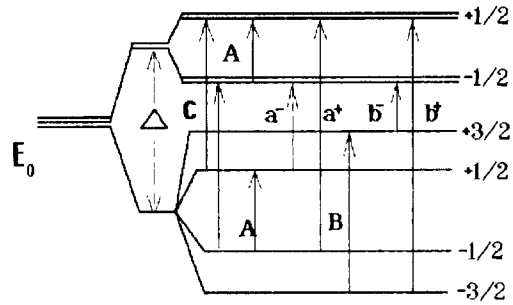

Fig. 51. Zeeman splitting of the lowest AE octet of the CH_3 group. Levels of the E state with $m = \pm 1/2$ are twice degenerate.

transitions, respectively. At liquid helium temperature the energy separation between the elastic central peak and the sidebands of inelastic scattering is equal to the tunneling frequency Δ. A typical example of spectrum is given in fig. 50 taken from Horsewill et al. [1987]. The spectrum dramatically changes when moving on from tunneling to thermally activated rotation (hopping). The sidebands disappear, and the quasielastic peak becomes Lorentzian, with halfwidth $\gamma = \frac{3}{2}\tau_h^{-1}$, where τ_h is the hopping time, i.e., the inverse rate constant $\tau_h^{-1} = k$.

In spin relaxation theory (see, e.g., Zweers and Brom [1977]) this quantity is equal to the correlation time of two-level Zeeman system (τ_c). The states A and E have total spins of protons $\frac{3}{2}$ and $\frac{1}{2}$, respectively. The diagram of Zeeman splitting of the lowest tunneling AE octet $n = 0$ is shown in fig. 51. Since the spin wavefunction belongs to the same symmetry group as that of the hindered rotation, the spin and rotational states are fully correlated, and the transitions observed in the NMR spectra $\Delta m = \pm 1$ and $\Delta m = \pm 2$ include, aside from the Zeeman frequencies, sidebands shifted by Δ. The special technique of dipole–dipole driven low-field NMR in the time and frequency domain [Weitenkamp et al. 1983; Clough et al. 1985] has allowed one to detect these sidebands directly.

Horsewill and Aibout [1989b] have also observed the transitions with $\Delta m = 0$. These transitions with conserved spin projection are due to the coupling of the tunneling and spin reservoirs in the vicinity of crossing of the Zeeman levels belonging to the tunneling states $(A, \frac{3}{2})$ and $(E, -\frac{1}{2})$, $(A, \frac{1}{2})$ and $(E, -\frac{1}{2})$ (see fig. 51). The NMR spectrum of thioanisole [Horsewill and Aibout, 1989b] is shown in fig. 52 demonstrating the change of the resonance frequencies with the magnetic field.

A more traditional technique for measuring the temperature dependence of the longitudinal spin–lattice relaxation time T_1 of methyl-group protons is also widely used for determining the tunneling frequencies Δ and τ_h. The interrelation between T_1, Δ and τ_h emerges due to dipole–dipole interactions between randomly moving protons, and it is described by Clough et al. [1982],

$$T_1^{-1} = C_1 [\tau_h/(1 + \omega_Z^2\tau_h^2) + 4\tau_h/(1 + 4\omega_Z^2\tau_h^2)] , \tag{6.24}$$

where ω_Z is the Zeeman frequency supposed to be greater than Δ, C_1 is the dipole–dipole lattice sum. The Arrhenius behavior of τ_h leads to the minimum of T_1 as a function of temperature at $\omega_Z\tau_h = 1$. The frequent observation of several minima in this function imply that there are several inequivalent methyl groups with different tunneling frequencies.

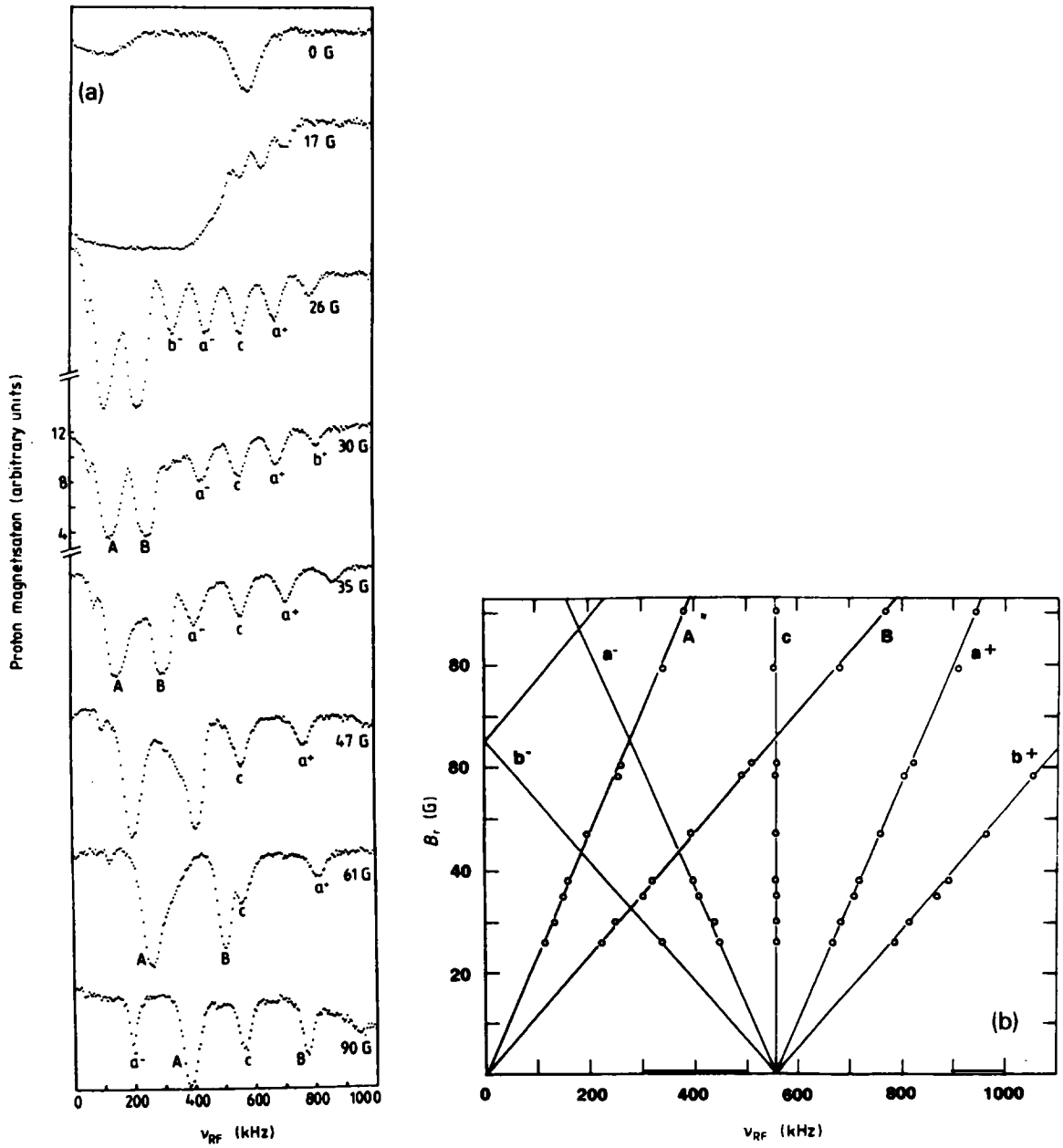

Fig. 52. (a) The frequency swept dipole–dipole driven NMR spectra of thioanisole recorded at a variety of magnetic fields. (b) The NMR and sideband transitions observed in the thioanisole data presented as a plot of magnetic field versus transition frequency. The transitions are defined in fig. 51.

A typical temperature dependence of T_1 is shown in fig. 53. Clough et al. [1981] have found a universal correlation between the temperature at which T_1 has a minimum, T_{min}, and Δ, when the measurements are performed at the same Zeeman frequency. This correlation, demonstrated in fig. 54, holds for all molecular solids studied so far, with Δ covering a range of four orders

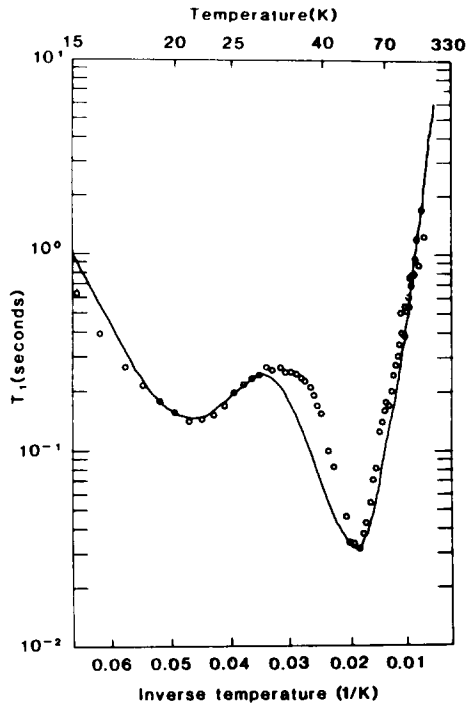

Fig. 53. The temperature dependence of T_1 in tiglic acid.

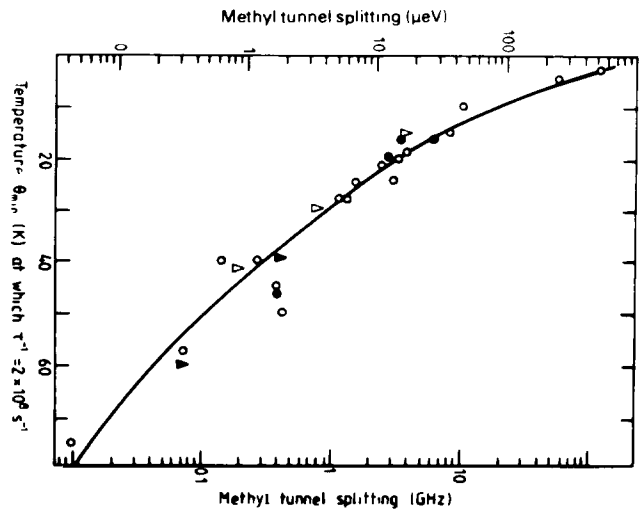

Fig. 54. Universal correlation between T_{min} and tunneling frequency Δ. The values of Δ are given in μeV (1 μeV = 8.066×10^{-3} cm^{-1} = 2.42×10^8 Hz). The Zeeman frequency equals 21 MHz. The points correspond to different chemical species.

of magnitude. The deviations are within a factor of 2. This correlation is the consequence of the fact that the barrier shape is approximately the same for different species. The barrier is overcome either by hopping [with the rate constant (2.14)], or tunneling [with frequency (2.20)], so that $\ln \Delta \propto -T_{min}$.

It is noteworthy that the above rule connects two quite different values, because the temperature dependence of T_1 is governed by the rate constant of incoherent processes, while Δ characterizes coherent tunneling. In actual fact, Δ is not measured directly, but it is calculated from the barrier height, extracted from the Arrhenius dependence $k(T)$. This dependence should level off to a low-temperature plateau at $T < T_{\min}$. This non-Arrhenius behavior of τ_c has actually been observed by Punnkinen [1980] in methane crystals (see fig. 1). A similar dependence, also depicted in fig. 1, has been observed by Geoffroy et al. [1979] for the radical

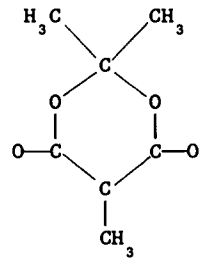

(6.25)

by using double electron–electron resonance. The values of k_c turn out to be several orders smaller than Δ, as should be expected from comparison of eqs. (2.18) and (2.20).

The WKB formula for the tunneling splitting is

$$\Delta = 3\,\frac{\omega_0}{2\pi}\exp\left(-\frac{1}{\hbar}\int_{\varphi_1}^{2\pi/3-\varphi_1} d\varphi\,\{2I[V(\varphi)-\tfrac{1}{2}\hbar\omega_0]\}^{1/2}\right), \tag{6.26}$$

where $\varphi_1 = \frac{1}{3}\cos^{-1}(1-\hbar\omega_0/V_0)$ is the turning point. The results of (6.26) are compared with the exact ones in table 4 taken from Peternelj and Jencic [1989].

As seen from this table, the WKB approximation is reasonably accurate even for very shallow potentials. At $T = 0$ the hindered rotation is a coherent tunneling process like that studied in section 2.3 for the double well. If, for instance, the system is initially prepared in one of the wells, say, with $\varphi = 0$, then the probability to find it in one of the other wells is $P(\pm\frac{2}{3}\pi, t) = \frac{4}{9}\sin^2(\frac{1}{2}\Delta t)$, while the survival probability equals $1 - \frac{8}{9}\sin^2(\frac{1}{2}\Delta t)$. The transition amplitude $A(t)$, defined as $P(\pm\frac{2}{3}\pi, t) = |A(t)|^2$, is connected with the tunneling frequency by

$$\lim_{t\to 0} t^{-1}|A(t)| = \tfrac{1}{3}\Delta\,. \tag{6.27}$$

The treatment of section 2.3 concerned with the destruction of coherence by the environment applies to this case.

Rotation of an end methyl group of a large molecule ($I \approx I_1$) implies transfer of the reduced mass $m = 3m_H m_C(3m_H + m_C)^{-1} = 2.4$ ($m = 4.0$ for CD_3) through the distance 1.74–1.79 Å. This tunneling distance is much greater than that typical of hydrogen transfer, and therefore tunneling rotation can be observed if the barrier is lower. The zero-point amplitude entering into (6.26), $\varphi_1^2 \simeq \frac{2}{9}\hbar\omega_0/V_0$, is 0.2 rad even for barriers as high as 3.5 kcal/mol ($\omega_0 \simeq 220\,\mathrm{cm}^{-1}$), so that the zero-point linear displacements of H atoms are 0.20–0.22 Å. Thus the torsion vibrations are actually the motions with large amplitudes, as compared with stretching modes. The temperature dependence of the zero-point angular amplitude, extracted from INS measurements, is described by (2.29). The tunneling frequencies detectable with INS and NMR lie in the intervals

Table 4
Tunneling frequencies of hindered rotation, in the potential (6.22)

$V_0/\hbar\omega_0$	Δ/ω_0, exact value	Δ/ω_0 from (6.26)
1.234	2.91×10^{-2}	3.79×10^{-2}
1.744	5.04×10^{-3}	5.76×10^{-3}
2.467	3.53×10^{-4}	3.77×10^{-4}
3.020	4.36×10^{-5}	4.54×10^{-5}
3.429	7.26×10^{-6}	7.46×10^{-6}

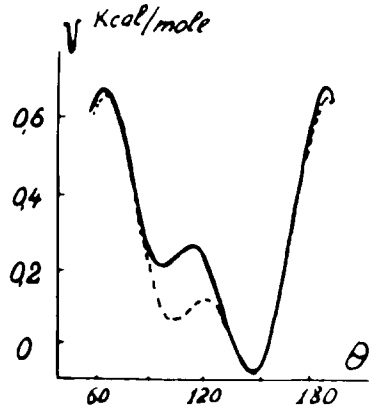

Fig. 55. The potential of hindered rotation of the CH_3 group in nitromethane (CH_3NO_2) crystal, (a) calculated from INS data, $V_3 = 0.586$ kcal/mol, $V_6 = 0.356$ kcal/mol, $\delta = 30°$, and (b) calculated with the atom–atom potential method [Cavagnat and Pesquer 1986]. The barrier height is 0.768 kcal/mol.

10^8–10^{11} and 10^5–$10^8\,s^{-1}$. This corresponds to barrier heights ranging from 0.3 to 3.5 kcal/mol. Incoherent transition occurring in the same barrier would have the rate constant k_c ranging from 10^7 to $10^{-3}\,s^{-1}$, as follows from (2.18) and (2.20) with a typical prefactor $\omega_0/2\pi = 10^{13}\,s^{-1}$. Most of hydrogen-transfer reactions actually lie in this interval. Thus the spectroscopic data correspond to the same barrier transparencies as tunneling chemical reactions.

Among numerous examples of the role of the chemical structure in tunneling rotation we select just one, connected with the effect of intramolecular hydrogen bond. In acetyl acetone in stable enol form

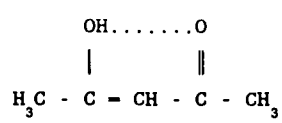

(6.28)

there are two chemically inequivalent methyl groups, with barrier heights equal to 0.45 and 1.18 kcal/mol [Horsewill et al. 1987]. If there were no proton tunneling at all, there would be two different static configurations of CH_3 fragments, each characterized by its own tunneling frequency, $\Delta_{1,2}$. In the opposite extreme case when the proton tunneling frequency Δ_h is much greater than $|\Delta_1 - \Delta_2|$, only one tunneling frequency should be observed. Seemingly the intermediate situation is actually observed.

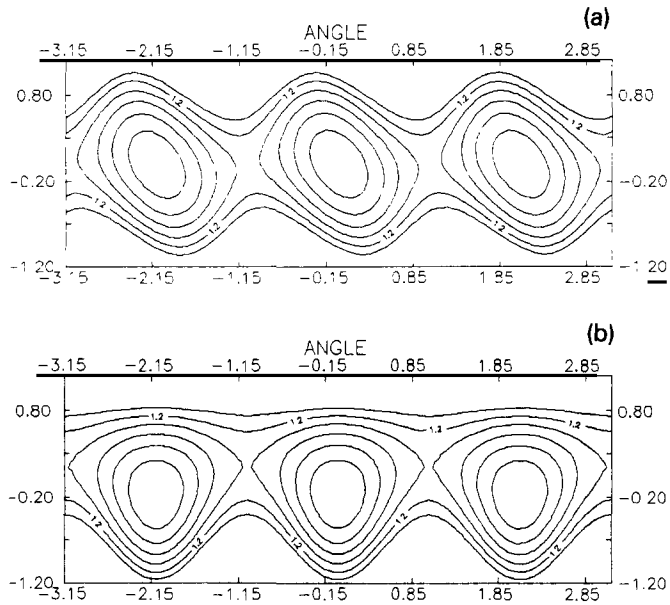

Fig. 56. Contour plots of (a) shaking and (b) breathing vibrations coupled to hindered rotation around the three-fold axis. The MEP is shown.

Although the rotation barrier is chiefly created by the high-frequency modes, it is necessary to consider coupling to low-frequency vibrations in order to account for subtler effects such as temperature shift and broadening of tunneling lines. The interaction with the vibrations q_n (with masses and frequencies m_n, ω_n) has the form

$$H_{\text{int}} = \sum_n C_n q_n \cos 3\varphi + C_n' q_n \sin 3\varphi . \tag{6.29}$$

The two terms correspond to different polarization of phonons. The cosine term corresponds to displacements along the rotation axis or the direction $\varphi = 0$. The sine contribution arises from the phonons polarized along the line $\varphi = \frac{1}{2}\pi$. The interaction (6.29) does not change the symmetry of the φ potential, and, in this respect, it is symmetric coupling, as defined in sections 2.3 and 2.5. Nonetheless, the role of the cosine and sine couplings is different. The former ("breathing modes") just modulate the barrier (6.22), while the latter ("shaking modes") displace the potential.

The contour plots and MEPs for both cases are demonstrated in fig. 56. The MEP in the total configuration space obeys the equation

$$q_n = -(C_n \cos 3\varphi + C_n' \sin 3\varphi)/2m_n\omega_n^2 , \tag{6.30}$$

and the adiabatic potential along the MEP is

$$V_{\text{ad}}(\varphi) = V(\varphi) - \sum_n (C_n \cos 3\varphi + C_n' \sin 3\varphi)^2/2m_n\omega_n^2 . \tag{6.31}$$

From (6.31) it follows that coupling contributes to the V_6 potential, even if the latter term is absent from the bare potential. Both shaking and breathing vibrations promote tunneling, but in

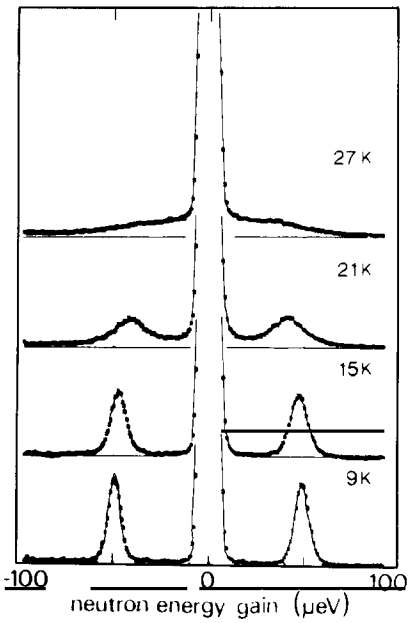

Fig. 57. The INS structure factor at different temperatures for rotational tunneling in a $(CH_3)_2SnCl_2$ crystal.

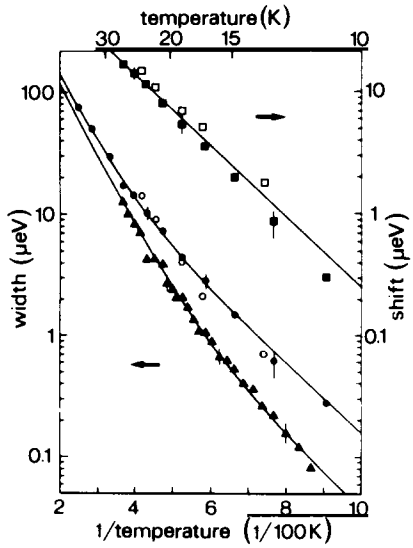

Fig. 58. Lower left-hand scale: Arrhenius plot of the linewidths (lower and upper curves, for inelastic and quasielastic peaks, respectively). Upper right-hand scale: Arrhenius plot of the shift of the inelastic peaks.

a different way. The former make the effective barrier narrower, while the latter lower it. One may define similarly to section 4.2 the parameter that characterizes the relative barrier modulation for the breathing modes ($C'_n = 0$) as

$$b = V_0^{-1} \sum C_n^2 / 2m_n \omega_n^2 , \tag{6.32}$$

and there is a similar expression for shaking modes. For nitromethane crystal (fig. 55) a rough estimate gives this parameter in the range 0.1–0.2.

The problem of temperature dependence of INS spectra is dealt with in many papers (see, e.g., Wûrger [1989], Hewson [1984], and Whittall and Gehring [1987]). An example of an INS spectrum at different temperatures is shown in fig. 57 taken from Wûrger and Heidemann [1990]. The shift of tunneling sidebands, their broadening, as well as the width of the quasielastic central peak display Arrhenius behavior with different activation energies (fig. 58). The quasielastic peak is narrower than the inelastic ones. In fact, we have already found the general expression for the linewidth, having noted that it appears only due to intermultiplet transitions [see eq. (2.52)].

In order to adapt that expression to the problem at hand, we note that interaction matrix elements for shaking and breathing modes are different. Namely, the matrix element $M'_{ll',\sigma} = \langle l, \sigma | \sin 3\varphi | l', \sigma \rangle$, where l denotes the multiplet number, σ is the symmetry index (A or E), is very small for even $l + l'$, while the cosine matrix element, $M_{ll',\sigma} = \langle l, \sigma | \cos 3\varphi | l', \sigma \rangle$ is minor for odd $l + l'$ [Wûrger 1989]. At low temperatures, when only $l' = l$ is accessible, the shaking

vibrations with sine matrix elements are dominant. The ensuing expression for the linewidth is

$$\Gamma_{AE} = (|M'_{01,A}|^2 + |M'_{01,E}|^2) J(E_{01}) \exp(-\beta E_{01}) ,$$
$$\Gamma_{E_a E_b} = 2|M'_{01,E}|^2 J(E_{01}) \exp(-\beta E_{01}) \tag{6.33}$$

for elastic and quasielastic lines, respectively. Here $J(E_{01})$ is the spectral density for shaking modes. Incorporation of breathing modes is straightforward, and they entail larger activation energies associated with participation of high multiplets.

The shift of the spectral line appears in the second order of the perturbation theory, and, with the assumption that the barrier is high enough, it equals

$$\Delta(T) - \Delta(0) = \sum_j \frac{C_j'^2}{\omega_j} \bar{n}(\omega_j) |M'_{01}|^2 \left(\frac{\Delta_1}{(E_{01} - \hbar\omega_j)^2 - \Delta_1^2} + \frac{\Delta_1}{(E_{01} + \hbar\omega_j)^2 - \Delta_1^2} \right) \tag{6.34}$$

where Δ_1 is the tunneling splitting in the first excited multiplet ($l = 1$), which, as argued before, is negative, and $\bar{n}(\omega_j)$ is the average phonon occupation number [cf. eq. (2.53)].

Hûller and Baetz [1988] have undertaken a numerical study of the role played by shaking vibrations. The vibration was supposed to change the phase of the rotational potential $V(\varphi - \alpha(t))$. The phase $\alpha(t)$ was a stochastic classical variable subject to the Langevin equation

$$I_\alpha \mathrm{d}^2\alpha/\mathrm{d}t^2 + \eta\, \mathrm{d}\alpha/\mathrm{d}t + \mathrm{d}U/\mathrm{d}\alpha + \langle\psi(t)|\partial V/\partial\alpha|\psi(t)\rangle = f(t) , \tag{6.35}$$

where I_α and $U(\alpha)$ are, respectively, the moment of inertia and angular potential for the α coordinate, $f(t)$ is the stochastic torque obeying the FDT relation (2.24). The matrix element is taken for the rotor wavefunction, which is subject to the Shrödinger equation,

$$\mathrm{i}\hbar\partial\psi(\varphi, t)/\partial t = [-(\hbar^2/2I)(\partial^2/\partial\varphi^2) + V(\varphi - \alpha(t))]\psi(\varphi, t) . \tag{6.36}$$

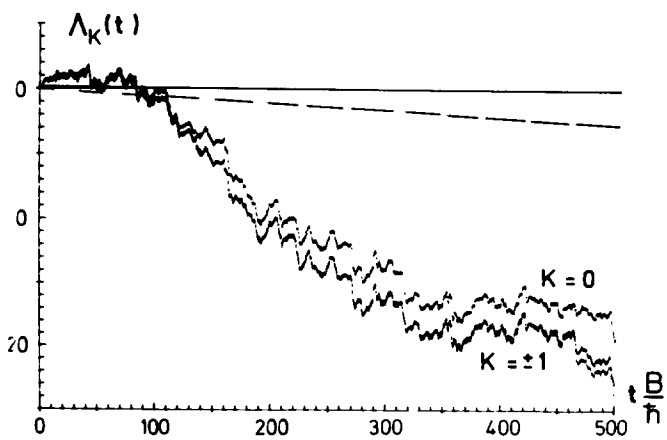

Fig. 59. Time dependence of phases Λ_A and Λ_E for a realization of stochastic force at $T = \frac{1}{8}T_c$. Also shown are the straight lines of the zero-temperature behavior of Λ_A (solid line) and Λ_E (dashed line). Time is measured in units $2I/\hbar$.

The evolution of a state with a certain symmetry was described as

$$\langle\psi_\sigma(t)|\psi_\sigma(0)\rangle = A_\sigma(t)\exp(\mathrm{i}\Lambda_\sigma t)\,. \tag{6.37}$$

The time dependence of the phases Λ_A and Λ_E is shown in fig. 59. Despite the erratic nature of these phases, it is seen that states of different symmetry develop in parallel. The states E_a and E_b show almost no difference. Moreover, at $T \approx \frac{1}{8}T_c$, the difference of phases in the E and A states is to a good accuracy the same as at $T = 0$. That is why the coupling to the stochastic reservoir violates coherence only slightly, and the tunneling splitting may be observed at temperatures up to T_c.

6.3. Tunneling in molecular dimers

In dimers composed of equal molecules the dimer components can replace each other through tunneling. This effect has been discovered by Dyke et al. [1972] as interconversion splitting of rotational levels of $(HF)_2$ in molecular beam electric resonance spectra. This dimer has been studied in many papers by microwave and far infrared tunable difference-frequency laser spectroscopy (see review papers by Truhlar [1990] and by Quack and Suhm [1991]). The dimer consists of two inequivalent HF molecules, the H atom of one of them participating in the hydrogen bond between the fluorine atoms (fig. 60). PES is a function of six variables indicated in this figure.

The experimental data as well as ab initio calculations show that the intramolecular HF distances are practically constant, and the dimer has a planar structure, so that practically the set of variables consists of the van der Waals stretch coordinate, R, and two angles, θ_1 and θ_2. The structure in the minima on the PES have C_s symmetry, while in the saddle point the symmetry is C_{2h}. The MEP turns out to be rather close to the linear path of geared transfer, $\theta_1 + \theta_2 =$ constant; that is, the reaction path has small curvature, suggesting use of the vibrationally adiabatic approximation in order to calculate the splitting. Figure 61 shows how θ_1, θ_2 and R change along the MEP calculated by Hancock et al. [1986] for the model PES of Barton and Howard [1982]. For this PES the interconversion barrier height is $302\,\mathrm{cm}^{-1}$. Later another PES was used with barrier height $385\,\mathrm{cm}^{-1}$ and a smaller tunneling distance [Hancock et al. 1988; Hancock and Truhlar 1989]. Figure 61 displays the promoting effect of the stretching intermolecular vibration at the initial part of MEP, where the angles are nearly constant while the F–F distance is decreased. The subsequent concerted rotation is accompanied by a slight increase in R.

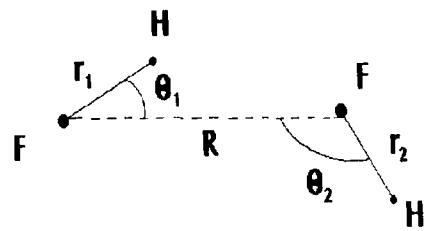

Fig. 60. Configuration and relevant coordinates of the planar HF dimer in stable and transition configurations. The angles and intermolecular distance are $\theta_1 = 9°$, $\theta_2 = 116°$, $R = 2.673$ Å in the stable configuration; $\theta_1 = \theta_2 = 54.9°$, $R = 2.567$ Å in the transition configuration. The HF bond lengths are constant within an accuracy of 0.003 Å.

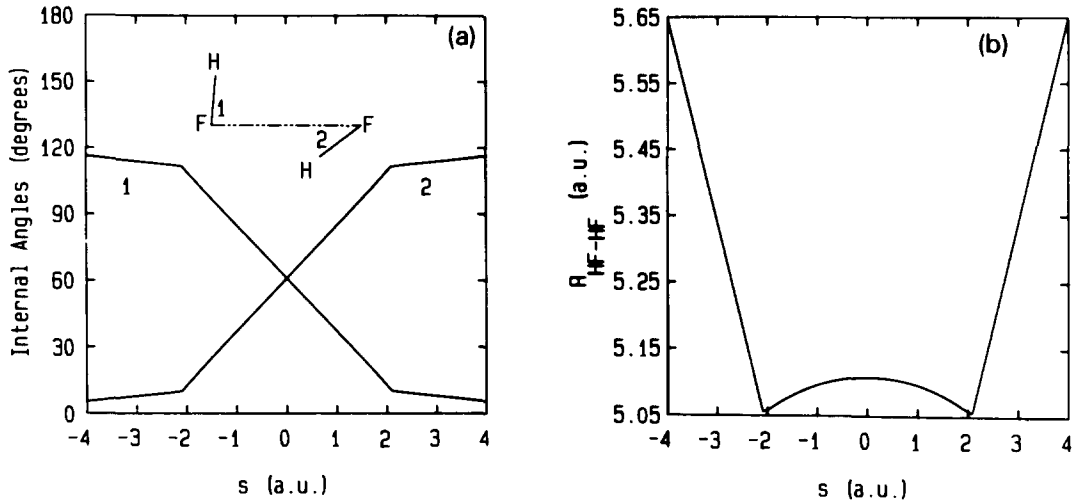

Fig. 61. Variation of angles θ_1 and θ_2 (curves 1 and 2) and intermolecular distance (b) along MEP for $(HF)_2$.

According to the Fukui theorem (see section 4.1) the initial part of the reaction path coincides with the direction of R, because it corresponds with the lowest frequency $174\,cm^{-1}$, whereas the disrotary combination of in-plane liberations ($\theta_1 + \theta_2 \simeq$ constant) has a larger frequency, $221\,cm^{-1}$. However, after passing this initial segment, the direction of concerted libration becomes the reaction coordinate with barrier frequency $\omega^{\#} = 197\,cm^{-1}$, while the stretching vibration is transverse with respect to the reaction path, with $\omega_t = 164\,cm^{-1}$. This leads to a sharp drop in the transverse frequency when moving on from the initial to the transition state, which, according to predictions of section 4.1, should lead to some decrease in the prefactor. This effect is still insignificant in this case, because ω_t does not change so strongly. The calculation gives a tunneling splitting $\Delta = 0.6$–$0.8\,cm^{-1}$, in excellent agreement with the experimental value $0.66\,cm^{-1}$.

Pine and Lafferty [1983] have discovered that tunneling splitting decreases by a factor three when intramolecular vibrations of hydrogen-bonded or free HF units are excited to the first level. Since the difference in frequency of these modes (about $60\,cm^{-1}$) is much greater than Δ, exciting one of them seems to lead to an energy bias that destroys any resonant tunneling, and it is surprising that splitting is still observed. Mills [1984] and Fraser [1989] suggested the vibrational exchange between two HF units, which symmetrizes the potential.

In essence, the initial asymmetric terms are analogous to the diabatic terms in the electronically nonadiabatic tunneling problem, while the vibrational exchange is the analogue of diabatic coupling. The diabatic and adiabatic terms are shown in fig. 62. As shown in section 3.5 and appendix B, diabatic coupling makes the adiabatic potential symmetric thus recovering the resonance. However, nonadiabaticity decreases the tunneling splitting, which is reflected in the prefactor in (3.92). Since the tunneling splitting in the adiabatic potential, Δ_{ad}, is just weakly dependent on the coupling V_d, the decrease in Δ should be ascribed to the Landau–Zener factor.

A straightforward calculation of Δ has been performed by Fraser [1989] within the framework of the one-dimensional model of concerted interconversion. The diabatic terms were taken in the form

$$V_{1,2}(Q) = V(Q) + \tfrac{1}{2}\hbar(\omega_1 + \omega_2) \pm \tfrac{1}{2}\hbar(\omega_1 - \omega_2)Q/Q_0\,, \quad Q = \theta_1 - \theta_2\,, \tag{6.38}$$

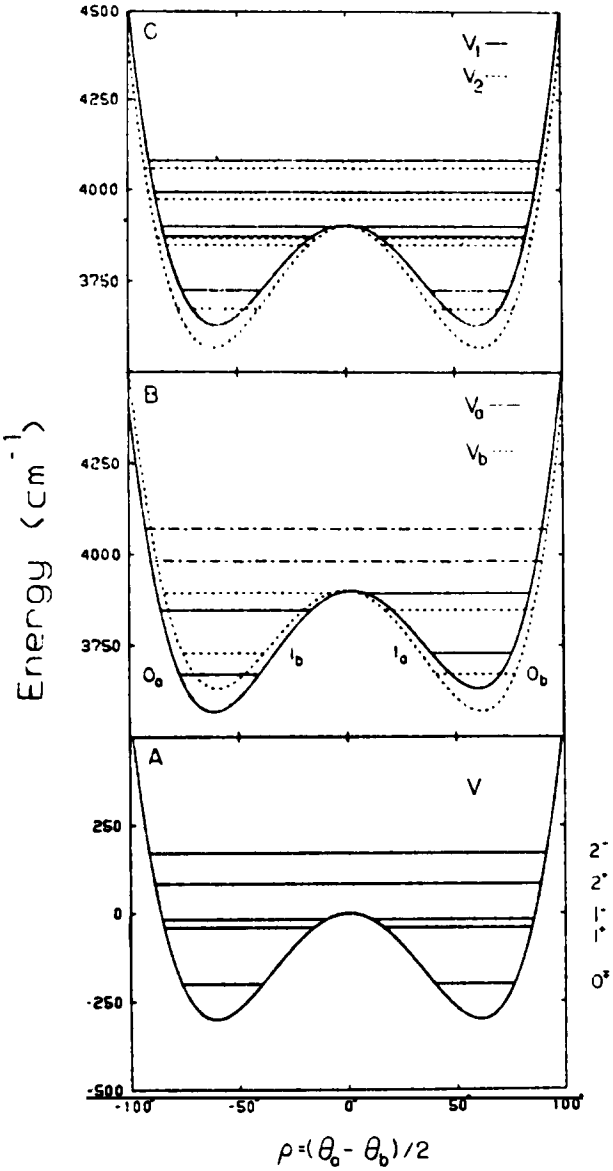

Fig. 62. HF dimer potentials as a function of $\frac{1}{2}(\theta_2-\theta_1)$ [$\frac{1}{2}(\theta_a-\theta_b)$ in the figure] in (A) ground state, (B) diabatic, V_a and V_b, and (C) adiabatic, V_+ and V_- terms of excited states. Diabatic terms correspond to excitation of stretching vibrations of hydrogen-bonded and free HF molecules. The energy levels for these potentials are shown.

where $V(Q)$ is the symmetric ground state potential, $\omega_{1,2}$ are the intramolecular vibration frequencies for the hydrogen bonded and free HF units, $\pm Q_0$ are the equilibrium positions. It was supposed that the major contribution to the diabatic coupling came from the transition–dipole interaction. It can be represented by a Fourier series,

$$V_d = (\mu_{01}^2/R^3)\sum c_n \cos nQ\ . \tag{6.39}$$

When V_d varied within the interval 1–8 cm^{-1}, the tunneling splitting was found to depend nearly linearly on V_d, in agreement with the semiclassical model of section 3.5 [see eq. (3.92)], and the prefactor Δ/Δ_{ad} ranged from 0.1 to 0.3, indicating nonadiabatic tunneling. Since this model is one-dimensional, it fails to explain the difference between splittings in the states with the ω_1 and ω_2 vibrations excited.

Usually nonadiabatic tunneling is considered to occur between electronic terms. We do not actually know any direct experimental evidence of the nonadiabatic regime, and it is difficult to estimate V_d and to separate the Landau–Zener prefactor from the leading exponential term, which is strongly dependent on the parameters of the problem. In the present case one deals with different nuclear (not electronic) states. Moreover, the barrier is relatively low, and coupling, having an electrostatic origin, can be estimated directly. A similar decrease of Δ in vibrationally excited states is observed in many other dimers, such as $(H_2O)_2$ [Huang and Miller 1988], $(HCl)_2$ [Blake et al. 1988] and $(C_2H_2)_2$ [Ohshima et al. 1988].

Tunneling interconversion is observed not only in hydrogen-bonded dimers but also in van der Waals bonded ones. In the latter very large masses may tunnel giving rise to small tunneling splittings. In particular, in $(SO_2)_2$ studied by Nelson et al. [1985] the tunneling splitting is 70 kHz.

In the recently studied dimer H_2O–NH_3 [Fraser and Suenram 1992] all the features of multidimensional nuclear tunneling show up. In the ground state the tunneling interconversion of the water molecule, resulting from the permutation of the hydrogen-bonded and free H atoms, leads to splitting of rotation-internal rotation levels. This process is promoted by nearly free rotation of NH_3. Since the N atom participates in the hydrogen bond OH ··· N, the inversion of NH_3 is suppressed by the asymmetry of the potential. However, excitation of the umbrella NH_3 vibration makes the inversion possible due to tunneling in the H_2O molecule, which symmetrizes the potential. That is, tunneling in both molecules is concerted and the transition state is two-fold, similarly to the situation considered in section 6.1.

The intensely developing technique of high-resolution IR-spectroscopy of dimers composed of two different molecules in supersonic cooled jets offers a new promising approach to the quantum dynamics of reaction complexes. In essence, this is a unique possibility of modelling low-temperature chemical reactions.

6.4. Tunneling of heavy particles

In the previous sections we have already encountered tunneling of particles with reduced masses greater than m_H. One more well-known example of this kind is the inversion splitting in ammonium. The planar transition state separates two equilibrium pyramid-shaped mirror-symmetric configurations of NH_3. The barrier height equals $V^{\#} = 5.94$ kcal/mol, ω_0 equals 950 and 745 cm^{-1} for NH_3 and ND_3, respectively. The inversion splitting Δ equals 0.8 cm^{-1} (0.053 cm^{-1} for ND_3) in the ground state and 36.5 cm^{-1} (3.9 cm^{-1} for ND_3) in the first vibrational state (see, e.g., Townes and Schawlow [1955]). The reduced mass that tunnels is $2.54m_H$ for NH_3 and $4.45m_H$ for ND_3. The tunneling distance, i.e., the displacement of the N atom with respect to the H_3 plane, equals 0.77 Å. The coupling of the tunneling coordinate with the rotations of the symmetric top leads to a promoting contribution as well as a reorganization energy because of centrifugal forces. Rotation around the symmetry axis flattens the pyramid thus lowering the barrier, while rotation around the perpendicular axis increases the barrier. Note that inversion of ND_3 is tunneling of a rather heavy mass throughout the barrier with the height and width typical of cryochemical reactions and with the tunneling amplitude $\Delta/\omega_0 \sim 10^{-3}$. It is natural then that, for the cryochemical reactions whose rates are 5–10 orders smaller than Δ (even allowing for the fact that the

incoherent tunneling rate is proportional to Δ^2), it is possible to observe tunneling of reduced masses (15–25)m_H.

The non-Arrhenius behavior of the inversion rate constant has been detected by [Deycard et al. 1988] for the oxyranyl radical,

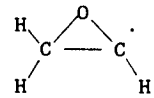

(6.40)

As stated by inequality (2.81) (see also section 4.2 and fig. 30), when the tunneling mass grows, the tunneling regime tends to be adiabatic, and the extremal trajectory approaches the MEP. The transition can be thought of as a one-dimensional tunneling in the vibrationally adiabatic barrier (1.10), and an estimate of k_c and T_c can be obtained on substitution of the parameters of this barrier in the one-dimensional formulae (2.6) and (2.7). The rate constant k_c falls into the interval available for measurements if, as the mass m is increased, the barrier parameters are decreased so that the quantity $d(V_0 m/m_H)^{1/2}$ remains approximately invariant.

Thus far the only known example of tunneling exchange of heavy particles is automerization of cyclobutadiene [Dewar et al. 1984; Carsky et al. 1988],

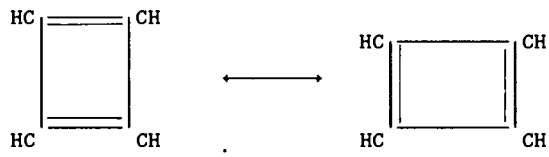

(6.41)

The automerization barrier arises, when passing from the initial rectangular configuration with the alternating bonds with lengths 1.56 Å and 1.33 Å to the transition square configuration with the bond length 1.45 Å, and has height 8–12 kcal/mol. In the space of the relevant coordinates (the C–C and C=C bond lengths) the transferred reduced mass equals $6.53m_H$. Owing to the weakness of the coupling of the reaction coordinate to other vibrations, the one-dimensional model is a good approximation giving sufficiently accurate results. For the same reason Δ changes only slightly for the excited vibrational levels (Δ = 4.2, 4.6 and 5.1 cm^{-1} for n = 0, 1, 2, respectively). The ground state splitting drops to 2.35 cm^{-1} for $^{13}C_4D_4$. Since the barrier is narrow, even at 350 K tunneling prevails over thermally activated hopping.

The low-temperature limit of the rate constant for the isomerization of the biradical

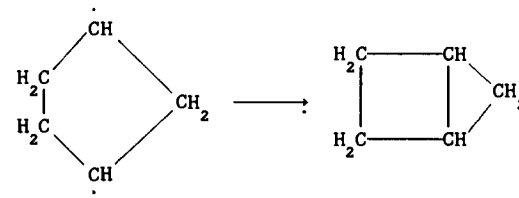

(6.42)

has been measured by Buchwalter and Closs [1979]. The cross-over temperature equals 15 K, $k_c = 6 \times 10^{-4} s^{-1}$. Above 20 K the apparent activation energy equals 2.3 kcal/mol; and the small apparent prefactor, according to (2.6), indicates the tunneling character of the transition. The smallness of isotope effect signifies that the contributions of the individual hydrogen-atom displacements to this reaction are immaterial. This is due to the off-plane bending vibration of the 5-membered ring. The experimental value of k_c corresponds to tunneling of reduced mass $\sim 7m_H \frac{1}{2}(m_c + 2m_H)$, associated with this vibration, through a distance 1.2 Å, which is approximately equal to the relative displacement of the CH_2 group needed to form the 4-membered ring.

In the numerous studies of the IR-spectra of the matrix-isolated reactants (see, e.g., Frei and Pimentele [1983]) there have been found a number of chemical conversions. Among them, from the point of view of the present review, the reaction NO with O_3 [Lucas and Pimentele 1979],

$$NO + O_3 \rightarrow NO_2 + O_2 , \tag{6.43}$$

is of interest. This reaction in the gas phase has enthalpy -47.1 kcal/mol and activation energy 2.3 kcal/mol. In the N_2 matrix at 10–20 K E_a is smaller than 0.11 kcal/mol, and $k = 1.4 \times 10^{-5} s^{-1}$ at 12 K. Experiments on ozon enriched with ^{18}O have revealed no isotope effect.

The structure of the van der Waals 1:1 complexes of $NO–O_3$ has been studied by Arnold et al. [1986]. In the planar complex (1) with symmetric position of the NO molecule relative to the O_3-symmetry axis the distance between the centers-of-mass of O_3 and NO is $R_{12} = 2.30$ Å, the bonding energy is 2.42 kcal/mol. In the complex (2) in which NO bond is perpendicular to the O_3 plane and $R_{12} = 2.15$ Å, the bonding energy goes up to 2.73 kcal/mol. The PES of the gas-phase reaction has been calculated by Viswanathan and Raff [1983].

The vibrationally excited products in the ground electronic state are created when the end O atom is abstracted from the O_3 molecule as a result of the approach of the NO molecule at an ONO angle of 110°. The barrier height equals 3.57 kcal/mol. The activation energy 2.13 kcal/mol is close to the measured one. In the transition state the saddle point is shifted towards the reactants valley and the distances R_{OO} and R_{NO} are equal, respectively, to 1.277 Å and 1.957 Å, while the equilibrium bond lengths in O_3 and NO are 1.272 Å and 1.150 Å. Comparison of the configurations of the van der Waals complex (1) and of the transition state shows that the arrangement of the reactants provides the same attack angle as in the gas-phase reaction. The O–O bond stretches by less than 0.2 Å. The O–NO length becomes reduced by 0.45 Å. Seemingly, intermolecular vibrations as well as the hindered rotation play a promoting role. Because of the low frequencies of these modes the low-temperature limit is not reached even at 10 K.

The chain polymerization of formaldehyde CH_2O was the first example of a chemical conversion for which the low-temperature limit of the rate constant was discovered (see reviews by Goldanskii [1976, 1979]). As found by Mansueto et al. [1989] and Mansueto and Wight [1989], the chain growth is driven by proton transfer at each step of adding a new link

$$(CH_2O)_{n-1}CH_2OH^+ + CH_2O \rightarrow (CH_2O)_nCH_2OH^+ . \tag{6.44}$$

The primary cation CH_2OH^+ is created in the cage reaction under photolysis of an impurity or γ-radiolysis. The rate constant of a one link growth, found from the kinetic post-polymerization curves, is constant in the interval 4.2–12 K where $k_c = 1.6 \times 10^2 s^{-1}$. Above 20 K the apparent activation energy goes up to 2.3 kcal/mol at 140 K, where $k \sim 10^5 s^{-1}$.

So the results obtained by different groups and with different methods display the existence of a completely unusual chemical conversion, polymerization at very low temperatures. Similar effects have been found in γ-irradiated acrylonitrile and acrolein [Gerasimov et al. 1980].

The mechanism of ion polymerization in formaldehyde crystals proposed by Basilevskii et al. [1982] rests on Semenov's [1960] assumption that solid-phase chain reactions are possible when the arrangement of the reactants in the crystal "prepares" the configuration of the future chain. The monomer crystals capable of low-temperature polymerization fulfill this condition. In the initial equilibrium state the monomer molecules are located in the lattice sites and the creation of a chemical bond requires surmounting a high barrier. However, upon creation of the primary dimer cation, the active center shifts to the intersite, and the barrier for the addition of the next link

diminishes. Since the intersite distance in the monomer lattice is much greater than that between the links of the polymer chain, the chain end-group has to shift towards the next monomer link, as a result of the previous reaction event. This diplacement, along with the reorientation of the monomer link, leads to the formation of a low-barrier configurations facilitating the next reaction event.

When it is added to the chain, the formaldehyde molecule rotates through $\sim 45°$ with respect to its axis. The C–O–C angle in the cation is $\sim 180°$ and it decreases to 120° after the addition of the next link, which involves overcoming a barrier of 2–3 kcal/mol. As a result of the two mentioned motions (rotation of the monomer molecule and isomerization of the end-group of the cation), the chain growth is associated (at $T < T_c$) with tunneling of the CH_3 group through the distance 0.6 Å. This mechanism is realized only in one of the possible crystalline structures of formaldehyde. In other structures the chain length is limited by the number of "suitably packed" molecules and it is below 8–10. This value agrees with the structure of crystalline formaldehyde found by Weng et al. [1989]. In this structure there are spatially selected groups, where the intermolecular distance is reduced to ~ 2.75 Å compared to the van der Waals one (3.22 Å).

The growth of long chains ($n \geq 10^2$) in the perfectly mixed 1:1 crystals of ethylene with chlorine and bromine at 20–70 K was studied in detail by Wight et al. [1993]. Active radicals were generated by pulse photolysis of Cl_2 or Br_2. The rate constant was found to be $k_c = 8\text{–}12\,s^{-1}$ below $T_c = 45$ K. The chain grows according to the well known radical mechanism including the reactions

$$C_2H_4Cl + Cl_2 \rightarrow C_2H_4Cl_2 + Cl\,, \qquad Cl + C_2H_4 \rightarrow C_2H_4Cl\,. \tag{6.45a, b}$$

The first slower reaction gives the product, while the second recovers the active radical. Reactions (6.45) in the gas phase result in formation of two stereo-isomers, gauche- and trans-1,2-dichloroethane $C_2H_4Cl_2$. In the low-temperature solid-state reaction only the trans-form is created. A specific feature of the mixed halogen–ethylene crystals is the alternating quasi-one-dimensional arrangement of reactants, which is due to the donor–acceptor interaction [Hassel and Romming 1962]. The stereo-specificity (formation of just one isomer) is due to the fact that the radical, created in reaction (6.45b) turns solely into the trans-form, abstracting the second halogen atom from the neighboring molecule.

If the lattices of reactants and products were incommensurate, the conversion would lead to accumulation of strains, which would stop the chain growth. As shown by simulations [Benderskii et al. 1991c; Wight et al. 1993], these lattices are however commensurate, and this fact permits propagation of chains along the direction in which the inter-reactant distance is shortest: the shortest diagonal of the (a, c) plane. The arrangement of reactants, active center of reaction (6.45a) and products in this plane are shown in fig. 63. Because of commensurability, the formation of the line of products does not preclude the growth of the chain along the neighbouring diagonals. In [Wight et al. 1993] 60–70% conversion was observed with mean chain length 260 ± 70 in the temperature interval 17–45 K. It has also been noted that the length is limited by defects randomly distributed in the bulk of crystal.

The $k(T)$ dependences for the reactions of C_2H_4 with Cl_2, Br_2 and HBr [Barkalov et al. 1980] practically coincide (fig. 1), despite the difference in the reactant masses. At 50–80 K the apparent activation energy is 1 kcal/mol, coinciding with E_a for the gas-phase reaction of C_2H_4Cl with Cl_2.

A multidimensional PES for the reaction (6.45a) has been calculated by Wight et al. [1993] with the aid of the atom–atom potential method combined with the semiempirical London–Eyring–Polanyi–Sato method (see, e.g., Eyring et al. [1983]). Because of high exoergicity, the PES

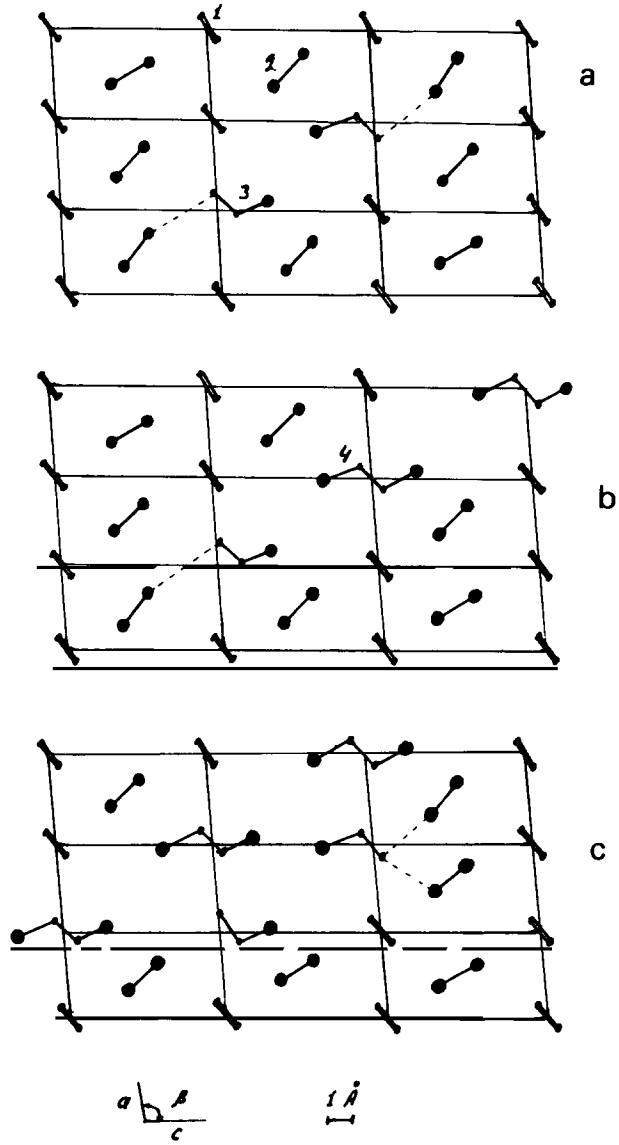

Fig. 63. Molecular arrangement in (a, c) plane of a mixed ethylene–chlorine binary crystal illustrating (a) radical pair formation, (b) single chain growth and (c) chain growth in the vicinity of product line. Molecules labelled 1–4 are ethylene (C_2H_4), chlorine, chloroethyl radical (C_2H_4Cl) and anti 1,2-dichloroethane ($C_2H_4Cl_2$), respectively.

is characterized by an early descent to the product valley; that is, the saddle point is strongly shifted towards the reactant valley, so that the reaction barrier is overcome practically without lengthening of the Cl–Cl broken bond. Since the angle between the valleys is greater than 90° and the intramolecular vibration frequencies are much greater than ω_0, the criterion (2.81) indicates the vibrationally adiabatic regime for these modes.

Analyses of MEP have shown that the displacement of the center-of-mass of the reactant is much smaller than the tunneling length, and the environment reorganization energy is just 0.12–0.17 kcal/mol, being considerably smaller than $V^{\#} \sim 2$ kcal/mol. This permits reduction of

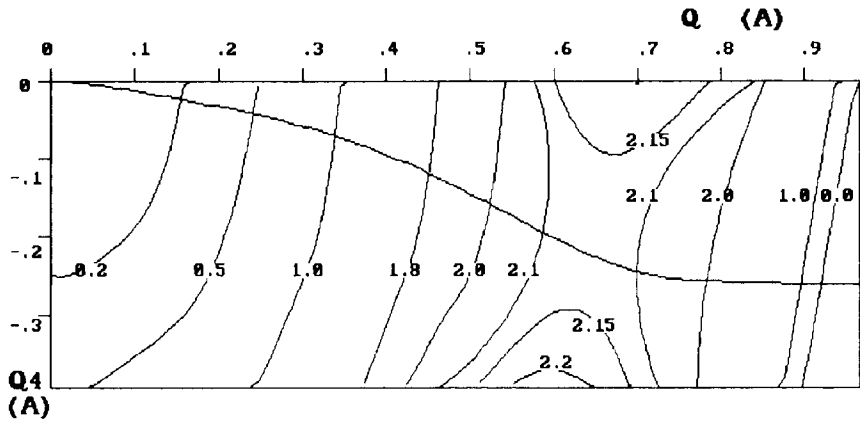

Fig. 64. The cut of PES and MEP of the reaction (6.45a) in coordinates q_4 and q. The coordinate q is a linear combination of q_5–q_7.

the number of freedom degrees to $N = 7$ by considering the Cl–Cl ··· C–C–Cl complex immersed in a fixed crystalline environment. Among the normal modes of the complex there are three high-frequency stretching vibrations of the chlorine molecule and radical (q_1–q_3), which in practice do not mix with the other modes. This allows further reduction of the dimension to four modes. The q_7 mode with the intermediate frequency is mainly due to bending of the radical. The low-frequency vibrations q_4–q_6 are assigned to intermolecular stretching and libration. The main contribution to the reaction path comes from the q_5 and q_6 vibrations, which correspond to the simultaneous relative approach and rotation of reactants.

It has been shown that there is a two-dimensional cut of the PES such that the MEP lies completely within it. The coordinates in this cut are q_4, and a linear combination of q_5–q_7. This cut is presented in fig. 64, along with the MEP. Motion along the reaction path is adiabatic with respect to the fast coordinates q_1–q_3 and nonadiabatic in the space of the slow coordinates q_4–q_7. Nevertheless, since the MEP has a small curvature, the deviation of the extremal trajectory from it is small. This small curvature approximation has been intensively used earlier [Skodje et al. 1981; Truhlar et al. 1982], in particular for calculating tunneling splittings in $(HF)_2$. The rate constant of reaction (6.45a) found in this way is characterized by the values $T_c = 20$–25 K, $k_c = 10^{-2}$–$10^{-1}\,s^{-1}$, $E_a = 1.4$ kcal/mol above T_c, which compare well with the experiment.

7. Summary and perspectives

The low-temperature chemistry evolved from the macroscopic description of a variety of chemical conversions in the condensed phase to microscopic models, merging with the general trend of present-day rate theory to include quantum effects and to work out a consistent quantal description of chemical reactions. Even though for unbound reactant and product states, i.e., for a gas-phase situation, the use of scattering theory allows one to introduce a formally exact concept of the rate constant as expressed via the flux–flux or related correlation functions, the applicability of this formulation to bound potential energy surfaces still remains an open question.

This question is closely related to the coherent–incoherent transition problem absent from the standard situation in the gas phase; namely, a "true" rate constant can be defined only when the tunneling dynamics is incoherent, i.e., once prepared in the initial state (reactant valley), the system

performs exponential relaxation to the equilibrium. Because the typical time scale of the flux–flux correlator ($\beta\hbar$) is shorter than the relevant time of tunneling transition, this quantity cannot tell directly whether the transition is coherent or incoherent. In this respect, the rate theory based on the flux–flux correlator goes no further than the imaginary-time instanton-type theories; they infer the long-time dynamics from propagators, calculated at much shorter times (real or imaginary), which are of the order of $\beta\hbar$. So one may expect a correct answer only if one knows in advance that the system possesses a rate constant, as is the case for unbound problems.

Therefore one can be much more successful in calculating the rate constant knowing in advance that it exists, rather than in answering the question whether it exists. Considerable progress in investigating this question was provided by the solution of the spin–boson problem [Leggett et al. 1987], which, however, has only a restricted relevance for any practical problem in chemistry, because it neglects the effects of interdoublet dynamics (vibrational relaxation) and does not describe thermally activated transitions. A number of attempts to go beyond the two-level system approximation have been undertaken [Parris and Silbey 1985; Dekker 1991] but the basic question how the vibrational relaxation affects the transition from coherent oscillations to the exponential decay awaits its quantitative solution, which may be expected to be obtained by numerically computing real-time path integrals for the density matrix using the influence functional technique.

Two-dimensional semiclassical studies described in section 4 and applied to some concrete problems in section 6 show that, when no additional assumptions (such as moving along a certain predetermined path) are made, and when the fluctuations around the extremal path are taken into account, the two-dimensional instanton theory is as accurate as the one-dimensional one, and for the tunneling problem in most cases its answer is very close to the exact numerical solution. Once the main difficulty of going from one dimension to two is circumvented, there seems to be no serious difficulty in extending the algorithm to more dimensions; that becomes necessary when the usual basis-set methods fail because of the exponentially increasing number of basis functions with the dimension.

Another attractive feature of the instanton method, as distinct from other semiclassical approaches, is that it shows a direct connection between tunneling trajectories and the temperature dependence of the rate constant; certain types of trajectories correspond to certain types of behavior of $k(T)$. For example, the presence of two-dimensional trajectories always extends the Arrhenius dependence to the region of low temperature making the transition from activated to tunneling dynamics less sharp. This explains the experimentally observed coexistence of tunneling (indicated by a strong isotope effect) with the Arrhenius-like behavior of $k(T)$. In general, for potentials with several saddle points like (6.13) there exist critical temperatures for which the behavior of the tunneling trajectories changes qualitatively.

In instanton picture, when the potential has only one saddle point, the transition from the thermally activated regime to tunneling comes about as the appearance of a nontrivial 2D trajectory, which deviates from the saddle point with decreasing temperature. At the same time, the old trivial solution proceeds to give exponentially decreasing contributions, because its action is inversely proportional to the temperature. Looking at this simplest 2D model, one may formulate the general requirement which a trajectory should satisfy in order to be a tunneling path at $T = 0$: it should spend infinitely long time in the initial state having potential $V = 0$; otherwise its action will be infinite at $T = 0$.

Keeping this in mind one may proceed to classify tunneling trajectories in the following way: choose a certain known trajectory at a given T then decrease T by δT, linearize the problem near that trajectory, and continuously transform to a new trajectory with a longer period. This way a family of trajectories arises which is parametrized by the period, i.e., by the temperature. In the

case of one saddle point [e.g., potentials (4.40) and (4.28)] there is only one such a family of 2D solutions below the cross-over temperature.*) Generally speaking, the above transformation may be singular at some points. These points correspond to the appearance of new tunneling pathways. An example is the potential (6.13) with two saddle points, for which two 2D trajectories eventually merge into a single 1D trajectory at a certain critical temperature.

In general, there may be several families of trajectories, so that they cannot be obtained from one another by a continuous transformation. The number of these families should be determined by the topology of the PES, i.e., by the number and positions of saddle points, minima and mixima. The problem of determining these families remains a challenge. The present status of instanton theory suggests relying on physical intuition in picking up relevant families of trajectories rather than on an exact topological treatment. (Although one might imagine a numerical scheme which would not miss any solutions, the numerical effort expended by this scheme would probably be too large for a complicated PES.)

For $T = 0$ the above requirement restricts the choice. For example, consider the potential for two-proton transfer, which is characterized by two global cis-minima, two local trans-minima, and four saddle points between them [Smedarchina et al. 1989]. At $T = 0$ there is a trajectory which starts out at the local minimum and which corresponds to the family of solutions that continuously collapse to the saddle point when the temperature rises. However, this trajectory cannot describe a tunneling event between the global minima, because its energy is always no less than the energy of the local minimum and it does not satisfy the above requirement of finite action. Nevertheless, it is this family that describes thermally activated transitions at higher temperatures. That is, the finite-action requirement suggests looking for another family of trajectories, which play a dominant role at sufficiently low temperatures.

Another problem which awaits its quantitative study is photochemical quantum dynamics, in particular tunneling dynamics in excited electronic states. From a theorist's point of view, this implies solving the curve-crossing tunneling problem for a multidimensional case. The methods described in section 4 together with the quasienergy ideas for integrating the pseudospin variable out of the problem may prove useful in this case. We believe that the experimental examples and theoretical ideas demonstrated in this review may foster new efforts towards studying the quantum dynamics of low-temperature chemical conversions, that is, the processes which are quantal in the full sense of these words.

Acknowledgements

We would like to thank Professors H. Dekker, J.T. Hynes, W.H. Miller, H. Nakamura, A.A. Ovchinnikov and M. Ya. Ovchinnikova for discussions and correspondence, Professor D.G. Truhlar for drawing our attention to tunneling in dimers, Professor C.A. Wight for many discussions about selection of experimental examples, Professor N. Makri and Dr. M. Topaler for discussions and providing their data prior to publication. We are grateful to our colleagues Dr. P.G. Grinevich, Dr. S. Yu. Grebenshchikov, Dr. E. Ya. Misochko, Dr. E.V. Vetoshkin and Dr. D.L. Pastur for collaboration on some of the topics of this review.

*) See Benderskii et al. [1993] for exceptions to this statement; the period may be not a good parameter to use for parametrizing this family because the action may be not a single-valued function of the period; however this difficulty is easily circumvented by parametrizing the solutions, for example, by their energy.

Appendix A. Derivation of eqs. (2.16) and (2.17)

Consider a potential like that in fig. 19. In the vicinity of the parabolic well ($\tau \to 0$) at $\beta \gg \omega_0^{-1}$ the instanton solution (3.34), corresponding to a harmonic oscillator in imaginary time, is given by

$$x = r\cosh(\omega_0\tau)\,, \qquad E = \tfrac{1}{2}\omega_0^2 r^2\,, \tag{A.1a, b}$$

where E is the instanton energy (we use mass-scaled coordinates and set $\hbar = 1$, $k_B = 1$). Let $r_0 \gg r$ be the coordinate of an arbitrary point still lying in the region where the harmonic approximation for $V(x)$ is correct within the (arbitrary) given accuracy. Then, if instanton starts out at $\tau = 0$, the time it takes to reach point r_0 equals

$$\tau_1 = \omega_0^{-1}\ln(2r_0/r)\,, \tag{A.2}$$

where we have replaced the hyperbolic cosine in (A.1a) by an exponent.

The total instanton period may be represented as

$$\beta = 2\tau_1 + \tau_2\,, \tag{A.3}$$

where τ_2 is the time during which the particle crosses the barrier and returns to the point r_0. The gist of the derivation is that, when $\beta \to \infty$ and, consequently, $r \to 0$, the time of lingering near the point $x = 0$, τ_1, goes to infinity, while the barrier passage time, τ_2, tends to some finite value, so that $\tau_1 \gg \tau_2$ for large enough β. Neglecting τ_2 in (A.3) and differentiating $\beta \simeq 2\tau_1$ with respect to E, we immediately obtain from (A.2) and (A.3) the following equation in E (A.4a) and its solution (A.4b):

$$\partial\beta/\partial E = (\omega_0 E)^{-1}\,, \qquad E = E_0\exp(-\beta\omega_0)\,. \tag{A.4a, b}$$

E depends on the constant E_0 which is determined by the actual shape of $V(x)$.

In order to find E_0 we study first the auxiliary problem of a cusp-shaped harmonic potential with a wall placed at $x = x_p$ (see fig. 7),

$$V(x) = \tfrac{1}{2}\omega_0^2 x^2\,, \quad x < x_p\,; \quad V(x) = -\infty\,, \quad x > x_p\,. \tag{A.5}$$

For this particular potential eq. (A.1a) is exact throughout the whole range of β and thus we can take $r_0 = x_p$ so that $\tau_2 \equiv 0$. From (A.1b)–(A.3) it is easy to see now that

$$E_0 = 2\omega_0^2 x_p^2 = 4V_0\,. \tag{A.6}$$

Then, given an arbitrary potential, we compare it to the reference potential (A.5) adjusting the width of the latter x_p such that the instanton periods β are equal when the energies E are the same. In other words we require

$$\lim_{E\to 0}\left(\int_r^{r'} \mathrm{d}x\,[2(V(x) - E)]^{-1/2} - \int_r^{x_p} \mathrm{d}x\,(\omega_0^2 x^2 - 2E)^{-1/2}\right) = 0\,, \tag{A.7}$$

where r is related to E by (A.1b) and r' is the second turning point for the potential $V(x)$ at given E. Equation (A.7) implicitly defines x_p for which the value of E_0 is the same for the both potentials.

Thus for an arbitrary potential we have $E_0 = 2\omega_0^2 x_p^2$ with x_p defined by (A.7). In particular, for the cubic parabola $V(x) = \frac{1}{2}\omega_0^2 x^2(1 - x/x_0)$ direct use of (A.7) leads to $x_p = 4x_0$ so that $E_0 = 32\omega_0^2 x_0^2$. Insertion of this into (2.6) and (2.7) gives (3.47).

Appendix B. Dissipative nonadiabatic tunneling at $T = 0$

In this appendix we shall show how the quasienergy ideas developed in section 5 can be applied to the problem of nonadiabatic tunneling. We use the Im F approach of section 3.3 for the multidimensional system with Hamiltonian

$$H = \{\tfrac{1}{2}P^2 + \tfrac{1}{2}[V_i(Q) + V_f(Q)]\}\,\mathbf{1} + \tfrac{1}{2}[V_f(Q) - V_i(Q)]\sigma_z + V_d(Q)\sigma_x + \sum[\tfrac{1}{2}p_j^2 + \tfrac{1}{2}\omega_j^2(x_j + C_jQ/\omega_j^2)^2]\,\mathbf{1}\,, \tag{B.1}$$

where V_i and V_f are the initial and final potential energy terms, V_d is the diabatic coupling between them, $\mathbf{1}$ is the unit 2×2 matrix and the σ are the Pauli matrices. Formally this is a Hamiltonian of a single particle with potential $\frac{1}{2}(V_i + V_f)$ (which may have no barrier at all) coupled to a two-level system and a bath of harmonic oscillators.

Following the Im F method, we study the partition function of the system with the aim to present it as a path integral over the $Q(\tau)$ paths solely. The oscillator degrees of freedom are traced out in a standard way producing the nonlocal action term, while integration over the TLS paths results in the quasienergy partition function $\tilde{Z} = 2\cosh(\beta\tilde{\varepsilon}[Q(\tau)])$. After taking the $\beta \to \infty$ limit only the lower quasienergy survives in $\tilde{Z}$, and one obtains

$$Z = \oint D[Q(\tau))]\exp\Bigg[-\int_0^\beta d\tau\Bigg(\tfrac{1}{2}\dot{Q}^2 + \tfrac{1}{2}[V_i(Q) + V_f(Q)] - [V_d^2(Q) + \varepsilon^2(Q)]^{1/2} + \int_0^\beta d\tau'\,K(\tau - \tau')Q(\tau)Q(\tau')\Bigg)\Bigg]\exp\Bigg(\beta\tilde{\varepsilon}[Q(\tau)] - \int_0^\beta d\tau\,[V_d^2(Q(\tau)) + \varepsilon^2(Q(\tau))]^{1/2}\Bigg)\,, \tag{B.2}$$

$$\varepsilon(Q) = \tfrac{1}{2}[V_i(Q) - V_f(Q)]\,. \tag{B.3}$$

We have multiplied and divided the path integral in (B.3) by the same factor $\exp(\beta\tilde{\varepsilon}_{ad})$, where

$$\tilde{\varepsilon}_{ad}[Q(\tau)] = \beta^{-1}\int_0^\beta d\tau\,[V_d^2(Q(\tau)) + \varepsilon^2(Q(\tau))]^{1/2} \tag{B.4}$$

is the quasienergy in the adiabatic approximation for TLS. Without the last exponent (B.2) would give the standard formula for dissipative adiabatic tunneling with the rate constant obtained in section 5.

Now we make the usual assumption in nonadiabatic transition theory that non-adiabaticity is essential only in the vicinity of the crossing point Q_c where $\varepsilon(Q_c) = 0$. Therefore, if the trajectory does not cross the dividing surface $Q = Q_c$, its contribution to the path integral is to a good accuracy described by adiabatic approximation, i.e., $\tilde{\varepsilon} = \tilde{\varepsilon}_{ad}$. Hence the real part of partition function, Z_0 is the same as in the adiabatic approximation. Then the rate constant may be written as

$$k = Bk_{ad} , \tag{B.5}$$

where k_{ad} is the rate of adiabatic tunneling in the potential

$$V_-(Q) = \tfrac{1}{2}[V_i(Q) + V_f(Q)] - [V_d^2(Q) + \varepsilon^2(Q)]^{1/2} , \tag{B.6}$$

and the prefactor B equals

$$B = \langle B[Q(\tau)]\rangle_{S_{ad}} = \langle \exp(\beta(\tilde{\varepsilon}[Q(\tau)] - \varepsilon_{ad})\rangle_{S_{ad}} , \tag{B.7}$$

where the symbol $\langle \cdots \rangle_{S_{ad}}$ means averaging over the paths with weight $\exp(-S_{ad})$,

$$S_{ad}[Q(\tau)] = \int_0^\beta d\tau \left(\tfrac{1}{2}\dot{Q}^2 + V_-(Q) + \int_0^\beta d\tau' K(\tau - \tau')Q(\tau)Q(\tau') \right) . \tag{B.8}$$

The equations for the quasienergies $\pm\tilde{\varepsilon}$ are

$$dc_1/d\tau = -\varepsilon(Q(\tau))c_1 + V_d(Q(\tau))c_2 , \qquad dc_2/d\tau = \varepsilon(Q(\tau))c_2 + V_d(Q(\tau))c_1 \tag{B.9}$$

with the condition

$$c_i(\tau + \beta) = \exp(\pm\beta\tilde{\varepsilon})c_i(\tau) . \tag{B.10}$$

Let $c_i(\tau)$ be an arbitrary solution to (B.9) which does not necessarily satisfy (B.9). Then it can be represented as a linear combination of exponentially increasing and decreasing linearly independent solutions (B.10). When $\beta \to \infty$, only the increasing solution survives after a long time, and one may write

$$\exp(\beta\tilde{\varepsilon}) = c_i(\beta + \tau)/c_i(\tau) , \tag{B.11}$$

where c_i is an arbitrary solution to (B.9) which is not subject to (B.10), and τ in (B.11) is sufficiently large. For this reason one does not have to take into consideration the boundary conditions (B.10).

Define the "phase" ϕ as

$$\exp[\phi(\tau_2|\tau_1)] = c_1(\tau_2)/c_1(\tau_1) . \tag{B.12}$$

Then $\beta\tilde{\varepsilon}$ may be thought of as the phase accumulated by the function $c_1(\tau)$ during the period β. To find B we should compare the phase $\phi(\beta + \tau|\tau)$ to that calculated in the adiabatic approximation

ϕ_{ad}. According the standard arguments of the Landau–Zener–Stueckelberg theory, this difference emerges mostly from passing the point $Q(\tau^*) = Q_c$ where the adiabaticity is violated. In the vicinity of this point eqs. (B.9) simplify to

$$dc_1/d\tau = -Fv(\tau - \tau^*)c_1 + V_d(Q_c)c_2\,, \qquad dc_2/d\tau = Fv(\tau - \tau^*)c_2 + V_d(Q_c)c_1 \tag{B.13}$$

$$F = \tfrac{1}{2}[dV_i/dQ - dV_f/dQ]_{Q=Q_c}\,, \qquad v = [dQ/d\tau]_{\tau=\tau^*}\,. \tag{B.14}$$

Adopting the dimensionless units $\tau - \tau^* = (2Fv)^{-1/2}\tau'$, $c_i = (2Fv)^{-1}c_i'$, we rewrite (B.13) as

$$dc_1'/d\tau' = -\tfrac{1}{2}\tau' c_1' + \delta^{1/2}c_2'\,, \qquad dc_2'/d\tau' = \tfrac{1}{2}\tau' c_2' + \delta^{1/2}c_1' \tag{B.15}$$

$$\delta = V_d^2(Q_c)/2Fv\,. \tag{B.16}$$

Equations (B.15) are exactly the same as those derived by Holstein [1978], and the following discussion draws on that paper. The pair of equations (B.15) may be represented as a single second-order differential equation

$$-d^2c_1/d\tau^2 + (\tfrac{1}{4}\tau^2 + \delta - \tfrac{1}{2})c_1 = 0\,, \tag{B.17}$$

where we have omitted for simplicity the primes. Its increasing solution at $\tau \to \infty$ is a parabolic cylinder function $D_{-\delta}(-\tau)$ with the asymptotic solutions

$$c_1(\tau) \propto \tau^{\delta}\exp(-\tfrac{1}{4}\tau^2)\,, \quad \tau < 0\,; \qquad c_1(\tau) \propto (2\pi)^{1/2}\tau^{\delta-1}\exp(\tfrac{1}{4}\tau^2)/\Gamma(\delta)\,, \quad \tau > 0\,, \tag{B.18a,b}$$

where $\Gamma(\delta)$ is the gamma function. By using the definition (B.12) we obtain

$$\exp(\phi(\tau|-\tau)) = c_1(\tau)/c_1(-\tau) = (2\pi)^{1/2}\tau^{2\delta-1}\exp(\tfrac{1}{2}\tau^2)/\Gamma(\delta) \tag{B.19}$$

This should be compared with the adiabatic result. To do this we look for a solution c_i of (B.15) in the form

$$c_i(\tau) = u_i(\tau)\exp\left(\int^{\tau}(\delta^2 + \tfrac{1}{4}\tau^2)^{1/2}\,d\tau\right). \tag{B.20}$$

Substituting this in (B.15) and neglecting the derivatives one gets

$$u_1[\tfrac{1}{2}\tau + (\tfrac{1}{4}\tau^2 + \delta)^{1/2}] = \delta^{1/2}u_2\,, \tag{B.21}$$

whence for $|\tau| \gg \delta^{1/2}$ the functions u_1 and u_2 are related by

$$u_1 \simeq \delta^{1/2}u_2/\tau\,, \quad \tau > 0\,; \qquad u_2 \simeq \delta^{1/2}u_1/|\tau|\,, \quad \tau < 0 \tag{B.22}$$

If we were to replace τ by $-\tau$ in (B.15), the solution u_1 would replace u_2 and vice versa. Therefore, one may write at $\tau > 0$

$$u_1(\tau) \simeq \delta^{1/2} u_2(\tau)/\tau = \delta^{1/2} u_1(-\tau)/\tau \,. \tag{B.23}$$

Thus for the adiabatic phase ϕ_{ad} one obtains

$$\exp[\phi_{ad}(\tau|-\tau)] = c_1(\tau)/c_1(-\tau)$$

$$= \tau^{-1}\delta^{1/2}\exp\left(\int_{-\tau}^{\tau}(\delta^2 + \tfrac{1}{4}\tau^2)^{1/2}\,\mathrm{d}\tau\right) \simeq \mathrm{e}^{\delta}\delta^{-\delta}\tau^{2\delta-1}\exp(\tfrac{1}{2}\tau^2)\,. \tag{B.24}$$

Comparing (B.19) with (B.24) one finds

$$B[Q(\tau)] = \exp[\beta(\tilde{\varepsilon} - \tilde{\varepsilon}_{ad})] \simeq \exp(n\phi(\tau|-\tau) - n\phi_{ad}(\tau|-\tau))$$

$$= [(2\pi/\delta)^{1/2}\mathrm{e}^{-\delta}\delta^{\delta}/\Gamma(\delta)]^n\,, \tag{B.25}$$

where n is the number of times the trajectory crosses the point Q_c.

The functional $B[Q(\tau)]$ actually depends only on the velocity $\mathrm{d}Q/\mathrm{d}\tau$ at the moment when the non-adiabaticity region is crossed. If we take the path integral by the method of steepest descents, considering that the prefactor $B[Q(\tau)]$ is much more weakly dependent on the realization of the path than $S_{ad}[Q(\tau)]$, we shall obtain the instanton trajectory for the adiabatic potential V_{ad}; then $B[Q(\tau)]$ will have to be calculated for that trajectory. Since the instanton trajectory crosses the dividing surface twice, we finally have

$$B = 2\pi\delta^{-1}\mathrm{e}^{-2\delta}\delta^{2\delta}/\Gamma^2(\delta)\,, \tag{B.26}$$

where the instanton velocity should be inserted for δ into eq. (B.16).

The ground state tunneling splitting for two symmetrically placed diabatic terms can be found in the same manner, as described in sections 2.4 and 4.2. Since the kink trajectory crosses the barrier once, we shall obtain

$$\Delta = \Delta_{ad} B^{1/2}\,, \tag{B.27}$$

where Δ_{ad} is the tunneling splitting in the adiabatic potential and B is defined by (B.26). In the nonadiabatic regime, $\delta \ll 1$, the tunneling splitting is proportional to V_d and inversely proportional to the square root of the instanton velocity.

References

Affleck, I., 1981, Phys. Rev. Lett. 46, 388.
Ambegaokar, V., 1987, Phys. Rev. B 37, 1624.
Amirav, A., U. Even and J. Jortner, 1980, Chem. Phys. 51, 31.
Arnold, V.I., 1978, Mathematical methods of Classical Mechanics (Springer, Berlin).

Arnold, C., N.S. Gettys, D.L. Thompson and L.M. Raff, 1986, J. Chem. Phys. 84, 3803.
Aslangul, C., N. Pottier and D. Saint-James, 1985, Phys. Lett. A 110, 249.
Auerbach, A., K.F. Freed and R. Gomer, 1987, J. Chem. Phys. 86, 2356.
Auerbach, A. and S. Kivelson, 1985, Nucl. Phys. B 257, 799.
Babamov, V.K. and R.A. Marcus, 1981, J. Chem. Phys. 74, 1790.
Babamov, V.K., V. Lopez and R.A. Marcus, 1983, J. Chem. Phys. 78, 5621.
Baer, M., 1982, Adv. Chem. Phys. 49, 191.
Balian, R. and C. Bloch, 1974, Ann. Phys. 85, 514.
Banghcum, S.L., Z. Smith, E.B. Wilson and R.W. Duerst, 1984, J. Am. Chem. Soc. 106, 2260.
Barbara, P.F., P.K. Walsh and L.E. Brus, 1989, J. Phys. Chem. 93, 29.
Barkalov, I.M., V.I. Goldanskii, D.P. Kiryukhin and A.M. Zanin, 1980, Chem. Phys. Lett. 73, 273.
Barton, A.E. and B.J. Howard, 1982, Faraday Disc. Chem. Soc. 73, 45.
Baś, A.I., Ya.B. Zeldovich and A.M. Perelomov, 1971, Scattering Reactions and Decays in the Non-relativistic Quantum Mechanics (Nauka, Moscow [in Russian)].
Basilevsky, M.V., G.N. Gerasimov and S.I. Petrochenko, 1982, Chem. Phys. 72, 493.
Bell, R.P., 1933, Proc. R. Soc. London A 139, 466.
Bell, R.P., 1935, Proc. R. Soc. London A 148, 241.
Bell, R.P., 1937, Proc. R. Soc. London A 158, 128.
Bell, R.P., 1973, The Proton in Chemistry, 2nd Ed. (Cornell Univ. Press, Ithaca, NY).
Bell, R.P., 1980, The Tunnel Effect in Chemistry (Chapman and Hall, London).
Benderskii, V.A. and V.I. Goldanskii, 1992, Int. Rev. Phys. Chem. 11, 1.
Benderskii, V.A. and D.E. Makarov, 1992, Phys. Lett. A 161, 535.
Benderskii, V.A., V.I. Goldanskii and A.A. Ovchinnikov, 1980, Chem. Phys. Lett. 73, 492.
Benderskii, V.A., V.I. Goldanskii and L.I. Trakhtenberg, 1989, Adv. Chem. Phys. 75, 349.
Benderskii, V.A., V.I. Goldanskii and D.E. Makarov, 1990, Chem. Phys. Lett. 171, 94.
Benderskii, V.A., V.I. Goldanskii and D.E. Makarov, 1991a, Chem. Phys. 154, 407.
Benderskii, V.A., V.I. Goldanskii and D.E. Makarov, 1991b, Chem. Phys. Lett. 186, 517.
Benderskii, V.A., V.I. Goldanskii, D.E. Makarov and E.Ya. Misochko, 1991c, Chem. Phys. Lett. 179, 334.
Benderskii, V.A., P.G. Grinevich, D.E. Makarov and D.L. Pastur, 1992a, Chem, Phys. 161, 51.
Benderskii, V.A., V.I. Goldanskii and D.E. Makarov, 1992b, Chem. Phys. 159, 29.
Benderskii, V.A., P.G. Grinevich and D.E. Makarov, 1993, Chem. Phys. 170, 275.
Bicerano, J., H.F. Schaefer and W.H. Miller, 1983, J. Am. Chem. Soc. 105, 2550.
Bixon, M. and J. Jortner, 1968, J. Chem. Phys. 48, 715.
Blake, G.A., K.L. Busarow, R.C. Cohen, K.B. Laughlin, Y.T. Lee and R.J. Saykally, 1988, J. Chem. Phys. 89, 6577.
Blanchet, G.B., N.J. Dinavolo and E.W. Plummer, 1982, Surf. Sci. 118, 496.
Blum, K., 1981, Density Matrix Theory and Applications (Plenum, New York).
Bolshakov, B.V., A.A. Stepanov and V.A. Tolkachev, 1980, Int. J. Chem. Kinet. 12, 271.
Borgis, D.C. and J.T. Hynes, 1991, J. Chem. Phys. 94, 3622.
Borgis, D.C., S. Lee and J.T. Hynes, 1989, Chem. Phys. Lett. 162, 19.
Bosch, E., M. Moreno, J.M. Lluch and J. Bertran, 1990, J. Chem. Phys. 93, 5685.
Bratan, S. and F. Strohbusch, 1980, J. Mol. Struct. 61, 409.
Buchwalter, S.L. and G.H. Closs, 1979, J. Am. Chem. Soc. 101, 4688.
Burton, G., J.A. Gray, D. Griller, L.R.C. Barclay and K.U. Ingold, 1978, J. Am. Chem. Soc. 100, 4197.
Buttenhoff, T.J. and C.B. Moore, 1988, J. Am. Chem. Soc. 110, 8336.
Caldeira, A.O. and A.J. Leggett, 1981, Phys. Rev. Lett. 46, 211.
Caldeira, A.O. and A.J. Leggett, 1983, Ann. Phys. 149, 374.
Callan, C.G. and S. Coleman, 1977, Phys. Rev. D 16, 1762.
Campion, A. and F. Williams, 1972, J. Am. Chem. Soc. 94, 7633.
Carrington, T. and W.H. Miller, 1986, J. Chem. Phys. 84, 4364.
Carsky, P., R.J. Bartlett, G. Fitzgerald, J. Noga and V. Spirko, 1988, J. Chem. Phys. 89, 3008.
Casati, G. and L. Molinari, 1989, Prog. Theor. Phys. Suppl. 98, 286.
Cavagnat, D. and M. Pesquer, 1986, J. Phys. Chem. 90, 3289.
Chakraborty, Z., P. Hedegard and M. Nylens, 1988, J. Phys. C 21, 3437.
Chandler, D., 1987, Introduction to Modern Statistical Mechanics (New York, Oxford).
Chapman, S., B.C. Garrett and W.H. Miller, 1975, J. Chem. Phys. 63, 2710.
Child, M.S., 1974, Molecular Collision Theory (Academic Press, London).
Clough, S., A. Heidemann, A.J. Horsewill, J.D. Lewis and M.N.J. Paley, 1981, J. Phys. C 14, L525.
Clough, S., A. Heidemann, A.J. Horsewill, J.D. Lewis and M.N.J. Paley, 1982, J. Phys. C 15, 2495.
Clough, S., A.J. Horsewill, P.J. McDonald and F.O. Zelaya, 1985, Phys. Rev. Lett. 55, 1794.
Coveney, P.V., M.S. Child and A. Barany, 1985, J. Phys. B 18, 4557.

Crossley, M.J., L.D. Field and M.M. Harding, 1988, J. Am. Chem. Soc. 109, 2335.
Dakhnovskii, Yu.I. and V.V. Nefedova, 1991, Phys. Lett. A 157, 301.
Dakhnovskii, Yu.I. and A.A. Ovchinnikov, 1985, Phys. Lett. A 113, 147.
Dakhnovskii, Yu.I. and M.B. Semenov, 1989, J. Chem. Phys. 92, 7606.
Dattaggupta, S., H. Grabert and R. Jung, 1989, J. Phys. Condens. Matter 1, 1405.
Dekker, H., 1987a, J. Phys. C 20, 3643.
Dekker, H., 1987b, Phys. Rev. A 35, 1436.
Dekker, H., 1991, Physica A 175, 485.
De la Vega, J.R., 1982, Account. Chem. Res. 15, 185.
De la Vega, J.R., J.H. Bush, J.H. Schauble, K.L. Kunze and B.E. Haggert, 1982, J. Am. Chem. Soc. 104, 3295.
DeVault, D., 1984, Quantum-Mechanical Tunneling in Biological Systems (Cambridge Univ. Press, Cambridge).
DeVault, D. and B. Chance, 1966, Biophys. J. 6, 825.
Dewar, M.J.S., K.M. Merz and J.J.P. Stewart, 1984, J. Am. Chem. Soc. 106, 4040.
Deycard, S., J. Lusztyk, K.U. Ingold, F. Zebretto, M.Z. Zgierski and W. Siebrand, 1988, J. Am. Chem. Soc. 110, 6721.
Difoggio, R. and R. Gomer, 1982, Phys. Rev. B 25, 3490.
Doba, T., K.U. Ingold, W. Siebrand and T.A. Wildman, 1984, J. Phys. Chem. 88, 3165.
Dogonadze, R.R. and A.M. Kuznetsov, 1975, Prog. Surf. Sci. 6, 1.
Dyke, T.R., B.J. Howard and W. Klemperer, 1972, J. Chem. Phys. 56, 2442.
Eyring, H., 1935, J. Chem. Phys. 3, 107.
Eyring, H., S.H. Lin and S.M. Lin, 1983, Basic Chemical Kinetics (Wiley, New York).
Feynman, R.P., 1972, Statistical Mechanics (Addison-Wesley, Reading, MA).
Feynman, R.P. and A.R. Hibbs, 1965, Quantum Mechanics and Path Integrals (McGraw-Hill, New York).
Feynman, R.P. and H.H. Kleinert, 1986, Phys. Rev. A 34, 5080.
Feynman, R.P. and F.L. Vernon, Ann. Phys. (NY) 24 (1963) 118.
Firth, D.W., P.F. Barbara and H.P. Trommsdorf, 1989, Chem. Phys. 136, 349.
Flynn, C.P. and A.M. Stoneham, 1970, Phys. Rev. B 1, 3967.
Ford, G.W., J.T. Lewis and R.F. O'Connel, 1988, Phys. Lett. A 128, 29; Phys. Rev. A 37, 4419.
Fraser, G.T., 1989, J. Chem. Phys. 90, 2097.
Fraser, G.T. and R.D. Suenram, 1992, J. Chem. Phys. 96, 7287.
Frei, H. and G.C. Pimentele, 1983, J. Chem. Phys. 78, 3698.
Frydman, L., F.C. Olivieri and L.E. Diaz, 1988, J. Am. Chem. Soc. 110, 336.
Fuke, K. and K. Kaya, 1989, J. Phys. Chem. 93, 614.
Furue, H. and P.D. Pacey, 1986, J. Phys. Chem. 90, 397.
Garg, A., J.N. Onuchic and V. Ambegaokar, 1985, J. Chem. Phys. 83, 4491.
Garrett, B.C. and D.G. Truhlar, 1983, J. Chem. Phys. 79, 4931.
Garrett, B.C. and D.G. Truhlar, 1991, J. Phys. Chem. 95, 10374.
Geoffroy, M., L.D. Kispert and J.S. Hwang, 1979, J. Chem. Phys. 70, 4238.
Gerasimov, G.N., S.N. Dolotov and D.A. Abkin, 1980, Int. J. Radiat. Phys. Chem. 15, 405.
Gillan, M.J., 1987, J. Phys. C 20, 3621.
Glasstone, S., K.J. Leidler and H. Eyring, 1941, The Theory of Rate Processes (McGraw-Hill, New York).
Goldanskii, V.I., 1959, Dokl. Akad. Nauk USSR 124, 1261; 127, 1037 [in Russian].
Goldanskii, V.I., 1976, Ann. Rev. Phys. Chem. 27, 85.
Goldanskii, V.I., 1979, Nature 279, 109.
Goldanskii, V.I., L.I. Trakhtenberg and V.N. Flerov, 1989, Tunneling Phenomena in Chemical Physics (Gordon and Breach, New York).
Grabert, H. and U. Weiss, 1984, Phys. Rev. Lett. 53, 1787.
Grabert, H., P. Olschowski and U. Weiss, 1987, Phys. Rev. B 36, 1931.
Grabert, H., U. Weiss and P. Hanggi, 1984a, Phys. Rev. Lett. 52. 2193.
Grabert, H., U. Weiss, P. Hanggi and P. Riseborough, 1984b, Phys. Lett. A 104, 10.
Grabert, H., D.N. Schramm and K.U. Ingold, 1988, Phys. Rep. 168, 115.
Grellmann, K.H., H. Weller and E. Tauer, 1983, Chem. Phys. Lett. 95, 195.
Grellmann, K.H., A. Mordzinski and A. Heinrich, 1989, Chem. Phys. 136, 201.
Grote, R.F. and J.T. Hynes, 1980, J. Chem. Phys, 73, 2715.
Gutzwiller, M.C., 1967, J. Math. Phys. 8, 1979.
Hancock, G.C. and D.G. Truhlar, 1989, J. Chem. Phys. 90, 3498.
Hancock, G.C., P. Rejto, R. Steckler, F.B. Brown, D.W. Schwenke and D.G. Truhlar, 1986, J. Chem. Phys. 85, 4997.
Hancock, G.C., D.G. Truhlar and C.E. Dykstra, 1988, J. Chem. Phys. 88, 1786.
Hancock, G.C., C.A. Mead, D.G. Truhlar and A.J.S. Varandas, 1989, J. Chem. Phys. 91, 3492.
Hanggi, P., 1986, J. Stat. Phys. 42, 105.
Hanggi, P. and W. Hontscha, 1988, J. Chem. Phys. 88, 4094.

Hanggi, P. and W. Hontscha, 1991, Ber. Bunsenges. Phys. Chem. 95, 379.
Hanggi, P., P. Talkner and M. Borkovec, 1990, Rev. Mod. Phys. 62, 251.
Hassel, O. and C. Romming, 1962, Quart, Rev. 14, 1.
(Heidemann, A., A. Magerl, M. Prager, D. Richter and T. Springer, eds, 1987, Quantum Aspects of Molecular Motions in Solids. Springer Proceedings in Physics, Vol. 17 (Springer, Berlin).
Hennig, J. and H.H. Limbach, 1979, J. Chem. Soc. Faraday Trans. Part 2, 75, 752.
Hewson, A.C., 1984, J. Phys. C 15, 3841, 3855.
Hill, J.R. and D.D. Dlott, 1988, J. Chem. Phys. 89, 830.
Hipes, P.G. and A. Kupperman, 1986, J. Phys. Chem. 90, 3630.
Holstein, T., 1959, Ann. Phys. 8, 325.
Holstein, T., 1978, Philos. Mag. B 37, 49.
Hontscha, W., P. Hanggi and E. Pollak, 1990, Phys. Rev. B 41, 2210.
Horsewill, A.J. and A. Aibout, 1989a, J. Phys. Condens. Mater 1, 9609.
Horsewill, A.J. and A. Aibout, 1989b, J. Phys. Condens. Mater 1, 10533.
Horsewill, A.J., A.M. Aslanoosi and C.J. Carlie, 1987, J. Phys. C 20, L869.
Huang, Z.S. and R.E. Miller, 1988, J. Chem. Phys. 88, 8008.
Huang, H., T.E. Feuchtwang, P.H. Cutler and E. Kazes, 1990, Phys. Rev. A 41, 32.
Hudson, P.L., M. Shiotani and F. Williams, 1977, Chem. Phys. Lett. 48, 193.
Hûller, A., 1980, Z. Phys. B 36, 215.
Hûller, A. and L. Baetz, 1988, Z. Phys. B 72, 47.
Hund, F., 1927, Z. Phys. 43, 805.
Idziak, S. and N. Pislewski, 1987, Chem. Phys. 111, 439.
Itzkovskii, A.S., A.Ya. Katunin and I.I. Lukashevich, 1986, Sov. Phys. – JETP 91, 1832.
Ivlev, B.I. and Yu.N. Ovchinnikov, 1987, Sov. Phys. – JETP 93, 668.
Jaquet, R. and W.H. Miller, 1985, J. Phys. Chem. 489, 2139.
Johnson, C.S., 1967, Mol. Phys. 12, 25.
Johnston, H.S., 1960, Adv. Chem. Phys. 3, 131.
Johnston, H.S. and D. Rapp, 1961, J. Am. Chem. Soc. 83, 1.
Jortner, J. and B. Pullman, eds, 1986, Tunneling (Reidel, Dordrecht).
Kagan Yu.M. and M.I. Klinger, 1974, J. Phys. C 7, 2791.
Kato, S., H. Kato and K. Fukui, 1977, J. Am. Chem. Soc. 99, 684.
Kramers, H., 1940, Physica 7, 284.
Kubo, R., 1957, J. Phys. Soc. Jpn. 12, 570.
Kubo, R. and S. Nakajima, 1957, J. Phys. Soc. Jpn. 12, 1203.
Kubo, R. and Y. Toyozava, 1955, Prog. Theor. Phys. 13, 160.
Kubo, R., M. Toda and N. Nashitsume, 1985, Statistical Physics. Non-equilibrium Statistical Mechanics (Springer, Berlin).
Laing, J.R., J.M. Yuan, H. Zimmerman, P.L. DeVries and T.F. George, 1977, J. Chem. Phys. 66, 2801.
Landau, L.D., 1932, Phys. Z. Sowjietunion 2, 46.
Landau, L.D. and E.M. Lifshitz, 1981, Quantum Mechanics (Pergamon, Oxford).
Langer, G.S., 1969, Ann. Phys. 54, 258.
Larkin, A.I. and Yu.N. Ovchinnikov, 1984, Sov. Phys. – JETP 59, 420.
Lauderdale, J.G. and D.G. Truhlar, 1985, Surf. Sci. 164, 558.
Lautie, A. and A. Novak, 1980, Chem. Phys. Lett. 71, 290
Lee, K.P., T. Miyazaki, K. Fueki and K. Gotoh, 1987, J. Phy. Chem. 91, 180.
Leggett, A.J., S. Chakravarty, A.T. Dorsey, M.P.A. Fisher, A. Garg and M. Zwerger, 1987, Rev. Mod. Phys. 59, 1.
Leidler, K.J., 1969, Theories of Chemical Kinetics (McGraw Hill, New York).
Le Roy, R.J., E.D. Sprague and F. Williams, 1972, J. Phys. Chem. 76, 545.
Le Roy, R.J., H. Murai and F. Williams, 1980, J. Am. Chem. Soc. 102, 2325.
Levine, A.M., W. Hontscha and E. Pollak, 1989, Phys. Rev. B 40, 2138.
Levit, S., J.W. Negele and Z. Paltiel, 1980a, Phys. Rev. C 21, 1603.
Levit, S., J.W. Negele and Z. Paltiel, 1980b, Phys. Rev. C 22, 1979.
Limbach, H.H., J. Hennig, D. Gerritzer and H. Rumpel, 1982, Faraday Disc. Chem. Soc. 74, 229.
Lippincott, E.R. and R. Schroeder, 1955, J. Chem. Phys. 23, 1099.
Lippincott, E.R. and R. Schroeder, 1957, J. Phys. Chem. 61, 921.
Loth, K., F. Graf and H. Gunthard, 1976, Chem. Phys. 13, 95.
Lucas, D. and G.C. Pimentele, 1979, J. Phys. Chem. 83, 2311.
Lynden-Bell, R.N., 1964, Mol. Phys. 8, 71.
Makri, N., 1991, J. Chem. Phys. 94, 4949.
Makri, N., 1992, Chem. Phys. Lett. 193, 435.
Makri, N. and W.H. Miller, 1987, J. Chem. Phys. 87, 5781.

Makri, N. and W.H. Miller, 1989, J. Chem. Phys. 91, 7026.
Mansuetto, E.S. and C.A. Wight, 1989, J. Am. Chem. Soc. 111, 1900.
Mansuetto, E.S., C.Y. Ju and C.A. Wight, 1989, J. Phys. Chem. 93, 4404.
Marcus, R.A., 1964, Ann. Rev. Phys. Chem. 15, 155.
McLaughlin, D.W., 1972, J. Math. Phys. 13, 1091.
Meier, B.H., F. Graf and R.R. Ernst, 1982, J. Chem. Phys. 76, 767.
Melnikov, V.I. and S.V. Meshkov, 1983, JETP Lett. 38, 130.
Mermin, N.D., 1991, Physica A 177, 561.
Meyer, R. and R.R. Ernst, 1987, J. Chem. Phys. 86, 784.
Miller, W.H., 1974, J. Chem. Phys. 61, 1823
Miller, W.H., 1975a, J. Chem. Phys. 62, 1899.
Miller, W.H., 1975b, J. Chem. Phys. 63, 1166.
Miller, W.H., 1976, Account. Chem. Res. 9, 36.
Miller, W.H., 1979, J. Phys. Chem. 83, 960.
Miller, W.H., 1983, J. Phys. Chem. 87, 3811.
Miller, W.H. and T.F. George, 1972, J. Chem. Phys. 56, 5668.
Miller, W.H., S.D. Schwartz and J.W. Tromp, 1983, J. Chem. Phys. 79, 4889.
Mills, I.M., 1984, J. Phys. Chem. 88, 532.
Miyazaki, T., 1991, Chem. Phys. Lett. 176, 99.
Miyazaki, T. and K.-P. Lee, 1986, J. Phys. Chem. 90, 400.
Miyazaki, T., K.-P. Lee, K. Fueki and A. Takeuchi, 1984, J. Phys. Chem. 88, 4959.
Miyazaki, T., N. Iwata, K.-P. Lee and K. Fueki, 1989, J. Phys. Chem. 93, 3352.
Miyazaki, T., H. Morikita, K. Fueki and T. Hiraku, 1991, Chem. Phys. Lett. 182, 35.
Mordzinski, A. and W. Kuhnle, 1986, J. Phys. Chem. 90, 1455.
Morillo, M. and R.I. Cukier, 1990, J. Chem. Phys. 92, 4833.
Morillo, M., D.Y. Yang and R.I. Cukier, 1989, J. Chem. Phys. 90, 5711.
Muttalib, K.A. and J. Sethna, 1985, Phys. Rev. B 32, 3462.
Nagaoka, S., T. Terao, F. Imashiro, N. Saika, N. Hirota and S. Nayashi, 1983, J. Chem. Phys. 79, 4694.
Nakamura, H., 1987, J. Chem. Phys. 87, 4031.
Nakamura, H., 1991, Int. Rev. Phys. Chem. 10, 123.
Nelson, D.D., G.T. Fraser and W. Klemperer, 1985, J. Chem. Phys. 83, 945.
Nikitin, E.E. and N.N. Korst, 1965, Theor. Exp. Chem. 1, 5.
Ohshima, Y., Y. Matsumoto, M. Takami and M. Kuchitsu, 1988, Chem. Phys. Lett. 147, 1.
Oppenlander, A., C. Rambaud, H.P. Trommsdorf and J.C. Vial, 1989, Phys. Rev. Lett. 63, 1432.
Ovchinnikov, A.A. and M.Ya. Ovchinnikova, 1982, Adv. Quantum Chem. 16, 161
Ovchinnikova, M.Ya., 1965, Dokl. Phys. Chem. 161, 259.
Ovchinnikova, M.Ya., 1979, Chem. Phys. 36, 15.
Pacey, P.D., 1979, J. Chem. Phys. 71, 2966.
Parris, P.E. and R. Silbey, 1985, J. Chem. Phys. 83, 5619.
Pertsin, A.J. and A.I. Kitaigorodskii, 1987, The Atom–Atom Potential Method. Application to Organic Molecular Solids (Springer, Berlin).
Peternelj, J. and I. Jencic, 1989, J. Phys. A 22, 1941.
Pine, A.S. and W.J. Lafferty, 1983, J. Chem. Phys. 78, 2154.
Pollak, E., 1986a, Phys. Rev. A 33, 4244.
Pollak, E., 1986b, J. Chem. Phys. 85, 865.
Polyakov, A.M., 1977, Nucl. Phys. B 121, 429.
Press, W., 1981, Single-Particle Rotations in Molecular Crystals. Springer Tracts in Modern Physics, Vol. 92 (Springer, Berlin).
Punnkinen, M., 1980, Phys. Rev. B 21, 54.
Quack, M. and M.A. Suhm, 1991, J. Chem. Phys. 95, 28.
Rajaraman, R., 1975, Phys. Rep. 21, 227.
Rambaud, C., A. Oppenlander, M. Pierre, H.P. Trommsdorf and J.C. Vial, 1989, Chem. Phys. 136, 335.
Rambaud, C., A. Oppenlander, H.P. Trommsdorf and J.C. Vial, 1990, J. Luminesc. 45, 310.
Razavy, M. and A. Pimpale, 1988, Phys. Rep. 168, 308.
Redington, R.L., 1990, J. Chem. Phys. 92, 6447.
Redington, R.L., Y. Chen, G.I. Scherer and R.W. Field, 1988, J. Chem. Phys. 88, 627.
Robinson, G.W. and R.P. Frosh, 1963, J. Chem. Phys. 37, 1962; 38, 1187.
Roginsky, S.Z. and L.V. Rozenkevitsch, 1930, Z. Phys. Chem. B 10, 47.
Rom, N., N. Moiseyev and R. Lefebvre, 1991, J. Chem. Phys. 95, 3562.
Rosetti, R. and L.E. Brus, 1980, J. Chem. Phys. 73, 1546.
Saitoh, T., K. Mori and R. Itoh, 1981, Chem. Phys. 60, 161.

Sana, M., G. Larry and J.L. Villaveces, 1984, Theor. Chim. Acta 65, 109.
Sarai, A., 1982, J. Chem. Phys. 76, 5554.
Sasetti, M. and U. Weiss, 1990, Phys. Rev. A 41, 5383.
Sato, N. and S. Iwata, 1988, J. Chem. Phys. 89, 2832.
Schlabach, M., B. Wehrle and H.H. Limbach, 1986, J. Am. Chem. Soc. 108, 3856.
Schmid, A., 1983, J. Low. Temp. Phys. 49, 609.
Schmid, A., 1986, Ann. Phys. 170, 333.
Sekiya, H., Y. Nagashima and Y. Nishima, 1990a, J. Chem. Phys. 92, 5761.
Sekiya, H., K. Sasaki, Y. Nishimura, A. Mori and H. Takeshita, 1990b, Chem. Phys. Lett. 174, 133.
Semenov, N.N., 1960, Khim. Tekh. Polimerov, 7–8, 196 [in Russian].
Sethna, J., 1981, Phys. Rev. B 24, 692.
Shian, W.-I., E.N. Duestler, I.C. Paul and D.Y. Curtin, 1980, J. Am. Chem. Soc. 102, 4546.
Shida, N., P.F. Barbara and J.E. Almlof, 1989, J. Chem. Phys. 91, 4061.
Shimanouchi, H. and Y. Sasada, 1973, Acta Crystallogr. B 29, 81.
Shimshoni, E. and Y. Cefen, 1991, Ann. Phys. (NY) 210, 16.
Shirley, J.H., 1965, Phys. Rev. B 138, 979.
Siebrand, W., 1967, J. Chem. Phys. 47, 2411.
Siebrand, W., T.A. Wildman and M.Z. Zgierski, 1984, J. Am. Chem. Soc. 106, 4083, 4089.
Silbey, R. and R.H. Harris, 1983, J. Chem. Phys. 78, 7330.
Silbey, R. and R.H. Harris, 1984, J. Chem. Phys. 80, 2615.
Silbey, R. and R.H. Harris, 1989, J. Phys. Chem. 93, 7062.
Silbey, R. and H.P. Trommsdorf, 1990, Chem. Phys. Lett. 165, 540.
Silvera, I.F., 1980, Rev. Mod. Phys. 52, 393.
Simonius, M., 1978, Phys. Rev. Lett. 26, 980.
Skinner, J.L. and H.P. Trommsdorf, 1988, J. Chem. Phys. 89, 897.
Skodje, R.T., D.G. Truhlar and B.C. Garrett, 1981, J. Phys. Chem. 85, 3019.
Smedarchina, Z., W. Siebrand and F. Zebretto, 1989, Chem. Phys. 136, 289.
Sokolov, N.D. and V.A. Savel'ev, 1977, Chem. Phys. 22, 383.
Someda, K. and H. Nakamura, 1991, J. Chem. Phys. 94, 4258.
Sprague, E.D. and F. Williams, 1971, J. Am. Chem. Soc. 93, 787.
Stuchebrukhov, A.A., 1991, J. Chem. Phys. 95, 4258.
Stueckelberg, E.C.G., 1932, Helv. Phys. Acta 5, 369.
Stunzes, P.A. and V.A. Benderskii, 1971, Sov. Optics Spectrosc. 30, 1041.
Suarez, A. and R. Silbey, 1991a, J. Chem. Phys. 94, 4809.
Suarez, A. and R. Silbey, 1991b, J. Chem. Phys. 95, 9115.
Tachibana, A. and K. Fukui, 1979, Theor. Chim. Acta 51, 189.
Takayanagi, T., N. Masaki, K. Nakamura, M. Okamoto and S. Sato, 1987, J. Chem. Phys. 86, 6133.
Tokumura, K., Y. Watanabe and M. Itoh, 1986, J. Phys. Chem. 90, 2362.
Topaler, M. and N. Makri, 1992, J. Chem. Phys. 97, 9001.
Topaler, M. and N. Makri, 1993, Chem. Phys. Lett. 210, 285.
Toriyama, K., K. Nunome and M. Iwasaki, 1977, J. Am. Chem. Soc. 99, 5823.
Toriyama, K. and M. Iwasaki, 1979, J. Am. Chem. Soc. 101, 2516.
Townes, C.H. and A.L. Schawlow, 1955, Microwave Spectroscopy (McGraw-Hill, New York).
Trakhtenberg, L.I., V.L. Klochikhin and S.Ya. Pshezhetskii, 1982, Chem. Phys. 69, 121.
Tringides, M. and R. Gomer, 1986, Surf. Sci. 166, 440.
Tromp, J.W. and W.H. Miller, 1986, J. Phys. Chem. 90, 3482.
Truhlar, D.G., 1990, in: Proc. NATO Workshop on Dynamics of Polyatomic van der Waals complexes, NATO Ser. B 227, 159.
Truhlar, D.G. and A. Kuppermann, 1971, J. Am. Chem. Soc. 93, 1840.
Truhlar, D.G., A.D. Isaacson, R.T. Skodje and B.C. Garrett, 1982, J. Phys. Chem. 86, 2252.
Truong, T. and D.G. Truhlar, 1987, J. Phys. Chem. 91, 6229.
Tsuji, T., H. Sekiya, Y. Nishimura, A. Mori and H. Takeshita, 1991, J. Chem. Phys. 95, 4802.
Turner, P., S.L. Banghcum, S.L. Coy and Z. Smith, 1984, J. Am. Chem. Soc. 106, 2265.
Ulstrup, L., 1979, Charge Transfer Process in Condensed Media (Springer, Berlin).
Vainshtein, A.I., V.I. Zakharov, V.A. Novikov and M.A. Shifman, 1982, Soviet Phys. – Usp. 25, 195.
Viswanathan, R. and L.M. Raff, 1983, J. Phys. Chem. 87, 3251.
Voth, G.A., D. Chandler and W.H. Miller, 1989a, J. Phys. Chem. 93, 7009.
Voth, G.A., D. Chandler and W.H. Miller, 1989b, J. Chem. Phys. 91, 7749.
Wang, S.C. and R. Gomer, 1985, J. Chem. Phys. 83, 4193.
Wartak, M.S. and S. Krzeminski, 1989, J. Phys. A 22, L1005.
Waxman, D. and A. Leggett, 1985, Phys. Rev. B 32, 4450.

Waxman, D., 1985, J. Phys. C 18, L421.
Weinhaus, F. and H. Meyer, 1972, Phys. Rev. B 7, 2974.
Weitenkamp, D.P., A. Bielecki, D. Zax, K. Zilm and A. Pines, 1983, Phys. Rev. Lett. 50, 1807.
Weng, S.-X., B.H. Torrie and B.M. Powell, 1989, Mol. Phys. 68, 25.
Whittall, M.W.G. and G.A. Gehring, 1987, J. Phys. C 20, 1619.
Wight, C.A., E.Ya. Misochko, E.V. Vetoshkin and V.I. Goldanskii, 1993, Chem. Phys. 170, 393.
Wigner, E., 1932, Z. Phys. Chem. B 19, 1903.
Wigner, E., 1938, Trans. Faraday Soc. 34, 29.
Wolynes, P.G., 1981, Phys. Rev. Lett. 47, 968.
Wolynes, P.G., 1987, J. Chem. Phys. 86, 1957.
Wûrger, A., 1989, Z. Phys. B 76, 65.
Wûrger, A. and A. Heidemann, 1990, Z. Phys. B 80, 113.
Yamamoto, T., 1960, J. Chem. Phys. 33, 281.
Zener, C., 1932, Proc. R. Soc. A 137, 696.
Zwanzig, R., 1964, Physica 30, 1109.
Zwanzig, R., 1973, J. Stat. Phys. 9, 215.
Zweers, A.E. and H.B. Brom, 1977, Physica B 85, 223.